

One-step full gradient suffices for low-rank fine-tuning, provably and efficiently

Yuanhe Zhang* Fanghui Liu† Yudong Chen‡

February 4, 2025

Abstract

This paper studies how to improve the performance of Low-Rank Adaption (LoRA) (Hu et al., 2022) as guided by our theoretical analysis. Our first set of theoretical results show that for random initialization and linear models, *i*) LoRA will align to the certain singular subspace of one-step gradient of full fine-tuning; *ii*) preconditioners improve convergence in the high-rank case. These insights motivate us to focus on preconditioned LoRA using a specific spectral initialization strategy for aligning with certain subspaces. For both linear and nonlinear models, we prove that alignment and generalization guarantees can be directly achieved at initialization, and the subsequent linear convergence can be also built. Our analysis leads to the *LoRA-One* algorithm (using *One*-step gradient and preconditioning), a theoretically grounded algorithm that achieves significant empirical improvement over vanilla LoRA and its variants on several benchmarks. Our theoretical analysis, based on decoupling the learning dynamics and characterizing how spectral initialization contributes to feature learning, may be of independent interest for understanding matrix sensing and deep learning theory. The source code can be found in the <https://github.com/YuanheZ/LoRA-One>.

1 Introduction

How to efficiently learn nonlinear models has been the recurring theme in machine learning (Alpaydin, 2020), especially in the era of large language models (LLMs) (Brown et al., 2020; Thoppilan et al., 2022). Parameter-efficient fine-tuning of LLMs (Achiam et al., 2023) aims to design scalable strategies to approximate/learn an unknown feature shift Δ such that LLMs perform well on new tasks while retain the knowledge from pre-trained models.

One typical parameter-efficient strategy is Low-Rank Adaptation (LoRA) (Hu et al., 2022), which learns a low-rank approximation of the unknown feature shift, $\Delta \approx \mathbf{A}\mathbf{B}$, using two low-rank matrices \mathbf{A} and \mathbf{B} . LoRA uses random Gaussian initialization for \mathbf{A} and zero initialization for \mathbf{B} :

$$[\mathbf{A}_0]_{ij} \sim \mathcal{N}(0, \alpha^2) \quad \text{and} \quad [\mathbf{B}_0]_{ij} = 0, \quad \alpha > 0. \quad (\text{LoRA-init})$$

*Department of Statistics, University of Warwick, United Kingdom; Email: yuanhe.zhang@warwick.ac.uk

†Department of Computer Science, also Centre for Discrete Mathematics and its Applications (DIMAP), University of Warwick, United Kingdom; Email: fanghui.liu@warwick.ac.uk (Corresponding author)

‡Department of Computer Sciences, University of Wisconsin-Madison, USA; e-mail: yudong.chen@wisc.edu

Table 1: Main results in the main text and appendix from subspace alignment to global convergence.

Model	Results	Algorithm	Initialization	Conclusion
Linear	Theorem 3.1	GD	(LoRA-init)	Subspace alignment of \mathbf{B}_t
	Theorem 3.2	GD	(LoRA-init)	Subspace alignment of \mathbf{A}_t
	Proposition 3.3	GD	(Spectral-init)	$\ \mathbf{A}_0\mathbf{B}_0 - \Delta\ _F$ is small
	Theorem 3.5	GD	(Spectral-init)	Linear convergence of $\ \mathbf{A}_t\mathbf{B}_t - \Delta\ _F$
	Theorem 3.6	Prec-GD	(Spectral-init)	Linear convergence rate independent of $\kappa(\Delta)$
Nonlinear	Theorem 4.3	Prec-GD	(Spectral-init)	Linear convergence rate independent of $\kappa(\Delta)$
	Theorem C.15	Smooth Prec-GD	(Spectral-init)	Linear convergence with less assumptions

To improve the performance in the downstream tasks, various LoRA-based algorithms have been proposed based on, e.g., refined initialization (Li et al., 2024), learning rates (Hayou et al., 2024), efficiency (Kopiczko et al., 2024), and gradient information (Meng et al., 2024; Wang et al., 2024a).

The goal of this work is to improve the practical performance of LoRA through theoretical insights. Although LoRA appears simple, its dynamics are inherently nonlinear and non-convex, and there is limited theoretical analysis of its behavior and generalization guarantees. Most prior theoretical studies are restricted to either lazy-training regimes (Jang et al., 2024; Malladi et al., 2023), or highly simplified settings such as when \mathbf{A}, \mathbf{B} are scalars (Hayou et al., 2024) or vectors (Dayi and Chen, 2024). It remains unclear how gradient updates in LoRA behave in the presence of data-adaptive and time-dependent nonlinearity. On the other hand, fine-tuning is ultimately an application-driven task. Therefore, when seeking a rigorous theoretical understanding of LoRA, we are equally (if not more) interested in leveraging our theoretical findings to guide practical algorithm design. This paper addresses two key questions sitting at the intersection of theory and practice:

- *Q1: How to characterize low-rank dynamics of LoRA and the associated subspace alignment in theory?*
- *Q2: How can our theoretical results contribute to algorithm design for LoRA in practice?*

1.1 Contributions and Algorithm Design Principles

In this work, we theoretically investigate the behavior of gradient descent (GD) update of LoRA parameters ($\mathbf{A}_t, \mathbf{B}_t$) and identify the subspaces they align with. Our analysis covers both linear and nonlinear models, with an overview of our results given in Table 1. Building on design principles distilled from these insights, we develop theoretically grounded algorithms that achieve enhanced performance in practical applications.

In Section 3, we start by analyzing LoRA for fine-tuning a multi-output linear model. Denoting one-step gradient of full fine-tuning as \mathbf{G}^\natural , we prove that the gradient update aligns \mathbf{A}_t with the singular subspace of \mathbf{G}^\natural while \mathbf{B}_t always stays in a certain singular subspace w.r.t. \mathbf{G}^\natural ; see Section 3.1 for details.

Consequently, by computing the singular value decomposition (SVD) of $\mathbf{G}^\natural = \tilde{\mathbf{U}}_{\mathbf{G}^\natural} \tilde{\mathbf{S}}_{\mathbf{G}^\natural} \tilde{\mathbf{V}}_{\mathbf{G}^\natural}^\top$ and we can directly achieve the above alignment if we use its certain singular subspaces for initialization:

$$\begin{aligned} \mathbf{A}_0 &= \sqrt{\gamma} \left[\tilde{\mathbf{U}}_{\mathbf{G}^\natural} \right]_{[:,1:r]} \left[\tilde{\mathbf{S}}_{\mathbf{G}^\natural}^{1/2} \right]_{[1:r]}, \\ \mathbf{B}_0 &= \sqrt{\gamma} \left[\tilde{\mathbf{S}}_{\mathbf{G}^\natural}^{1/2} \right]_{[1:r]} \left[\tilde{\mathbf{V}}_{\mathbf{G}^\natural} \right]_{[:,1:r]}^\top, \end{aligned} \tag{Spectral-init}$$

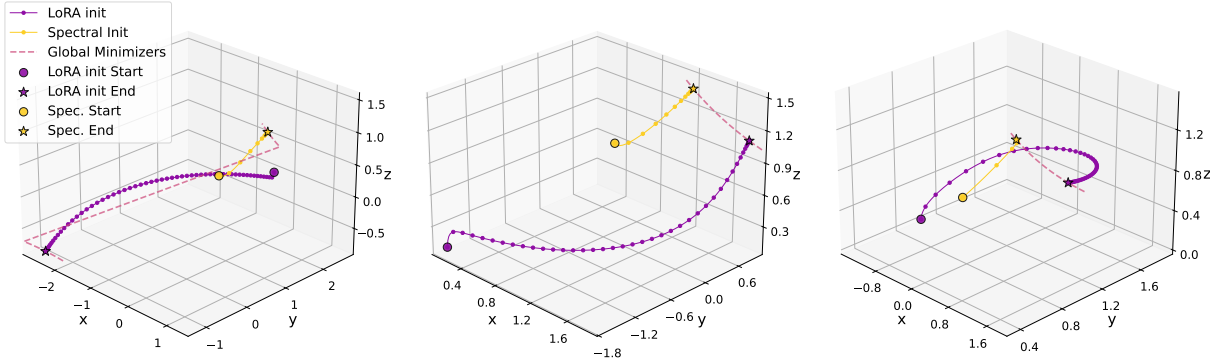


Figure 1: Comparison of the GD trajectories under (**LoRA-init**) and (**Spectral-init**) with three different starting points. We can observe that the starting points initialized by (**Spectral-init**) are consistently closer to the set of global minimizers, whereas those initialized by (**LoRA-init**) tend to be farther away across different random seeds. Moreover, running gradient descent from points initialized by (**Spectral-init**) requires significantly fewer steps to reach a global minimizer, demonstrating the advantages of (**Spectral-init**). More details can be found in Appendix F.1.

where γ is a tuning parameter. In Section 3.2, we prove that the initial iterate $(\mathbf{A}_0, \mathbf{B}_0)$ computed by (**Spectral-init**) approximately recovers the downstream target shift Δ , thereby showing the **sufficiency of using one-step full gradient**, which can be numerically verified on several benchmarks in Table 2 of Section 5. In Fig. 1, we present a toy experiment to intuitively illustrate the advantages of Eq. (**Spectral-init**) over Eq. (**LoRA-init**).

Continuing the GD update for $(\mathbf{A}_t, \mathbf{B}_t)$, we further establish the linear convergence rate of $\|\mathbf{A}_t \mathbf{B}_t - \Delta\|_F$. However, this linear rate is sensitive to the condition number $\kappa(\Delta)$ of Δ , leading to unsatisfactory convergence performance if Δ is ill-conditioned. To address this issue, we rigorously show that adding preconditioners into the GD update eliminates the dependence on the condition number; see Section 3.3.

In Section 4, we extend our theoretical results to nonlinear models with ReLU activation. We prove that the sufficiency of using one-step full gradient still holds under (**Spectral-init**) and further establish linear convergence rate of $\|\mathbf{A}_t \mathbf{B}_t - \Delta\|_F$. Besides, stronger convergence guarantees can be given by modifying the gradient update.

From the above theoretical results, we derive the following two algorithm design principles:

- #1: Proper spectral initialization by (**Spectral-init**) helps alignment and achieves better performance.
- #2: Preconditioners accelerate LoRA updates in the high-rank or ill-conditioned case.

Fig. 2 demonstrates the power of these two principles. This leads to our theoretically grounded algorithm, *LoRA-One*, which uses *one*-step full gradient and preconditioners and is given in Section 5. Our experiments demonstrate that *LoRA-One* achieves promising performance when compared to LoRA and its variants on natural language processing (NLP) tasks and LLMs under various tasks. More experimental details can be found in Appendix F. Besides, our theory and empirical observations also point to potential limitations of previous LoRA variants that are based on gradient alignment, e.g., LoRA-GA (Wang et al., 2024a); see the discussion in Section 5.

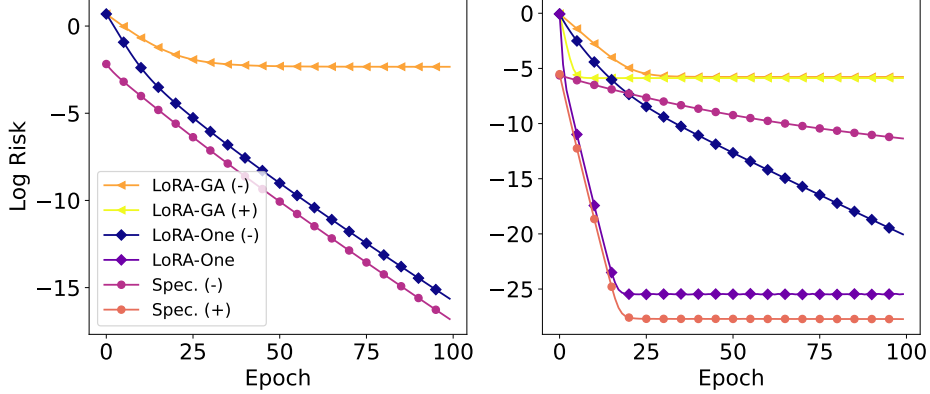


Figure 2: The log-risk curve under (Spectral-init), LoRA-GA (Wang et al., 2024a), and LoRA-One in Algorithm 1, trained via (Prec-)GD on fine-tuning task (2.2). (–) indicates that preconditioners is not added into GD. The risk is defined as $\frac{1}{2} \|\mathbf{A}_t \mathbf{B}_t - \Delta\|_{\text{F}}^2$. We compare the risk convergence of these algorithms under *Left*: GD in the exact-ranked setting; *Right*: adding preconditioners or not in the ill-conditioned setting. More experimental details and GD trajectories comparisons can be found in Appendix F.1.

Notations For a matrix \mathbf{A} , let $\|\mathbf{A}\|_{op}$ denote its operator and $\|\mathbf{A}\|_{\text{F}}$ its Frobenius norm. Let \odot denote the Hadamard (i.e., entrywise) matrix product. We use \mathbf{I}_n to denote the $\mathbb{R}^{n \times n}$ -valued identity matrix. The notation $\mathbf{U}_{\mathbf{A}}$ denotes the left singular matrix of the compact SVD of \mathbf{A} and $\mathbf{U}_{\mathbf{A}, \perp}$ denotes the corresponding orthogonal complement. Similarly, $\mathbf{V}_{\mathbf{A}}$ denotes the right singular matrix of \mathbf{A} and $\mathbf{V}_{\mathbf{A}, \perp}$ denotes its orthogonal complement. Let $\mathbf{U}_{r^*}(\mathbf{A})$ denote the left singular subspace spanned by the r^* largest singular values of \mathbf{A} and $\mathbf{U}_{r^*, \perp}(\mathbf{A})$ denote the left singular subspace orthogonal to $\mathbf{U}_{r^*}(\mathbf{A})$. Similarly define $\mathbf{V}_{r^*}(\mathbf{A})$ and $\mathbf{V}_{r^*, \perp}(\mathbf{A})$ for the right singular subspace. A complete list notations can be found in Table 7 of Appendix A.

1.2 Related Work

Parameter-Efficient Fine-Tuning (PEFT): LoRA (Hu et al., 2022) and its variants have received great attention for downstream applications. The variants of LoRA focus on imbalance stepsize (Hayou et al., 2024), initialization using SVD of pre-trained weights (Meng et al., 2024), gradient approximation (Wang et al., 2024a,b) for better performance, reducing parameters (Kopiczko et al., 2024) efficiency, preconditioned algorithm (Zhang and Pilanci, 2024) for stability.

In theory, the training dynamics and generalization ability of LoRA are rarely discovered. Based on the empirical evidence of kernel behavior of LoRA in Malladi et al. (2023); Jang et al. (2024) prove that LoRA with rank $\mathcal{O}(\sqrt{N})$ trained via gradient descent with N data can admit global minimizer under neural tangent kernel (Jacot et al., 2018) regime. Beyond kernel regime, Dayi and Chen (2024) explores the SGD dynamics of rank-1 LoRA. However, their setting is unrealistic since they only train \mathbf{A} which is a vector and restricted to the rank-1 setting. In our work, we simultaneously train \mathbf{A} and \mathbf{B} and have flexible choice for LoRA ranks. Moreover, we discover the relationship between LoRA and full fine-tuning from dynamics.

Matrix Sensing under Gradient Descent: Since LoRA performs fine-tuning using a Burer-Monterio factorization, it admits similarities with matrix sensing problems, including the symmetric

matrix problem with $r = r^*$ (Li et al., 2018) and $r \geq r^*$ (Stöger and Soltanolkotabi, 2021); asymmetric problem with $r \geq r^*$ (Soltanolkotabi et al., 2023; Xiong et al., 2023). Regarding initialization, small initialization (Ding et al., 2022) and spectral initialization (Ma et al., 2021) help convergence with theoretical guarantees. Besides, adding preconditioner (Zhang et al., 2021; Tong et al., 2021; Xu et al., 2023; Zhang et al., 2023) is beneficial to solve the problem of ill-conditioned ground truth matrix.

Technically, for the alignment part, our theory leverages some techniques from Soltanolkotabi et al. (2023). However, the symmetrization technique used in prior work cannot be applied to decouple the GD dynamics of $(\mathbf{A}_t, \mathbf{B}_t)$, posing a challenge in analyzing their individual spectral behaviors. To overcome this limitation, we develop a novel approach that enables a detailed analysis of the distinct spectral dynamics of \mathbf{A}_t and \mathbf{B}_t , which is one technical contribution of this work. Besides, for the nonlinear model part, dynamical analysis are normally based on classical gradient-based algorithm (Damian et al., 2022; Lee et al., 2024). How such model behaves under low-rank updates under (Spectral-init) has been unclear to our knowledge.

2 Problem Settings

In this section, we introduce the problem setting of fine-tuning pre-trained linear and nonlinear models with the following assumptions.

2.1 Basic Assumptions

We consider both linear and nonlinear pre-trained models with multiple outputs and thus matrix parameters (instead of vectors), which is consistent with LoRA in practice.

Assumption 2.1 (Pre-trained model). For the input $\mathbf{x} \in \mathbb{R}^d$, we denote by $\mathbf{W}^{\natural} \in \mathbb{R}^{d \times k}$ the **known** pre-trained parameter matrix. We assume that the pre-trained model can be linear or nonlinear with $\sigma(\cdot) = \max\{0, \cdot\}$ is the (entry-wise) ReLU activation function.

$$f_{\text{pre}}(\mathbf{x}) := \begin{cases} (\mathbf{x}^\top \mathbf{W}^{\natural})^\top \in \mathbb{R}^k & \text{linear} \\ \sigma[(\mathbf{x}^\top \mathbf{W}^{\natural})^\top] \in \mathbb{R}^k & \text{nonlinear} \end{cases}.$$

Note that our results can handle large dimension d and k . Next, we assume there exists an **unknown** low-rank feature shift Δ on \mathbf{W}^{\natural} that we aim to estimate.

Assumption 2.2. The downstream feature matrix $\widetilde{\mathbf{W}}^{\natural} := \mathbf{W}^{\natural} + \Delta$ admits an **unknown** low-rank feature shift $\Delta \in \mathbb{R}^{d \times k}$, where $\text{Rank}(\Delta) = r^* < \min\{d, k\}$.

This assumption is widely used in the literature on LoRA analysis and matrix factorization (Zhang et al., 2021; Stöger and Soltanolkotabi, 2021; Soltanolkotabi et al., 2023; Xiong et al., 2023). Besides, we also assume that the data is well-behaved, e.g., (Gaussian/sub-Gaussian) concentration.

Assumption 2.3 (Downstream data for fine-tuning). We consider the label-noiseless setting for fine-tuning linear and nonlinear models. Given the unknown $\widetilde{\mathbf{W}}^{\natural}$, the N downstream data points $\{(\tilde{\mathbf{x}}_i, \tilde{\mathbf{y}}_i)\}_{i=1}^N$ are i.i.d. and satisfy the following data generation process:

$$\tilde{\mathbf{y}} := \begin{cases} (\tilde{\mathbf{x}}^\top \widetilde{\mathbf{W}}^{\natural})^\top \in \mathbb{R}^k, & \{\tilde{\mathbf{x}}_i\}_{i=1}^N \stackrel{i.i.d.}{\sim} SG, & \text{linear} \\ \sigma[(\tilde{\mathbf{x}}^\top \widetilde{\mathbf{W}}^{\natural})^\top], & \{\tilde{\mathbf{x}}_i\}_{i=1}^N \stackrel{i.i.d.}{\sim} \mathcal{N}(\mathbf{0}, \mathbf{I}_d) & \text{nonlinear} \end{cases},$$

where SG denotes the probability distribution for isotropic centered sub-Gaussian random vectors.

Note that the nonlinear model can be regarded as a special case of multi-index model (Damian et al., 2022; Abbe et al., 2022; Bietti et al., 2023) and Gaussian data is a common assumption in the analysis of single/multi-index models (Damian et al., 2022; Lee et al., 2024; Oko et al., 2024). We additionally assume that $d < N$, which coincides with practical settings of LoRA for Llama 2-7b (Touvron et al., 2023) on real-world datasets, e.g., MetaMathQA (Yu et al., 2023) and Code-Feedback (Zheng et al., 2024), where $d = 1024$ and N is on the order of 10^5 .

2.2 Full Fine-tuning and LoRA

Our goal is to efficiently recover Δ by fine-tuning on the downstream data. Let the complete SVD of $\Delta \in \mathbb{R}^{d \times k}$ be

$$\Delta = \tilde{\mathbf{U}} \tilde{\mathbf{S}}^* \tilde{\mathbf{V}}^\top := [\mathbf{U} \quad \mathbf{U}_\perp] \begin{bmatrix} \mathbf{S}^* & \mathbf{0} \\ \mathbf{0} & \mathbf{0} \end{bmatrix} \begin{bmatrix} \mathbf{V}^\top \\ \mathbf{V}_\perp^\top \end{bmatrix}, \quad (2.1)$$

where $\tilde{\mathbf{U}} \in \mathbb{R}^{d \times d}$ and $\tilde{\mathbf{V}} \in \mathbb{R}^{k \times k}$ are the left and right singular matrices, and $\tilde{\mathbf{S}}^* \in \mathbb{R}^{d \times k}$ is a rank- r^* diagonal matrix with nonzero singular values $\{\lambda_i^*\}_{i=1}^{r^*}$. It admits the compact SVD $\Delta = \mathbf{U} \mathbf{S}^* \mathbf{V}^\top$ with $\mathbf{U} \in \mathbb{R}^{d \times r^*}$, $\mathbf{V}^\top \in \mathbb{R}^{r^* \times k}$, and $\mathbf{S}^* \in \mathbb{R}^{r^* \times r^*}$. The left/right singular subspaces spanned by \mathbf{U} and \mathbf{V} play an important role in our analysis.

We write the downstream data in a compact form $\tilde{\mathbf{X}} = [\tilde{\mathbf{x}}_1, \dots, \tilde{\mathbf{x}}_N]^\top \in \mathbb{R}^{N \times d}$ and the label matrix $\tilde{\mathbf{Y}} = [\tilde{\mathbf{y}}_1 \cdots \tilde{\mathbf{y}}_N]^\top \in \mathbb{R}^{N \times k}$ is generated by either linear or nonlinear target functions in Assumption 2.3. We introduce the training based on full fine-tuning and LoRA below.

Full Fine-tuning: We consider the following empirical risk minimization with a squared loss

$$L(\mathbf{W}) := \frac{1}{2N} \begin{cases} \|\tilde{\mathbf{X}}\mathbf{W} - \tilde{\mathbf{Y}}\|_{\text{F}}^2 & \text{linear,} \\ \|\sigma(\tilde{\mathbf{X}}\mathbf{W}) - \tilde{\mathbf{Y}}\|_{\text{F}}^2 & \text{nonlinear} \end{cases}, \quad (2.2)$$

where the parameter \mathbf{W} can be learned by gradient descent (GD) initialized at \mathbf{W}^\natural , i.e., $\mathbf{W}_0 := \mathbf{W}^\natural$.

LoRA: LoRA updates two low-rank matrices $\mathbf{A} \in \mathbb{R}^{d \times r}$, $\mathbf{B} \in \mathbb{R}^{r \times k}$ for efficiency with the following empirical risk

$$\tilde{L}(\mathbf{A}, \mathbf{B}) := \frac{1}{2N} \begin{cases} \|\tilde{\mathbf{X}}(\mathbf{W}^\natural + \mathbf{A}\mathbf{B}) - \tilde{\mathbf{Y}}\|_{\text{F}}^2, & \text{linear,} \\ \|\sigma(\tilde{\mathbf{X}}(\mathbf{W}^\natural + \mathbf{A}\mathbf{B})) - \tilde{\mathbf{Y}}\|_{\text{F}}^2, & \text{nonlinear} \end{cases}$$

which can be minimized using GD

$$\begin{aligned} \mathbf{A}_{t+1} &= \mathbf{A}_t - \eta_1 \nabla_{\mathbf{A}} \tilde{\mathcal{L}}(\mathbf{A}_t, \mathbf{B}_t), \\ \mathbf{B}_{t+1} &= \mathbf{B}_t - \eta_2 \nabla_{\mathbf{B}} \tilde{\mathcal{L}}(\mathbf{A}_t, \mathbf{B}_t), \end{aligned} \quad (2.3)$$

with stepsizes $\eta_1, \eta_2 > 0$. Notice that our results are able to handle imbalanced step-sizes, i.e., $\eta_1 \neq \eta_2$ in Hayou et al. (2024).

Since the true rank r^* of Δ is unknown in LoRA, our results will cover two cases: *over-ranked* ($r \geq r^*$) and *exact-ranked* ($r = r^*$).¹ Our results allow for large d, k while $r, r^* = \Theta(1)$, which coincides with common practice.

Optimization and Generalization: We are interested in the error $\|\mathbf{A}_t \mathbf{B}_t - \Delta\|_{\text{F}}^2$ under the LoRA training dynamics. Bounds on this error also imply generalization performance, because the generalization error for a new data $(\tilde{\mathbf{x}}, \tilde{\mathbf{y}})$ satisfies $\mathbb{E}_{\tilde{\mathbf{x}}} \|\tilde{\mathbf{y}} - \sigma(\mathbf{W}^{\natural} + \mathbf{A}_t \mathbf{B}_t)^{\top} \tilde{\mathbf{x}}\|_2^2 \leq \|\mathbf{A}_t \mathbf{B}_t - \Delta\|_{\text{F}}^2$ in the nonlinear setting, with equality in the linear setting.

3 Analysis of LoRA under Linear Model

In this section, we establish the alignment between LoRA and one gradient of full fine-tuning. This result guides us to design new strategies for speeding up practical LoRA-based algorithms, which achieve this alignment at initialization.

We formally define the negative gradient of full fine-tuning in Eq. (2.2) for the linear setting after the first step as

$$\mathbf{G}^{\natural} := -\nabla_{\mathbf{W}} L(\mathbf{W}^{\natural}) = \frac{1}{N} \widetilde{\mathbf{X}}^{\top} (\widetilde{\mathbf{Y}} - \widetilde{\mathbf{X}} \mathbf{W}^{\natural}). \quad (3.1)$$

Note that $\widetilde{\mathbf{X}}^{\top} \widetilde{\mathbf{X}}$ is a non-singular square matrix by Zeng and Lee (2023, Lemma 6). Since left multiplication by a non-singular square matrix does not change the rank by Horn and Johnson (2012, 0.4.6 (b)), we have $\text{Rank}(\mathbf{G}^{\natural}) = \text{Rank}(\Delta) = r^*$. Denote by $\{\lambda_i(\mathbf{G}^{\natural})\}_{i=1}^{r^*}$ the singular values of \mathbf{G}^{\natural} in non-increasing order.

3.1 Alignment under LoRA Initialization

We first present the results for the alignment of \mathbf{B}_t by recalling the notations $\mathbf{V}_{r^*}(\cdot)$ and $\mathbf{V}_{r^*, \perp}(\cdot)$.

Theorem 3.1 (Alignment between \mathbf{G}^{\natural} and \mathbf{B}_t). Under assumptions in Section 2.1 for the linear setting, consider the LoRA updates (2.3) with (LoRA-init). We have

$$\left\| \mathbf{V}_{r^*, \perp}^{\top} \left(\mathbf{G}^{\natural} \right) \mathbf{V}_{r^*}(\mathbf{B}_t) \right\|_{op} = 0, \quad \forall t \in \mathbb{N}_+.$$

One can see that, due to the zero initialization of \mathbf{B}_0 in (LoRA-init), after the first GD step, it holds that $\mathbf{B}_1 = \eta_1 \mathbf{A}_0^{\top} \mathbf{G}^{\natural}$, which has rank $\leq r^*$ and lies in the right top- r^* singular subspace of \mathbf{G}^{\natural} . The subsequent GD dynamics of \mathbf{B}_t is always restricted to this invariant subspace.

Next we build the alignment for \mathbf{A}_t with the notations $\mathbf{U}_{r^*}(\cdot)$, $\mathbf{U}_{r^*, \perp}(\cdot)$ and κ^{\natural} as the condition number of \mathbf{G}^{\natural} .

Theorem 3.2 (Alignment between \mathbf{G}^{\natural} and \mathbf{A}_t . Simplified version of Theorem B.9). For the $r \geq 2r^*$ case, under assumptions in Section 2.1 for the linear setting, we consider the LoRA updates (2.3) with $[\mathbf{A}_0]_{ij} \sim \mathcal{N}(0, \alpha^2)$ in (LoRA-init). Then for any constant $\theta \in (0, 1)$, by taking $\alpha = \mathcal{O}\left(\theta^{\frac{3}{2}\kappa^{\natural}} d^{-\frac{3}{4}\kappa^{\natural} - \frac{1}{2}} \|\mathbf{G}^{\natural}\|_{op}^{\frac{1}{2}}\right)$, and running gradient descent for t^* steps with

$$t^* \lesssim \frac{\ln\left(\frac{\sqrt{d}}{\theta}\right)}{\ln\left(1 + \sqrt{\eta_1 \eta_2} \lambda_{r^*}(\mathbf{G}^{\natural})\right)}, \quad (3.2)$$

¹In the matrix sensing/completion literature, they are often called *over-* and *exact-parameterized*, respectively.

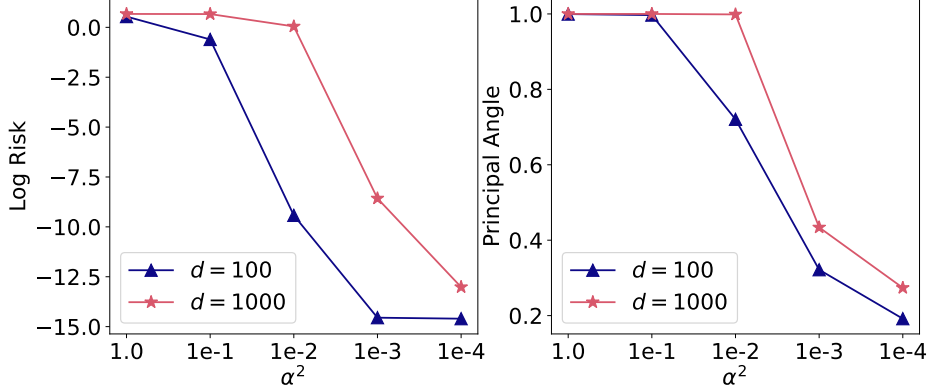


Figure 3: Under (LoRA-init), the log-risk and the angle of alignment to full one-step GD of LoRA with different α^2 and d , trained via GD on task (2.2). *Left*: the log risk under different initialization variance α^2 . The risk is defined as $\frac{1}{2} \|\mathbf{A}_t \mathbf{B}_t - \Delta\|_F^2$. *Right*: the best principal angle between the top- r singular subspace of \mathbf{G}^\natural and \mathbf{A}_t during training. Smaller is closer. The principal angle is defined as $\min_t \|\mathbf{U}_{r^*, \perp}^\top(\mathbf{G}^\natural) \mathbf{U}_{r^*}(\mathbf{A}_t)\|_{op}$. More experimental details can be found in Appendix F.1.

we achieve the following the alignment on the left singular subspace between \mathbf{G}^\natural and \mathbf{A}_{t^*} as below

$$\left\| \mathbf{U}_{r^*, \perp}^\top(\mathbf{G}^\natural) \mathbf{U}_{r^*}(\mathbf{A}_{t^*}) \right\|_{op} \lesssim \theta, \quad (3.3)$$

with probability at least $1 - C_1 \exp(-d) - C_2 \exp(-r) - C_3 \exp(-N)$ for some constants C_1, C_2, C_3 .

The result under the $r^* \leq r < 2r^*$ case is more complex and we defer this result to Theorem B.9.

Remark: We make the following remarks:

- The choice of α in Theorem 3.2 shows that after $t^* = \Theta\left(\frac{\ln d}{\lambda_{r^*}(\mathbf{G}^\natural)}\right)$ in Eq. (3.2), the alignment can be achieved. Our results can cover the standard He-initialization (He et al., 2015) if $\|\mathbf{G}^\natural\|_{op} \geq \Omega\left(d^{\frac{3}{4} \kappa^\natural}\right)$. Requirement on $\|\mathbf{G}^\natural\|_{op}$ can be relaxed under smaller initialization, illustrated by Fig. 3.
- Using imbalanced step-size, e.g., increasing η_2 while fixing η_1 , can reduce the time steps needed for alignment. In particular, if we fix η_1 , increasing the step-size ratio $\sqrt{\eta_2/\eta_1}$ in Eq. (3.2) reduces the alignment time, theoretically support for LoRA+ (Hayou et al., 2024).
- Note that we can select any pair of stepsizes (η_1, η_2) that satisfies the conditions $t^* > 1$, $\eta_2 \geq \eta_1$, and $\zeta(\eta_1, \eta_2) = \Theta(1)$.

The above two theorems characterize the alignment between \mathbf{G}^\natural and $(\mathbf{A}_t, \mathbf{B}_t)$. Fig. 3 empirically validates Theorem 3.2 in two folds:

- Smaller initialization (α^2 in the x-axis) encourages better alignment (evaluated by the principal angle), and then better generalization performance of fine-tuning (evaluated by the risk). But in practice, a smaller initialization would increase the training time for convergence, as a double-edge sword.

- ii) Increasing d leads to longer alignment time, illustrated by Eq. (3.2), and worse alignment performance, illustrated by the formulation of α .

We remark that previous work on matrix sensing (Stöger and Soltanolkotabi, 2021; Soltanolkotabi et al., 2023) via a symmetrization technique cannot be directly applied to our setting. Such symmetrization technique prevents the alignment results decoupling into two factorized matrices. We extend their technique to decouple the alignment for \mathbf{A}_t and \mathbf{B}_t individually via Schur decomposition of \mathbf{H} .

3.2 Spectral Initialization for Global Convergence

Theorem 3.2 has demonstrated the alignment on the rank- r^* singular space of \mathbf{G}^\natural and $(\mathbf{A}_t, \mathbf{B}_t)$. In other words, if we take the SVD of \mathbf{G}^\natural and choose the certain singular subspace for initialization in (Spectral-init), we can directly achieve the alignment at the initialization (without training) and recover Δ to some extent, which is the main target of this work.

By the following standard concentration result for (sub)-Gaussian data: with probability at least $1 - 2C \exp(-\epsilon^2 N)$ for some constants $C > 0$, we have

$$\left\| \widehat{\Sigma} - \mathbf{I}_d \right\|_{op} \leq \epsilon := \min \left\{ \frac{1}{2\kappa}, \frac{c}{\kappa^3} \right\} \leq \frac{1}{2}. \quad (3.4)$$

Recall κ is the condition number of Δ and $\lambda_{r^*}^*$ is the r^* -th singular value of Δ , we have the following result at the spectral initialization.

Proposition 3.3. [One-step gradient suffices] Under assumptions in Section 2.1 for the linear setting via (Spectral-init), taking ϵ in Eq. (3.4), then with probability at least $1 - 2C \exp(-\epsilon^2 N)$ for constant $C > 0$, we have

$$\|\mathbf{A}_0 \mathbf{B}_0 - \Delta\|_{op} \leq \epsilon \|\Delta\|_{op} \leq \frac{\lambda_{r^*}^*}{2}.$$

Proposition 3.3 demonstrates that, after one-step full gradient, i.e., using spectral initialization (Spectral-init), $\mathbf{A}_0 \mathbf{B}_0$ is able to recover Δ with small error. Besides, under (Spectral-init), the alignment between Δ and \mathbf{B}_t in Theorem 3.1 via (LoRA-init) can be simplified as below.

Lemma 3.4. Under assumptions in Section 2.1 for the linear setting, and spectral initialization (Spectral-init), we always have $\mathbf{B}_t \mathbf{V}_\perp = \mathbf{0}_{d \times (d-r^*)}$ for any $t \in \mathbb{N}^+$, where \mathbf{V}_\perp comes from the complete SVD of Δ in Eq. (2.1).

Lemma 3.4 shows that \mathbf{B}_t 's dynamics always stays in the low-dimensional target (right singular) subspace under the spectral initialization, which contributes to track the behavior of $\|\mathbf{A}_t \mathbf{B}_t - \Delta\|_{op}$. In this regime, there is no significant difference on setting different step-size η_1 and η_2 . For ease of description, we set $\eta_1 = \eta_2 := \eta$ for the later analysis.

Theorem 3.5 (Global convergence. Simplified version of Theorem B.17). Under assumptions in Section 2.1 for the linear setting, suppose we use the initialization scheme (Spectral-init), and take ϵ in Eq. (3.4) and $r \geq r^*$, $\eta = \mathcal{O}(1/\kappa \lambda_1^*)$. Then with probability at least $1 - 2C \exp(-\epsilon^2 N)$ for a universal constant $C > 0$, we have

$$\|\mathbf{A}_t \mathbf{B}_t - \Delta\|_F \leq \sqrt{2r^*} \left(1 - \eta \frac{\lambda_{r^*}^*}{64\kappa} \right)^t \lambda_{r^*}^*(\Delta), \quad \forall t \geq 1.$$

Remark: The above convergence rate is independent of the choice of LoRA rank r if $r \geq r^*$. It achieves an ε -risk in $\mathcal{O}(\kappa^3 \ln(1/\varepsilon))$ iterations.

3.3 Preconditioned GD under Spectral Initialization

By Theorem 3.5, the linear convergence rate heavily depends on κ . The convergence will be slow if the downstream feature shift Δ is ill-conditioned (i.e., κ is extremely large). This motivates us to add preconditioners, which is a key technique to accelerate convergence in matrix factorization/sensing (Tong et al., 2021; Zhang et al., 2021, 2023; Jia et al., 2024). We apply to analysis of LoRA as well as algorithm design. In the over-ranked setting ($r > r^*$), $\mathbf{B}_t \mathbf{B}_t^\top$ and $\mathbf{A}_t^\top \mathbf{A}_t$ are not necessarily invertible. Hence we add the following preconditioners to vanilla GD (2.3)

$$\begin{aligned} \mathbf{A}_{t+1} &= \mathbf{A}_t - \eta \widehat{\Sigma} (\mathbf{A}_t \mathbf{B}_t - \Delta) (\mathbf{B}_t)^\top \left(\mathbf{B}_t \mathbf{B}_t^\top \right)^\dagger, \\ \mathbf{B}_{t+1} &= \mathbf{B}_t - \eta \left(\mathbf{A}_t^\top \mathbf{A}_t \right)^\dagger \mathbf{A}_t^\top \widehat{\Sigma} (\mathbf{A}_t \mathbf{B}_t - \Delta), \end{aligned} \quad (3.5)$$

where \mathbf{M}^\dagger denotes the pseudo-inverse of a matrix \mathbf{M} . Such modified preconditioners are also considered in Li et al. (2024). Under (Spectral-init), similar to Lemma 3.4, the dynamics of \mathbf{B}_t under precondition GD are still limited to the r^* -dimensional singular subspace \mathbf{V} of Δ , i.e., $\mathbf{B}_t \mathbf{V}_\perp = \mathbf{0}_{r \times (k-r^*)}$; see the proof in Lemma B.18 in the appendix. We also have the following linear convergence under preconditioners.

Theorem 3.6. Under assumptions in Section 2.1 for the linear setting, using precondition GD in Eq. (3.5) under spectral initialization (Spectral-init), we choose $\epsilon \leq \min \left\{ \frac{1}{2\sqrt{r^* \kappa}}, \frac{1}{4} \right\}$ and set $\eta \in \left(0, \frac{0.5-2\epsilon}{(1+\epsilon)^2} \right)$, then with probability at least $1 - 2C \exp(-\epsilon^2 N)$ for a universal constant $C > 0$, we have

$$\|\mathbf{A}_t \mathbf{B}_t - \Delta\|_F \leq \frac{1}{2} \left(1 - \frac{\eta}{2} \right)^t \lambda_{r^*}^*(\Delta), \quad \forall t \geq 0.$$

The convergence rate is independent of the condition number of κ . The choice of stepsize η is upper bounded by $\frac{0.5-2\epsilon}{(1+\epsilon)^2} \in (0, 0.5)$, which is a decreasing function of ϵ . Therefore, if the condition number κ is very large and thus ϵ is chosen as sufficiently small, then η can reach 0.5 and we still have a fast convergence rate independent of κ . This is particularly useful in practical fine-tuning tasks, where the adapted matrix can be highly ill-conditioned when its rank increases. We can empirically observe the ill-conditioned issues in real-world benchmarks, as shown in Fig. 4. For the difference matrix between pre-trained weight and fine-tuned weight, the singular values decrease drastically as the index increases, indicating an ill-conditioned behavior during fine-tuning.

4 Analysis of LoRA under Nonlinear Models

Now we focus on the nonlinear setting described in Section 2, where we consider the exact-rank case $r = r^*$ for delivery. We will demonstrate the linear convergence rate in the linear setting can still hold for the nonlinear setting.

Following Section 3.3, we continue to consider preconditioned GD on $(\mathbf{A}_t, \mathbf{B}_t)$ with the same

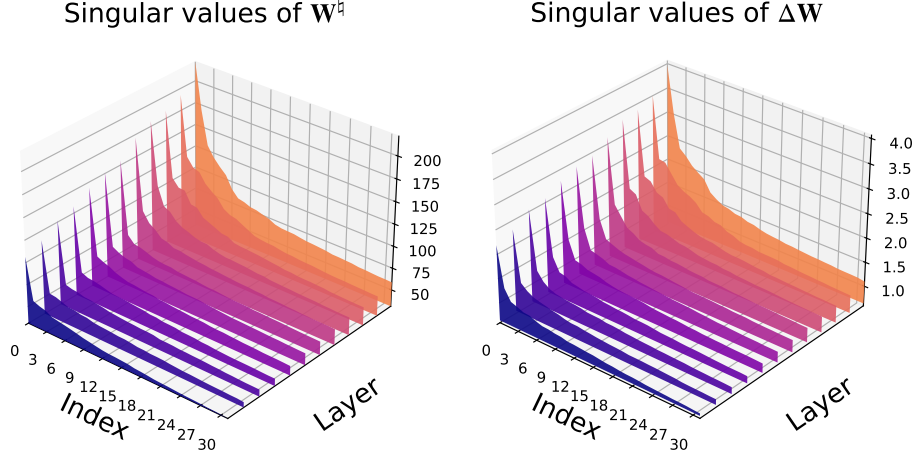


Figure 4: Fine-tuning T5 base model (Raffel et al., 2020) on SST2 from GLUE dataset (Wang, 2018). The experimental details can be found in Appendix F.5. *Left*: top-32 singular values for each pre-trained weight matrices \mathbf{W}^d . *Right*: top-32 singular values for each difference matrices $\Delta\mathbf{W} = \mathbf{W}_{\text{fine-tuned}} - \mathbf{W}^d$ after full fine-tuning. The Index is ranked from the largest to the smallest singular values.

step-size η for convenience:

$$\begin{aligned} \mathbf{A}_{t+1} &= \mathbf{A}_t - \eta \nabla_{\mathbf{A}} \tilde{L}(\mathbf{A}_t, \mathbf{B}_t) \left(\mathbf{B}_t \mathbf{B}_t^\top \right)^{-1}, \\ \mathbf{B}_{t+1} &= \mathbf{B}_t - \eta \left(\mathbf{A}_t^\top \mathbf{A}_t \right)^{-1} \nabla_{\mathbf{B}} \tilde{L}(\mathbf{A}_t, \mathbf{B}_t). \end{aligned} \quad (4.1)$$

Notice that here we use standard matrix inversion since we can prove that \mathbf{A}_t and \mathbf{B}_t stay non-singular across all $t \geq 0$. By denoting $\mathbf{W}_t := \mathbf{W}^d + \mathbf{A}_t \mathbf{B}_t$, we have the gradients

$$\nabla_{\mathbf{A}} \tilde{L}(\mathbf{A}_t, \mathbf{B}_t) = -\mathbf{J}_{\mathbf{W}_t} \mathbf{B}_t^\top, \quad \nabla_{\mathbf{B}} \tilde{L}(\mathbf{A}_t, \mathbf{B}_t) = -\mathbf{A}_t^\top \mathbf{J}_{\mathbf{W}_t},$$

where we define

$$\mathbf{J}_{\mathbf{W}_t} := \frac{1}{N} \tilde{\mathbf{X}}^\top \left[\sigma(\tilde{\mathbf{X}} \tilde{\mathbf{W}}^d) - \frac{1}{N} \tilde{\mathbf{X}}^\top \sigma(\tilde{\mathbf{X}} \mathbf{W}_t) \right] \odot \sigma'(\tilde{\mathbf{X}} \mathbf{W}_t).$$

To deliver the proof, apart from the above-mentioned assumptions in Section 2.1 for the the nonlinear setting, we also need the following additional assumptions.

Assumption 4.1. We assume that \mathbf{W}^d has orthonormal columns and its row space is orthogonal to that of Δ .

Assumption 4.2. We assume that $\|\Delta\|_{op} \leq \frac{\sqrt{2}-1}{2}$ with $\text{Rank}(\Delta) = r^*$ where $k + r^* \leq d$ and $r^* \ll \min\{d, k\}$.

Remark: Assumption 4.1 ensures rich task diversity between pre-trained model and downstream tasks. We notice that such assumption is also considered in Dayi and Chen (2024). Assumption 4.2 restricts the norm of downstream feature shift since the signal of adapted weight is generally smaller than the pre-trained weight. We can empirically assess the validity of this assumption in Fig. 4.

Here we can show that, for the nonlinear model, LoRA training can achieve global linear convergence under (**Spectral-init**) via preconditioned GD in Eq. (4.1).

Theorem 4.3 (Simplified version of Theorem C.10). Under assumptions in Section 2.1 for the nonlinear setting, Assumption 4.1, and 4.2, with training conducted by Eq. (4.1) and initialization via (**Spectral-init**), we take $\epsilon = \mathcal{O}\left(\frac{1}{r^* \kappa \sqrt{d}}\right)$ and $\rho \leq 0.01$ such that we set

$$\gamma \in \left[\frac{1}{c_H} - \frac{\rho}{3c_H \kappa \sqrt{2r^*}}, \frac{1}{c_H} + \frac{\rho}{3c_H \kappa \sqrt{2r^*}} \right] \quad (4.2)$$

with $c_H := \frac{1}{4} + \frac{1}{4\pi} \sum_{\substack{n \geq 1, \\ n \text{ odd}}} 2^{-n} n^{-2} (n!)^{-2}$. Then choosing $\eta \in \left(c_\eta, \frac{1}{2c_H}\right)$ for a small constant $c_\eta > 0$, with probability at least $1 - 2Cdk \exp(-\epsilon^2 N)$ for a universal constant $C > 0$, we have

$$\|\mathbf{A}_t \mathbf{B}_t - \Delta\|_F \leq \left(1 - \frac{c_H}{10} \eta\right)^t \rho \lambda_{r^*}^*, \forall t \geq 0. \quad (4.3)$$

Remark: We make the following remarks:

- This theorem is based on $\|\mathbf{A}_0 \mathbf{B}_0 - \Delta\|_F \leq \rho \lambda_{r^*}^*$ at initialization (Assumption 4.2 is not needed), see Lemma C.5 for details, which demonstrates the ability of one-step full gradient can improve feature learning.
- The final rate is independent of condition number κ of downstream feature shift Δ , which coincides with the results from linear model. This provide us evidence that adding preconditioners can also work for nonlinear model.

Proof Sketch: The complete proof can be found in Appendix C.2.1. By Hermite decomposition, we can compute the expectation of $\mathbf{J}_{\mathbf{W}_t}$ (see Lemma C.2) and decompose $\mathbf{J}_{\mathbf{W}_t}$ into $c_H (\mathbf{A}_t \mathbf{B}_t - \Delta) + \mathbf{\Xi}_t$, where $\mathbf{\Xi}_t$ is defined in Lemma C.6. The first term is the signal term which can dominate the preconditioned GD dynamics. The second term $\mathbf{\Xi}_t := T1 + T2$ consists of two parts (details see Lemma C.7): the first part $T1$ is the higher-order residual terms from $\mathbb{E}_{\tilde{\mathbf{x}}}[\mathbf{J}_{\mathbf{W}_t}]$ which related to Hermite decomposition. Since the decay of Hermite coefficients of σ is faster than polynomial decay, it can be well controlled. For the second term $T2$, it comes from the concentration error of $\mathbf{J}_{\mathbf{W}_t}$, which can also controlled by large sample size N .

To handle $\|\mathbf{A}_t \mathbf{B}_t - \Delta\|_F$, we explore its recursion relationship in Lemma C.6. The key part is to control $\|(\mathbf{I}_d - \mathbf{U}_{\mathbf{A}_t} \mathbf{U}_{\mathbf{A}_t}^\top) \Delta (\mathbf{I}_k - \mathbf{V}_{\mathbf{B}_t} \mathbf{V}_{\mathbf{B}_t}^\top)\|_F$ as well as its complementary part in Lemma C.9 and higher order term in Lemma C.8. We deliver the complete proof to Appendix C.2.1.

Note that the above two assumptions are not required if we modify the gradient update of Eq. (4.1) by removing the mask matrix $\sigma'(\tilde{\mathbf{X}} \mathbf{W}_t)$, a smoothing technique from Kalai and Sastry (2009); Kakade et al. (2011); Wu et al. (2023), i.e.,

$$\mathbf{J}_{\mathbf{W}_t}^{\text{GLM}} := \frac{1}{N} \tilde{\mathbf{X}}^\top \left(\sigma(\tilde{\mathbf{X}} \tilde{\mathbf{W}}^\natural) - \sigma(\tilde{\mathbf{X}} \mathbf{W}_t) \right).$$

In this case, we reformulate Eq. (4.1) as

$$\begin{aligned} \mathbf{A}_{t+1} &= \mathbf{A}_t + \eta \mathbf{J}_{\mathbf{W}_t}^{\text{GLM}} \mathbf{B}_t^\top \left(\mathbf{B}_t \mathbf{B}_t^\top \right)^{-1}, \\ \mathbf{B}_{t+1} &= \mathbf{B}_t + \eta \left(\mathbf{A}_t^\top \mathbf{A}_t \right)^{-1} \mathbf{A}_t^\top \mathbf{J}_{\mathbf{W}_t}^{\text{GLM}}. \end{aligned} \quad (4.4)$$

And we propose to use $\mathbf{G}^\natural := \mathbf{J}_{\mathbf{W}_t}^{\text{GLM}}$ for (Spectral-init) to initialize \mathbf{A}_0 and \mathbf{B}_0 . The global linear convergence results are given as below.

Theorem 4.4 (Simplified version of Theorem C.15). Under assumptions in Section 2.1 for the nonlinear setting, with training conducted by Eq. (4.4) and initialization via (Spectral-init) by taking $\mathbf{G}^\natural := \mathbf{J}_{\mathbf{W}_t}^{\text{GLM}}$, suppose $\epsilon = \mathcal{O}\left(\frac{1}{r^*\kappa\sqrt{d}}\right)$ and $\rho \leq \frac{1}{20}$, we take

$$\gamma \in \left[2 - \frac{2\rho}{3\kappa\sqrt{2r^*}}, 2 + \frac{2\rho}{3\kappa\sqrt{2r^*}}\right],$$

and set $\eta \in (c_\eta^{\text{GLM}}, 1)$ where $c_\eta^{\text{GLM}} > 0$ is a small constant, then with probability at least $1 - 2Cdk \exp(-\epsilon^2 N)$ for a universal constant $C > 0$, we have

$$\|\mathbf{A}_t \mathbf{B}_t - \Delta\|_{\text{F}} \leq \left(1 - \frac{\eta}{4}\right)^t \rho \lambda_{r^*}^*.$$

Remark: Removing the mask matrix $\sigma'(\widetilde{\mathbf{X}}\mathbf{W}_t)$ in Eq. (4.1) allows for better linear convergence performance with $(1 - \eta/4)^t$ than that in Eq. (4.3), albeit without Assumption 4.1, 4.2.

Proof Sketch: The proof strategy is similar to Theorem 4.3. The key difference is that the corresponding Ξ_t under Eq. (4.4) does not have the residual terms from Hermite decomposition. We deliver the complete proof to Appendix C.2.2.

5 Algorithm and Experiments

In this section, we firstly present our algorithm, *LoRA-One*, and compare with previous gradient alignment based algorithm for fine-tuning. Then we evaluate LoRA-One against typical LoRA based algorithms across multiple NLP benchmarks and conduct an ablation study.

Algorithm and Discussion: We formally present our LoRA-One algorithm in Algorithm 1, which is driven by spectral initialization (Spectral-init) (shown in line 4-6) and the pre-condition strategy (shown in line 10-11). To ensure numerical stability, we slightly modify (Spectral-init) in our Algorithm 1 (shown in line 5-6) inspired by the trick in Wang et al. (2024a). This is because $\widetilde{\mathbf{S}}_{\mathbf{G}_t}$ is highly ill-conditioned and numerically unstable, and has some difficulty for hyperparameter search in practice, see the Ablation Study part.

We remark that our initialization strategy in Algorithm 1 (line 4-6) shares some similarity with gradient alignment work, e.g., LoRA-GA (Wang et al., 2024a), LoRA-pro (Wang et al., 2024b), but the mechanisms for gradient alignment differ significantly.

More importantly, the spirit of LoRA-GA might not help recover Δ , as verified by our theory as well as the empirical results in Fig. 2, where LoRA-GA fails to generalize and remain at a high-risk level throughout training. We provide more discussion in Appendix E. Furthermore, we notice that Zhang and Pilanci (2024) propose to add preconditioners to AdamW (Loshchilov, 2017) in the view of stability. In contrast, our focus is on addressing the potential issue of ill-conditioning in the downstream tasks, which is theoretically proven to accelerate convergence, as demonstrated in Theorems 3.6, 4.3 and 4.4.

Experiments on NLU tasks: We evaluate Algorithm 1 on multiple natural language understanding (NLU) benchmarks, e.g., MNLI, SST2, CoLA, QNLI, and MRPC via a comprehensive comparison

Algorithm 1 LoRA-One training for a specific layer

Input: Pre-trained weight \mathbf{W}^{\natural} , batched data $\{\mathcal{D}_t\}_{t=1}^T$, LoRA rank r , LoRA alpha α , loss function L , stable parameter s , damping parameter λ

Initialize:

- 1: Compute $\nabla_{\mathbf{W}}L(\mathbf{W}^{\natural})$
- 2: $d_{\text{in}}, d_{\text{out}} \leftarrow \text{size}(\nabla_{\mathbf{W}}L(\mathbf{W}^{\natural}))$
- 3: $\gamma \leftarrow \frac{\sqrt{d_{\text{out}}}}{s}$
- 4: $\mathbf{U}, \mathbf{S}, \mathbf{V} \leftarrow \text{SVD}(\nabla_{\mathbf{W}}L(\mathbf{W}^{\natural}))$
- 5: $\mathbf{A}_0 \leftarrow \sqrt{\gamma} \cdot \mathbf{U}_{[:,1:r]}$
- 6: $\mathbf{B}_0 \leftarrow \sqrt{\gamma} \cdot \mathbf{V}_{[:,1:r]}^{\top}$
- 7: $\mathbf{W}^{\natural} \leftarrow \mathbf{W}^{\natural} - \frac{\alpha}{\sqrt{r}} \mathbf{A}_0 \mathbf{B}_0$
- 8: Clear $\nabla_{\mathbf{W}}L(\mathbf{W}^{\natural})$

Train:

- 9: **for** $t = 1, \dots, T$ **do**
- 10: Compute preconditioned gradients given \mathcal{D}_t :
 $\mathbf{G}_t^A \leftarrow \nabla_{\mathbf{A}} \tilde{L}(\mathbf{A}_{t-1}, \mathbf{B}_{t-1}) (\mathbf{B}_{t-1} \mathbf{B}_{t-1}^{\top} + \lambda \mathbf{I}_r)^{-1}$
 $\mathbf{G}_t^B \leftarrow (\mathbf{A}_{t-1}^{\top} \mathbf{A}_{t-1} + \lambda \mathbf{I}_r)^{-1} \nabla_{\mathbf{B}} \tilde{L}(\mathbf{A}_{t-1}, \mathbf{B}_{t-1})$
- 11: Update $\mathbf{A}_t, \mathbf{B}_t \leftarrow \text{AdamW}(\mathbf{G}_t^A, \mathbf{G}_t^B)$
- 12: **end for**

Return: $\mathbf{W}^{\natural} + \frac{\alpha}{\sqrt{r}} \mathbf{A}_T \mathbf{B}_T$

with full fine-tuning, LoRA (Hu et al., 2022), LoRA+ (Hayou et al., 2024), Preconditioned LoRA (denoted as P-LoRA) (Zhang and Pilanci, 2024), LoRA-GA (Wang et al., 2024a). More experimental details can be found in Appendix F.2. We use these algorithms to fine-tune T5-base model (Raffel et al., 2020). Table 2 demonstrates the superior performance of our theoretically grounded algorithm LoRA-One.

Experiments on LLM: Apart from NLU tasks, we also fine-tune the Llama 2-7B (Touvron et al., 2023) on two tasks: math and code generation, to evaluate the performance of Algorithm 1. The training and evaluation details are as follows: 1) *Math task*: we fine-tune the model using a 100k subset from MetaMathQA (Yu et al., 2023) and test on GSM8K (Cobbe et al., 2021) evaluation dataset. We take accuracy as the performance metric. 2) *Code Task*: we fine-tune the model using a 100k subset from Code-Feedback (Zheng et al., 2024) and evaluate on HumanEval (Chen et al., 2021a). We take the PASS@1 metric. More experimental details can be found in Appendix F.3. Table 3 shows that our method LoRA-One can achieve the best performance over both datasets. For rank 8, we achieve significant improvements over vanilla LoRA, with a margin of 6.91 on GSM8K and 5.35 on HumanEval. LoRA-One outperforms LoRA-GA over all three ranks with notable improvements, which demonstrates the power of using top- r^* singular subspace as suggested by our theory and the good scalability in high ranks from preconditioning.

Ablation study: We perform two types of ablation study. First, in Table 2, comparing “One-step GD” and “Pre-trained”, we see that one-step full gradient descent significantly improves on pre-training and even performs better than LoRA on CoLA and MRPC. This supports our claim on one-step full gradient.

Second, Fig. 5 compares the accuracy of LoRA-One and LoRA-GA, with and without preconditioners. Our choice of top- r^* singular subspace can be seen to be empirically better than LoRA-GA’s

Table 2: Accuracy comparison on various NLP tasks from GLUE across several typical LoRA based algorithms. Results are reported as accuracy (%) with standard deviations with 3 runs (best in **bold**). The subscript indicates the used rank. “-” on MNLI indicates that the test accuracy remains zero after one-step update, see Appendix F.2 for illustration.

Dataset Size	MNLI 393k	SST-2 67k	CoLA 8.5k	QNLI 105k	MRPC 3.7k
Full	86.33 \pm 0.00	94.75 \pm 0.21	80.70 \pm 0.24	93.19 \pm 0.22	84.56 \pm 0.73
Pre-trained	-	89.79	59.03	49.28	63.48
One-step GD	-	90.48	73.00	69.13	68.38
LoRA ₈	85.30 \pm 0.04	94.04 \pm 0.09	72.84 \pm 1.25	93.02 \pm 0.07	68.38 \pm 0.01
LoRA ₃₂	85.23 \pm 0.11	94.08 \pm 0.05	70.66 \pm 0.41	92.87 \pm 0.05	67.24 \pm 0.58
LoRA ₁₂₈	85.53 \pm 0.13	93.96 \pm 0.05	69.45 \pm 0.25	92.91 \pm 0.13	65.36 \pm 0.31
LoRA+ ₈	85.81 \pm 0.09	93.85 \pm 0.24	77.53 \pm 0.20	93.14 \pm 0.03	74.43 \pm 1.39
LoRA+ ₃₂	85.88 \pm 0.16	94.15 \pm 0.25	79.29 \pm 0.96	93.25 \pm 0.08	79.49 \pm 0.64
LoRA+ ₁₂₈	86.07 \pm 0.15	94.08 \pm 0.30	78.59 \pm 0.73	93.06 \pm 0.23	78.76 \pm 0.12
P-LoRA ₈	85.28 \pm 0.15	93.88 \pm 0.11	79.58 \pm 0.67	93.00 \pm 0.07	83.91 \pm 1.16
P-LoRA ₃₂	85.07 \pm 0.11	94.08 \pm 0.14	76.54 \pm 1.29	93.00 \pm 0.08	79.49 \pm 0.50
P-LoRA ₁₂₈	85.38 \pm 0.11	93.96 \pm 0.24	72.04 \pm 1.89	92.98 \pm 0.06	79.66 \pm 1.44
LoRA-GA ₈	85.70 \pm 0.09	94.11 \pm 0.18	80.57 \pm 0.20	93.18 \pm 0.06	85.29 \pm 0.24
LoRA-GA ₃₂	83.32 \pm 0.10	94.49 \pm 0.32	80.86 \pm 0.23	93.06 \pm 0.14	86.36 \pm 0.42
LoRA-GA ₁₂₈	84.75 \pm 0.06	94.19 \pm 0.14	80.95 \pm 0.35	93.12 \pm 0.11	85.46 \pm 0.23
LoRA-One ₈ (Ours)	85.81 \pm 0.03	94.69 \pm 0.05	81.08 \pm 0.36	93.22 \pm 0.12	86.77 \pm 0.53
LoRA-One ₃₂	86.08 \pm 0.01	94.73 \pm 0.37	81.34 \pm 0.51	93.19 \pm 0.02	87.34 \pm 0.31
LoRA-One ₁₂₈	86.22 \pm 0.08	94.65 \pm 0.19	81.53 \pm 0.36	93.34 \pm 0.11	88.40 \pm 0.70

choice. Moreover, LoRA-One and LoRA-One (-) exhibit comparable performance when the rank is $r = 8$ or $r = 32$. Notably, LoRA-One (-) surpasses LoRA-One in the MRPC task at $r = 8$. These findings suggest that incorporating preconditioners may not be necessary for lower-rank settings. In contrast, for larger ranks ($r = 128$), LoRA-One consistently outperforms LoRA-One (-). Therefore, we recommend using LoRA-One (-) for small-rank cases and LoRA-One for high-rank cases.

Moreover, from Table 4, the performance of LoRA-One (-) is close to Spectral (-), even better for MRPC dataset. This demonstrates the validity of using lines 4–6 in Algorithm 1 for initialization instead of using \mathbf{G}^{\natural} directly for a practical consideration. More details are provided in Appendix F.4.

6 Conclusion

This paper theoretically demonstrates how LoRA can be improved from our theoretical analysis in both linear and nonlinear models: the alignment between LoRA’s gradient update ($\mathbf{A}_t, \mathbf{B}_t$) and the singular subspace of \mathbf{G}^{\natural} , and adding preconditioners. Our theory clarifies some potential issues behind gradient alignment work and the theory-grounded algorithm, LoRA-One, obtains promising performance in practical fine-tuning benchmarks.

Table 3: Performance comparison across different methods on GSM8K, and Human-eval benchmarks. Results are reported as accuracy (%) with standard deviations with 3 runs (higher is better). The subscript indicates the rank of LoRA.

	GSM8K	Human-eval
Full	59.36 \pm 0.85	35.31 \pm 2.13
LoRA ₈	46.89 \pm 0.05	15.67 \pm 0.60
LoRA-GA ₈	53.60 \pm 0.13	20.45 \pm 0.92
LoRA-GA ₃₂	55.12 \pm 0.30	20.18 \pm 0.19
LoRA-GA ₁₂₈	55.07 \pm 0.18	23.05 \pm 0.37
LoRA-One ₈	53.80 \pm 0.44	21.02 \pm 0.01
LoRA-One ₃₂	56.61 \pm 0.29	23.86 \pm 0.01
LoRA-One ₁₂₈	58.10 \pm 0.10	26.79 \pm 0.21

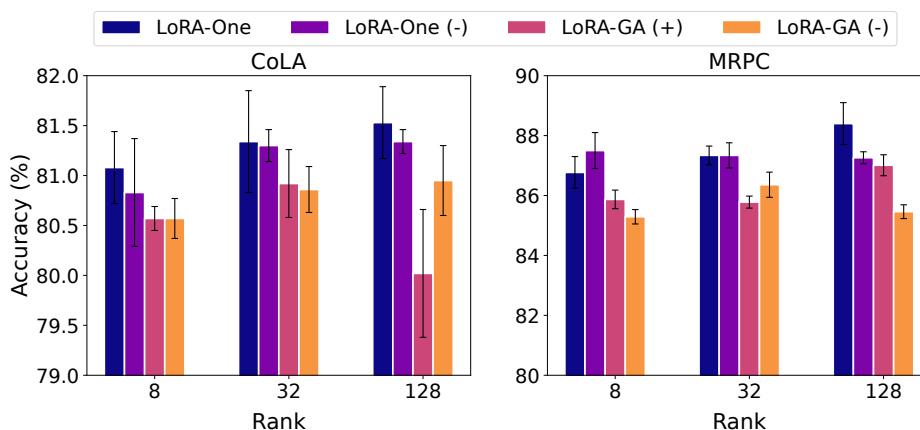


Figure 5: Ablation study of LoRA-One (Algorithm 1), LoRA-One (-) (without preconditioners), LoRA-GA (-) (original LoRA-GA from Wang et al. 2024a), and LoRA-GA (+) (with preconditioners) on CoLA and MRPC from GLUE (Wang, 2018) under ranks $r = 8, 32, 128$.

Table 4: Accuracy comparison across different methods on MRPC and CoLA from GLUE (Wang, 2018) under ranks $r = 8, 32, 128$. LoRA-One (-) stands for training with AdamW without preconditioning under initialization by lines 1–8 in Algorithm 1.

CoLA				MRPC			
r	LoRA-One	LoRA-One (-)	Spectral (-)	r	LoRA-One	LoRA-One (-)	Spectral (-)
8	81.08 \pm 0.36	80.83 \pm 0.54	81.40 \pm 0.31	8	86.77 \pm 0.53	87.50 \pm 0.60	86.19 \pm 0.42
32	81.34 \pm 0.51	81.30 \pm 0.16	81.18 \pm 0.30	32	87.34 \pm 0.31	87.34 \pm 0.42	86.02 \pm 0.20
128	81.53 \pm 0.36	81.34 \pm 0.12	81.62 \pm 0.48	128	88.40 \pm 0.70	87.26 \pm 0.20	86.03 \pm 0.20

Acknowledgment

F. Liu was supported by Royal Society KTP R1 241011 Kan Tong Po Visiting Fellowships. Y. Chen was supported in part by National Science Foundation grants CCF-2233152.

References

- ABBE, E., ADSERA, E. B. and MISIAKIEWICZ, T. (2022). The merged-staircase property: a necessary and nearly sufficient condition for SGD learning of sparse functions on two-layer neural networks. In *Conference on Learning Theory*. PMLR.
- ACHIAM, J., ADLER, S., AGARWAL, S., AHMAD, L., AKKAYA, I., ALEMAN, F. L., ALMEIDA, D., ALTENSCHMIDT, J., ALTMAN, S., ANADKAT, S. ET AL. (2023). GPT-4 technical report. *arXiv preprint arXiv:2303.08774* .
- ALPAYDIN, E. (2020). *Introduction to machine learning*. MIT press.
- AROUS, G. B., GHEISSARI, R. and JAGANNATH, A. (2021). Online stochastic gradient descent on non-convex losses from high-dimensional inference. *Journal of Machine Learning Research* **22** 1–51.
- BIETTI, A., BRUNA, J. and PILLAUD-VIVIEN, L. (2023). On learning gaussian multi-index models with gradient flow. *arXiv preprint arXiv:2310.19793* .
- BROWN, T., MANN, B., RYDER, N., SUBBIAH, M., KAPLAN, J. D., DHARIWAL, P., NEELAKANTAN, A., SHYAM, P., SASTRY, G., ASKELL, A. ET AL. (2020). Language models are few-shot learners. In *Advances in neural information processing systems*.
- CHEN, M., TWOREK, J., JUN, H., YUAN, Q., PINTO, H. P. D. O., KAPLAN, J., EDWARDS, H., BURDA, Y., JOSEPH, N., BROCKMAN, G. ET AL. (2021a). Evaluating large language models trained on code. *arXiv preprint arXiv:2107.03374* .
- CHEN, Y., CHI, Y., FAN, J., MA, C. ET AL. (2021b). Spectral methods for data science: A statistical perspective. *Foundations and Trends® in Machine Learning* **14** 566–806.
- COBBE, K., KOSARAJU, V., BAVARIAN, M., CHEN, M., JUN, H., KAISER, L., PLAPPERT, M., TWOREK, J., HILTON, J., NAKANO, R. ET AL. (2021). Training verifiers to solve math word problems. *arXiv preprint arXiv:2110.14168* .
- DAMIAN, A., LEE, J. and SOLTANOLKOTABI, M. (2022). Neural networks can learn representations with gradient descent. In *Conference on Learning Theory*. PMLR.
- DAYI, A. K. and CHEN, S. (2024). Gradient dynamics for low-rank fine-tuning beyond kernels.
- DING, L., QIN, Z., JIANG, L., ZHOU, J. and ZHU, Z. (2022). A validation approach to over-parameterized matrix and image recovery. *arXiv preprint arXiv:2209.10675* .
- HAYOU, S., GHOSH, N. and YU, B. (2024). LoRA+: Efficient low rank adaptation of large models. *arXiv preprint arXiv:2402.12354* .
- HE, K., ZHANG, X., REN, S. and SUN, J. (2015). Delving deep into rectifiers: Surpassing human-level performance on imagenet classification. In *Proceedings of the IEEE international conference on computer vision*.
- HORN, R. A. and JOHNSON, C. R. (2012). *Matrix analysis*. Cambridge university press.

- HU, E. J., WALLIS, P., ALLEN-ZHU, Z., LI, Y., WANG, S., WANG, L., CHEN, W. ET AL. (2022). LoRA: Low-rank adaptation of large language models. In *International Conference on Learning Representations*.
- JACOT, A., GABRIEL, F. and HONGLER, C. (2018). Neural tangent kernel: Convergence and generalization in neural networks. *Advances in neural information processing systems* **31**.
- JANG, U., LEE, J. D. and RYU, E. K. (2024). LoRA training in the NTK regime has no spurious local minima. In *International Conference on Machine Learning*.
- JIA, X., WANG, H., PENG, J., FENG, X. and MENG, D. (2024). Preconditioning matters: Fast global convergence of non-convex matrix factorization via scaled gradient descent. *Advances in Neural Information Processing Systems* **36**.
- KAKADE, S. M., KANADE, V., SHAMIR, O. and KALAI, A. (2011). Efficient learning of generalized linear and single index models with isotonic regression. *Advances in Neural Information Processing Systems* **24**.
- KALAI, A. T. and SASTRY, R. (2009). The isotron algorithm: High-dimensional isotonic regression. In *COLT*, vol. 1.
- KOPICZKO, D. J., BLANKEVOORT, T. and ASANO, Y. M. (2024). Vera: Vector-based random matrix adaptation. In *The Twelfth International Conference on Learning Representations*.
- LEE, J. D., OKO, K., SUZUKI, T. and WU, D. (2024). Neural network learns low-dimensional polynomials with sgd near the information-theoretic limit. *arXiv preprint arXiv:2406.01581* .
- LI, B., ZHANG, L., MOKHTARI, A. and HE, N. (2024). On the crucial role of initialization for matrix factorization.
- LI, Y., MA, T. and ZHANG, H. (2018). Algorithmic regularization in over-parameterized matrix sensing and neural networks with quadratic activations. In *Conference On Learning Theory*. PMLR.
- LOSHCHILOV, I. (2017). Decoupled weight decay regularization. *arXiv preprint arXiv:1711.05101* .
- LV, K., YANG, Y., LIU, T., GAO, Q., GUO, Q. and QIU, X. (2023). Full parameter fine-tuning for large language models with limited resources. *arXiv preprint arXiv:2306.09782* .
- MA, C., LI, Y. and CHI, Y. (2021). Beyond procrustes: Balancing-free gradient descent for asymmetric low-rank matrix sensing. *IEEE Transactions on Signal Processing* **69** 867–877.
- MALLADI, S., WETTIG, A., YU, D., CHEN, D. and ARORA, S. (2023). A kernel-based view of language model fine-tuning. In *International Conference on Machine Learning*. PMLR.
- MENG, F., WANG, Z. and ZHANG, M. (2024). Pissa: Principal singular values and singular vectors adaptation of large language models. *arXiv preprint arXiv:2404.02948* .
- OJA, E. (1982). Simplified neuron model as a principal component analyzer. *Journal of mathematical biology* **15** 267–273.

- OKO, K., SONG, Y., SUZUKI, T. and WU, D. (2024). Pretrained transformer efficiently learns low-dimensional target functions in-context. *arXiv preprint arXiv:2411.02544* .
- PONKSHE, K., SINGHAL, R., GORBUNOV, E., TUMANOV, A., HORVATH, S. and VEPAKOMMA, P. (2024). Initialization using update approximation is a silver bullet for extremely efficient low-rank fine-tuning. *arXiv preprint arXiv:2411.19557* .
- RAFFEL, C., SHAZEER, N., ROBERTS, A., LEE, K., NARANG, S., MATENA, M., ZHOU, Y., LI, W. and LIU, P. J. (2020). Exploring the limits of transfer learning with a unified text-to-text transformer. *Journal of machine learning research* **21** 1–67.
- SOLTANOLKOTABI, M., STÖGER, D. and XIE, C. (2023). Implicit balancing and regularization: Generalization and convergence guarantees for overparameterized asymmetric matrix sensing. In *The Thirty Sixth Annual Conference on Learning Theory*. PMLR.
- STÖGER, D. and SOLTANOLKOTABI, M. (2021). Small random initialization is akin to spectral learning: Optimization and generalization guarantees for overparameterized low-rank matrix reconstruction. In *Advances in Neural Information Processing Systems*.
- THOPPILAN, R., DE FREITAS, D., HALL, J., SHAZEER, N., KULSHRESHTHA, A., CHENG, H.-T., JIN, A., BOS, T., BAKER, L., DU, Y. ET AL. (2022). Lamda: Language models for dialog applications. *arXiv preprint arXiv:2201.08239* .
- TONG, T., MA, C. and CHI, Y. (2021). Accelerating ill-conditioned low-rank matrix estimation via scaled gradient descent. *Journal of Machine Learning Research* **22** 1–63.
- TOUVRON, H., MARTIN, L., STONE, K., ALBERT, P., ALMAHAIRI, A., BABAEI, Y., BASHLYKOV, N., BATRA, S., BHARGAVA, P., BHOSALE, S. ET AL. (2023). Llama 2: Open foundation and fine-tuned chat models. *arXiv preprint arXiv:2307.09288* .
- VERSHYNIN, R. (2010). Introduction to the non-asymptotic analysis of random matrices. *arXiv preprint arXiv:1011.3027* .
- VERSHYNIN, R. (2018). *High-dimensional probability: An introduction with applications in data science*, vol. 47. Cambridge university press.
- WANG, A. (2018). Glue: A multi-task benchmark and analysis platform for natural language understanding. *arXiv preprint arXiv:1804.07461* .
- WANG, S., YU, L. and LI, J. (2024a). LoRA-GA: Low-rank adaptation with gradient approximation. In *The Thirty-eighth Annual Conference on Neural Information Processing Systems*.
- WANG, Z., LIANG, J., HE, R., WANG, Z. and TAN, T. (2024b). LoRA-Pro: Are low-rank adapters properly optimized? *arXiv preprint arXiv:2407.18242* .
- WEDIN, P.-Å. (1972). Perturbation bounds in connection with singular value decomposition. *BIT Numerical Mathematics* **12** 99–111.
- WU, J., ZOU, D., CHEN, Z., BRAVERMAN, V., GU, Q. and KAKADE, S. M. (2023). Finite-sample analysis of learning high-dimensional single relu neuron. In *International Conference on Machine Learning*. PMLR.

- XIONG, N., DING, L. and DU, S. S. (2023). How over-parameterization slows down gradient descent in matrix sensing: The curses of symmetry and initialization. *arXiv preprint arXiv:2310.01769* .
- XU, X., SHEN, Y., CHI, Y. and MA, C. (2023). The power of preconditioning in overparameterized low-rank matrix sensing. In *International Conference on Machine Learning*. PMLR.
- YU, L., JIANG, W., SHI, H., YU, J., LIU, Z., ZHANG, Y., KWOK, J. T., LI, Z., WELLER, A. and LIU, W. (2023). Metamath: Bootstrap your own mathematical questions for large language models. *arXiv preprint arXiv:2309.12284* .
- ZENG, Y. and LEE, K. (2023). The expressive power of low-rank adaptation. *arXiv preprint arXiv:2310.17513* .
- ZHANG, F. and PILANCI, M. (2024). Riemannian preconditioned lora for fine-tuning foundation models. *arXiv preprint arXiv:2402.02347* .
- ZHANG, G., FATTAHI, S. and ZHANG, R. Y. (2023). Preconditioned gradient descent for overparameterized nonconvex burer–monteiro factorization with global optimality certification. *Journal of Machine Learning Research* **24** 1–55.
- ZHANG, J., FATTAHI, S. and ZHANG, R. Y. (2021). Preconditioned gradient descent for overparameterized nonconvex matrix factorization. *Advances in Neural Information Processing Systems* **34** 5985–5996.
- ZHENG, T., ZHANG, G., SHEN, T., LIU, X., LIN, B. Y., FU, J., CHEN, W. and YUE, X. (2024). Opencodeinterpreter: Integrating code generation with execution and refinement. *arXiv preprint arXiv:2402.14658* .

Contents

A Symbols and Notations	22
B Proofs for Linear Model	23
B.1 Proofs for LoRA under Random Initialization	23
B.1.1 SVD and Schur Decomposition	23
B.1.2 Dynamics of Linear Approximation	26
B.1.3 Alignment to Negative Gradient of Full Fine-tuning	31
B.2 Gradient Descent under Spectral Initialization	36
B.3 Preconditioned Gradient Descent under Spectral Initialization	48
C Proofs for Nonlinear Model	52
C.1 Problem Settings and Spectral Initialization	52
C.1.1 Computation of Full Population Gradients	53
C.1.2 Concentration of Empirical Gradients	58
C.2 LoRA Training under Spectral Initialization	62
C.2.1 Preconditioned Gradient Descent	62
C.2.2 Preconditioned Smoothed-Gradient Descent	75
D Auxiliary Results for Proofs	79
E Discussion on Prior Work Based on Gradient Alignment	81
F Experimental Settings and Additional Results	82
F.1 Small-Scale Experiments	82
F.2 Natural Language Understanding	83
F.3 Experiments on LLM	84
F.4 Ablation Study	84
F.5 Comparison of Singular Values	86

A Symbols and Notations

Symbol	Dimension(s)	Definition
$\mathcal{N}(\boldsymbol{\mu}, \boldsymbol{\sigma})$	-	Multivariate normal distribution with mean vector $\boldsymbol{\mu}$ and covariance matrix $\boldsymbol{\sigma}$
$\mathcal{O}, o, \Omega, \Theta$	-	Bachmann–Landau asymptotic notation
$\ \boldsymbol{w}\ _2$	-	Euclidean norm of vector \boldsymbol{w}
$\ \mathbf{M}\ _{op}$	-	Operator norm of matrix \mathbf{M}
$\ \mathbf{M}\ _F$	-	Frobenius norm of matrix \mathbf{M}
$\langle \boldsymbol{u}, \boldsymbol{v} \rangle$	-	Dot product of vectors \boldsymbol{u} and \boldsymbol{v}
$\mathbf{M} \odot \mathbf{N}$	-	Hadamard product of matrix \mathbf{M} and \mathbf{N}
\mathbf{W}^{\natural}	$\mathbb{R}^{d \times k}$	Pre-trained weight matrix
Δ	$\mathbb{R}^{d \times k}$	Downstream feature shift matrix
$\widetilde{\mathbf{W}}^{\natural}$	$\mathbb{R}^{d \times k}$	Downstream weight matrix $\widetilde{\mathbf{W}}^{\natural} = \mathbf{W}^{\natural} + \Delta$
\mathbf{G}^{\natural}	$\mathbb{R}^{d \times k}$	The initial gradient matrix under full fine-tuning
$\mathbf{A}_t, \mathbf{B}_t$	$\mathbb{R}^{d \times r}, \mathbb{R}^{r \times k}$	Learnable low-rank adapters at step t
$\boldsymbol{w}_i^{\natural}$	\mathbb{R}^d	i^{th} column of pre-trained weight matrix \mathbf{W}^{\natural}
$\widetilde{\boldsymbol{w}}_i^{\natural}$	\mathbb{R}^d	i^{th} column of downstream weight matrix $\widetilde{\mathbf{W}}^{\natural}$
$\boldsymbol{w}_{t,i}$	\mathbb{R}^d	i^{th} column of adapted weight matrix $(\mathbf{W}^{\natural} + \mathbf{A}_t \mathbf{B}_t)$ at step t
Δ_i	\mathbb{R}^d	i^{th} column of downstream feature matrix Δ
$[\mathbf{A}_t \mathbf{B}_t]_i$	\mathbb{R}^d	i^{th} column of the product of adapters $\mathbf{A}_t \mathbf{B}_t$
$\widetilde{\mathbf{X}}$	$\mathbb{R}^{N \times d}$	Downstream data matrix
$\widetilde{\mathbf{Y}}$	$\mathbb{R}^{N \times d}$	Downstream label matrix
$\widetilde{\boldsymbol{x}}_n$	\mathbb{R}^d	n^{th} downstream data point
\mathbf{M}^{-1}	-	Inverse of matrix \mathbf{M}
\mathbf{M}^{\dagger}	-	Pseudo-inverse of matrix \mathbf{M}
$\lambda_i(\mathbf{M})$	\mathbb{R}	i^{th} singular value of matrix \mathbf{M}
λ_i^*	\mathbb{R}	i^{th} singular value of downstream feature shift matrix Δ
$\kappa(\mathbf{M})$	\mathbb{R}	The condition number of matrix \mathbf{M}
κ	\mathbb{R}	The condition number of Δ : $\kappa = \lambda_{\max}^* / \lambda_{\min}^*$
κ^{\natural}	\mathbb{R}	The condition number of \mathbf{G}^{\natural} : $\kappa^{\natural} = \lambda_{\max}(\mathbf{G}^{\natural}) / \lambda_{\min}(\mathbf{G}^{\natural})$
$\mathbf{U}_m(\mathbf{M})$	-	The left singular subspace spanned by the m largest singular values of the input matrix \mathbf{M}
$\mathbf{U}_{m,\perp}(\mathbf{M})$	-	The left singular subspace orthogonal to $\mathbf{U}_m(\mathbf{M})$
$\mathbf{V}_m(\mathbf{M})$	-	The right singular subspace spanned by the m largest singular values of the input matrix \mathbf{M}
$\mathbf{V}_{m,\perp}(\mathbf{M})$	-	The right singular subspace orthogonal to $\mathbf{V}_m(\mathbf{M})$
$\mathbf{U}_{\mathbf{A}}$	-	The left singular matrix of the compact SVD of \mathbf{A}
$\mathbf{U}_{\mathbf{A},\perp}$	-	The corresponding orthogonal complement of $\mathbf{U}_{\mathbf{A}}$
$\mathbf{V}_{\mathbf{A}}$	-	The right singular matrix of the compact SVD of \mathbf{A}
$\mathbf{V}_{\mathbf{A},\perp}$	-	The corresponding orthogonal complement of $\mathbf{V}_{\mathbf{A}}$
$\sigma(\cdot)$	-	ReLU activation function
$\sigma'(\cdot)$	-	The derivative of ReLU activation function
c_j	\mathbb{R}	j^{th} Hermite coefficient of ReLU activation function
$\text{He}_j(\cdot)$	-	j^{th} Hermite polynomial
$\nabla_{\mathbf{W}} f(\mathbf{W})$	-	The gradient matrix of function f w.r.t. input matrix \mathbf{W}
$\widetilde{L}(\mathbf{A}, \mathbf{B})$	-	Loss function under LoRA fine-tuning
$L(\mathbf{W})$	-	Loss function under full fine-tuning
N	-	Number of downstream data
d	-	Input dimension of the data
k	-	Output dimension of the label
η, η_1, η_2	-	Learning rates
α	-	Random initialization scale of low-rank adapter \mathbf{A}_0

Table 7: Essential symbols and notations in this paper.

B Proofs for Linear Model

In Appendix B.1, we deliver the proofs for alignment in Section 3.1. In Appendix B.2, we present the proofs for the main results in Section 3.2 under spectral initialization. In Appendix B.3, we give the proofs for precondition GD in Section 3.3.

B.1 Proofs for LoRA under Random Initialization

Let $\widetilde{\mathbf{X}}$ be the fine-tuned data with $\widetilde{\mathbf{X}} \in \mathbb{R}^{N \times d}$ and the multi-output $\widetilde{\mathbf{Y}} \in \mathbb{R}^{N \times k}$. For simplicity, we define the initial residual error $\widetilde{\mathbf{Y}}_\Delta := \widetilde{\mathbf{Y}} - \widetilde{\mathbf{X}}\mathbf{W}^\natural = \widetilde{\mathbf{X}}\Delta$. Then, denote the negative gradient of Full Fine-tuning after the first step as

$$\mathbf{G}^\natural = -\nabla_{\mathbf{W}} L(\mathbf{W}^\natural) = -\frac{1}{N} \widetilde{\mathbf{X}}^\top (\widetilde{\mathbf{X}}\mathbf{W}^\natural - \widetilde{\mathbf{Y}}) = \frac{1}{N} \widetilde{\mathbf{X}}^\top \widetilde{\mathbf{Y}}_\Delta \in \mathbb{R}^{d \times k}.$$

Recall the gradient update for LoRA

$$\begin{aligned} \mathbf{A}_{t+1} &= \mathbf{A}_t - \frac{\eta_1}{N} \widetilde{\mathbf{X}}^\top \left(\widetilde{\mathbf{X}}(\mathbf{W}^\natural + \mathbf{A}_t \mathbf{B}_t) - \widetilde{\mathbf{Y}} \right) \mathbf{B}_t^\top, \\ \mathbf{B}_{t+1} &= \mathbf{B}_t - \frac{\eta_2}{N} \mathbf{A}_t^\top \widetilde{\mathbf{X}}^\top \left(\widetilde{\mathbf{X}}(\mathbf{W}^\natural + \mathbf{A}_t \mathbf{B}_t) - \widetilde{\mathbf{Y}} \right), \end{aligned}$$

we rewrite it in a compact form

$$\begin{aligned} \begin{bmatrix} \mathbf{A}_{t+1} \\ \mathbf{B}_{t+1}^\top \end{bmatrix} &= \begin{bmatrix} \mathbf{A}_t \\ \mathbf{B}_t^\top \end{bmatrix} + \underbrace{\begin{bmatrix} \mathbf{0} & \eta_1 \mathbf{G}^\natural \\ \eta_2 \mathbf{G}^{\natural\top} & \mathbf{0} \end{bmatrix}}_{:=\mathbf{H}} \begin{bmatrix} \mathbf{A}_t \\ \mathbf{B}_t^\top \end{bmatrix} - \frac{1}{N} \begin{bmatrix} \mathbf{0} & \eta_1 \widetilde{\mathbf{X}}^\top \widetilde{\mathbf{X}} \mathbf{A}_t \mathbf{B}_t \\ \eta_2 \mathbf{B}_t^\top \mathbf{A}_t^\top \widetilde{\mathbf{X}}^\top \widetilde{\mathbf{X}} & \mathbf{0} \end{bmatrix} \begin{bmatrix} \mathbf{A}_t \\ \mathbf{B}_t^\top \end{bmatrix} \\ &= \underbrace{\begin{bmatrix} \mathbf{I}_d & \eta_1 \mathbf{G}^\natural \\ \eta_2 \mathbf{G}^{\natural\top} & \mathbf{I}_k \end{bmatrix}}_{:=\mathbf{H}} \begin{bmatrix} \mathbf{A}_t \\ \mathbf{B}_t^\top \end{bmatrix} - \underbrace{\frac{1}{N} \begin{bmatrix} \mathbf{0} & \eta_1 \widetilde{\mathbf{X}}^\top \widetilde{\mathbf{X}} \mathbf{A}_t \mathbf{B}_t \\ \eta_2 \mathbf{B}_t^\top \mathbf{A}_t^\top \widetilde{\mathbf{X}}^\top \widetilde{\mathbf{X}} & \mathbf{0} \end{bmatrix}}_{:=\widehat{\mathbf{E}}_{t+1}} \begin{bmatrix} \mathbf{A}_t \\ \mathbf{B}_t^\top \end{bmatrix}. \end{aligned} \tag{B.1}$$

By defining a stack iterate

$$\mathbf{Z}_t := \begin{bmatrix} \mathbf{A}_t \\ \mathbf{B}_t^\top \end{bmatrix}, \quad \text{and} \quad \mathbf{Z}_0 := \begin{bmatrix} \mathbf{A}_0 \\ \mathbf{0} \end{bmatrix} \in \mathbb{R}^{(d+k) \times r}, \tag{B.2}$$

we can formulate Eq. (B.1) as a compact form of a nonlinear dynamical system

$$\mathbf{Z}_{t+1} = \mathbf{H} \mathbf{Z}_t - \widehat{\mathbf{E}}_{t+1}, \tag{B.3}$$

where \mathbf{H} is a time-independent matrix corresponding to the linear part, and $\widehat{\mathbf{E}}_{t+1}$ corresponds to the nonlinear part.

B.1.1 SVD and Schur Decomposition

We recall the complete SVD of $\Delta \in \mathbb{R}^{d \times k}$

$$\Delta = \widetilde{\mathbf{U}} \widetilde{\mathbf{S}} \widetilde{\mathbf{V}}^\top = [\mathbf{U} \quad \mathbf{U}_\perp] \begin{bmatrix} \mathbf{S}^* & \mathbf{0}_{r^* \times (k-r^*)} \\ \mathbf{0}_{(d-r^*) \times r^*} & \mathbf{0}_{(d-r^*) \times (k-r^*)} \end{bmatrix} \begin{bmatrix} \mathbf{V}^\top \\ \mathbf{V}_\perp^\top \end{bmatrix}, \quad \text{where } \mathbf{S}^* = \text{Diag}(\lambda_1^*, \dots, \lambda_{r^*}^*).$$

Similarly, we recall the complete SVD of \mathbf{G}^\natural as $\mathbf{G}^\natural = \tilde{\mathbf{U}}_{\mathbf{G}^\natural} \tilde{\mathbf{S}}_{\mathbf{G}^\natural} \tilde{\mathbf{V}}_{\mathbf{G}^\natural}^\top$. We derive the Schur decomposition of \mathbf{H} under the special case $d = k$ in Lemma B.1 and then extend to $d \neq k$ in Lemma B.3 via zero padding on SVD in Lemma B.2.

Lemma B.1 (Schur Decomposition of \mathbf{H} under $d = k$). Under assumptions in Section 2.1 for the linear setting, given $\mathbf{G}^\natural \in \mathbb{R}^{d \times k}$ in Eq. (3.1) and its complete SVD $\tilde{\mathbf{U}}_{\mathbf{G}^\natural} \tilde{\mathbf{S}}_{\mathbf{G}^\natural} \tilde{\mathbf{V}}_{\mathbf{G}^\natural}^\top$, if $d = k$, then the block matrix \mathbf{H} admits the following Schur decomposition

$$\mathbf{H} = \begin{bmatrix} \mathbf{I}_d & \eta_1 \mathbf{G}^\natural \\ \eta_2 (\mathbf{G}^\natural)^\top & \mathbf{I}_d \end{bmatrix} = \mathbf{C} \mathbf{T} \mathbf{C}^\top,$$

where \mathbf{C} is an orthogonal matrix and \mathbf{T} is a block upper triangular matrix

$$\mathbf{C} = \frac{1}{\sqrt{1 + \frac{\eta_2}{\eta_1}}} \begin{bmatrix} \tilde{\mathbf{U}}_{\mathbf{G}^\natural} & -\sqrt{\frac{\eta_2}{\eta_1}} \tilde{\mathbf{U}}_{\mathbf{G}^\natural} \\ \sqrt{\frac{\eta_2}{\eta_1}} \tilde{\mathbf{V}}_{\mathbf{G}^\natural} & \tilde{\mathbf{V}}_{\mathbf{G}^\natural} \end{bmatrix}, \quad \text{and} \quad \mathbf{T} = \begin{bmatrix} \mathbf{I}_d + \sqrt{\eta_1 \eta_2} \tilde{\mathbf{S}}_{\mathbf{G}^\natural} & (\eta_1 - \eta_2) \tilde{\mathbf{S}}_{\mathbf{G}^\natural} \\ \mathbf{0} & \mathbf{I}_d - \sqrt{\eta_1 \eta_2} \tilde{\mathbf{S}}_{\mathbf{G}^\natural} \end{bmatrix}.$$

Proof. We prove by verifying the claim. Starting with

$$\begin{aligned} & \begin{bmatrix} \tilde{\mathbf{U}}_{\mathbf{G}^\natural} & -\sqrt{\frac{\eta_2}{\eta_1}} \tilde{\mathbf{U}}_{\mathbf{G}^\natural} \\ \sqrt{\frac{\eta_2}{\eta_1}} \tilde{\mathbf{V}}_{\mathbf{G}^\natural} & \tilde{\mathbf{V}}_{\mathbf{G}^\natural} \end{bmatrix} \begin{bmatrix} \mathbf{I}_d + \sqrt{\eta_1 \eta_2} \tilde{\mathbf{S}}_{\mathbf{G}^\natural} & (\eta_1 - \eta_2) \tilde{\mathbf{S}}_{\mathbf{G}^\natural} \\ \mathbf{0} & \mathbf{I}_d - \sqrt{\eta_1 \eta_2} \tilde{\mathbf{S}}_{\mathbf{G}^\natural} \end{bmatrix} \\ &= \begin{bmatrix} \tilde{\mathbf{U}}_{\mathbf{G}^\natural} + \sqrt{\eta_1 \eta_2} \tilde{\mathbf{U}}_{\mathbf{G}^\natural} \tilde{\mathbf{S}}_{\mathbf{G}^\natural} & \eta_1 \tilde{\mathbf{U}}_{\mathbf{G}^\natural} \tilde{\mathbf{S}}_{\mathbf{G}^\natural} - \sqrt{\frac{\eta_2}{\eta_1}} \tilde{\mathbf{U}}_{\mathbf{G}^\natural} \\ \sqrt{\frac{\eta_2}{\eta_1}} \tilde{\mathbf{V}}_{\mathbf{G}^\natural} + \eta_2 \tilde{\mathbf{V}}_{\mathbf{G}^\natural} \tilde{\mathbf{S}}_{\mathbf{G}^\natural} & \sqrt{\frac{\eta_2}{\eta_1}} (\eta_1 - \eta_2) \tilde{\mathbf{V}}_{\mathbf{G}^\natural} \tilde{\mathbf{S}}_{\mathbf{G}^\natural} + \tilde{\mathbf{V}}_{\mathbf{G}^\natural} - \sqrt{\eta_1 \eta_2} \tilde{\mathbf{V}}_{\mathbf{G}^\natural} \tilde{\mathbf{S}}_{\mathbf{G}^\natural} \end{bmatrix} =: \mathbf{\Xi}, \end{aligned}$$

then we can verify that

$$\begin{aligned} & \frac{\eta_1}{\eta_1 + \eta_2} \times \mathbf{\Xi} \times \begin{bmatrix} \tilde{\mathbf{U}}_{\mathbf{G}^\natural}^\top & \sqrt{\frac{\eta_2}{\eta_1}} \tilde{\mathbf{V}}_{\mathbf{G}^\natural}^\top \\ -\sqrt{\frac{\eta_2}{\eta_1}} \tilde{\mathbf{U}}_{\mathbf{G}^\natural}^\top & \tilde{\mathbf{V}}_{\mathbf{G}^\natural}^\top \end{bmatrix} \\ &= \frac{\eta_1}{\eta_1 + \eta_2} \times \begin{bmatrix} \left(1 + \frac{\eta_2}{\eta_1}\right) \mathbf{I}_d & (\eta_1 + \eta_2) \tilde{\mathbf{U}}_{\mathbf{G}^\natural} \tilde{\mathbf{S}}_{\mathbf{G}^\natural} \tilde{\mathbf{V}}_{\mathbf{G}^\natural}^\top \\ \eta_2 \left(1 + \frac{\eta_2}{\eta_1}\right) \tilde{\mathbf{V}}_{\mathbf{G}^\natural} \tilde{\mathbf{S}}_{\mathbf{G}^\natural} \tilde{\mathbf{U}}_{\mathbf{G}^\natural}^\top & \left(1 + \frac{\eta_2}{\eta_1}\right) \mathbf{I}_d \end{bmatrix} \\ &= \begin{bmatrix} \mathbf{I}_d & \eta_1 \tilde{\mathbf{U}}_{\mathbf{G}^\natural} \tilde{\mathbf{S}}_{\mathbf{G}^\natural} \tilde{\mathbf{V}}_{\mathbf{G}^\natural}^\top \\ \eta_2 \tilde{\mathbf{V}}_{\mathbf{G}^\natural} \tilde{\mathbf{S}}_{\mathbf{G}^\natural} \tilde{\mathbf{U}}_{\mathbf{G}^\natural}^\top & \mathbf{I}_d \end{bmatrix} = \mathbf{H}. \end{aligned}$$

Accordingly, we conclude the result. □

Next, we consider the case of $d \neq k$.

Case 1 ($d > k$): by zero padding, \mathbf{G}^\natural and related matrices are given by

$$\underline{\mathbf{G}}^\natural = [\mathbf{G}^\natural \quad \mathbf{0}_{d \times (d-k)}], \quad \underline{\mathbf{H}} = \begin{bmatrix} \mathbf{I}_d & \eta_1 \mathbf{G}^\natural \\ \eta_2 (\underline{\mathbf{G}}^\natural)^\top & \mathbf{I}_d \end{bmatrix},$$

and for any $t \geq 0$, we have the following related matrices

$$\underline{\mathbf{B}}_t = [\mathbf{B}_t \quad \mathbf{0}_{r \times (d-k)}], \quad \underline{\mathbf{Z}}_t = \begin{bmatrix} \mathbf{A}_t \\ (\underline{\mathbf{B}}_t)^\top \end{bmatrix}, \quad \tilde{\underline{\mathbf{Z}}}_t = \begin{bmatrix} \mathbf{A}_t^{\text{lin}} \\ (\underline{\mathbf{B}}_t^{\text{lin}})^\top \end{bmatrix} = \underline{\mathbf{H}}^t \underline{\mathbf{Z}}_0.$$

Case 2 ($d < k$): Similarly, by zero padding, we define

$$\underline{\mathbf{G}}^\natural = \begin{bmatrix} \mathbf{G}^\natural \\ \mathbf{0}_{(k-d) \times k} \end{bmatrix}, \quad \underline{\mathbf{H}} = \begin{bmatrix} \mathbf{I}_k & \eta_1 \underline{\mathbf{G}}^\natural \\ \eta_2 (\underline{\mathbf{G}}^\natural)^\top & \mathbf{I}_k \end{bmatrix},$$

and for $\forall t \geq 0$, we define

$$\underline{\mathbf{A}}_t = \begin{bmatrix} \mathbf{A}_t \\ \mathbf{0}_{(k-d) \times r} \end{bmatrix}, \quad \underline{\mathbf{Z}}_t = \begin{bmatrix} \underline{\mathbf{A}}_t \\ (\underline{\mathbf{B}}_t)^\top \end{bmatrix}, \quad \tilde{\underline{\mathbf{Z}}}_t = \begin{bmatrix} \underline{\mathbf{A}}_t^{\text{lin}} \\ (\underline{\mathbf{B}}_t^{\text{lin}})^\top \end{bmatrix} = \underline{\mathbf{H}}^t \underline{\mathbf{Z}}_0.$$

Then we have the following lemma on the SVD of $\underline{\mathbf{G}}^\natural$.

Lemma B.2. If $d > k$, then we have the following SVD of $\underline{\mathbf{G}}^\natural$

$$\underline{\mathbf{G}}^\natural = \tilde{\underline{\mathbf{U}}}_{\mathbf{G}^\natural} \tilde{\underline{\mathbf{S}}}_{\mathbf{G}^\natural} \tilde{\underline{\mathbf{V}}}_{\mathbf{G}^\natural}^\top,$$

where

$$\tilde{\underline{\mathbf{V}}}_{\mathbf{G}^\natural} = \begin{bmatrix} \tilde{\mathbf{V}}_{\mathbf{G}^\natural} & \mathbf{0}_{k \times (d-k)} \\ \mathbf{0}_{(d-k) \times k} & \mathbf{I}_{(d-k)} \end{bmatrix}, \quad \text{and} \quad \tilde{\underline{\mathbf{S}}}_{\mathbf{G}^\natural} = \begin{bmatrix} \tilde{\mathbf{S}}_{\mathbf{G}^\natural} & \mathbf{0}_{d \times (d-k)} \end{bmatrix}.$$

If $d < k$, then we have the following SVD of $\underline{\mathbf{G}}^\natural$

$$\underline{\mathbf{G}}^\natural = \tilde{\underline{\mathbf{U}}}_{\mathbf{G}^\natural} \tilde{\underline{\mathbf{S}}}_{\mathbf{G}^\natural} \tilde{\underline{\mathbf{V}}}_{\mathbf{G}^\natural}^\top,$$

where

$$\tilde{\underline{\mathbf{U}}}_{\mathbf{G}^\natural} = \begin{bmatrix} \tilde{\mathbf{U}}_{\mathbf{G}^\natural} & \mathbf{0}_{k \times (k-d)} \\ \mathbf{0}_{(k-d) \times k} & \mathbf{I}_{(k-d)} \end{bmatrix}, \quad \text{and} \quad \tilde{\underline{\mathbf{S}}}_{\mathbf{G}^\natural} = \begin{bmatrix} \tilde{\mathbf{S}}_{\mathbf{G}^\natural} \\ \mathbf{0}_{(k-d) \times k} \end{bmatrix}.$$

Proof. The block construction does not affect the original part of the SVD. It only appends zeros to the singular values and grows the corresponding orthonormal bases as partial identity matrices appropriately. \square

Now we can apply Lemma B.2 for Lemma B.1 to extend to $d \neq k$ via the following lemma. The proof is direct and we omit it here.

Lemma B.3 (Schur decomposition of \mathbf{H} under $d \neq k$). Given the defined block matrix $\underline{\mathbf{H}} \in \mathbb{R}^{2s \times 2s}$ with $s := \max\{d, k\}$, we have the following decomposition

$$\underline{\mathbf{H}} = \underline{\mathbf{C}} \underline{\mathbf{T}} \underline{\mathbf{C}}^\top,$$

If $d > k$,

$$\mathbf{C} = \frac{1}{\sqrt{1 + \frac{\eta_2}{\eta_1}}} \begin{bmatrix} \tilde{\mathbf{U}}_{\mathbf{G}^\natural} & -\sqrt{\frac{\eta_2}{\eta_1}} \tilde{\mathbf{U}}_{\mathbf{G}^\natural} \\ \sqrt{\frac{\eta_2}{\eta_1}} \tilde{\mathbf{V}}_{\mathbf{G}^\natural} & \tilde{\mathbf{V}}_{\mathbf{G}^\natural} \end{bmatrix}, \quad \mathbf{T} = \begin{bmatrix} \mathbf{I}_d + \sqrt{\eta_1 \eta_2} \tilde{\mathbf{S}}_{\mathbf{G}^\natural} & (\eta_1 - \eta_2) \tilde{\mathbf{S}}_{\mathbf{G}^\natural} \\ \mathbf{0} & \mathbf{I}_d - \sqrt{\eta_1 \eta_2} \tilde{\mathbf{S}}_{\mathbf{G}^\natural} \end{bmatrix}.$$

If $d < k$,

$$\mathbf{C} = \frac{1}{\sqrt{1 + \frac{\eta_2}{\eta_1}}} \begin{bmatrix} \tilde{\mathbf{U}}_{\mathbf{G}^\natural} & -\sqrt{\frac{\eta_2}{\eta_1}} \tilde{\mathbf{U}}_{\mathbf{G}^\natural} \\ \sqrt{\frac{\eta_2}{\eta_1}} \tilde{\mathbf{V}}_{\mathbf{G}^\natural} & \tilde{\mathbf{V}}_{\mathbf{G}^\natural} \end{bmatrix}, \quad \mathbf{T} = \begin{bmatrix} \mathbf{I}_k + \sqrt{\eta_1 \eta_2} \tilde{\mathbf{S}}_{\mathbf{G}^\natural} & (\eta_1 - \eta_2) \tilde{\mathbf{S}}_{\mathbf{G}^\natural} \\ \mathbf{0} & \mathbf{I}_k - \sqrt{\eta_1 \eta_2} \tilde{\mathbf{S}}_{\mathbf{G}^\natural} \end{bmatrix}.$$

B.1.2 Dynamics of Linear Approximation

The target of our proof is to demonstrate that $\hat{\mathbf{E}}_{t+1}$ does not effect the dynamics too much such that the dynamics of \mathbf{Z}_t is close to the following pseudo iterate

$$\mathbf{Z}_t^{\text{lin}} := \mathbf{H}^t \mathbf{Z}_0 =: \begin{bmatrix} \mathbf{A}_t^{\text{lin}} \\ (\mathbf{B}_t^{\text{lin}})^\top \end{bmatrix}. \quad (\text{B.4})$$

The updates of the pseudo iterate follow the trajectory of Oja's Power Method (Oja, 1982). Therefore, we aim to prove that the error between the actual iterate \mathbf{Z}_t and the pseudo iterate $\mathbf{Z}_t^{\text{lin}}$ is sufficiently small, which is equivalent to that the actual iterate \mathbf{Z}_t performs a power iteration during the early steps. First, we obtain the difference between \mathbf{Z}_t and $\mathbf{Z}_t^{\text{lin}}$ by the following lemma.

Lemma B.4 (Formulation of \mathbf{E}_t). Under assumptions in Section 2.1 for the linear setting, given the nonlinear dynamical system (B.3) and its linear part (B.4), their difference admits

$$\mathbf{E}_t := \mathbf{Z}_t - \mathbf{Z}_t^{\text{lin}} = - \sum_{i=1}^t \mathbf{H}^{t-i} \hat{\mathbf{E}}_i, \quad \forall t \in \mathbb{N}^+, \quad (\text{B.5})$$

where $\hat{\mathbf{E}}_i$ corresponds to the nonlinear part in Eq. (B.1).

Proof of Lemma B.4. We prove it by induction. Recall the formulation of the nonlinear dynamical system $\mathbf{Z}_{t+1} = \mathbf{H} \mathbf{Z}_t - \hat{\mathbf{E}}_{t+1}$, we start with the base case $t = 1$ such that

$$\mathbf{Z}_1 = \mathbf{H} \mathbf{Z}_0 - \hat{\mathbf{E}}_1 = \tilde{\mathbf{Z}}_1 - \hat{\mathbf{E}}_1,$$

which proves the claim. Next, we assume Eq. (B.5) holds for $t \geq 2$, then for $t + 1$, we have

$$\begin{aligned} \mathbf{Z}_{t+1} &= \mathbf{H} \mathbf{Z}_t - \hat{\mathbf{E}}_{t+1} \\ &= \mathbf{H} \left(\mathbf{Z}_t^{\text{lin}} - \sum_{i=1}^t \mathbf{H}^{t-i} \hat{\mathbf{E}}_i \right) - \hat{\mathbf{E}}_{t+1} \\ &= \mathbf{Z}_{t+1}^{\text{lin}} - \sum_{i=1}^t \mathbf{H}^{t+1-i} \hat{\mathbf{E}}_i - \hat{\mathbf{E}}_{t+1} \\ &= \mathbf{Z}_{t+1}^{\text{lin}} - \sum_{i=1}^{t+1} \mathbf{H}^{t+1-i} \hat{\mathbf{E}}_i, \end{aligned}$$

which proves the claim. \square

If $\|\mathbf{E}_t\|_{op}$ is sufficiently small within a certain period, e.g., $t \leq T$, then we could approximate the early dynamics by

$$\mathbf{Z}_{t+1} := \begin{bmatrix} \mathbf{A}_{t+1} \\ \mathbf{B}_{t+1}^\top \end{bmatrix} \approx \mathbf{Z}_t^{\text{lin}} := \begin{bmatrix} \mathbf{A}_{t+1}^{\text{lin}} \\ (\mathbf{B}_{t+1}^{\text{lin}})^\top \end{bmatrix} = \begin{bmatrix} \mathbf{A}_t^{\text{lin}} \\ (\mathbf{B}_t^{\text{lin}})^\top \end{bmatrix} + \begin{bmatrix} \mathbf{0} & \eta_1 \mathbf{G}^\natural \\ \eta_2 \mathbf{G}^\natural^\top & \mathbf{0} \end{bmatrix} \begin{bmatrix} \mathbf{A}_t^{\text{lin}} \\ (\mathbf{B}_t^{\text{lin}})^\top \end{bmatrix},$$

via

$$\left\| \begin{bmatrix} \mathbf{A}_t \\ \mathbf{B}_t^\top \end{bmatrix} - \begin{bmatrix} \mathbf{A}_t^{\text{lin}} \\ (\mathbf{B}_t^{\text{lin}})^\top \end{bmatrix} \right\|_{op} \leq \|\mathbf{E}_t\|_{op}.$$

In this subsection, we will bound $\|\mathbf{E}_t\|_{op}$ to show that it is actually small up to the initialization. To prove it, we first conduct the dynamical analysis of $\mathbf{Z}_t^{\text{lin}}$ via the structure of \mathbf{H} .

Part I: Dynamics of $\mathbf{Z}_t^{\text{lin}}$

With the algebra fact above, we can derive the precise spectral dynamics of $\mathbf{Z}_t^{\text{lin}}$, i.e., $\mathbf{A}_t^{\text{lin}}$ and $\mathbf{B}_t^{\text{lin}}$ separately.

Lemma B.5. Under assumptions in Section 2.1 for the linear setting, given the pseudo iterate (B.4) on $\mathbf{Z}_t^{\text{lin}}$, where two components $\mathbf{A}_t^{\text{lin}}$ and $\mathbf{B}_t^{\text{lin}}$ admit the following recursion

$$\begin{cases} \mathbf{A}_t^{\text{lin}} = \frac{1}{2} \tilde{\mathbf{U}}_{\mathbf{G}^\natural} \underbrace{\left((\mathbf{I}_d + \sqrt{\eta_1 \eta_2} \tilde{\mathbf{S}}_{\mathbf{G}^\natural})^t + (\mathbf{I}_d - \sqrt{\eta_1 \eta_2} \tilde{\mathbf{S}}_{\mathbf{G}^\natural})^t \right)}_{:= \mathbf{P}_t^{\mathbf{A}}} \tilde{\mathbf{U}}_{\mathbf{G}^\natural}^\top \mathbf{A}_0, \\ (\mathbf{B}_t^{\text{lin}})^\top = \frac{1}{2} \sqrt{\frac{\eta_2}{\eta_1}} \tilde{\mathbf{V}}_{\mathbf{G}^\natural} \underbrace{\left((\mathbf{I}_d + \sqrt{\eta_1 \eta_2} \tilde{\mathbf{S}}_{\mathbf{G}^\natural})^t - (\mathbf{I}_d - \sqrt{\eta_1 \eta_2} \tilde{\mathbf{S}}_{\mathbf{G}^\natural})^t \right)}_{:= \mathbf{P}_t^{\mathbf{B}}} \tilde{\mathbf{U}}_{\mathbf{G}^\natural}^\top \mathbf{A}_0. \end{cases}$$

Furthermore, if $\tilde{\mathbf{X}}^\top \tilde{\mathbf{X}}$ is non-singular, $\mathbf{P}_t^{\mathbf{A}}$ is a full rank matrix and singular values are 1 after the r^* -th order. $\mathbf{P}_t^{\mathbf{B}}$ is a rank- r^* matrix.

Proof. We start with the special case $d = k$ and then discuss the case of $d \neq k$. For the case of $d = k$, we have

$$\mathbf{Z}_t^{\text{lin}} = \mathbf{H}^t \mathbf{Z}_0 = (\mathbf{C} \mathbf{T} \mathbf{C}^\top)^t \mathbf{Z}_0 = \mathbf{C} \mathbf{T}^t \mathbf{C}^\top \mathbf{Z}_0,$$

where the last equality follows from the fact that \mathbf{C} is an orthogonal matrix. Next, we compute \mathbf{T}^t

$$\mathbf{T}^t = \begin{bmatrix} \left(\mathbf{I}_d + \sqrt{\eta_1 \eta_2} \tilde{\mathbf{S}}_{\mathbf{G}^\natural} \right)^t & \underbrace{(\eta_1 - \eta_2) \tilde{\mathbf{S}}_{\mathbf{G}^\natural} \left(\sum_{j=0}^{t-1} \left(\mathbf{I}_d - \sqrt{\eta_1 \eta_2} \tilde{\mathbf{S}}_{\mathbf{G}^\natural} \right)^{t-j-1} \left(\mathbf{I}_d + \sqrt{\eta_1 \eta_2} \tilde{\mathbf{S}}_{\mathbf{G}^\natural} \right)^j \right)}_{:= \mathbf{D}^t} \\ \mathbf{0}_{d \times d} & \left(\mathbf{I}_d - \sqrt{\eta_1 \eta_2} \tilde{\mathbf{S}}_{\mathbf{G}^\natural} \right)^t \end{bmatrix}. \quad (\text{B.6})$$

We first deal with the upper-right part \mathbf{D}^t . It is a mix of several diagonal matrices under addition and multiplications, leading to be a diagonal matrix again, i.e., $\mathbf{D}_{(i,j)}^t = 0, \forall i \neq j$. Note that the diagonal matrix $\tilde{\mathbf{S}}_{\mathbf{G}^\natural}$ is a rank- r^* matrix, we have $\mathbf{D}_{(i,i)}^t = 0$ for $(r^* + 1) \leq i \leq d$. Accordingly, we only need to handle $\mathbf{D}_{(i,i)}^t$ in the $1 \leq i \leq r^*$ part

$$\begin{aligned} \mathbf{D}_{(i,i)}^t &= (\eta_1 - \eta_2) \sigma_i^* \left(\sum_{j=0}^{t-1} (1 - \sqrt{\eta_1 \eta_2} \sigma_i^*)^{t-j-1} (1 + \sqrt{\eta_1 \eta_2} \sigma_i^*)^j \right) \\ &= (\eta_1 - \eta_2) \sigma_i^* \frac{(1 + \sqrt{\eta_1 \eta_2} \sigma_i^*)^t - (1 - \sqrt{\eta_1 \eta_2} \sigma_i^*)^t}{2\sqrt{\eta_1 \eta_2} \sigma_i^*} \\ &= \frac{\eta_1 - \eta_2}{2\sqrt{\eta_1 \eta_2}} \left((1 + \sqrt{\eta_1 \eta_2} \sigma_i^*)^t - (1 - \sqrt{\eta_1 \eta_2} \sigma_i^*)^t \right), \end{aligned}$$

where we use $\sum_{j=0}^{t-1} x^{t-j-1} y^j = \frac{x^t - y^t}{x - y}$. Therefore, we can conclude

$$\mathbf{T}^t = \begin{bmatrix} \left(\mathbf{I}_d + \sqrt{\eta_1 \eta_2} \tilde{\mathbf{S}}_{\mathbf{G}^\natural} \right)^t & \frac{\eta_1 - \eta_2}{2\sqrt{\eta_1 \eta_2}} \left(\left(\mathbf{I}_d + \sqrt{\eta_1 \eta_2} \tilde{\mathbf{S}}_{\mathbf{G}^\natural} \right)^t - \left(\mathbf{I}_d - \sqrt{\eta_1 \eta_2} \tilde{\mathbf{S}}_{\mathbf{G}^\natural} \right)^t \right) \\ \mathbf{0}_{d \times d} & \left(\mathbf{I}_d - \sqrt{\eta_1 \eta_2} \tilde{\mathbf{S}}_{\mathbf{G}^\natural} \right)^t \end{bmatrix}.$$

Finally, we can derive the following recursion

$$\begin{aligned} \mathbf{Z}_t^{\text{lin}} &= \mathbf{H}^t \mathbf{Z}_0 \\ &= \frac{1}{\sqrt{1 + \frac{\eta_2}{\eta_1}}} \begin{bmatrix} \tilde{\mathbf{U}}_{\mathbf{G}^\natural} & -\sqrt{\frac{\eta_2}{\eta_1}} \tilde{\mathbf{U}}_{\mathbf{G}^\natural} \\ \sqrt{\frac{\eta_2}{\eta_1}} \tilde{\mathbf{V}}_{\mathbf{G}^\natural} & \tilde{\mathbf{V}}_{\mathbf{G}^\natural} \end{bmatrix} \\ &\quad \times \begin{bmatrix} \left(\mathbf{I}_d + \sqrt{\eta_1 \eta_2} \tilde{\mathbf{S}}_{\mathbf{G}^\natural} \right)^t & \frac{\eta_1 - \eta_2}{2\sqrt{\eta_1 \eta_2}} \left(\left(\mathbf{I}_d + \sqrt{\eta_1 \eta_2} \tilde{\mathbf{S}}_{\mathbf{G}^\natural} \right)^t - \left(\mathbf{I}_d - \sqrt{\eta_1 \eta_2} \tilde{\mathbf{S}}_{\mathbf{G}^\natural} \right)^t \right) \\ \mathbf{0}_{d \times d} & \left(\mathbf{I}_d - \sqrt{\eta_1 \eta_2} \tilde{\mathbf{S}}_{\mathbf{G}^\natural} \right)^t \end{bmatrix} \mathbf{C}^\top \mathbf{Z}_0 \\ &= \begin{bmatrix} \tilde{\mathbf{U}}_{\mathbf{G}^\natural} \left(\mathbf{I}_d + \sqrt{\eta_1 \eta_2} \tilde{\mathbf{S}}_{\mathbf{G}^\natural} \right)^t & \frac{\eta_1 - \eta_2}{2\sqrt{\eta_1 \eta_2}} \tilde{\mathbf{U}}_{\mathbf{G}^\natural} \left(\mathbf{I}_d + \sqrt{\eta_1 \eta_2} \tilde{\mathbf{S}}_{\mathbf{G}^\natural} \right)^t - \frac{1}{2} \left(\sqrt{\frac{\eta_1}{\eta_2}} + \sqrt{\frac{\eta_2}{\eta_1}} \right) \tilde{\mathbf{U}}_{\mathbf{G}^\natural} \left(\mathbf{I}_d - \sqrt{\eta_1 \eta_2} \tilde{\mathbf{S}}_{\mathbf{G}^\natural} \right)^t \\ \sqrt{\frac{\eta_2}{\eta_1}} \tilde{\mathbf{V}}_{\mathbf{G}^\natural} \left(\mathbf{I}_d + \sqrt{\eta_1 \eta_2} \tilde{\mathbf{S}}_{\mathbf{G}^\natural} \right)^t & \frac{1}{2} \left(1 - \frac{\eta_2}{\eta_1} \right) \tilde{\mathbf{V}}_{\mathbf{G}^\natural} \left(\mathbf{I}_d + \sqrt{\eta_1 \eta_2} \tilde{\mathbf{S}}_{\mathbf{G}^\natural} \right)^t + \frac{1}{2} \left(1 + \frac{\eta_2}{\eta_1} \right) \tilde{\mathbf{V}}_{\mathbf{G}^\natural} \left(\mathbf{I}_d - \sqrt{\eta_1 \eta_2} \tilde{\mathbf{S}}_{\mathbf{G}^\natural} \right)^t \end{bmatrix} \\ &\quad \times \frac{\mathbf{C}^\top \mathbf{Z}_0}{\sqrt{1 + \frac{\eta_2}{\eta_1}}} \\ &= \begin{bmatrix} \frac{1}{2} \tilde{\mathbf{U}}_{\mathbf{G}^\natural} \left(\left(\mathbf{I}_d + \sqrt{\eta_1 \eta_2} \tilde{\mathbf{S}}_{\mathbf{G}^\natural} \right)^t + \left(\mathbf{I}_d - \sqrt{\eta_1 \eta_2} \tilde{\mathbf{S}}_{\mathbf{G}^\natural} \right)^t \right) \tilde{\mathbf{U}}_{\mathbf{G}^\natural}^\top & * \\ \frac{1}{2} \sqrt{\frac{\eta_2}{\eta_1}} \tilde{\mathbf{V}}_{\mathbf{G}^\natural} \left(\left(\mathbf{I}_d + \sqrt{\eta_1 \eta_2} \tilde{\mathbf{S}}_{\mathbf{G}^\natural} \right)^t - \left(\mathbf{I}_d - \sqrt{\eta_1 \eta_2} \tilde{\mathbf{S}}_{\mathbf{G}^\natural} \right)^t \right) \tilde{\mathbf{U}}_{\mathbf{G}^\natural}^\top & * \end{bmatrix} \begin{bmatrix} \mathbf{A}_0 \\ \mathbf{0} \end{bmatrix} \\ &= \begin{bmatrix} \frac{1}{2} \tilde{\mathbf{U}}_{\mathbf{G}^\natural} \left(\left(\mathbf{I}_d + \sqrt{\eta_1 \eta_2} \tilde{\mathbf{S}}_{\mathbf{G}^\natural} \right)^t + \left(\mathbf{I}_d - \sqrt{\eta_1 \eta_2} \tilde{\mathbf{S}}_{\mathbf{G}^\natural} \right)^t \right) \tilde{\mathbf{U}}_{\mathbf{G}^\natural}^\top \mathbf{A}_0 \\ \frac{1}{2} \sqrt{\frac{\eta_2}{\eta_1}} \tilde{\mathbf{V}}_{\mathbf{G}^\natural} \left(\left(\mathbf{I}_d + \sqrt{\eta_1 \eta_2} \tilde{\mathbf{S}}_{\mathbf{G}^\natural} \right)^t - \left(\mathbf{I}_d - \sqrt{\eta_1 \eta_2} \tilde{\mathbf{S}}_{\mathbf{G}^\natural} \right)^t \right) \tilde{\mathbf{U}}_{\mathbf{G}^\natural}^\top \mathbf{A}_0 \end{bmatrix}. \end{aligned}$$

Next, we extend the results above to $d \neq k$. Here we take $d > k$,

$$\begin{aligned} \underline{\mathbf{B}}_t^{\text{lin}} &= \frac{1}{2} \sqrt{\frac{\eta_2}{\eta_1}} \tilde{\mathbf{V}}_{\mathbf{G}^\natural} \left(\left(\mathbf{I}_d + \sqrt{\eta_1 \eta_2} \tilde{\mathbf{S}}_{\mathbf{G}^\natural} \right)^t - \left(\mathbf{I}_d - \sqrt{\eta_1 \eta_2} \tilde{\mathbf{S}}_{\mathbf{G}^\natural} \right)^t \right) \tilde{\mathbf{U}}_{\mathbf{G}^\natural}^\top \mathbf{A}_0 \\ &= \left[\frac{1}{2} \sqrt{\frac{\eta_2}{\eta_1}} \tilde{\mathbf{V}}_{\mathbf{G}^\natural} \left(\left(\mathbf{I}_d + \sqrt{\eta_1 \eta_2} \tilde{\mathbf{S}}_{\mathbf{G}^\natural} \right)^t - \left(\mathbf{I}_d - \sqrt{\eta_1 \eta_2} \tilde{\mathbf{S}}_{\mathbf{G}^\natural} \right)^t \right) \tilde{\mathbf{U}}_{\mathbf{G}^\natural}^\top \mathbf{A}_0 \quad \mathbf{0}_{r \times (d-k)} \right], \end{aligned}$$

which proves the claim. Lastly, we take $d < k$,

$$\begin{aligned} \underline{\mathbf{A}}_t^{\text{lin}} &= \frac{1}{2} \tilde{\mathbf{U}}_{\mathbf{G}^\natural} \left(\left(\mathbf{I}_k + \sqrt{\eta_1 \eta_2} \tilde{\mathbf{S}}_{\mathbf{G}^\natural} \right)^t + \left(\mathbf{I}_k - \sqrt{\eta_1 \eta_2} \tilde{\mathbf{S}}_{\mathbf{G}^\natural} \right)^t \right) \tilde{\mathbf{U}}_{\mathbf{G}^\natural}^\top \mathbf{A}_0 \\ &\quad \left[\begin{array}{c} \frac{1}{2} \tilde{\mathbf{U}}_{\mathbf{G}^\natural} \left(\left(\mathbf{I}_d + \sqrt{\eta_1 \eta_2} \tilde{\mathbf{S}}_{\mathbf{G}^\natural} \right)^t + \left(\mathbf{I}_d - \sqrt{\eta_1 \eta_2} \tilde{\mathbf{S}}_{\mathbf{G}^\natural} \right)^t \right) \tilde{\mathbf{U}}_{\mathbf{G}^\natural}^\top \mathbf{A}_0 \\ \mathbf{0}_{(k-d) \times r} \end{array} \right], \end{aligned}$$

which completes the proof.

Besides, we discuss about some properties of $\mathbf{P}_t^{\mathbf{A}}$ and $\mathbf{P}_t^{\mathbf{B}}$. Recall $\text{Rank}(\mathbf{G}^\natural) = \text{Rank}(\Delta) = r^*$, then we have

$$\lambda_{r^*+i}(\mathbf{P}_t^{\mathbf{A}}) = \frac{1}{2} \lambda_{r^*+i} \left(\left(\mathbf{I}_d + \sqrt{\eta_1 \eta_2} \tilde{\mathbf{S}}_{\mathbf{G}^\natural} \right)^t + \left(\mathbf{I}_d - \sqrt{\eta_1 \eta_2} \tilde{\mathbf{S}}_{\mathbf{G}^\natural} \right)^t \right) = 1, \quad \text{for } \forall 1 \leq i \leq (d - r^*).$$

That means $\mathbf{P}_t^{\mathbf{A}} \in \mathbb{R}^{d \times d}$ is a full rank matrix and the singular values are 1 after the r^* -th order. However $\mathbf{P}_t^{\mathbf{B}} \in \mathbb{R}^{k \times k}$ is a rank- r^* matrix. □

Part II: Control $\|\mathbf{E}_t\|_{op}$

Based on the above results, we are ready to prove that $\|\mathbf{E}_t\|_{op}$ is small.

Lemma B.6. Under assumptions in Section 2.1 for the linear setting, with LoRA initialization (**LoRA-init**), given $\|\mathbf{A}_0\|_{op}$ and \mathbf{G}^\natural in Eq. (3.1) and its largest singular value $\lambda_1(\mathbf{G}^\natural)$, consider the following time period

$$t \leq t^* := \frac{\ln \left(\frac{\lambda_1(\mathbf{G}^\natural)}{6 \zeta(\eta_1, \eta_2) \|\mathbf{A}_0\|_{op}^2} \right)}{3 \ln \left(1 + \sqrt{\eta_1 \eta_2} \lambda_1(\mathbf{G}^\natural) \right)},$$

where $\zeta(\eta_1, \eta_2)$ is a function of η_1, η_2 defined as

$$\zeta(\eta_1, \eta_2) := \max \left\{ 1, \frac{1}{2} \sqrt{\frac{\eta_2}{\eta_1}} \right\} \times \max \left\{ \left(\sqrt{\frac{\eta_2}{\eta_1}} + \frac{1}{2} \right), \left(\sqrt{\frac{\eta_1}{\eta_2}} + \sqrt{\frac{\eta_2}{\eta_1}} \right) \right\}, \quad (\text{B.7})$$

then the following statement holds with probability at least $1 - 2C \exp(-N)$ for a universal constant C over random Gaussian data

$$\|\mathbf{E}_t\|_{op} \leq \|\mathbf{A}_0\|_{op}. \quad (\text{B.8})$$

Remark: By choosing proper random initialization variance over \mathbf{A}_0 , we can ensure $t^* > 1$ to avoid vacuous upper bound.

Proof. We will prove by induction. Starting from $t = 0$, this is trivially true since $\mathbf{Z}_0 = \mathbf{Z}_0^{\text{lin}}$. Next,

we assume Eq. (B.8) holds for $t - 1$ with $t \geq 1$ and prove $\|\mathbf{E}_t\|_{op} \leq \|\mathbf{A}_0\|_{op}$. To deliver the proof, denote $a_0 := \|\mathbf{A}_0\|_{op}$, from Lemma B.5, we know that

$$\|\mathbf{A}_{t-1}^{\text{lin}}\|_{op} \leq \left(1 + \sqrt{\eta_1 \eta_2} \lambda_1(\mathbf{G}^\natural)\right)^{t-1} a_0, \quad \|\mathbf{B}_{t-1}^{\text{lin}}\|_{op} \leq \frac{1}{2} \sqrt{\frac{\eta_1}{\eta_2}} \left(1 + \sqrt{\eta_1 \eta_2} \lambda_1(\mathbf{G}^\natural)\right)^{t-1} a_0. \quad (\text{B.9})$$

Besides, since $(\mathbf{A}_t - \mathbf{A}_t^{\text{lin}})$ and $(\mathbf{B}_t - \mathbf{B}_t^{\text{lin}})$ are the sub-matrices of the error term \mathbf{E}_t , our condition $\|\mathbf{E}_{t-1}\|_{op} \leq \|\mathbf{A}_0\|_{op}$ we have

$$\|\mathbf{A}_{t-1} - \mathbf{A}_{t-1}^{\text{lin}}\|_{op} \leq \|\mathbf{E}_{t-1}\|_{op}, \quad \|\mathbf{B}_{t-1} - \mathbf{B}_{t-1}^{\text{lin}}\|_{op} \leq \|\mathbf{E}_{t-1}\|_{op}. \quad (\text{B.10})$$

It implies that

$$\begin{aligned} \|\mathbf{A}_{t-1}\|_{op} &\leq \left(1 + \sqrt{\eta_1 \eta_2} \lambda_1(\mathbf{G}^\natural)\right)^{t-1} a_0 + \|\mathbf{E}_{t-1}\|_{op}, \\ \|\mathbf{B}_{t-1}\|_{op} &\leq \frac{1}{2} \sqrt{\frac{\eta_1}{\eta_2}} \left(1 + \sqrt{\eta_1 \eta_2} \lambda_1(\mathbf{G}^\natural)\right)^{t-1} a_0 + \|\mathbf{E}_{t-1}\|_{op}. \end{aligned} \quad (\text{B.11})$$

Besides, according to covariance matrix estimation in the operator norm in Lemma D.1, with probability at least $1 - 2C \exp(-N\epsilon^2)$ for a universal constant $C > 0$, we have (taking $\epsilon = 1$)

$$\left\| \frac{1}{N} \widetilde{\mathbf{X}}^\top \widetilde{\mathbf{X}} - \mathbf{I}_d \right\|_{op} \leq \epsilon = 1. \quad (\text{B.12})$$

Accordingly, with probability at least $1 - 2C \exp(-N)$, $\|\widehat{\mathbf{E}}_t\|_{op}$ can be upper bounded by

$$\begin{aligned} \|\widehat{\mathbf{E}}_t\|_{op} &\leq \eta_1 \left\| \frac{1}{N} \widetilde{\mathbf{X}}^\top \widetilde{\mathbf{X}} \mathbf{A}_{t-1} \mathbf{B}_{t-1} \mathbf{B}_{t-1}^\top \right\|_{op} + \eta_2 \left\| \mathbf{B}_{t-1}^\top \mathbf{A}_{t-1}^\top \frac{1}{N} \widetilde{\mathbf{X}}^\top \widetilde{\mathbf{X}} \mathbf{A}_{t-1} \right\|_{op} \\ &\leq \eta_1 (1 + \epsilon) \|\mathbf{A}_{t-1}\|_{op} \|\mathbf{B}_{t-1}\|_{op}^2 + \eta_2 (1 + \epsilon) \|\mathbf{A}_{t-1}\|_{op}^2 \|\mathbf{B}_{t-1}\|_{op} \quad [\text{using Eq. (B.12)}] \\ &\leq (1 + \epsilon) (\|\mathbf{A}_{t-1}^{\text{lin}}\|_{op} + \|\mathbf{E}_{t-1}\|_{op}) (\|\mathbf{B}_{t-1}^{\text{lin}}\|_{op} + \|\mathbf{E}_{t-1}\|_{op}) \times \\ &\quad (\eta_1 \|\mathbf{B}_{t-1}^{\text{lin}}\|_{op} + \eta_2 \|\mathbf{A}_{t-1}^{\text{lin}}\|_{op} + (\eta_1 + \eta_2) \|\mathbf{E}_{t-1}\|_{op}) \quad [\text{using Eq. (B.10)}] \\ &\leq (1 + \epsilon) \sqrt{\eta_1 \eta_2} \left(\left(1 + \sqrt{\eta_1 \eta_2} \lambda_1(\mathbf{G}^\natural)\right)^{t-1} a_0 + \|\mathbf{E}_{t-1}\|_{op} \right) \quad [\text{using Eq. (B.11)}] \\ &\quad \times \left(\frac{1}{2} \sqrt{\frac{\eta_2}{\eta_1}} \left(1 + \sqrt{\eta_1 \eta_2} \lambda_1(\mathbf{G}^\natural)\right)^{t-1} a_0 + \|\mathbf{E}_{t-1}\|_{op} \right) \\ &\quad \times \left(\left(\sqrt{\frac{\eta_2}{\eta_1}} + \frac{1}{2} \right) \left(1 + \sqrt{\eta_1 \eta_2} \lambda_1(\mathbf{G}^\natural)\right)^{t-1} a_0 + \left(\sqrt{\frac{\eta_1}{\eta_2}} + \sqrt{\frac{\eta_2}{\eta_1}} \right) \|\mathbf{E}_{t-1}\|_{op} \right) \\ &\leq (1 + \epsilon) \underbrace{\max \left\{ 1, \frac{1}{2} \sqrt{\frac{\eta_2}{\eta_1}} \right\} \times \max \left\{ \left(\sqrt{\frac{\eta_2}{\eta_1}} + \frac{1}{2} \right), \left(\sqrt{\frac{\eta_1}{\eta_2}} + \sqrt{\frac{\eta_2}{\eta_1}} \right) \right\}}_{:=\zeta(\eta_1, \eta_2)} \times \\ &\quad \left(\left(1 + \sqrt{\eta_1 \eta_2} \lambda_1(\mathbf{G}^\natural)\right)^{t-1} a_0 + \|\mathbf{E}_{t-1}\|_{op} \right)^3 \\ &\leq 4(1 + \epsilon) \sqrt{\eta_1 \eta_2} \zeta(\eta_1, \eta_2) \left(\left(1 + \sqrt{\eta_1 \eta_2} \lambda_1(\mathbf{G}^\natural)\right)^{3t-3} a_0^3 + \|\mathbf{E}_{t-1}\|_{op}^3 \right) \\ &\leq 12 \sqrt{\eta_1 \eta_2} \zeta(\eta_1, \eta_2) \left(1 + \sqrt{\eta_1 \eta_2} \lambda_1(\mathbf{G}^\natural)\right)^{3t-3} a_0^3. \quad [\text{from our inductive hypothesis}] \end{aligned}$$

Then, by Lemma B.4, we can conclude that

$$\begin{aligned}
\|\mathbf{E}_t\|_{op} &= \left\| \sum_{i=1}^t \mathbf{H}^{t-i} \widehat{\mathbf{E}}_i \right\|_{op} \leq \sum_{i=1}^t \|\mathbf{H}\|_{op}^{t-i} \|\widehat{\mathbf{E}}_i\|_{op} \\
&\leq 12\sqrt{\eta_1\eta_2} \zeta(\eta_1, \eta_2) a_0^3 \times \sum_{i=1}^t \left(1 + \sqrt{\eta_1\eta_2} \lambda_1(\mathbf{G}^\natural)\right)^{t+2i-3} \quad \text{[using Lemma B.1]} \\
&= 12\sqrt{\eta_1\eta_2} \zeta(\eta_1, \eta_2) a_0^3 \times \left(1 + \sqrt{\eta_1\eta_2} \lambda_1(\mathbf{G}^\natural)\right)^{t-1} \sum_{i=1}^t \left(1 + \sqrt{\eta_1\eta_2} \lambda_1(\mathbf{G}^\natural)\right)^{2i-2} \\
&= 12\sqrt{\eta_1\eta_2} \zeta(\eta_1, \eta_2) a_0^3 \times \left(1 + \sqrt{\eta_1\eta_2} \lambda_1(\mathbf{G}^\natural)\right)^{t-1} \frac{\left(1 + \sqrt{\eta_1\eta_2} \lambda_1(\mathbf{G}^\natural)\right)^{2t} - 1}{\left(1 + \sqrt{\eta_1\eta_2} \lambda_1(\mathbf{G}^\natural)\right)^2 - 1} \\
&\quad \text{[geometric series]} \\
&\leq 12\sqrt{\eta_1\eta_2} \zeta(\eta_1, \eta_2) a_0^3 \times \left(1 + \sqrt{\eta_1\eta_2} \lambda_1(\mathbf{G}^\natural)\right)^{t-1} \frac{\left(1 + \sqrt{\eta_1\eta_2} \lambda_1(\mathbf{G}^\natural)\right)^{2t+1}}{2\sqrt{\eta_1\eta_2} \lambda_1(\mathbf{G}^\natural)} \\
&\leq 6\zeta(\eta_1, \eta_2) \left(1 + \sqrt{\eta_1\eta_2} \lambda_1(\mathbf{G}^\natural)\right)^{3t} \frac{a_0^3}{\lambda_1(\mathbf{G}^\natural)}. \tag{B.13}
\end{aligned}$$

Accordingly, when $t \leq t^* := \frac{\ln\left(\frac{\lambda_1(\mathbf{G}^\natural)}{6\zeta(\eta_1, \eta_2)\|\mathbf{A}_0\|_{op}^2}\right)}{3\ln\left(1 + \sqrt{\eta_1\eta_2} \lambda_1(\mathbf{G}^\natural)\right)}$, we have

$$\|\mathbf{E}_t\|_{op} \leq \|\mathbf{A}_0\|_{op},$$

which proves the claim. \square

B.1.3 Alignment to Negative Gradient of Full Fine-tuning

Now we can apply Lemma B.6 to obtain

$$\|\mathbf{A}_t - \mathbf{A}_t^{\text{1in}}\|_{op} \leq \|\mathbf{A}_0\|_{op}.$$

Recall Lemma B.5, we can observe that the dynamic of $\mathbf{A}_t^{\text{1in}}$ also follows an Oja's Power Method (Oja, 1982), which aligns $\mathbf{A}_t^{\text{1in}}$'s left singular subspace to the left subspace of the initial negative gradient step \mathbf{G}^\natural of full fine-tuning. We anticipate that $\lambda_{r^*}(\mathbf{A}_t) \gg \lambda_{r^*+1}(\mathbf{A}_t)$ for sufficiently large t . Furthermore, if $\|\mathbf{E}_t\|_{op}$ remains small, then the top- r^* left singular subspace of \mathbf{A}_t can closely align to \mathbf{G}^\natural 's. To prove this alignment, we modify Stöger and Soltanolkotabi (2021, Lemma 8.3) to obtain the following results.

Lemma B.7. Under assumptions in Section 2.1 for the linear setting, recall

$$\mathbf{P}_t^{\mathbf{A}} := \frac{1}{2} \tilde{\mathbf{U}}_{\mathbf{G}^\natural} \left(\left(\mathbf{I}_d + \sqrt{\eta_1\eta_2} \tilde{\mathbf{S}}_{\mathbf{G}^\natural} \right)^t + \left(\mathbf{I}_d - \sqrt{\eta_1\eta_2} \tilde{\mathbf{S}}_{\mathbf{G}^\natural} \right)^t \right) \tilde{\mathbf{U}}_{\mathbf{G}^\natural}^\top$$

as an $\mathbb{R}^{d \times d}$ -valued symmetric matrix in Lemma B.5, we assume that

$$\lambda_{r^*+1}(\mathbf{P}_t^{\mathbf{A}}) \|\mathbf{A}_0\|_{op} + \|\mathbf{E}_t\|_{op} < \lambda_{r^*}(\mathbf{P}_t^{\mathbf{A}}) \lambda_{\min}(\mathbf{U}_{r^*}^\top(\mathbf{P}_t^{\mathbf{A}})\mathbf{A}_0),$$

that can be satisfied under certain conditions (discussed later). Then the following three inequalities hold:

$$\lambda_{r^*}(\mathbf{P}_t^{\mathbf{A}} \mathbf{A}_0 + \mathbf{E}_t) \geq \lambda_{r^*}(\mathbf{P}_t^{\mathbf{A}}) \lambda_{\min}(\mathbf{U}_{r^*}^{\top}(\mathbf{P}_t^{\mathbf{A}}) \mathbf{A}_0) - \|\mathbf{E}_t\|_{op}, \quad (\text{B.14})$$

$$\lambda_{r^*+1}(\mathbf{P}_t^{\mathbf{A}} \mathbf{A}_0 + \mathbf{E}_t) \leq \lambda_{r^*+1}(\mathbf{P}_t^{\mathbf{A}}) \|\mathbf{A}_0\|_{op} + \|\mathbf{E}_t\|_{op}, \quad (\text{B.15})$$

$$\|\mathbf{U}_{r^*,\perp}^{\top}(\mathbf{P}_t^{\mathbf{A}}) \mathbf{U}_{r^*}(\mathbf{P}_t^{\mathbf{A}} \mathbf{A}_0 + \mathbf{E}_t)\|_{op} \leq \frac{\lambda_{r^*+1}(\mathbf{P}_t^{\mathbf{A}}) \|\mathbf{A}_0\|_{op} + \|\mathbf{E}_t\|_{op}}{\lambda_{r^*}(\mathbf{P}_t^{\mathbf{A}}) \lambda_{\min}(\mathbf{U}_{r^*}^{\top}(\mathbf{P}_t^{\mathbf{A}}) \mathbf{A}_0) - \lambda_{r^*+1}(\mathbf{P}_t^{\mathbf{A}}) \|\mathbf{A}_0\|_{op} - \|\mathbf{E}_t\|_{op}}, \quad (\text{B.16})$$

where $\mathbf{U}_k(\mathbf{M})$ denotes the left singular subspace spanned by the k largest singular values of the input matrix \mathbf{M} and $\mathbf{U}_{k,\perp}(\mathbf{M})$ denotes the left singular subspace orthogonal to $\mathbf{U}_k(\mathbf{M})$.

This lemma can help us derive the principle angle of the left singular subspace between $\mathbf{A}_t^{\text{lin}}$ and \mathbf{A}_t . Note that the assumption comes from the necessary condition of Wedin's $\sin \theta$ theorem (Wedin, 1972). In the next lemma, we aim to derive the time threshold which can fulfill this assumption.

Lemma B.8. Under assumptions in Section 2.1 for the linear setting, given $\|\mathbf{A}_0\|_{op}$, for any $\theta \in (0, 1)$, taking

$$t \leq \frac{\ln\left(\frac{8\|\mathbf{A}_0\|_{op}}{\theta \lambda_{\min}(\mathbf{U}_{r^*}^{\top}(\mathbf{P}_t^{\mathbf{A}}) \mathbf{A}_0)}\right)}{\ln\left(1 + \sqrt{\eta_1 \eta_2} \lambda_{r^*}(\mathbf{G}^{\natural})\right)},$$

then Eq. (B.16) holds with probability at least $1 - 2C \exp(-N)$ for a universal constant C over random Gaussian data, i.e.

$$\|\mathbf{U}_{r^*,\perp}^{\top}(\mathbf{P}_t^{\mathbf{A}}) \mathbf{U}_{r^*}(\mathbf{P}_t^{\mathbf{A}} \mathbf{A}_0 + \mathbf{E}_t)\|_{op} \leq \theta.$$

Remark: To ensure that the θ -alignment phase still falls into the early phase in Lemma B.6 for $\|\mathbf{E}_t\|_{op} \leq \|\mathbf{A}_0\|_{op}$, we need to choose proper initialization for \mathbf{A}_0 . We will detail this in Theorem 3.2 later.

Proof. First, $\lambda_{r^*}(\mathbf{P}_t^{\mathbf{A}})$ in Lemma B.5 can be lower bounded by

$$\begin{aligned} \lambda_{r^*}(\mathbf{P}_t^{\mathbf{A}}) &= \frac{1}{2} \lambda_{r^*} \left((\mathbf{I}_d + \sqrt{\eta_1 \eta_2} \tilde{\mathbf{S}}_{\mathbf{G}^{\natural}})^t + (\mathbf{I}_d - \sqrt{\eta_1 \eta_2} \tilde{\mathbf{S}}_{\mathbf{G}^{\natural}})^t \right) \\ &\geq \frac{1}{2} \lambda_{r^*} \left((\mathbf{I}_d + \sqrt{\eta_1 \eta_2} \tilde{\mathbf{S}}_{\mathbf{G}^{\natural}})^t \right) \\ &= \frac{1}{2} \left(1 + \sqrt{\eta_1 \eta_2} \lambda_{r^*}(\mathbf{G}^{\natural}) \right)^t. \end{aligned} \quad (\text{B.17})$$

Recall Lemma B.5, we have $\lambda_{r^*+1}(\mathbf{P}_t^{\mathbf{A}}) = 1$ and Lemma B.6 with $\|\mathbf{E}_t\|_{op} \leq \|\mathbf{A}_0\|_{op}$, we define the following threshold γ and upper bound it

$$\begin{aligned} \gamma &:= \frac{\lambda_{r^*+1}(\mathbf{P}_t^{\mathbf{A}}) \|\mathbf{A}_0\|_{op} + \|\mathbf{E}_t\|_{op}}{\lambda_{r^*}(\mathbf{P}_t^{\mathbf{A}}) \lambda_{\min}(\mathbf{U}_{r^*}^{\top}(\mathbf{P}_t^{\mathbf{A}}) \mathbf{A}_0)} \\ &\leq \frac{2\|\mathbf{A}_0\|_{op}}{\frac{1}{2} \left(1 + \sqrt{\eta_1 \eta_2} \lambda_{r^*}(\mathbf{G}^{\natural}) \right)^t \lambda_{\min}(\mathbf{U}_{r^*}^{\top}(\mathbf{P}_t^{\mathbf{A}}) \mathbf{A}_0)} \quad [\text{using Lemma B.5, B.6}] \\ &= \exp\left(-\ln\left(1 + \sqrt{\eta_1 \eta_2} \lambda_{r^*}(\mathbf{G}^{\natural})\right) \cdot t\right) \cdot \frac{4\|\mathbf{A}_0\|_{op}}{\lambda_{\min}(\mathbf{U}_{r^*}^{\top}(\mathbf{P}_t^{\mathbf{A}}) \mathbf{A}_0)}. \end{aligned} \quad (\text{B.18})$$

Set $\theta \in (0, 1)$, let Eq.(B.18) $\leq \frac{\theta}{2}$, then we have that

$$\|\mathbf{U}_{r^*, \perp}^\top (\mathbf{P}_t^{\mathbf{A}}) \mathbf{U}_{r^*} (\mathbf{P}_t^{\mathbf{A}} \mathbf{A}_0 + \mathbf{E}_t)\|_{op} \leq \theta.$$

The time t to achieve this angle θ can be upper bounded by

$$\exp\left(-\ln\left(1 + \sqrt{\eta_1 \eta_2} \lambda_{r^*}(\mathbf{G}^{\natural})\right) \cdot t\right) \cdot \frac{4\|\mathbf{A}_0\|_{op}}{\lambda_{\min}(\mathbf{U}_{r^*}^\top (\mathbf{P}_t^{\mathbf{A}}) \mathbf{A}_0)} \leq \frac{\theta}{2},$$

which implies that

$$t \leq \frac{\ln\left(\frac{8\|\mathbf{A}_0\|_{op}}{\theta \lambda_{\min}(\mathbf{U}_{r^*}^\top (\mathbf{P}_t^{\mathbf{A}}) \mathbf{A}_0)}\right)}{\ln\left(1 + \sqrt{\eta_1 \eta_2} \lambda_{r^*}(\mathbf{G}^{\natural})\right)}.$$

Finally we conclude the proof. \square

Theorem B.9. [Full version of Theorem 3.2] Under assumptions in Section 2.1 for the linear setting, recall \mathbf{G}^{\natural} defined in Eq. (3.1) with its condition number κ^{\natural} , we consider random Gaussian initialization $\mathbf{A}_0 \in \mathbb{R}^{d \times r}$ with $[\mathbf{A}_0]_{ij} \sim \mathcal{N}(0, \alpha^2)$ in (LoRA-init), for any $\theta \in (0, 1)$, let $\xi = o(1)$ be chosen such that

$$\alpha \leq \begin{cases} \left(\frac{\theta \xi}{24r\sqrt{d}}\right)^{\frac{3\kappa^{\natural}}{2}} \sqrt{\frac{\lambda_1(\mathbf{G}^{\natural})}{54d\zeta(\eta_1, \eta_2)}} & \text{if } r^* \leq r < 2r^*, \\ \left(\frac{\theta}{24\sqrt{d}}\right)^{\frac{3\kappa^{\natural}}{2}} \sqrt{\frac{\lambda_1(\mathbf{G}^{\natural})}{54d\zeta(\eta_1, \eta_2)}} & \text{if } r \geq 2r^*, \end{cases}$$

where $\zeta(\eta_1, \eta_2)$ is defined in Eq. (B.7) and satisfies $\zeta(\eta_1, \eta_2) = \Theta(1)$. Then if we run gradient descent for t^* steps with

$$t^* \lesssim \begin{cases} \frac{\ln\left(\frac{24r\sqrt{d}}{\theta \xi}\right)}{\ln\left(1 + \sqrt{\eta_1 \eta_2} \lambda_{r^*}(\mathbf{G}^{\natural})\right)} & \text{if } r^* \leq r < 2r^*, \\ \frac{\ln\left(\frac{24\sqrt{d}}{\theta}\right)}{\ln\left(1 + \sqrt{\eta_1 \eta_2} \lambda_{r^*}(\mathbf{G}^{\natural})\right)} & \text{if } r \geq 2r^*, \end{cases}$$

we have the following alignment on the left singular subspace between \mathbf{G}^{\natural} and \mathbf{A}_{t^*}

$$\left\| \mathbf{U}_{r^*, \perp}^\top (\mathbf{G}^{\natural}) \mathbf{U}_{r^*} (\mathbf{A}_{t^*}) \right\|_{op} \lesssim \theta,$$

$$\text{with probability at least } \begin{cases} 1 - C_1 \exp(-d) - (C_2 \xi)^{r-r^*+1} - C_3 \exp(-r) - C \exp(-N) & \text{if } r^* \leq r < 2r^*, \\ 1 - C_4 \exp(-d) - C_5 \exp(-r) - C \exp(-N) & \text{if } r \geq 2r^*, \end{cases}$$

for some positive constants $C, C_1, C_2, C_3, C_4, C_5$. Here $\mathbf{U}_{r^*}(\mathbf{A}_{t^*})$ denotes the left singular subspace spanned by the r^* largest singular values of \mathbf{A}_{t^*} and $\mathbf{U}_{r^*, \perp}(\mathbf{M})$ denotes the left singular subspace orthogonal to $\mathbf{U}_{r^*}(\mathbf{M})$. Note that we can select any pair of stepsizes (η_1, η_2) that satisfies the conditions $t^* > 1$, $\eta_2 \geq \eta_1$, and $\zeta(\eta_1, \eta_2) = \Theta(1)$.

Proof. For ease of description, we denote $\mathbf{A}_0 := \alpha \mathbf{T} \in \mathbb{R}^{d \times r}$ where \mathbf{T} is a standard random Gaussian matrix with zero-mean and unit variance. Here we aim to choose a proper α to ensure that

θ -alignment phase in Lemma B.8 still falls into the early phase in Lemma B.6, i.e.

$$\begin{aligned}
& \frac{\ln\left(\frac{8\|\mathbf{A}_0\|_{op}}{\theta\lambda_{\min}(\mathbf{U}_{r^*}^\top(\mathbf{P}_t^{\mathbf{A}})\mathbf{A}_0)}\right)}{\ln\left(1+\sqrt{\eta_1\eta_2}\lambda_{r^*}(\mathbf{G}^\natural)\right)} = \frac{\ln\left(\frac{\lambda_1(\mathbf{G}^\natural)}{6\zeta(\eta_1,\eta_2)\|\mathbf{A}_0\|_{op}^2}\right)}{3\ln\left(1+\sqrt{\eta_1\eta_2}\lambda_1(\mathbf{G}^\natural)\right)} = t^* \\
\Leftrightarrow & \ln\left(\frac{8\|\mathbf{A}_0\|_{op}}{\theta\lambda_{\min}(\mathbf{U}_{r^*}^\top(\mathbf{P}_t^{\mathbf{A}})\mathbf{A}_0)}\right) = \frac{\ln\left(1+\sqrt{\eta_1\eta_2}\lambda_{r^*}(\mathbf{G}^\natural)\right)}{3\ln\left(1+\sqrt{\eta_1\eta_2}\lambda_1(\mathbf{G}^\natural)\right)} \ln\left(\frac{\lambda_1(\mathbf{G}^\natural)}{6\zeta(\eta_1,\eta_2)\|\mathbf{A}_0\|_{op}^2}\right) \\
\Leftrightarrow & \frac{8\|\mathbf{A}_0\|_{op}}{\theta\lambda_{\min}(\mathbf{U}_{r^*}^\top(\mathbf{P}_t^{\mathbf{A}})\mathbf{A}_0)} = \left(\frac{\lambda_1(\mathbf{G}^\natural)}{6\zeta(\eta_1,\eta_2)\|\mathbf{A}_0\|_{op}^2}\right)^{\frac{\ln\left(1+\sqrt{\eta_1\eta_2}\lambda_{r^*}(\mathbf{G}^\natural)\right)}{3\ln\left(1+\sqrt{\eta_1\eta_2}\lambda_1(\mathbf{G}^\natural)\right)}} \\
\Leftrightarrow & \theta = \frac{8\|\mathbf{A}_0\|_{op}}{\lambda_{\min}(\mathbf{U}_{r^*}^\top(\mathbf{P}_t^{\mathbf{A}})\mathbf{A}_0)} \left(\frac{6\zeta(\eta_1,\eta_2)\|\mathbf{A}_0\|_{op}^2}{\lambda_1(\mathbf{G}^\natural)}\right)^{\frac{\ln\left(1+\sqrt{\eta_1\eta_2}\lambda_{r^*}(\mathbf{G}^\natural)\right)}{3\ln\left(1+\sqrt{\eta_1\eta_2}\lambda_1(\mathbf{G}^\natural)\right)}} \\
& = \frac{8\|\mathbf{T}\|_{op}}{\lambda_{\min}(\mathbf{U}_{r^*}^\top(\mathbf{P}_t^{\mathbf{A}})\mathbf{T})} \left(\frac{6\zeta(\eta_1,\eta_2)\|\mathbf{T}\|_{op}^2}{\lambda_1(\mathbf{G}^\natural)}\right)^\iota \alpha^{2\iota}. \quad \left[\text{by setting } \iota := \frac{\ln\left(1+\sqrt{\eta_1\eta_2}\lambda_{r^*}(\mathbf{G}^\natural)\right)}{3\ln\left(1+\sqrt{\eta_1\eta_2}\lambda_1(\mathbf{G}^\natural)\right)}\right]
\end{aligned}$$

In the next, we will discuss how to pick up α . According to Lemma D.3, we need to consider the following two cases on the relationship between r^* and r .

Case 1. $r^* \leq r < 2r^*$: by Lemma D.2 and Lemma D.3, with probability at least $1 - C_1 \exp(-d) - (C_2\xi)^{r-r^*+1} - C_3 \exp(-r)$ for some positive constants C_1, C_2, C_3 , we have

$$\frac{\|\mathbf{T}\|_{op}}{3\sqrt{d}} \leq 1, \quad \frac{\xi}{r\lambda_{\min}(\mathbf{U}_{r^*}^\top(\mathbf{P}_t^{\mathbf{A}})\mathbf{T})} \lesssim 1. \quad (\text{B.19})$$

Here we pick

$$\alpha \leq \left(\frac{\theta\xi}{24r\sqrt{d}}\right)^{\frac{3\kappa^\natural}{2}} \sqrt{\frac{\lambda_1(\mathbf{G}^\natural)}{54\zeta(\eta_1,\eta_2)d}},$$

then recall Lemma B.8 on the alignment, we take α here

$$\begin{aligned}
& \left\| \mathbf{U}_{r^*}^\top \left(-\nabla_{\mathbf{W}} \tilde{L}(\mathbf{W}^\natural) \right) \mathbf{U}_{r^*}(\mathbf{A}_{t^*}) \right\|_{op} \\
& \leq \frac{8\|\mathbf{T}\|_{op}}{\lambda_{\min}(\mathbf{U}_{r^*}^\top(\mathbf{P}_t^{\mathbf{A}})\mathbf{T})} \left(\frac{6\zeta(\eta_1,\eta_2)\|\mathbf{S}\|_{op}^2}{\lambda_1(\mathbf{G}^\natural)}\right)^\iota \alpha^{2\iota} \\
& = \frac{8\|\mathbf{T}\|_{op}}{\lambda_{\min}(\mathbf{U}_{r^*}^\top(\mathbf{P}_t^{\mathbf{A}})\mathbf{T})} \left(\frac{6\zeta(\eta_1,\eta_2)\|\mathbf{S}\|_{op}^2}{\lambda_1(\mathbf{G}^\natural)}\right)^\iota \left(\frac{\theta\xi}{24r\sqrt{d}}\right)^{3\kappa^\natural\iota} \left(\frac{\lambda_1(\mathbf{G}^\natural)}{54\zeta(\eta_1,\eta_2)d}\right)^\iota \\
& = \frac{8\|\mathbf{T}\|_{op}}{\lambda_{\min}(\mathbf{U}_{r^*}^\top(\mathbf{P}_t^{\mathbf{A}})\mathbf{T})} \left(\frac{\|\mathbf{T}\|_{op}^2}{9d}\right)^\iota \left(\frac{\theta\xi}{24r\sqrt{d}}\right)^{3\kappa^\natural\iota} \\
& \leq \frac{\|\mathbf{T}\|_{op}\theta\xi}{3r\sqrt{d}\lambda_{\min}(\mathbf{U}_{r^*}^\top(\mathbf{P}_t^{\mathbf{A}})\mathbf{T})} \left(\frac{\|\mathbf{T}\|_{op}^2}{9d}\right)^\iota. \quad \left[\text{since } \iota \geq 1/3\kappa^\natural \text{ and } \frac{\theta\xi}{24r\sqrt{d}} \in (0,1)\right]
\end{aligned}$$

Then using Eq. (B.19), with probability at least $1 - C_1 \exp(-d) - (C_2\xi)^{r-r^*+1} - C_3 \exp(-r)$ for

some positive constants C_1, C_2, C_3 , we have

$$\left\| \mathbf{U}_{r^*, \perp}^\top \left(-\nabla_{\mathbf{W}} \tilde{L}(\mathbf{W}^\natural) \right) \mathbf{U}_{r^*}(\mathbf{A}_{t^*}) \right\|_{op} \lesssim \theta.$$

And we can compute the upper bound of t^* as

$$t^* = \frac{\ln \left(\frac{8 \|\mathbf{A}\|_{op}}{\theta \lambda_{\min}(\mathbf{U}_{r^*}^\top (\mathbf{P}_t^{\mathbf{A}}) \mathbf{A})} \right)}{\ln \left(1 + \sqrt{\eta_1 \eta_2} \lambda_{r^*}(\mathbf{G}^\natural) \right)} \lesssim \frac{\ln \left(\frac{24r\sqrt{d}}{\theta \xi} \right)}{\ln \left(1 + \sqrt{\eta_1 \eta_2} \lambda_{r^*}(\mathbf{G}^\natural) \right)}.$$

Case 2. $r \geq 2r^*$: by Lemma D.2 and Lemma D.3, with probability at least $1 - C_4 \exp(-d) - C_5 \exp(-r)$ for some positive constants C_4, C_5 , we have

$$\frac{\|\mathbf{T}\|_{op}}{3\sqrt{d}} \leq 1, \quad \frac{1}{\lambda_{\min}(\mathbf{U}_{r^*}^\top (\mathbf{P}_t^{\mathbf{A}}) \mathbf{T})} \lesssim 1.$$

Here we pick

$$\alpha \leq \left(\frac{\theta}{24\sqrt{d}} \right)^{\frac{3\kappa^\natural}{2}} \sqrt{\frac{\lambda_1(\mathbf{G}^\natural)}{54d \zeta(\eta_1, \eta_2)}}.$$

Similarly, we can obtain

$$\left\| \mathbf{U}_{r^*, \perp}^\top \left(-\nabla_{\mathbf{W}} \tilde{L}(\mathbf{W}^\natural) \right) \mathbf{U}_{r^*}(\mathbf{A}_t) \right\|_{op} \leq \frac{\|\mathbf{T}\|_{op} \theta}{3\sqrt{d} \lambda_{\min}(\mathbf{U}_{r^*}^\top (\mathbf{P}_t^{\mathbf{A}}) \mathbf{S})} \left(\frac{\|\mathbf{S}\|_{op}^2}{9d} \right)^t \lesssim \theta.$$

And we can compute the upper bound of t^* as

$$t^* \leq \frac{\ln \left(\frac{24\sqrt{d}}{\theta} \right)}{\ln \left(1 + \sqrt{\eta_1 \eta_2} \lambda_{r^*}(\mathbf{G}^\natural) \right)}.$$

□

Theorem B.10. Under assumptions in Section 2.1 for the linear setting, using the LoRA initialization for $\mathbf{B}_0 = \mathbf{0}$, then for any time-step $t \in \mathbb{N}_+$, we have

$$\left\| \mathbf{V}_{r^*, \perp}^\top \left(-\nabla_{\mathbf{W}} \tilde{L}(\mathbf{W}^\natural) \right) \mathbf{V}_{r^*}(\mathbf{B}_t) \right\|_{op} = 0.$$

Proof. We prove by induction. Recall the complete SVD of Δ in Eq. (2.1) as

$$\Delta = \tilde{\mathbf{U}} \tilde{\mathbf{S}}^* \tilde{\mathbf{V}}^\top = \begin{bmatrix} \mathbf{U} & \mathbf{U}_\perp \end{bmatrix} \begin{bmatrix} \mathbf{S}^* & \mathbf{0}_{r^* \times (d-r^*)} \\ \mathbf{0}_{(d-r^*) \times r^*} & \mathbf{0}_{(d-r^*) \times (d-r^*)} \end{bmatrix} \begin{bmatrix} \mathbf{V}^\top \\ \mathbf{V}_\perp^\top \end{bmatrix}.$$

For $t = 1$, recall $\mathbf{G}^\natural = \frac{1}{N} \tilde{\mathbf{X}}^\top \tilde{\mathbf{X}} \Delta$ in Eq. (3.1), we have

$$\mathbf{B}_1 \mathbf{V}_\perp = \frac{\eta_2}{N} \mathbf{A}_0^\top \mathbf{G}^\natural \mathbf{V}_\perp = \frac{\eta_2}{N} \mathbf{A}_0^\top \tilde{\mathbf{X}}^\top \tilde{\mathbf{X}} \Delta \mathbf{V}_\perp = \mathbf{0}_{r \times (d-r^*)}.$$

Assume $\mathbf{B}_t \mathbf{V}_\perp = \mathbf{0}_{r \times (d-r^*)}$ holds for any $t \in \mathbb{N}_+$ and $t \geq 2$, then

$$\mathbf{B}_{t+1} \mathbf{V}_\perp = \mathbf{B}_t \mathbf{V}_\perp - \frac{\eta_2}{N} \mathbf{A}_t^\top \widetilde{\mathbf{X}}^\top \widetilde{\mathbf{X}} \mathbf{A}_t \mathbf{B}_t \mathbf{V}_\perp + \frac{\eta_2}{N} \mathbf{A}_t^\top \mathbf{G}^\natural \mathbf{V}_\perp = \mathbf{0}_{r \times (d-r^*)},$$

which completes the claim. \square

B.2 Gradient Descent under Spectral Initialization

For notational simplicity, we denote $\widehat{\boldsymbol{\Sigma}} := \frac{1}{N} \widetilde{\mathbf{X}}^\top \widetilde{\mathbf{X}}$ in the following content. Recall the negative gradient of Full Fine-tuning at the first step in Eq. (3.1), we write it here again

$$\mathbf{G}^\natural = -\nabla_{\mathbf{W}} \widetilde{L}(\mathbf{W}^\natural) = \frac{1}{N} \widetilde{\mathbf{X}}^\top \widetilde{\mathbf{Y}}_\Delta = \widehat{\boldsymbol{\Sigma}} \Delta = \widetilde{\mathbf{U}}_{\mathbf{G}^\natural} \widetilde{\mathbf{S}}_{\mathbf{G}^\natural} \widetilde{\mathbf{V}}_{\mathbf{G}^\natural}^\top. \quad (\text{B.20})$$

In this section, according to Lemma D.1, the following statement

$$\left\| \widehat{\boldsymbol{\Sigma}} - \mathbf{I}_d \right\|_{op} = \epsilon \leq \min \left\{ \frac{1}{2\kappa}, \frac{c}{\kappa^3} \right\} \leq \frac{1}{2}, \quad \text{for some small constant } c, \quad (\text{B.21})$$

holds with probability at least $1 - 2C \exp(-\epsilon^2 N)$ for a universal constant $C > 0$. We propose the following initialization scheme (**Spectral-init**)

$$\mathbf{A}_0 = \left[\widetilde{\mathbf{U}}_{\mathbf{G}^\natural} \right]_{[:,1:r]} \left[\widetilde{\mathbf{S}}_{\mathbf{G}^\natural}^{1/2} \right]_{[1:r]}, \quad \mathbf{B}_0 = \left[\widetilde{\mathbf{S}}_{\mathbf{G}^\natural}^{1/2} \right]_{[1:r]} \left[\widetilde{\mathbf{V}}_{\mathbf{G}^\natural} \right]_{[:,1:r]}^\top.$$

First, we have the following lemma.

Lemma B.11. Under assumptions in Section 2.1 for the linear setting, with spectral initialization (**Spectral-init**), recall $\kappa := \lambda_1^*(\Delta) / \lambda_{r^*}^*(\Delta)$, then with probability at least with probability $1 - 2C \exp(-\epsilon^2 N)$ for a universal constant $C > 0$, we have

$$\|\mathbf{A}_0 \mathbf{B}_0 - \Delta\|_{op} \leq \epsilon \|\Delta\|_{op} \leq \frac{\lambda_{r^*}^*}{2}, \quad (\text{B.22})$$

and

$$\lambda_{r^*}(\mathbf{A}_0) \geq \frac{\sqrt{\lambda_{r^*}^*}}{2}, \quad \lambda_{r^*}(\mathbf{B}_0) \geq \frac{\sqrt{\lambda_{r^*}^*}}{2}. \quad (\text{B.23})$$

Proof. Due to $\text{rank}(\mathbf{G}^\natural) = r^*$ and $r \geq r^*$, then $\mathbf{A}_0 \mathbf{B}_0 = \mathbf{G}^\natural$, so we have

$$\begin{aligned} \|\mathbf{A}_0 \mathbf{B}_0 - \Delta\|_{op} &\leq \left\| \mathbf{A}_0 \mathbf{B}_0 - \mathbf{G}^\natural \right\|_{op} + \left\| \mathbf{G}^\natural - \Delta \right\|_{op} \\ &= \left\| \mathbf{G}^\natural - \Delta \right\|_{op} \\ &= \left\| \left(\widehat{\boldsymbol{\Sigma}} - \mathbf{I}_d \right) \Delta \right\|_{op} && \text{[using Eq. (B.20)]} \\ &\leq \left\| \widehat{\boldsymbol{\Sigma}} - \mathbf{I}_d \right\|_{op} \|\Delta\|_{op}. \end{aligned}$$

Accordingly, by Eq. (B.21), with probability at least $1 - 2 \exp(-c\epsilon^2 N)$, we have

$$\begin{aligned} \|\mathbf{A}_0 \mathbf{B}_0 - \Delta\|_{op} &\leq \epsilon \|\Delta\|_{op} \\ &\leq \frac{1}{2\kappa} \|\Delta\|_{op} && \text{[using Eq. (B.21)]} \\ &= \frac{\lambda_{r^*}^*}{2}. \end{aligned}$$

Then, using the above result and Weyl's inequality, we have the upper bound $\lambda_{r^*}(\mathbf{A}_0 \mathbf{B}_0) \leq \lambda_1(\mathbf{A}_0) \lambda_{r^*}(\mathbf{B}_0)$ and the lower bound

$$\lambda_{r^*}(\mathbf{A}_0 \mathbf{B}_0) = \lambda_{r^*}(\mathbf{G}^\natural) \geq \lambda_{r^*}(\Delta) - \|\mathbf{G}^\natural - \Delta\|_{op} = \lambda_{r^*}(\Delta) - \|\mathbf{A}_0 \mathbf{B}_0 - \Delta\|_{op} \geq \frac{\lambda_{r^*}^*}{2}.$$

Now we are ready to give the lower bound of $\lambda_{r^*}(\mathbf{B}_0)$. Because of $\mathbf{A}_0 \mathbf{B}_0 = \mathbf{G}^\natural$ under spectral initialization, we have

$$\lambda_1(\mathbf{A}_0) \leq \sqrt{\lambda_1(\mathbf{G}^\natural)} \leq \sqrt{\|\widehat{\Sigma} - \mathbf{I}_d\|_{op}} \lambda_1(\Delta) \leq \sqrt{\epsilon \lambda_1(\Delta)}, \quad \text{with high probability at least } 1 - 2C \exp(-\epsilon^2 N).$$

where we use $\mathbf{G}^\natural = \widehat{\Sigma} \Delta$ and the concentration results on $\widehat{\Sigma}$. Then combining the above two inequalities, $\lambda_{r^*}(\mathbf{B}_0)$ is lower bounded by

$$\lambda_{r^*}(\mathbf{B}_0) \geq \frac{\lambda_{r^*}(\mathbf{A}_0 \mathbf{B}_0)}{\lambda_1(\mathbf{A}_0)} \geq \frac{\lambda_{r^*}^*/2}{\lambda_1(\mathbf{A}_0)} \geq \frac{\sqrt{\lambda_{r^*}^*}}{2},$$

by taking $\epsilon \leq \frac{1}{2\kappa}$. The lower bound of $\lambda_{r^*}(\mathbf{A}_0)$ can be obtained similarly. \square

The following lemma indicates \mathbf{B}_t 's GD dynamics stay in the low-dimensional target subspace under the spectral initialization.

Lemma B.12. Under assumptions in Section 2.1 for the linear setting, with spectral initialization (**Spectral-init**), during the iteration, for any $t \in \mathbb{N}^+$, we always have $\mathbf{B}_t \mathbf{V}_\perp = \mathbf{0}_{d \times (d-r^*)}$, where \mathbf{V}_\perp comes from the complete SVD of Δ in Eq. (2.1).

Proof. We prove it by induction. First, recall the SVD of Δ in Eq. (2.1), we have

$$\mathbf{G}^\natural \mathbf{V}_\perp = \widetilde{\Sigma} \Delta \mathbf{V}_\perp = \mathbf{0}_{d \times (d-r^*)},$$

and

$$\begin{aligned} \mathbf{B}_0 \mathbf{V}_\perp &= \begin{bmatrix} \widetilde{\mathbf{S}}_{\mathbf{G}^\natural}^{1/2} \end{bmatrix}_{[1:r]} \begin{bmatrix} \widetilde{\mathbf{V}}_{\mathbf{G}^\natural}^\top \end{bmatrix}_{[:,1:r]} \mathbf{V}_\perp \\ &= \begin{bmatrix} \widetilde{\mathbf{S}}_{\mathbf{G}^\natural}^{-1/2} \end{bmatrix}_{[1:r]} \begin{bmatrix} \widetilde{\mathbf{U}}_{\mathbf{G}^\natural}^\top \end{bmatrix}_{[:,1:r]} \mathbf{G}^\natural \mathbf{V}_\perp \\ &= \begin{bmatrix} \widetilde{\mathbf{S}}_{\mathbf{G}^\natural}^{-1/2} \end{bmatrix}_{[1:r]} \begin{bmatrix} \widetilde{\mathbf{U}}_{\mathbf{G}^\natural}^\top \end{bmatrix}_{[:,1:r]} \widehat{\Sigma} \Delta \mathbf{V}_\perp \\ &= \mathbf{0}_{d \times (d-r^*)}. \end{aligned}$$

Next, We prove by induction. Starting from $t = 1$, using the above two equations, we have

$$\begin{aligned} \mathbf{B}_1 \mathbf{V}_\perp &= \mathbf{B}_0 \mathbf{V}_\perp - \frac{\eta_2}{N} \mathbf{A}_0^\top \widetilde{\mathbf{X}}^\top \left(\widetilde{\mathbf{X}} (\mathbf{W}^\natural + \mathbf{A}_0 \mathbf{B}_0) - \widetilde{\mathbf{Y}} \right) \mathbf{V}_\perp \\ &= \mathbf{B}_0 \mathbf{V}_\perp - \frac{\eta_2}{N} \mathbf{A}_0^\top \widetilde{\mathbf{X}}^\top \widetilde{\mathbf{X}} \mathbf{A}_0 \mathbf{B}_0 \mathbf{V}_\perp + \eta_2 \mathbf{A}_0^\top \mathbf{G}^\natural \mathbf{V}_\perp \\ &= \mathbf{0}_{d \times (d-r^*)}. \end{aligned}$$

Assume $\mathbf{B}_t \mathbf{V}_\perp = \mathbf{0}_{d \times (d-r^*)}$ holds for any $t = 2, 3, \dots$, then at $t + 1$, we have

$$\begin{aligned} \mathbf{B}_{t+1} \mathbf{V}_\perp &= \mathbf{B}_t \mathbf{V}_\perp - \frac{\eta}{N} \mathbf{A}_t^\top \widetilde{\mathbf{X}}^\top \widetilde{\mathbf{X}} \mathbf{A}_t \mathbf{B}_t \mathbf{V}_\perp + \eta_2 \mathbf{A}_t^\top \mathbf{G}^\natural \mathbf{V}_\perp \\ &= \mathbf{0}_{d \times (d-r^*)}. \end{aligned}$$

Accordingly we finish the proof. \square

Under spectral initialization, we have already demonstrated that $\mathbf{A}_0 \mathbf{B}_0$ is close to Δ . In the following content, we aim to track how $\|\mathbf{A}_t \mathbf{B}_t - \Delta\|_{op}$ behaves (in a local sense), which is a critical ingredient to study both the loss and risk of LoRA training. In this regime, there is no significant difference on setting different step-size η_1 and η_2 . For ease of description, we set $\eta_1 = \eta_2 := \eta$.

Here we can characterize the operator norm of $(\mathbf{A}_t \mathbf{B}_t - \Delta)$ as

$$\begin{aligned} \|\mathbf{A}_t \mathbf{B}_t - \Delta\|_{op} &= \left\| \left(\mathbf{A}_t \mathbf{B}_t - \Delta \right) \begin{bmatrix} \mathbf{V} & \mathbf{V}_\perp \end{bmatrix} \right\|_{op} && \text{[by unitary invariance of operator norm]} \\ &= \|\mathbf{A}_t \mathbf{B}_t \mathbf{V} - \mathbf{U} \mathbf{S}^*\|_{op} && \text{[by Lemma B.12]} \\ &= \left\| \left(\mathbf{U} \mathbf{U}^\top + \mathbf{U}_\perp \mathbf{U}_\perp^\top \right) \left(\mathbf{A}_t \mathbf{B}_t \mathbf{V} - \mathbf{U} \mathbf{S}^* \right) \right\|_{op} \\ &= \left\| \mathbf{U} \left(\mathbf{U}^\top \mathbf{A}_t \mathbf{B}_t \mathbf{V} - \mathbf{S}^* \right) \right\|_{op} + \left\| \mathbf{U}_\perp \mathbf{U}_\perp^\top \mathbf{A}_t \mathbf{B}_t \mathbf{V} \right\|_{op} \\ &\leq \underbrace{\left\| \mathbf{U}^\top \mathbf{A}_t \mathbf{B}_t \mathbf{V} - \mathbf{S}^* \right\|_{op}}_{\text{signal space}} + \underbrace{\left\| \mathbf{U}_\perp^\top \mathbf{A}_t \mathbf{B}_t \mathbf{V} \right\|_{op}}_{\text{complementary}}, \end{aligned} \tag{B.24}$$

where the first term denotes the loss in the signal space $\|\mathbf{U}^\top \mathbf{A} \mathbf{B} \mathbf{V} - \mathbf{S}^*\|_{op}$ and the second term denotes the complementary space decay $\|\mathbf{U}_\perp^\top \mathbf{A} \mathbf{B} \mathbf{V}\|_{op}$. Next, we need a new parametrization to track the dynamics of these two terms. Recall the complete SVD of Δ in Eq. (2.1) as

$$\Delta = \widetilde{\mathbf{U}} \widetilde{\mathbf{S}}^* \widetilde{\mathbf{V}}^\top = \begin{bmatrix} \mathbf{U} & \mathbf{U}_\perp \end{bmatrix} \begin{bmatrix} \mathbf{S}^* & \mathbf{0}_{r^* \times (d-r^*)} \\ \mathbf{0}_{(d-r^*) \times r^*} & \mathbf{0}_{(d-r^*) \times (d-r^*)} \end{bmatrix} \begin{bmatrix} \mathbf{V}^\top \\ \mathbf{V}_\perp^\top \end{bmatrix}.$$

For notational simplicity, we denote

$$\mathbf{A}_t^U := \mathbf{U}^\top \mathbf{A}_t, \quad \mathbf{A}_t^{U_\perp} := \mathbf{U}_\perp^\top \mathbf{A}_t, \quad \mathbf{B}_t^V := \mathbf{B}_t^V, \quad \mathbf{B}_t^{V_\perp} := \mathbf{B}_t^{V_\perp}.$$

and thus

$$\mathbf{R}_t := (\mathbf{A}_t \mathbf{B}_t - \Delta) \mathbf{V}, \quad \mathbf{R}_t^* := \mathbf{A}_t^U \mathbf{B}_t^V - \mathbf{S}^*, \quad \mathbf{R}_t^\perp := \mathbf{A}_t^{U_\perp} \mathbf{B}_t^V.$$

Accordingly, Eq. (B.24) can be reformulated as $\|\mathbf{R}_t\|_{op} \leq \|\mathbf{R}_t^*\|_{op} + \|\mathbf{R}_t^\perp\|_{op}$. By Lemma B.12, we have $\mathbf{B}^{\mathbf{V}\perp} = \mathbf{0}_{r \times (k-r^*)}$ for $\forall t \in \mathbb{N}^+$. Next, we can track \mathbf{R}_t^* and \mathbf{R}_t^\perp via the following two lemmas.

Lemma B.13. Under assumptions in Section 2.1 for the linear setting, with spectral initialization (Spectral-init), we have the following reparametrized iterates

$$\mathbf{A}_{t+1}^U = \mathbf{A}_t^U - \eta \mathbf{R}_t^* (\mathbf{B}_t^{\mathbf{V}})^\top - \eta \mathbf{U}^\top (\widehat{\Sigma} - \mathbf{I}_d) \mathbf{R}_t (\mathbf{B}_t^{\mathbf{V}})^\top, \quad (\text{B.25})$$

$$\mathbf{A}_{t+1}^{U\perp} = \mathbf{A}_t^{U\perp} - \eta \mathbf{R}_t^\perp (\mathbf{B}_t^{\mathbf{V}})^\top - \eta \mathbf{U}_\perp^\top (\widehat{\Sigma} - \mathbf{I}_d) \mathbf{R}_t (\mathbf{B}_t^{\mathbf{V}})^\top, \quad (\text{B.26})$$

$$\begin{aligned} \mathbf{B}_{t+1}^{\mathbf{V}} &= \mathbf{B}_t^{\mathbf{V}} - \eta (\mathbf{A}_t^U)^\top \mathbf{R}_t^* - \eta (\mathbf{A}_t^{U\perp})^\top \mathbf{R}_t^\perp \\ &\quad - \eta (\mathbf{A}_t^U)^\top \mathbf{U}^\top (\widehat{\Sigma} - \mathbf{I}_d) \mathbf{R}_t - \eta (\mathbf{A}_t^{U\perp})^\top \mathbf{U}_\perp^\top (\widehat{\Sigma} - \mathbf{I}_d) \mathbf{R}_t. \end{aligned} \quad (\text{B.27})$$

Proof. Recall the gradient update for \mathbf{A}_{t+1} , we have

$$\begin{aligned} \mathbf{A}_{t+1} &= \mathbf{A}_t - \eta \widehat{\Sigma} (\mathbf{A}_t \mathbf{B}_t - \Delta) (\mathbf{B}_t)^\top \\ &= \mathbf{A}_t - \eta (\mathbf{A}_t \mathbf{B}_t - \Delta) (\mathbf{B}_t)^\top - \eta (\widehat{\Sigma} - \mathbf{I}_d) (\mathbf{A}_t \mathbf{B}_t - \Delta) (\mathbf{B}_t)^\top. \end{aligned}$$

Recall $\mathbf{R}_t := (\mathbf{A}_t \mathbf{B}_t - \Delta) \mathbf{V}$ and $\Delta = \mathbf{U} \mathbf{S}^* \mathbf{V}^\top$, we have

$$\begin{aligned} \mathbf{U}^\top \mathbf{A}_{t+1} &= \mathbf{U}^\top \mathbf{A}_t - \eta \mathbf{U}^\top (\mathbf{A}_t \mathbf{B}_t - \Delta) (\mathbf{V} \mathbf{V}^\top + \mathbf{V}_\perp \mathbf{V}_\perp^\top) (\mathbf{B}_t)^\top \\ &\quad - \eta \mathbf{U}^\top (\widehat{\Sigma} - \mathbf{I}_d) (\mathbf{A}_t \mathbf{B}_t - \Delta) (\mathbf{V} \mathbf{V}^\top + \mathbf{V}_\perp \mathbf{V}_\perp^\top) (\mathbf{B}_t)^\top \\ &= \mathbf{U}^\top \mathbf{A}_t - \eta \mathbf{U}^\top (\mathbf{A}_t \mathbf{B}_t \mathbf{V} - \Delta \mathbf{V}) (\mathbf{B}_t \mathbf{V})^\top - \eta \mathbf{U}^\top (\widehat{\Sigma} - \mathbf{I}_d) (\mathbf{A}_t \mathbf{B}_t \mathbf{V} - \Delta \mathbf{V}) (\mathbf{B}_t \mathbf{V})^\top \\ &\quad \text{[by Lemma B.12]} \\ &= \mathbf{U}^\top \mathbf{A}_t - \eta (\mathbf{U}^\top \mathbf{A}_t \mathbf{B}_t \mathbf{V} - \mathbf{S}^*) (\mathbf{B}_t \mathbf{V})^\top - \eta \mathbf{U}^\top (\widehat{\Sigma} - \mathbf{I}_d) \mathbf{R}_t (\mathbf{B}_t \mathbf{V})^\top. \end{aligned}$$

Accordingly, the recursion for \mathbf{A}_{t+1}^U is reformulated as

$$\mathbf{A}_{t+1}^U = \mathbf{A}_t^U - \eta \mathbf{R}_t^* (\mathbf{B}_t^{\mathbf{V}})^\top - \eta \mathbf{U}^\top (\widehat{\Sigma} - \mathbf{I}_d) \mathbf{R}_t (\mathbf{B}_t^{\mathbf{V}})^\top.$$

Similarly, we can obtain

$$\mathbf{A}_{t+1}^{U\perp} = \mathbf{A}_t^{U\perp} - \eta \mathbf{R}_t^\perp (\mathbf{B}_t^{\mathbf{V}})^\top - \eta \mathbf{U}_\perp^\top (\widehat{\Sigma} - \mathbf{I}_d) \mathbf{R}_t (\mathbf{B}_t^{\mathbf{V}})^\top.$$

Regarding the recursion for \mathbf{B}_{t+1} , we can derive in a similar way

$$\begin{aligned} \mathbf{B}_{t+1} \mathbf{V} &= \mathbf{B}_t \mathbf{V} - \eta (\mathbf{A}_t)^\top \widehat{\Sigma} (\mathbf{A}_t \mathbf{B}_t - \Delta) \mathbf{V} \\ &= \mathbf{B}_t \mathbf{V} - \eta (\mathbf{A}_t)^\top (\mathbf{U} \mathbf{U}^\top + \mathbf{U}_\perp \mathbf{U}_\perp^\top) (\mathbf{A}_t \mathbf{B}_t - \Delta) \mathbf{V} \\ &\quad - \eta (\mathbf{A}_t)^\top (\mathbf{U} \mathbf{U}^\top + \mathbf{U}_\perp \mathbf{U}_\perp^\top) (\widehat{\Sigma} - \mathbf{I}_d) (\mathbf{A}_t \mathbf{B}_t - \Delta) \mathbf{V}, \end{aligned}$$

which implies

$$\mathbf{B}_{t+1}^V = \mathbf{B}_t^V - \eta (\mathbf{A}_t^U)^\top \mathbf{R}_t^* - \eta (\mathbf{A}_t^{U\perp})^\top \mathbf{R}_t^\perp - \eta (\mathbf{A}_t^U)^\top \mathbf{U}^\top (\widehat{\Sigma} - \mathbf{I}_d) \mathbf{R}_t - \eta (\mathbf{A}_t^{U\perp})^\top \mathbf{U}_\perp^\top (\widehat{\Sigma} - \mathbf{I}_d) \mathbf{R}_t.$$

□

In the next, we are able to characterize the upper bound of $\|\mathbf{R}_{t+1}^*\|_{op}$.

Lemma B.14. Denote $\mathcal{M}_t := \max \left\{ \|\mathbf{R}_t^*\|_{op}, \|\mathbf{R}_t^\perp\|_{op} \right\}$, under assumptions in Section 2.1 for the linear setting, with spectral initialization (**Spectral-init**), then we choose ϵ with probability at least $1 - 2C \exp(-\epsilon^2 N)$ for a universal constant $C > 0$, we have

$$\begin{aligned} \|\mathbf{R}_{t+1}^*\|_{op} &\leq \left(1 - \eta (\lambda_{r^*}^2(\mathbf{A}_t^U) + \lambda_{r^*}^2(\mathbf{B}_t^V)) \right) \mathcal{M}_t \\ &\quad + 2\eta\epsilon \|\mathbf{B}_t^V\|_{op}^2 \mathcal{M}_t + \eta^2 \|\mathbf{A}_t^U\|_{op} \|\mathbf{B}_t^V\|_{op} \mathcal{M}_t^2 + 2\eta^2\epsilon \|\mathbf{A}_t^U\|_{op} \|\mathbf{B}_t^V\|_{op} \mathcal{M}_t^2 \\ &\quad + \eta \|\mathbf{A}_t^U\|_{op} \|\mathbf{A}_t^{U\perp}\|_{op} \mathcal{M}_t + \eta^2 \|\mathbf{B}_t^V\|_{op} \|\mathbf{A}_t^{U\perp}\|_{op} \mathcal{M}_t^2 \\ &\quad + 2\eta^2\epsilon \|\mathbf{B}_t^V\|_{op} \|\mathbf{A}_t^{U\perp}\|_{op} \mathcal{M}_t^2 + 2\eta\epsilon \|\mathbf{A}_t^U\|_{op}^2 \mathcal{M}_t \\ &\quad + 2\eta^2\epsilon \|\mathbf{A}_t^U\|_{op} \|\mathbf{B}_t^V\|_{op} \mathcal{M}_t + 4\eta^2\epsilon^2 \|\mathbf{A}_t^U\|_{op} \|\mathbf{B}_t^V\|_{op} \mathcal{M}_t^2 \\ &\quad + 2\eta\epsilon \|\mathbf{A}_t^U\|_{op} \|\mathbf{A}_t^{U\perp}\|_{op} \mathcal{M}_t + 2\eta^2\epsilon \|\mathbf{A}_t^{U\perp}\|_{op} \|\mathbf{B}_t^V\|_{op} \mathcal{M}_t^2 \\ &\quad + 4\eta^2\epsilon^2 \|\mathbf{A}_t^{U\perp}\|_{op} \|\mathbf{B}_t^V\|_{op} \mathcal{M}_t^2, \end{aligned}$$

and

$$\begin{aligned} \|\mathbf{R}_{t+1}^\perp\|_{op} &\leq \left(1 - \eta (\lambda_{\min}^2(\mathbf{A}_t^{U\perp}) + \lambda_{r^*}^2(\mathbf{B}_t^V)) \right) \mathcal{M}_t \tag{B.28} \\ &\quad + 2\eta\epsilon \|\mathbf{B}_t^V\|_{op}^2 \mathcal{M}_t + \eta^2 \|\mathbf{A}_t^U\|_{op} \|\mathbf{B}_t^V\|_{op} \mathcal{M}_t^2 + 2\eta^2\epsilon \|\mathbf{A}_t^U\|_{op} \|\mathbf{B}_t^V\|_{op} \mathcal{M}_t^2 \\ &\quad + \eta \|\mathbf{A}_t^U\|_{op} \|\mathbf{A}_t^{U\perp}\|_{op} \mathcal{M}_t + \eta^2 \|\mathbf{B}_t^V\|_{op} \|\mathbf{A}_t^{U\perp}\|_{op} \mathcal{M}_t^2 \\ &\quad + 2\eta^2\epsilon \|\mathbf{B}_t^V\|_{op} \|\mathbf{A}_t^{U\perp}\|_{op} \mathcal{M}_t^2 + 2\eta\epsilon \|\mathbf{A}_t^U\|_{op} \|\mathbf{A}_t^{U\perp}\|_{op} \mathcal{M}_t \\ &\quad + 2\eta^2\epsilon \|\mathbf{A}_t^U\|_{op} \|\mathbf{B}_t^V\|_{op} \mathcal{M}_t + 4\eta^2\epsilon^2 \|\mathbf{A}_t^U\|_{op} \|\mathbf{B}_t^V\|_{op} \mathcal{M}_t^2 \\ &\quad + 2\eta\epsilon \|\mathbf{A}_t^{U\perp}\|_{op}^2 \mathcal{M}_t + 2\eta^2\epsilon \|\mathbf{A}_t^{U\perp}\|_{op} \|\mathbf{B}_t^V\|_{op} \mathcal{M}_t^2 \\ &\quad + 4\eta^2\epsilon^2 \|\mathbf{A}_t^{U\perp}\|_{op} \|\mathbf{B}_t^V\|_{op} \mathcal{M}_t^2. \end{aligned}$$

Proof. Here we first track the dynamics of \mathbf{R}_t^* . We have

$$\begin{aligned}
\mathbf{R}_{t+1}^* &= \mathbf{A}_{t+1}^U \mathbf{B}_{t+1}^V - \mathbf{S}^* \\
&= \mathbf{R}_t^* - \eta \mathbf{R}_t^* (\mathbf{B}_t^V)^\top \mathbf{B}_t^V - \eta \mathbf{U}^\top (\widehat{\Sigma} - \mathbf{I}_d) \mathbf{R}_t (\mathbf{B}_t^V)^\top \mathbf{B}_t^V \\
&\quad - \eta \mathbf{A}_t^U (\mathbf{A}_t^U)^\top \mathbf{R}_t^* + \eta^2 \mathbf{R}_t^* (\mathbf{B}_t^V)^\top (\mathbf{A}_t^U)^\top \mathbf{R}_t^* + \eta^2 \mathbf{U}^\top (\widehat{\Sigma} - \mathbf{I}_d) \mathbf{R}_t (\mathbf{B}_t^V)^\top (\mathbf{A}_t^U)^\top \mathbf{R}_t^* \\
&\quad - \eta \mathbf{A}_t^U (\mathbf{A}_t^{U\perp})^\top \mathbf{R}_t^\perp + \eta^2 \mathbf{R}_t^* (\mathbf{B}_t^V)^\top (\mathbf{A}_t^{U\perp})^\top \mathbf{R}_t^\perp + \eta^2 \mathbf{U}^\top (\widehat{\Sigma} - \mathbf{I}_d) \mathbf{R}_t (\mathbf{B}_t^V)^\top (\mathbf{A}_t^{U\perp})^\top \mathbf{R}_t^\perp \\
&\quad - \eta \mathbf{A}_t^U (\mathbf{A}_t^U)^\top \mathbf{U}^\top (\widehat{\Sigma} - \mathbf{I}_d) \mathbf{R}_t \\
&\quad + \eta^2 \mathbf{R}_t^* (\mathbf{B}_t^V)^\top (\mathbf{A}_t^U)^\top \mathbf{U}^\top (\widehat{\Sigma} - \mathbf{I}_d) \mathbf{R}_t \\
&\quad + \eta^2 \mathbf{U}^\top (\widehat{\Sigma} - \mathbf{I}_d) \mathbf{R}_t (\mathbf{B}_t^V)^\top (\mathbf{A}_t^U)^\top \mathbf{U}^\top (\widehat{\Sigma} - \mathbf{I}_d) \mathbf{R}_t \\
&\quad - \eta \mathbf{A}_t^U (\mathbf{A}_t^{U\perp})^\top \mathbf{U}_\perp^\top (\widehat{\Sigma} - \mathbf{I}_d) \mathbf{R}_t \\
&\quad + \eta^2 \mathbf{R}_t^* (\mathbf{B}_t^V)^\top (\mathbf{A}_t^{U\perp})^\top \mathbf{U}_\perp^\top (\widehat{\Sigma} - \mathbf{I}_d) \mathbf{R}_t \\
&\quad + \eta^2 \mathbf{U}^\top (\widehat{\Sigma} - \mathbf{I}_d) \mathbf{R}_t (\mathbf{B}_t^V)^\top (\mathbf{A}_t^{U\perp})^\top \mathbf{U}_\perp^\top (\widehat{\Sigma} - \mathbf{I}_d) \mathbf{R}_t.
\end{aligned}$$

Then, we take operator norm over the above equation. Hence, with probability at least $1 - 2C \exp(-\epsilon^2 N)$ for a universal constant $C > 0$, we have

$$\begin{aligned}
\|\mathbf{R}_{t+1}^*\|_{op} &\leq \left(1 - \eta (\lambda_{r^*}^2(\mathbf{A}_t^U) + \lambda_{r^*}^2(\mathbf{B}_t^V))\right) \|\mathbf{R}_t^*\|_{op} \\
&\quad + \eta \epsilon \|\mathbf{B}_t^V\|_{op}^2 \|\mathbf{R}_t\|_{op} + \eta^2 \|\mathbf{A}_t^U\|_{op} \|\mathbf{B}_t^V\|_{op} \|\mathbf{R}_t^*\|_{op}^2 + \eta^2 \epsilon \|\mathbf{A}_t^U\|_{op} \|\mathbf{B}_t^V\|_{op} \|\mathbf{R}_t^*\|_{op} \|\mathbf{R}_t\|_{op} \\
&\quad + \eta \|\mathbf{A}_t^U\|_{op} \|\mathbf{A}_t^{U\perp}\|_{op} \|\mathbf{R}_t^\perp\|_{op} + \eta^2 \|\mathbf{B}_t^V\|_{op} \|\mathbf{A}_t^{U\perp}\|_{op} \|\mathbf{R}_t^\perp\|_{op} \|\mathbf{R}_t^*\|_{op} \\
&\quad + \eta^2 \epsilon \|\mathbf{B}_t^V\|_{op} \|\mathbf{A}_t^{U\perp}\|_{op} \|\mathbf{R}_t^\perp\|_{op} \|\mathbf{R}_t\|_{op} + \eta \epsilon \|\mathbf{A}_t^U\|_{op}^2 \|\mathbf{R}_t\|_{op} \\
&\quad + \eta^2 \epsilon \|\mathbf{A}_t^U\|_{op} \|\mathbf{B}_t^V\|_{op} \|\mathbf{R}_t\|_{op} + \eta^2 \epsilon^2 \|\mathbf{A}_t^U\|_{op} \|\mathbf{B}_t^V\|_{op} \|\mathbf{R}_t\|_{op}^2 \\
&\quad + \eta \epsilon \|\mathbf{A}_t^U\|_{op} \|\mathbf{A}_t^{U\perp}\|_{op} \|\mathbf{R}_t\|_{op} + \eta^2 \epsilon \|\mathbf{A}_t^{U\perp}\|_{op} \|\mathbf{B}_t^V\|_{op} \|\mathbf{R}_t^*\|_{op} \|\mathbf{R}_t\|_{op} \\
&\quad + \eta^2 \epsilon^2 \|\mathbf{A}_t^{U\perp}\|_{op} \|\mathbf{B}_t^V\|_{op} \|\mathbf{R}_t\|_{op}^2.
\end{aligned}$$

Next, we take maximum over $\|\mathbf{R}_t^*\|_{op}$ and $\|\mathbf{R}_t^\perp\|_{op}$ on the right hand side above. Recall $\mathcal{M}_t =$

$\max \left\{ \|\mathbf{R}_t^*\|_{op}, \|\mathbf{R}_t^\perp\|_{op} \right\}$, using the fact that $\|\mathbf{R}_t\|_{op} \leq 2\mathcal{M}_t$, we have:

$$\begin{aligned}
\|\mathbf{R}_{t+1}^*\|_{op} &\leq \left(1 - \eta (\lambda_{r^*}^2 (\mathbf{A}_t^U) + \lambda_{r^*}^2 (\mathbf{B}_t^V)) \right) \mathcal{M}_t \\
&\quad + 2\eta\epsilon \|\mathbf{B}_t^V\|_{op}^2 \mathcal{M}_t + \eta^2 \|\mathbf{A}_t^U\|_{op} \|\mathbf{B}_t^V\|_{op} \mathcal{M}_t^2 + 2\eta^2\epsilon \|\mathbf{A}_t^U\|_{op} \|\mathbf{B}_t^V\|_{op} \mathcal{M}_t^2 \\
&\quad + \eta \|\mathbf{A}_t^U\|_{op} \|\mathbf{A}_t^{U\perp}\|_{op} \mathcal{M}_t + \eta^2 \|\mathbf{B}_t^V\|_{op} \|\mathbf{A}_t^{U\perp}\|_{op} \mathcal{M}_t^2 \\
&\quad + 2\eta^2\epsilon \|\mathbf{B}_t^V\|_{op} \|\mathbf{A}_t^{U\perp}\|_{op} \mathcal{M}_t^2 + 2\eta\epsilon \|\mathbf{A}_t^U\|_{op}^2 \mathcal{M}_t \\
&\quad + 2\eta^2\epsilon \|\mathbf{A}_t^U\|_{op} \|\mathbf{B}_t^V\|_{op} \mathcal{M}_t + 4\eta^2\epsilon^2 \|\mathbf{A}_t^U\|_{op} \|\mathbf{B}_t^V\|_{op} \mathcal{M}_t^2 \\
&\quad + 2\eta\epsilon \|\mathbf{A}_t^U\|_{op} \|\mathbf{A}_t^{U\perp}\|_{op} \mathcal{M}_t + 2\eta^2\epsilon \|\mathbf{A}_t^{U\perp}\|_{op} \|\mathbf{B}_t^V\|_{op} \mathcal{M}_t^2 \\
&\quad + 4\eta^2\epsilon^2 \|\mathbf{A}_t^{U\perp}\|_{op} \|\mathbf{B}_t^V\|_{op} \mathcal{M}_t^2.
\end{aligned}$$

Next, we track the dynamics of \mathbf{R}_t^\perp . We have

$$\begin{aligned}
\mathbf{R}_{t+1}^\perp &= \mathbf{A}_{t+1}^{U\perp} \mathbf{B}_{t+1}^V \\
&= \mathbf{R}_t^\perp - \eta \mathbf{R}_t^\perp (\mathbf{B}_t^V)^\top \mathbf{B}_t^V - \eta \mathbf{U}_\perp^\top (\widehat{\Sigma} - \mathbf{I}_d) \mathbf{R}_t (\mathbf{B}_t^V)^\top \mathbf{B}_t^V \\
&\quad - \eta \mathbf{A}_t^{U\perp} (\mathbf{A}_t^U)^\top \mathbf{R}_t^* + \eta^2 \mathbf{R}_t^\perp (\mathbf{B}_t^V)^\top (\mathbf{A}_t^U)^\top \mathbf{R}_t^* + \eta^2 \mathbf{U}_\perp^\top (\widehat{\Sigma} - \mathbf{I}_d) \mathbf{R}_t (\mathbf{B}_t^V)^\top (\mathbf{A}_t^U)^\top \mathbf{R}_t^* \\
&\quad - \eta \mathbf{A}_t^{U\perp} (\mathbf{A}_t^{U\perp})^\top \mathbf{R}_t^\perp + \eta^2 \mathbf{R}_t^\perp (\mathbf{B}_t^V)^\top (\mathbf{A}_t^{U\perp})^\top \mathbf{R}_t^\perp + \eta^2 \mathbf{U}_\perp^\top (\widehat{\Sigma} - \mathbf{I}_d) \mathbf{R}_t (\mathbf{B}_t^V)^\top (\mathbf{A}_t^{U\perp})^\top \mathbf{R}_t^\perp \\
&\quad - \eta \mathbf{A}_t^{U\perp} (\mathbf{A}_t^U)^\top \mathbf{U}^\top (\widehat{\Sigma} - \mathbf{I}_d) \mathbf{R}_t \\
&\quad + \eta^2 \mathbf{R}_t^\perp (\mathbf{B}_t^V)^\top (\mathbf{A}_t^U)^\top \mathbf{U}^\top (\widehat{\Sigma} - \mathbf{I}_d) \mathbf{R}_t \\
&\quad + \eta^2 \mathbf{U}_\perp^\top (\widehat{\Sigma} - \mathbf{I}_d) \mathbf{R}_t (\mathbf{B}_t^V)^\top (\mathbf{A}_t^U)^\top \mathbf{U}^\top (\widehat{\Sigma} - \mathbf{I}_d) \mathbf{R}_t \\
&\quad - \eta \mathbf{A}_t^{U\perp} (\mathbf{A}_t^{U\perp})^\top \mathbf{U}_\perp^\top (\widehat{\Sigma} - \mathbf{I}_d) \mathbf{R}_t \\
&\quad + \eta^2 \mathbf{R}_t^\perp (\mathbf{B}_t^V)^\top (\mathbf{A}_t^{U\perp})^\top \mathbf{U}_\perp^\top (\widehat{\Sigma} - \mathbf{I}_d) \mathbf{R}_t \\
&\quad + \eta^2 \mathbf{U}_\perp^\top (\widehat{\Sigma} - \mathbf{I}_d) \mathbf{R}_t (\mathbf{B}_t^V)^\top (\mathbf{A}_t^{U\perp})^\top \mathbf{U}_\perp^\top (\widehat{\Sigma} - \mathbf{I}_d) \mathbf{R}_t.
\end{aligned}$$

Then, we take operator norm over the above equation. With probability at least $1 - 2C \exp(-\epsilon^2 N)$

for a universal constant $C > 0$, we have

$$\begin{aligned}
\|\mathbf{R}_{t+1}^\perp\|_{op} &\leq \left(1 - \eta \left(\lambda_{\min}^2(\mathbf{A}_t^{U^\perp}) + \lambda_{r^*}^2(\mathbf{B}_t^V)\right)\right) \|\mathbf{R}_t^\perp\|_{op} \\
&\quad + \eta\epsilon \|\mathbf{B}_t^V\|_{op}^2 \|\mathbf{R}_t\|_{op} + \eta^2 \|\mathbf{A}_t^U\|_{op} \|\mathbf{B}_t^V\|_{op} \|\mathbf{R}_t^*\|_{op} \|\mathbf{R}_t^\perp\|_{op} + \eta^2\epsilon \|\mathbf{A}_t^U\|_{op} \|\mathbf{B}_t^V\|_{op} \|\mathbf{R}_t^*\|_{op} \|\mathbf{R}_t\|_{op} \\
&\quad + \eta \|\mathbf{A}_t^U\|_{op} \|\mathbf{A}_t^{U^\perp}\|_{op} \|\mathbf{R}_t^*\|_{op} + \eta^2 \|\mathbf{B}_t^V\|_{op} \|\mathbf{A}_t^{U^\perp}\|_{op} \|\mathbf{R}_t^\perp\|_{op}^2 \\
&\quad + \eta^2\epsilon \|\mathbf{B}_t^V\|_{op} \|\mathbf{A}_t^{U^\perp}\|_{op} \|\mathbf{R}_t^\perp\|_{op} \|\mathbf{R}_t\|_{op} + \eta\epsilon \|\mathbf{A}_t^U\|_{op} \|\mathbf{A}_t^{U^\perp}\|_{op} \|\mathbf{R}_t\|_{op} \\
&\quad + \eta^2\epsilon \|\mathbf{A}_t^U\|_{op} \|\mathbf{B}_t^V\|_{op} \|\mathbf{R}_t\|_{op} + \eta^2\epsilon^2 \|\mathbf{A}_t^U\|_{op} \|\mathbf{B}_t^V\|_{op} \|\mathbf{R}_t\|_{op}^2 \\
&\quad + \eta\epsilon \|\mathbf{A}_t^{U^\perp}\|_{op}^2 \|\mathbf{R}_t\|_{op} + \eta^2\epsilon \|\mathbf{A}_t^{U^\perp}\|_{op} \|\mathbf{B}_t^V\|_{op} \|\mathbf{R}_t^\perp\|_{op} \|\mathbf{R}_t\|_{op} \\
&\quad + \eta^2\epsilon^2 \|\mathbf{A}_t^{U^\perp}\|_{op} \|\mathbf{B}_t^V\|_{op} \|\mathbf{R}_t\|_{op}^2.
\end{aligned}$$

Next, we take maximum over $\|\mathbf{R}_t^*\|_{op}$ and $\|\mathbf{R}_t^\perp\|_{op}$ on the right hand side above. Recall $\mathcal{M}_t = \max\{\|\mathbf{R}_t^*\|_{op}, \|\mathbf{R}_t^\perp\|_{op}\}$, using the fact that $\|\mathbf{R}_t\|_{op} \leq 2\mathcal{M}_t$, we have:

$$\begin{aligned}
\|\mathbf{R}_{t+1}^\perp\|_{op} &\leq \left(1 - \eta \left(\lambda_{\min}^2(\mathbf{A}_t^{U^\perp}) + \lambda_{r^*}^2(\mathbf{B}_t^V)\right)\right) \mathcal{M}_t \\
&\quad + 2\eta\epsilon \|\mathbf{B}_t^V\|_{op}^2 \mathcal{M}_t + \eta^2 \|\mathbf{A}_t^U\|_{op} \|\mathbf{B}_t^V\|_{op} \mathcal{M}_t^2 + 2\eta^2\epsilon \|\mathbf{A}_t^U\|_{op} \|\mathbf{B}_t^V\|_{op} \mathcal{M}_t^2 \\
&\quad + \eta \|\mathbf{A}_t^U\|_{op} \|\mathbf{A}_t^{U^\perp}\|_{op} \mathcal{M}_t + \eta^2 \|\mathbf{B}_t^V\|_{op} \|\mathbf{A}_t^{U^\perp}\|_{op} \mathcal{M}_t^2 \\
&\quad + 2\eta^2\epsilon \|\mathbf{B}_t^V\|_{op} \|\mathbf{A}_t^{U^\perp}\|_{op} \mathcal{M}_t^2 + 2\eta\epsilon \|\mathbf{A}_t^U\|_{op} \|\mathbf{A}_t^{U^\perp}\|_{op} \mathcal{M}_t \\
&\quad + 2\eta^2\epsilon \|\mathbf{A}_t^U\|_{op} \|\mathbf{B}_t^V\|_{op} \mathcal{M}_t + 4\eta^2\epsilon^2 \|\mathbf{A}_t^U\|_{op} \|\mathbf{B}_t^V\|_{op} \mathcal{M}_t^2 \\
&\quad + 2\eta\epsilon \|\mathbf{A}_t^{U^\perp}\|_{op}^2 \mathcal{M}_t + 2\eta^2\epsilon \|\mathbf{A}_t^{U^\perp}\|_{op} \|\mathbf{B}_t^V\|_{op} \mathcal{M}_t^2 \\
&\quad + 4\eta^2\epsilon^2 \|\mathbf{A}_t^{U^\perp}\|_{op} \|\mathbf{B}_t^V\|_{op} \mathcal{M}_t^2.
\end{aligned}$$

Finally we conclude the proof. \square

Before we move to the main proof, we need to establish a strict upper bound on \mathbf{A}_t and \mathbf{B}_t .

Lemma B.15. Under assumptions in Section 2.1 for the linear setting, suppose $\|\mathbf{A}_t^\top \mathbf{A}_t - \mathbf{B}_t^\top \mathbf{B}_t\|_{op} + \epsilon \|\mathbf{R}_t\|_{op} \leq \lambda_1^*$ and $\eta \leq \frac{1}{10\lambda_1^*}$, if $\|\mathbf{A}_t\|_{op} \leq 2\sqrt{\lambda_1^*}$ and $\|\mathbf{B}_t\|_{op} \leq 2\sqrt{\lambda_1^*}$, we choose ϵ satisfying Eq. (B.21), then with probability $1 - 2C \exp(-\epsilon^2 N)$ for a universal constant $C > 0$, we have

$$\|\mathbf{A}_{t+1}\|_{op} \leq 2\sqrt{\lambda_1^*}, \quad \|\mathbf{B}_{t+1}\|_{op} \leq 2\sqrt{\lambda_1^*}.$$

Proof. Inspired by Soltanolkotabi et al. (2023), we recall the stacked iterate \mathbf{Z}_t defined in Eq. (B.2) and construct an anti-iterate

$$\underline{\mathbf{Z}}_t := \begin{bmatrix} \mathbf{A}_t \\ -\mathbf{B}_t^\top \end{bmatrix}.$$

Additionally, we define a perturbation matrix

$$\Xi_t := \begin{bmatrix} \mathbf{0}_{d \times d} & (\tilde{\Sigma} - \mathbf{I}_d) \mathbf{R}_t \\ \mathbf{R}_t^\top (\tilde{\Sigma} - \mathbf{I}_d) & \mathbf{0}_{k \times k} \end{bmatrix}.$$

Then, we can reformulate the recursion of \mathbf{Z}_{t+1} as

$$\begin{aligned} \mathbf{Z}_{t+1} &= \mathbf{Z}_t - \eta \left(\mathbf{Z}_t \mathbf{Z}_t^\top - \underline{\mathbf{Z}}_t \underline{\mathbf{Z}}_t^\top - \Gamma \right) \mathbf{Z}_t + \eta \Xi_t \mathbf{Z}_t \\ &= \left(\mathbf{I}_{2d} - \eta \mathbf{Z}_t \mathbf{Z}_t^\top \right) \mathbf{Z}_t + \eta \underline{\mathbf{Z}}_t \underline{\mathbf{Z}}_t^\top \mathbf{Z}_t - \eta \Gamma \mathbf{Z}_t + \eta \Xi_t \mathbf{Z}_t, \end{aligned}$$

where Γ is defined as

$$\Gamma := \begin{bmatrix} \mathbf{0}_{d \times d} & \Delta \\ \Delta^\top & \mathbf{0}_{k \times k} \end{bmatrix}.$$

Then, by the triangle inequality, with probability $1 - 2C \exp(-\epsilon^2 N)$ for a universal constant $C > 0$, we have

$$\begin{aligned} \|\mathbf{Z}_{t+1}\|_{op} &\leq \left\| \left(\mathbf{I}_{2d} - \eta \mathbf{Z}_t \mathbf{Z}_t^\top \right) \mathbf{Z}_t \right\|_{op} + \eta \left\| \underline{\mathbf{Z}}_t \underline{\mathbf{Z}}_t^\top \mathbf{Z}_t \right\|_{op} + \eta \|\Gamma \mathbf{Z}_t\|_{op} + \eta \|\Xi_t \mathbf{Z}_t\|_{op} \\ &\leq \left(1 - \eta \|\mathbf{Z}_t\|_{op}^2 \right) \|\mathbf{Z}_t\|_{op} \quad \text{[by simultaneous diagonalization]} \\ &\quad + \eta \left\| \underline{\mathbf{Z}}_t \underline{\mathbf{Z}}_t^\top \mathbf{Z}_t \right\|_{op} + \eta \|\Gamma \mathbf{Z}_t\|_{op} + \eta \|\Xi_t \mathbf{Z}_t\|_{op} \\ &\leq \left(1 - \eta \|\mathbf{Z}_t\|_{op}^2 \right) \|\mathbf{Z}_t\|_{op} + \eta \left\| \underline{\mathbf{Z}}_t^\top \mathbf{Z}_t \right\|_{op} \|\mathbf{Z}_t\|_{op} + \eta \lambda_1^* \|\mathbf{Z}_t\|_{op} + \eta \epsilon \|\mathbf{R}_t\|_{op} \|\mathbf{Z}_t\|_{op}, \end{aligned}$$

where the last inequality follows from the fact that

$$\begin{aligned} \|\underline{\mathbf{Z}}_t\|_{op} &= \|\mathbf{Z}_t\|_{op}, \\ \|\Gamma\|_{op} &= \lambda_1^*, \\ \|\Xi_t\|_{op} &= \left\| \left(\tilde{\Sigma} - \mathbf{I}_d \right) \mathbf{R}_t \right\|_{op} \leq \epsilon \|\mathbf{R}_t\|_{op}, \quad \text{w.h.p. } 1 - 2C \exp(-\epsilon^2 N). \end{aligned}$$

Using the assumption

$$\left\| \underline{\mathbf{Z}}_t^\top \mathbf{Z}_t \right\|_{op} + \epsilon \|\mathbf{R}_t\|_{op} = \left\| \mathbf{A}_t^\top \mathbf{A}_t - \mathbf{B}_t^\top \mathbf{B}_t \right\|_{op} + \epsilon \|\mathbf{R}_t\|_{op} \leq \lambda_1^*,$$

then $\|\mathbf{Z}_{t+1}\|_{op}$ can be further bounded by

$$\|\mathbf{Z}_{t+1}\|_{op} \leq \left(1 - \eta \|\mathbf{Z}_t\|_{op}^2 + 2\eta \lambda_1^* \right) \|\mathbf{Z}_t\|_{op}. \quad (\text{B.29})$$

Denote $x = \|\mathbf{Z}_t\|_{op}$ and $f(x) = (1 - \eta x^2 + 2\eta \lambda_1^*) x$, we have $f'(x) = 1 + 2\eta \lambda_1^* - 3\eta x^2$ and $f''(x) = -6\eta x$. Then, we know $f'(x^*) = 0$ for $x > 0$ attained at $x^* = \sqrt{\frac{1+2\eta \lambda_1^*}{3\eta}} = \sqrt{\frac{1}{3\eta} + \frac{2}{3} \lambda_1^*}$. As we pick $\eta \leq \frac{1}{10\lambda_1^*}$, then $x^* \geq 2\sqrt{\lambda_1^*}$, which implies the maximum of $f(x)$ attained at $x^* = 2\sqrt{\lambda_1^*}$ over

$x \in [0, 2\lambda_1^*]$ since $\|\mathbf{Z}_t\|_{op} \leq 2\sqrt{\lambda_1^*}$ and

$$f(2\sqrt{\lambda_1^*}) = 2(1 - 4\eta\lambda_1^* + 2\eta\lambda_1^*)\sqrt{\lambda_1^*} = 2\sqrt{\lambda_1^*} - 4\eta\lambda_1^* \leq 2\sqrt{\lambda_1^*},$$

which directly implies $\|\mathbf{Z}_{t+1}\|_{op} \leq 2\sqrt{\lambda_1^*}$. By consequence, $\|\mathbf{A}_{t+1}\|_{op}, \|\mathbf{B}_{t+1}\|_{op} \leq 2\sqrt{\lambda_1^*}$ if $\|\mathbf{A}_t\|_{op}, \|\mathbf{B}_t\|_{op} \leq 2\sqrt{\lambda_1^*}$, since \mathbf{A}_{t+1} and \mathbf{B}_{t+1} are sub-matrices of \mathbf{Z}_{t+1} . \square

Based on the above results, we are ready to present the following intermediate results.

Lemma B.16. Under assumptions in Section 2.1 for the linear setting, with spectral initialization (**Spectral-init**), we take ϵ in data concentration as

$$\epsilon \leq \min \left\{ \frac{1}{2\kappa}, \frac{\lambda_{r^*}^*}{32\kappa(32\lambda_1^* + 128\kappa^2)} \right\},$$

and set the step-size as

$$\eta \leq \min \left\{ \frac{1}{128\kappa\lambda_1^*}, \frac{(1 - \epsilon/\kappa)}{1152\lambda_1^*} \right\},$$

then with probability at least with probability $1 - 2C \exp(-\epsilon^2 N)$ for a universal constant $C > 0$, we have that for $\forall t \geq 0$

$$\mathcal{M}_t \leq \frac{\lambda_{r^*}^*}{2} \tag{B.30}$$

$$\max \left\{ \|\mathbf{A}_t\|_{op}, \|\mathbf{B}_t\|_{op} \right\} \leq 2\sqrt{\lambda_1^*}, \tag{B.31}$$

$$\lambda_{r^*}^*(\mathbf{A}_t), \lambda_{r^*}^*(\mathbf{B}_t) \geq \frac{\sqrt{\lambda_{r^*}^*}}{4\sqrt{\kappa}}, \tag{B.32}$$

$$\|\mathbf{A}_t^{U\perp}\|_{op} \leq \frac{32\kappa\epsilon\sqrt{\lambda_1^*}}{\lambda_{r^*}^*}. \tag{B.33}$$

Also, we can obtain

$$\mathcal{M}_{t+1} \leq \left(1 - \eta \frac{\lambda_{r^*}^*}{64\kappa}\right) \mathcal{M}_t. \tag{B.34}$$

Proof. Inspired by the matrix sensing technique from Xiong et al. (2023), we develop an inductive approach to prove the claims on our settings. At $t = 0$, Eq. (B.30)-Eq. (B.33) can be adopted from Lemma B.11. We assume Eq. (B.30)-Eq. (B.33) hold at $t \geq 1$, recall Eq. (B.26), we have

$$\begin{aligned} \|\mathbf{A}_{t+1}^{U\perp}\|_{op} &\leq (1 - \eta\lambda_{r^*}^2(\mathbf{B}_t^V)) \|\mathbf{A}_t^{U\perp}\|_{op} + \eta\epsilon \|\mathbf{R}_t\|_{op} \|\mathbf{B}_t^V\|_{op} \\ &\leq (1 - \eta\lambda_{r^*}^2(\mathbf{B}_t^V)) \|\mathbf{A}_t^{U\perp}\|_{op} + 4\eta\epsilon\mathcal{M}_t\sqrt{\lambda_1^*} \\ &\leq \left(1 - \eta \frac{(\lambda_{r^*}^*)^2}{16\kappa}\right) \|\mathbf{A}_t^{U\perp}\|_{op} + 2\eta\epsilon\lambda_{r^*}^*\sqrt{\lambda_1^*} \\ &\leq \frac{32\kappa\epsilon\sqrt{\lambda_1^*}}{\lambda_{r^*}^*}, \quad \left[\text{by } \|\mathbf{A}_t^{U\perp}\|_{op} \leq \frac{32\kappa\epsilon\sqrt{\lambda_1^*}}{\lambda_{r^*}^*} \right] \end{aligned}$$

which proves the Eq. (B.33) at $t + 1$. Next, by Lemma B.14, we have

$$\begin{aligned}
\|\mathbf{R}_{t+1}^*\|_{op} &\leq \left(1 - \eta \frac{\lambda_{r^*}^*}{8\kappa}\right) \mathcal{M}_t \\
&\quad + 8\eta\epsilon\lambda_1^* \mathcal{M}_t + 2\eta^2\lambda_1^* \lambda_{r^*}^* \mathcal{M}_t + 4\eta^2\epsilon\lambda_1^* \lambda_{r^*}^* \mathcal{M}_t + 64\eta\epsilon\kappa^2 \mathcal{M}_t + 32\eta^2\kappa^2\epsilon\lambda_{r^*}^* \mathcal{M}_t + 128\eta^2\epsilon^3\kappa^2\lambda_{r^*}^* \mathcal{M}_t \\
&\quad + 64\eta^2\epsilon^2\kappa^2\lambda_{r^*}^* \mathcal{M}_t + 8\eta\epsilon\lambda_1^* \mathcal{M}_t + 8\eta^2\epsilon\lambda_1^* \mathcal{M}_t + 8\eta^2\epsilon^2\lambda_1^* \lambda_{r^*}^* \mathcal{M}_t + 128\eta\epsilon^2\kappa^2 \mathcal{M}_t + 64\eta^2\epsilon^2\kappa^2\lambda_{r^*}^* \mathcal{M}_t \\
&= \left(1 - \eta \frac{\lambda_{r^*}^*}{8\kappa}\right) \mathcal{M}_t \\
&\quad + \eta \left\{ 16\epsilon\lambda_1^* + 64\epsilon\kappa^2 + 2\eta\lambda_1^* \lambda_{r^*}^* + \eta\epsilon (4\lambda_1^* \lambda_{r^*}^* + 32\kappa^2\lambda_{r^*}^* + 8\lambda_1^*) + 128\epsilon^2\kappa^2 \right. \\
&\quad \left. + \eta (128\eta\epsilon^2\kappa^2\lambda_{r^*}^* + 8\eta\epsilon^2\lambda_1^* \lambda_{r^*}^*) + 128\eta\epsilon^3\kappa^2\lambda_{r^*}^* \right\} \mathcal{M}_t \\
&\leq \left(1 - \eta \frac{\lambda_{r^*}^*}{8\kappa}\right) \mathcal{M}_t + 2\eta \left(16\epsilon\lambda_1^* + 64\epsilon\kappa^2 + 2\eta\lambda_1^* \lambda_{r^*}^*\right) \mathcal{M}_t && \text{[due to the order dominance]} \\
&\leq \left(1 - \eta \frac{\lambda_{r^*}^*}{16\kappa}\right) \mathcal{M}_t + 2\eta \left(16\epsilon\lambda_1^* + 64\epsilon\kappa^2\right) \mathcal{M}_t && \text{[by } \eta \leq \frac{1}{64\kappa\lambda_1^*}] \\
&\leq \left(1 - \eta \frac{\lambda_{r^*}^*}{32\kappa}\right) \mathcal{M}_t, && \text{[by } \epsilon \leq \frac{\lambda_{r^*}^*}{16\kappa(32\lambda_1^* + 128\kappa^2)}]
\end{aligned}$$

where the order dominance from the second inequality follows from the fact that η and ϵ are sufficiently small constant such that the terms in $\mathcal{O}(\eta\epsilon)$, $\mathcal{O}(\epsilon^2)$, $\mathcal{O}(\eta^2\epsilon^2)$, $\mathcal{O}(\eta\epsilon^3)$ are significantly smaller the terms in $\mathcal{O}(\eta)$ and $\mathcal{O}(\epsilon)$.

Similarly, we can obtain

$$\begin{aligned}
\|\mathbf{R}_{t+1}^\perp\|_{op} &\leq \left(1 - \eta \frac{\lambda_{r^*}^*}{16\kappa}\right) \mathcal{M}_t && \text{[since } \lambda_{\min}(\mathbf{A}_t^{U^\perp}) \geq 0] \\
&\quad + \eta \left\{ 8\epsilon\lambda_1^* + 2\eta\lambda_1^* \lambda_{r^*}^* + 4\eta\epsilon\lambda_1^* \lambda_{r^*}^* + 64\epsilon\kappa^2 + 32\eta\epsilon\kappa^2\lambda_{r^*}^* + 64\eta\epsilon\kappa^2\lambda_{r^*}^* + 128\epsilon^2\kappa^2 \right. \\
&\quad \left. + 8\eta\epsilon\lambda_1^* + 8\eta\epsilon^2\lambda_1^* \lambda_{r^*}^* + 2048\epsilon^3 \frac{\kappa^3}{\lambda_{r^*}^*} + 64\eta\epsilon^2\kappa^2 + 128\eta\epsilon^3\kappa^2 \right\} \mathcal{M}_t \\
&\leq \left(1 - \eta \frac{\lambda_{r^*}^*}{16\kappa}\right) \mathcal{M}_t + 2\eta \left\{ 8\epsilon\lambda_1^* + 2\eta\lambda_1^* \lambda_{r^*}^* + 64\epsilon\kappa^2 \right\} \mathcal{M}_t && \text{[due to the order dominance]} \\
&\leq \left(1 - \eta \frac{\lambda_{r^*}^*}{32\kappa}\right) \mathcal{M}_t + 2\eta \left\{ 8\epsilon\lambda_1^* + 64\epsilon\kappa^2 \right\} \mathcal{M}_t && \text{[by } \eta \leq \frac{1}{128\kappa\lambda_1^*}] \\
&\leq \left(1 - \eta \frac{\lambda_{r^*}^*}{64\kappa}\right) \mathcal{M}_t, && \text{[by } \epsilon \leq \frac{\lambda_{r^*}^*}{32\kappa(32\lambda_1^* + 128\kappa^2)}]
\end{aligned}$$

which proves the Eq. (B.30) at $t + 1$.

Therefore, we can conclude that

$$\mathcal{M}_{t+1} \leq \left(1 - \eta \frac{\lambda_{r^*}^*}{64\kappa}\right) \mathcal{M}_t.$$

Next, assume Eq. (B.30)-Eq. (B.33) hold at $t \geq 1$, we have

$$\begin{aligned} \left(\mathbf{A}_{t+1}^\top \mathbf{A}_{t+1} - \mathbf{B}_{t+1} \mathbf{B}_{t+1}^\top\right) - \left(\mathbf{A}_t^\top \mathbf{A}_t - \mathbf{B}_t \mathbf{B}_t^\top\right) &= \eta^2 \mathbf{B}_t (\mathbf{A}_t \mathbf{B}_t - \Delta)^\top \widehat{\Sigma} \widehat{\Sigma} (\mathbf{A}_t \mathbf{B}_t - \Delta) \mathbf{B}_t^\top \\ &\quad + \eta^2 \mathbf{A}_t^\top \widehat{\Sigma} (\mathbf{A}_t \mathbf{B}_t - \Delta) (\mathbf{A}_t \mathbf{B}_t - \Delta)^\top \widehat{\Sigma} \mathbf{A}_t. \end{aligned}$$

Accordingly, we can derive

$$\begin{aligned} &\left\| \left(\mathbf{A}_{t+1}^\top \mathbf{A}_{t+1} - \mathbf{B}_{t+1} \mathbf{B}_{t+1}^\top\right) - \left(\mathbf{A}_0^\top \mathbf{A}_0 - \mathbf{B}_0 \mathbf{B}_0^\top\right) \right\|_{op} \\ &= \sum_{i=1}^{t+1} \left\| \left(\mathbf{A}_i^\top \mathbf{A}_i - \mathbf{B}_i \mathbf{B}_i^\top\right) - \left(\mathbf{A}_{i-1}^\top \mathbf{A}_{i-1} - \mathbf{B}_{i-1} \mathbf{B}_{i-1}^\top\right) \right\|_{op} \\ &= \sum_{i=1}^{t+1} 2\eta^2 \|\widehat{\Sigma}\|_{op}^2 \|\mathbf{R}_{i-1}\|_{op}^2 \max\{\|\mathbf{A}_{i-1}\|_{op}^2, \|\mathbf{B}_{i-1}\|_{op}^2\} \\ &= \sum_{i=1}^{t+1} 72\eta^2 \mathcal{M}_{i-1}^2 \lambda_1^* \tag{by Eq. (B.21)} \\ &\leq \sum_{i=1}^{t+1} 18\eta^2 \left(1 - \eta \frac{\lambda_{r^*}^*}{64\kappa}\right)^{2(i-1)} (\lambda_{r^*}^*)^2 \lambda_1^* \\ &\leq 18\eta^2 (\lambda_{r^*}^*)^2 \lambda_1^* \sum_{i=0}^{\infty} \left(1 - \eta \frac{\lambda_{r^*}^*}{64\kappa}\right)^{2i} \\ &\leq 18\eta^2 (\lambda_{r^*}^*)^2 \lambda_1^* \frac{64\kappa}{\eta \lambda_{r^*}^*} \\ &= 1152\eta \lambda_1^* \lambda_{r^*}^* \kappa \\ &\leq (1 - \epsilon/\kappa) \lambda_1^*. \tag{by } \eta \leq \frac{(1-\epsilon/\kappa)}{1152\lambda_1^*} \end{aligned}$$

Since $\|(\mathbf{A}_0^\top \mathbf{A}_0 - \mathbf{B}_0 \mathbf{B}_0^\top)\|_{op} = 0$ due to the spectral initialization (**Spectral-init**), by triangle inequality, $\|(\mathbf{A}_{t+1}^\top \mathbf{A}_{t+1} - \mathbf{B}_{t+1} \mathbf{B}_{t+1}^\top)\|_{op} \leq (1 - \epsilon/\kappa) \lambda_1^*$. Next, by Lemma B.15, we can obtain

$$\|\mathbf{A}_{t+1}\|_{op} \leq 2\sqrt{\lambda_1^*}, \quad \|\mathbf{B}_{t+1}\|_{op} \leq 2\sqrt{\lambda_1^*},$$

which proves the Eq. (B.31) at $t + 1$. Lastly, assume Eq. (B.30)-Eq. (B.33) hold at $t \geq 1$, by Weyl's inequality, combine with $\mathcal{M}_{t+1} \leq \frac{\lambda_{r^*}^*}{2}$, we have

$$\frac{\lambda_{r^*}^*}{2} \geq \|\mathbf{A}_{t+1}^U \mathbf{B}_{t+1}^V - \mathbf{S}^*\|_{op} \geq \lambda_{r^*}^* - \lambda_{r^*}(\mathbf{A}_{t+1}^U \mathbf{B}_{t+1}^V) \Rightarrow \lambda_{r^*}(\mathbf{A}_{t+1}^U \mathbf{B}_{t+1}^V) \geq \frac{\lambda_{r^*}^*}{2}.$$

Again by Weyl's inequality and the Eq. (B.31) at time $t + 1$ we can get

$$2\sqrt{\lambda_1^*} \cdot \lambda_{r^*}(\mathbf{B}_{t+1}^V) \geq \lambda_1(\mathbf{A}_{t+1}^U) \lambda_{r^*}(\mathbf{B}_{t+1}^V) \geq \lambda_{r^*}(\mathbf{A}_{t+1}^U \mathbf{B}_{t+1}^V) \geq \frac{\lambda_{r^*}^*}{2} \Rightarrow \lambda_{r^*}(\mathbf{B}_{t+1}^V) \geq \frac{\sqrt{\lambda_{r^*}^*}}{4\sqrt{\kappa}}.$$

Besides, $\lambda_{r^*}(\mathbf{A}_{t+1}^U)$ follows similar derivation. We prove all the claims. \square

Theorem B.17. Under assumptions in Section 2.1 for the linear setting, with spectral initialization (Spectral-init), we take ϵ in data concentration as

$$\epsilon \leq \min \left\{ \frac{1}{2\kappa}, \frac{\lambda_{r^*}^*}{32\kappa(32\lambda_1^* + 128\kappa^2)} \right\},$$

and set the step-size as

$$\eta \leq \min \left\{ \frac{1}{128\kappa\lambda_1^*}, \frac{(1 - \epsilon/\kappa)}{1152\lambda_1^*} \right\}, \quad (\text{B.35})$$

then with probability at least with probability $1 - 2C \exp(-\epsilon^2 N)$ for a universal constant $C > 0$, we have that for $\forall t \geq 0$

$$\|\mathbf{A}_t \mathbf{B}_t - \Delta\|_F \leq \sqrt{2r^*} \left(1 - \eta \frac{\lambda_{r^*}^*}{64\kappa} \right)^t \cdot \lambda_{r^*}^*.$$

Proof. By Lemma B.16, with probability at least with probability $1 - 2C \exp(-\epsilon^2 N)$ for a universal constant $C > 0$, we can obtain the linear convergence of generalization risk

$$\begin{aligned} \|\mathbf{A}_t \mathbf{B}_t - \Delta\|_F &\leq \sqrt{2r^*} \|\mathbf{A}_t \mathbf{B}_t - \Delta\|_{op} \quad [\text{Rank}(\mathbf{A}_t \mathbf{B}_t) = r^* \text{ by Lemma B.12 and Rank}(\Delta) = r^*] \\ &\leq \sqrt{2r^*} \left(1 - \eta \frac{\lambda_{r^*}^*}{64\kappa} \right)^t \cdot \lambda_{r^*}^*, \end{aligned}$$

which is independent of the choice of LoRA rank r if $r \geq r^*$. \square

B.3 Preconditioned Gradient Descent under Spectral Initialization

Here we present the proof for preconditioned gradient descent.

$$\begin{aligned} \mathbf{A}_{t+1} &= \mathbf{A}_t - \frac{\eta}{N} \widetilde{\mathbf{X}}^\top \left(\widetilde{\mathbf{X}} \left(\mathbf{W}^\natural + \mathbf{A}_t \mathbf{B}_t \right) - \widetilde{\mathbf{Y}} \right) \mathbf{B}_t^\top \left(\mathbf{B}_t \mathbf{B}_t^\top \right)^\dagger, \\ \mathbf{B}_{t+1} &= \mathbf{B}_t - \frac{\eta}{N} \left(\mathbf{A}_t^\top \mathbf{A}_t \right)^\dagger \mathbf{A}_t^\top \widetilde{\mathbf{X}}^\top \left(\widetilde{\mathbf{X}} \left(\mathbf{W}^\natural + \mathbf{A}_t \mathbf{B}_t \right) - \widetilde{\mathbf{Y}} \right). \end{aligned} \quad (\text{Prec-GD})$$

In the following proofs, we will prove that the LoRA fine-tuning can achieve faster linear convergence which is independent of condition number κ under (Spectral-init) and (Prec-GD). Similar to Lemma B.12, the dynamics of \mathbf{B}_t are still limited to the r^* -dimensional singular subspace \mathbf{V} of Δ under (Spectral-init). We can verify this fact by the following lemma.

Lemma B.18. For any natural number $t \geq 0$, under assumptions in Section 2.1 for the linear

setting, with (Spectral-init) and (Prec-GD), we have

$$\mathbf{B}_t \mathbf{V}_\perp = \mathbf{0}_{r \times (k-r^*)}.$$

Proof. For $t = 0$, recall the SVD of \mathbf{G}^\natural , i.e. $\tilde{\mathbf{U}}_{\mathbf{G}^\natural} \tilde{\mathbf{S}}_{\mathbf{G}^\natural} \tilde{\mathbf{V}}_{\mathbf{G}^\natural}^\top$ in Eq. (B.20), we have

$$\mathbf{B}_0 \mathbf{V}_\perp = \left[\tilde{\mathbf{S}}_{\mathbf{G}^\natural}^{-1/2} \right]_{[1:r]} \left[\tilde{\mathbf{U}}_{\mathbf{G}^\natural}^\top \right]_{[:,1:r]} \mathbf{G}^\natural \mathbf{V}_\perp = \left[\tilde{\mathbf{S}}_{\mathbf{G}^\natural}^{-1/2} \right]_{[1:r]} \left[\tilde{\mathbf{U}}_{\mathbf{G}^\natural}^\top \right]_{[:,1:r]} \hat{\Sigma} \Delta \mathbf{V}_\perp = \mathbf{0}_{r \times (k-r^*)}.$$

Assume $\mathbf{B}_t \mathbf{V}_\perp = \mathbf{0}_{d \times (d-r^*)}$ holds for any natural number $t \geq 1$, then

$$\begin{aligned} \mathbf{B}_{t+1} \mathbf{V}_\perp &= \mathbf{B}_t \mathbf{V}_\perp - \frac{\eta}{N} \left(\mathbf{A}_t^\top \mathbf{A}_t \right)^\dagger \mathbf{A}_t^\top \tilde{\mathbf{X}}^\top \left(\tilde{\mathbf{X}} \left(\mathbf{W}^\natural + \mathbf{A}_t \mathbf{B}_t \right) - \tilde{\mathbf{Y}} \right) \mathbf{V}_\perp \\ &= \mathbf{B}_t \mathbf{V}_\perp - \eta \left(\mathbf{A}_t^\top \mathbf{A}_t \right)^\dagger \mathbf{A}_t^\top \hat{\Sigma} \left(\mathbf{A}_t \mathbf{B}_t - \Delta \right) \mathbf{V}_\perp \\ &= \mathbf{0}_{r \times (k-r^*)}, \end{aligned} \quad \text{[by our inductive hypothesis]}$$

which proves the claim. \square

We can re-formulate (Prec-GD) to be

$$\mathbf{A}_{t+1} = \mathbf{A}_t - \eta \hat{\Sigma} \left(\mathbf{A}_t \mathbf{B}_t - \Delta \right) \left(\mathbf{B}_t \right)^\top \left(\mathbf{B}_t \mathbf{B}_t^\top \right)^\dagger, \quad (\text{B.36})$$

$$\mathbf{B}_{t+1} = \mathbf{B}_t - \eta \left(\mathbf{A}_t^\top \mathbf{A}_t \right)^\dagger \mathbf{A}_t^\top \hat{\Sigma} \left(\mathbf{A}_t \mathbf{B}_t - \Delta \right). \quad (\text{B.37})$$

Before we start our main proofs, we first define the following notations

- SVD of product matrix $\mathbf{A}_t \mathbf{B}_t := \mathbf{U}_t \mathcal{S}_t \mathcal{V}_t^\top$, where $\mathbf{U}_t \in \mathbb{R}^{d \times r^*}$, $\mathcal{S}_t \in \mathbb{R}^{r^* \times r^*}$, and $\mathcal{V}_t \in \mathbb{R}^{k \times r^*}$. Notice that here we employ rank- r^* SVD of $\mathbf{A}_t \mathbf{B}_t$ since $\text{Rank}(\mathbf{A}_t \mathbf{B}_t) \leq r^*$ due to Lemma B.18 and $\lambda_{r^*}(\mathbf{A}_t \mathbf{B}_t) > 0$ strictly which we will obtain from Theorem B.21.
- The left compact singular matrix of \mathbf{A}_t as $\mathbf{U}_{\mathbf{A}_t} \in \mathbb{R}^{d \times r}$.
- The right compact singular matrix of \mathbf{B}_t as $\mathbf{V}_{\mathbf{B}_t} \in \mathbb{R}^{k \times r^*}$. Notice that here we take the top- r^* right singular subspace of \mathbf{B}_t due to Lemma B.18.

By the pseudo inverse theorem and Jia et al. (2024, Lemma 14), we can obtain

$$\mathbf{A}_t \left(\mathbf{A}_t^\top \mathbf{A}_t \right)^\dagger \mathbf{A}_t^\top = \mathbf{U}_{\mathbf{A}_t} \mathbf{U}_{\mathbf{A}_t}^\top, \quad (\text{B.38})$$

$$\left(\mathbf{B}_t \right)^\top \left(\mathbf{B}_t \mathbf{B}_t^\top \right)^\dagger \mathbf{B}_t = \mathbf{V}_{\mathbf{B}_t} \mathbf{V}_{\mathbf{B}_t}^\top. \quad (\text{B.39})$$

$$\left(\mathbf{B}_t \right)^\top \left(\mathbf{B}_t \mathbf{B}_t^\top \right)^\dagger \left(\mathbf{A}_t^\top \mathbf{A}_t \right)^\dagger \mathbf{A}_t^\top = \mathcal{V}_t \mathcal{S}_t^{-1} \mathbf{U}_t^\top. \quad (\text{B.40})$$

Lemma B.19. Denote $\mathbf{R}_t := \mathbf{A}_t \mathbf{B}_t - \Delta$, $\Xi := \hat{\Sigma} - \mathbf{I}_d$, under assumptions in Section 2.1 for the linear setting, with (Prec-GD), then we have

$$\mathbf{R}_{t+1} = \mathbf{R}_t - \eta \mathbf{U}_{\mathbf{A}_t} \mathbf{U}_{\mathbf{A}_t}^\top \mathbf{R}_t - \eta \mathbf{R}_t \mathbf{V}_{\mathbf{B}_t} \mathbf{V}_{\mathbf{B}_t}^\top - \eta \mathbf{U}_{\mathbf{A}_t} \mathbf{U}_{\mathbf{A}_t}^\top \Xi \mathbf{R}_t - \eta \Xi \mathbf{R}_t \mathbf{V}_{\mathbf{B}_t} \mathbf{V}_{\mathbf{B}_t}^\top + \eta^2 \hat{\Sigma} \mathbf{R}_t \mathcal{V}_t \mathcal{S}_t^{-1} \mathbf{U}_t^\top \hat{\Sigma} \mathbf{R}_t.$$

Proof. With Eq. (B.36) and Eq. (B.37), we can construct

$$\begin{aligned}
\mathbf{R}_{t+1} &= \mathbf{A}_{t+1}\mathbf{B}_{t+1} - \Delta \\
&= \mathbf{A}_t\mathbf{B}_t - \Delta \\
&\quad - \eta\mathbf{A}_t \left(\mathbf{A}_t^\top \mathbf{A}_t \right)^\dagger \mathbf{A}_t^\top \widehat{\Sigma} (\mathbf{A}_t\mathbf{B}_t - \Delta) \\
&\quad - \eta \widehat{\Sigma} (\mathbf{A}_t\mathbf{B}_t - \Delta) (\mathbf{B}_t)^\top \left(\mathbf{B}_t\mathbf{B}_t^\top \right)^\dagger \mathbf{B}_t \\
&\quad + \eta^2 \widehat{\Sigma} (\mathbf{A}_t\mathbf{B}_t - \Delta) (\mathbf{B}_t)^\top \left(\mathbf{B}_t\mathbf{B}_t^\top \right)^\dagger \left(\mathbf{A}_t^\top \mathbf{A}_t \right)^\dagger \mathbf{A}_t^\top \widehat{\Sigma} (\mathbf{A}_t\mathbf{B}_t - \Delta) \\
&= \mathbf{R}_t - \eta\mathbf{U}_{\mathbf{A}_t}\mathbf{U}_{\mathbf{A}_t}^\top \widehat{\Sigma}\mathbf{R}_t - \eta \widehat{\Sigma}\mathbf{R}_t\mathbf{V}_{\mathbf{B}_t}\mathbf{V}_{\mathbf{B}_t}^\top \quad [\text{by Eq. (B.38) and Eq. (B.39)}] \\
&\quad + \eta^2 \widehat{\Sigma}\mathbf{R}_t\mathcal{V}_t\mathcal{S}_t^{-1}\mathcal{U}_t^\top \widehat{\Sigma}\mathbf{R}_t \quad [\text{by Eq. (B.40)}] \\
&= \mathbf{R}_t - \eta\mathbf{U}_{\mathbf{A}_t}\mathbf{U}_{\mathbf{A}_t}^\top \mathbf{R}_t - \eta\mathbf{R}_t\mathbf{V}_{\mathbf{B}_t}\mathbf{V}_{\mathbf{B}_t}^\top - \eta\mathbf{U}_{\mathbf{A}_t}\mathbf{U}_{\mathbf{A}_t}^\top \Xi\mathbf{R}_t - \eta\Xi\mathbf{R}_t\mathbf{V}_{\mathbf{B}_t}\mathbf{V}_{\mathbf{B}_t}^\top + \eta^2 \widehat{\Sigma}\mathbf{R}_t\mathcal{V}_t\mathcal{S}_t^{-1}\mathcal{U}_t^\top \widehat{\Sigma}\mathbf{R}_t,
\end{aligned}$$

which proves the claim. \square

In the next, we aim to estimate the signal part $\mathbf{R}_t - \eta\mathbf{U}_{\mathbf{A}_t}\mathbf{U}_{\mathbf{A}_t}^\top \mathbf{R}_t - \eta\mathbf{R}_t\mathbf{V}_{\mathbf{B}_t}\mathbf{V}_{\mathbf{B}_t}^\top$.

Lemma B.20. Recall $\mathbf{R}_t := \mathbf{A}_t\mathbf{B}_t - \Delta$, under assumptions in Section 2.1 for the linear setting, with (Prec-GD), then

$$\left\| \mathbf{R}_t - \eta\mathbf{U}_{\mathbf{A}_t}\mathbf{U}_{\mathbf{A}_t}^\top \mathbf{R}_t - \eta\mathbf{R}_t\mathbf{V}_{\mathbf{B}_t}\mathbf{V}_{\mathbf{B}_t}^\top \right\|_{\mathbb{F}} \leq (1 - \eta) \|\mathbf{R}_t\|_{\mathbb{F}}.$$

Proof.

$$\begin{aligned}
&\left\| \mathbf{R}_t - \eta\mathbf{U}_{\mathbf{A}_t}\mathbf{U}_{\mathbf{A}_t}^\top \mathbf{R}_t - \eta\mathbf{R}_t\mathbf{V}_{\mathbf{B}_t}\mathbf{V}_{\mathbf{B}_t}^\top \right\|_{\mathbb{F}} \\
&= \left\| \mathbf{R}_t \left(\mathbf{V}_{\mathbf{B}_t}\mathbf{V}_{\mathbf{B}_t}^\top + \mathbf{I}_k - \mathbf{V}_{\mathbf{B}_t}\mathbf{V}_{\mathbf{B}_t}^\top \right) - \eta\mathbf{U}_{\mathbf{A}_t}\mathbf{U}_{\mathbf{A}_t}^\top \mathbf{R}_t \left(\mathbf{V}_{\mathbf{B}_t}\mathbf{V}_{\mathbf{B}_t}^\top + \mathbf{I}_k - \mathbf{V}_{\mathbf{B}_t}\mathbf{V}_{\mathbf{B}_t}^\top \right) - \eta\mathbf{R}_t\mathbf{V}_{\mathbf{B}_t}\mathbf{V}_{\mathbf{B}_t}^\top \right\|_{\mathbb{F}} \\
&= \left\| \mathbf{R}_t\mathbf{V}_{\mathbf{B}_t}\mathbf{V}_{\mathbf{B}_t}^\top - \eta\mathbf{U}_{\mathbf{A}_t}\mathbf{U}_{\mathbf{A}_t}^\top \mathbf{R}_t\mathbf{V}_{\mathbf{B}_t}\mathbf{V}_{\mathbf{B}_t}^\top - \eta\mathbf{R}_t\mathbf{V}_{\mathbf{B}_t}\mathbf{V}_{\mathbf{B}_t}^\top \right\|_{\mathbb{F}} \quad [\text{since } \mathbf{R}_t(\mathbf{I}_k - \mathbf{V}_{\mathbf{B}_t}\mathbf{V}_{\mathbf{B}_t}^\top) = \mathbf{0} \text{ by Lemma B.18}] \\
&= \left\| \left(\mathbf{I}_d - \eta \left(\mathbf{I}_d + \mathbf{U}_{\mathbf{A}_t}\mathbf{U}_{\mathbf{A}_t}^\top \right) \right) \mathbf{R}_t\mathbf{V}_{\mathbf{B}_t}\mathbf{V}_{\mathbf{B}_t}^\top \right\|_{\mathbb{F}} \\
&= \left\| \mathbf{I}_d - \eta \left(\mathbf{I}_d + \mathbf{U}_{\mathbf{A}_t}\mathbf{U}_{\mathbf{A}_t}^\top \right) \right\|_{op} \left\| \mathbf{R}_t\mathbf{V}_{\mathbf{B}_t}\mathbf{V}_{\mathbf{B}_t}^\top \right\|_{\mathbb{F}} \\
&\leq (1 - \eta) \|\mathbf{R}_t\|_{\mathbb{F}}, \\
&\quad \left[\left\| \mathbf{I}_d - \eta \left(\mathbf{I}_d + \mathbf{U}_{\mathbf{A}_t}\mathbf{U}_{\mathbf{A}_t}^\top \right) \right\|_{op} \leq 1 - \eta, \text{ since } \mathbf{U}_{\mathbf{A}_t}\mathbf{U}_{\mathbf{A}_t}^\top \text{ is a rank-}r \text{ projection matrix} \right]
\end{aligned}$$

which concludes the proof. \square

Theorem B.21. Under assumptions in Section 2.1 for the linear setting, with (Spectral-init) and (Prec-GD), we choose

$$\epsilon \leq \min \left\{ \frac{1}{2\sqrt{r^*\kappa}}, \frac{1}{4} \right\}$$

and set $\eta \in \left(0, \frac{0.5-2\epsilon}{(1+\epsilon)^2} \right)$, then with probability at least $1 - 2C \exp(-\epsilon^2 N)$ for a universal constant

$C > 0$, we have

$$\|\mathbf{A}_t \mathbf{B}_t - \Delta\|_{\text{F}} \leq \frac{1}{2} \left(1 - \frac{\eta}{2}\right)^t \lambda_{r^*}^*.$$

Proof. We prove it by induction. We suppose the following two inductive hypothesis

$$\lambda_{r^*}(\mathbf{A}_t \mathbf{B}_t) \geq \frac{\lambda_{r^*}^*}{2}, \quad (\text{B.41})$$

$$\|\mathbf{A}_0 \mathbf{B}_0 - \Delta\|_{\text{F}} \leq \frac{\lambda_{r^*}^*}{2}. \quad (\text{B.42})$$

Starting from $t = 0$, under **(Spectral-init)**, with probability at least $1 - 2C \exp(-\epsilon^2 N)$ for a universal constant $C > 0$, we have

$$\begin{aligned} \|\mathbf{A}_0 \mathbf{B}_0 - \Delta\|_{\text{F}} &= \|\mathbf{G}^{\dagger} - \Delta\|_{\text{F}} \\ &= \left\| \left(\widehat{\Sigma} - \mathbf{I}_d \right) \Delta \right\|_{\text{F}} && \text{[by Eq. (B.20)]} \\ &\leq \epsilon \|\Delta\|_{\text{F}} \\ &\leq \epsilon \sqrt{r^*} \|\Delta\|_{\text{op}} && \text{[since Rank}(\Delta) = r^*] \\ &\leq \frac{\lambda_{r^*}^*}{2}. && \text{[since } \epsilon \leq 1/2\sqrt{r^* \kappa}] \end{aligned}$$

Then, by Weyl's inequality, we have

$$\lambda_{r^*}(\Delta) - \lambda_{r^*}(\mathbf{A}_0 \mathbf{B}_0) \leq \|\mathbf{A}_0 \mathbf{B}_0 - \Delta\|_{\text{op}} \leq \|\mathbf{A}_0 \mathbf{B}_0 - \Delta\|_{\text{F}},$$

which implies

$$\lambda_{r^*}(\mathbf{A}_0 \mathbf{B}_0) \geq \frac{\lambda_{r^*}^*}{2}. \quad (\text{B.43})$$

Therefore, we verify Eq. (B.41) and Eq. (B.42) at $t = 0$. We assume Eq. (B.41) and Eq. (B.42) hold at $t = 2, 3, \dots$, then by Lemma B.19, with probability at least with probability $1 - 2C \exp(-\epsilon^2 N)$ for a universal constant $C > 0$, we have

$$\begin{aligned} \|\mathbf{R}_{t+1}\|_{\text{F}} &\leq \left\| \mathbf{R}_t - \eta \mathbf{U}_{\mathbf{A}_t} \mathbf{U}_{\mathbf{A}_t}^{\top} \mathbf{R}_t - \eta \mathbf{R}_t \mathbf{V}_{\mathbf{B}_t} \mathbf{V}_{\mathbf{B}_t}^{\top} \right\|_{\text{F}} \\ &\quad + \eta \left\| \mathbf{U}_{\mathbf{A}_t} \mathbf{U}_{\mathbf{A}_t}^{\top} \Xi \mathbf{R}_t \right\|_{\text{F}} + \eta \left\| \Xi \mathbf{R}_t \mathbf{V}_{\mathbf{B}_t} \mathbf{V}_{\mathbf{B}_t}^{\top} \right\|_{\text{F}} + \eta^2 \left\| \widehat{\Sigma} \mathbf{R}_t \mathcal{V}_t \mathcal{S}_t^{-1} \mathcal{U}_t^{\top} \widehat{\Sigma} \mathbf{R}_t \right\|_{\text{F}} \\ &\leq (1 - \eta) \|\mathbf{R}_t\|_{\text{F}} && \text{[by Lemma B.20]} \\ &\quad + \eta \epsilon \left\| \mathbf{U}_{\mathbf{A}_t} \mathbf{U}_{\mathbf{A}_t}^{\top} \mathbf{R}_t \right\|_{\text{F}} + \eta \epsilon \left\| \mathbf{R}_t \mathbf{V}_{\mathbf{B}_t} \mathbf{V}_{\mathbf{B}_t}^{\top} \right\|_{\text{F}} + \eta^2 (1 + \epsilon)^2 \frac{\|\mathbf{R}_t\|_{\text{F}}^2}{\lambda_{r^*}(\mathbf{A}_t \mathbf{B}_t)} && \text{[by } \|\Xi\|_{\text{op}} \leq \epsilon] \\ &\leq (1 - \eta) \|\mathbf{R}_t\|_{\text{F}} \\ &\quad + \eta \epsilon \|\mathbf{R}_t\|_{\text{F}} + \eta \epsilon \|\mathbf{R}_t\|_{\text{F}} + \eta^2 (1 + \epsilon)^2 \|\mathbf{R}_t\|_{\text{F}} && \text{[since Eq. (B.41) and Eq. (B.42) hold at } t] \\ &= (1 - (1 - 2\epsilon)\eta + \eta^2 (1 + \epsilon)^2) \|\mathbf{R}_t\|_{\text{F}} \\ &\leq \left(1 - \frac{\eta}{2}\right) \|\mathbf{R}_t\|_{\text{F}}. && \text{[taking } \eta \leq \frac{0.5 - 2\epsilon}{(1 + \epsilon)^2}] \end{aligned}$$

This implies Eq. (B.42) at time $t + 1$. By consequence, we can obtain Eq. (B.41) at time $t + 1$ again by Weyl's inequality. \square

C Proofs for Nonlinear Model

We deliver the proofs for nonlinear models in Section 4 here. The problem setting and results for $\|\mathbf{A}_0\mathbf{B}_0 - \Delta\|_F$ are presented in Appendix C.1. In Appendix C.2, we present the proofs of Theorem 4.3 as well as proofs for smoothed GD.

C.1 Problem Settings and Spectral Initialization

Recall the pre-training model from Assumption 2.1

$$f_{\text{pre}}(\mathbf{x}) = \sigma(\mathbf{x}^\top \mathbf{W}^\natural)^\top \in \mathbb{R}^k, \quad \mathbf{W}^\natural \in \mathbb{R}^{d \times k}, \quad (\text{C.1})$$

and the downstream teacher weights from Assumption 2.2

$$\widetilde{\mathbf{W}}^\natural = \mathbf{W}^\natural + \Delta \in \mathbb{R}^{d \times k}, \quad \text{with } \widetilde{\mathbf{W}}^\natural := [\widetilde{\mathbf{w}}_1^\natural, \widetilde{\mathbf{w}}_2^\natural, \dots, \widetilde{\mathbf{w}}_k^\natural].$$

The empirical loss of LoRA fine-tuning is defined as

$$\widetilde{L}(\mathbf{A}_t, \mathbf{B}_t) = \frac{1}{2N} \left\| \sigma(\widetilde{\mathbf{X}}(\mathbf{W}^\natural + \mathbf{A}_t\mathbf{B}_t)) - \sigma(\widetilde{\mathbf{X}}\widetilde{\mathbf{W}}^\natural) \right\|_F^2.$$

Next, we can derive the empirical gradients for \mathbf{A}_t and \mathbf{B}_t respectively.

$$\begin{aligned} \nabla_{\mathbf{A}} \widetilde{L}(\mathbf{A}_t, \mathbf{B}_t) &= \frac{1}{N} \widetilde{\mathbf{X}}^\top \left[\sigma(\widetilde{\mathbf{X}}(\mathbf{W}^\natural + \mathbf{A}_t\mathbf{B}_t)) - \sigma(\widetilde{\mathbf{X}}\widetilde{\mathbf{W}}^\natural) \right] \odot \sigma'(\widetilde{\mathbf{X}}(\mathbf{W}^\natural + \mathbf{A}_t\mathbf{B}_t)) \mathbf{B}_t^\top \\ &:= \frac{1}{N} \widetilde{\mathbf{X}}^\top \left[\sigma(\widetilde{\mathbf{X}}(\mathbf{W}_t)) - \sigma(\widetilde{\mathbf{X}}\widetilde{\mathbf{W}}^\natural) \right] \odot \sigma'(\widetilde{\mathbf{X}}\mathbf{W}_t) \mathbf{B}_t^\top \\ &\hspace{25em} \text{[denote } \mathbf{W}_t := \mathbf{W}^\natural + \mathbf{A}_t\mathbf{B}_t] \\ &= - \left[\underbrace{\frac{1}{N} \widetilde{\mathbf{X}}^\top \sigma(\widetilde{\mathbf{X}}\widetilde{\mathbf{W}}^\natural) \odot \sigma'(\widetilde{\mathbf{X}}\mathbf{W}_t)}_{:=\Gamma_{1,t}} - \underbrace{\frac{1}{N} \widetilde{\mathbf{X}}^\top \sigma(\widetilde{\mathbf{X}}\mathbf{W}_t) \odot \sigma'(\widetilde{\mathbf{X}}\mathbf{W}_t)}_{:=\Gamma_{2,t}} \right] \mathbf{B}_t^\top \quad (\text{C.2}) \\ &:= -\mathbf{J}_{\mathbf{W}_t} \mathbf{B}_t^\top \hspace{15em} \text{[denote } \mathbf{J}_{\mathbf{W}_t} := \Gamma_{1,t} - \Gamma_{2,t}] \end{aligned}$$

where the matrix operator $\mathbf{J}_{\mathbf{W}} : \mathbb{R}^{d \times k} \rightarrow \mathbb{R}^{d \times k}$ is formally defined as (by denoting $\mathbf{W}_t := \mathbf{W}^\natural + \mathbf{A}_t\mathbf{B}_t$)

$$\mathbf{J}_{\mathbf{W}} : \mathbf{W} \rightarrow \frac{1}{N} \widetilde{\mathbf{X}}^\top \left[\sigma(\widetilde{\mathbf{X}}\widetilde{\mathbf{W}}^\natural) - \sigma(\widetilde{\mathbf{X}}(\mathbf{W})) \right] \odot \sigma'(\widetilde{\mathbf{X}}\mathbf{W}). \quad (\text{C.3})$$

Similarly, we can compute

$$\begin{aligned} \nabla_{\mathbf{B}} \widetilde{L}(\mathbf{A}_t, \mathbf{B}_t) &= \frac{1}{N} \mathbf{A}_t^\top \widetilde{\mathbf{X}}^\top \left[\sigma(\widetilde{\mathbf{X}}(\mathbf{W}_t)) - \sigma(\widetilde{\mathbf{X}}\widetilde{\mathbf{W}}^\natural) \right] \odot \sigma'(\widetilde{\mathbf{X}}\mathbf{W}_t) \\ &= -\mathbf{A}_t^\top \mathbf{J}_{\mathbf{W}_t}. \end{aligned}$$

For full fine-tuning, we consider the following empirical loss function over $\mathbf{K} \in \mathbb{R}^{d \times k}$

$$L(\mathbf{K}) = \frac{1}{2N} \left\| \sigma(\tilde{\mathbf{X}}\mathbf{K}) - \sigma(\tilde{\mathbf{X}}\tilde{\mathbf{W}}^\natural) \right\|_{\text{F}}^2.$$

The gradient w.r.t. \mathbf{K} is

$$\nabla L(\mathbf{K}) = \frac{1}{N} \tilde{\mathbf{X}}^\top \left[\sigma(\tilde{\mathbf{X}}\mathbf{K}) - \sigma(\tilde{\mathbf{X}}\tilde{\mathbf{W}}^\natural) \right] \odot \sigma'(\tilde{\mathbf{X}}\mathbf{K})$$

Next, we can define the one-step negative gradient of full fine-tuning in the nonlinear case as

$$\begin{aligned} \mathbf{G}^\natural &:= -\nabla L(\mathbf{W}^\natural) \\ &= \frac{1}{N} \tilde{\mathbf{X}}^\top \left[\sigma(\tilde{\mathbf{X}}\tilde{\mathbf{W}}^\natural) - \sigma(\tilde{\mathbf{X}}\mathbf{W}^\natural) \right] \odot \sigma'(\tilde{\mathbf{X}}\mathbf{W}^\natural) \\ &= \mathbf{J}_{\mathbf{W}^\natural}. \end{aligned} \quad \text{[by definition of } \mathbf{J}_{\mathbf{W}} \text{ in Eq. (C.3)]}$$

Additionally, we define

$$\begin{aligned} \mathbf{\Gamma}_1^\natural &= \frac{1}{N} \tilde{\mathbf{X}}^\top \sigma(\tilde{\mathbf{X}}\tilde{\mathbf{W}}^\natural) \odot \sigma'(\tilde{\mathbf{X}}\mathbf{W}^\natural), \\ \mathbf{\Gamma}_2^\natural &= \frac{1}{N} \tilde{\mathbf{X}}^\top \sigma(\tilde{\mathbf{X}}\mathbf{W}^\natural) \odot \sigma'(\tilde{\mathbf{X}}\mathbf{W}^\natural). \end{aligned} \quad (\text{C.4})$$

In this section, we aim to analyze the initial properties of low-rank adapters under **(Spectral-init)** in a nonlinear context. The high-level proof strategy begins with examining the spectral properties of the one-step full gradient matrix, \mathbf{G}^\natural . Unlike the linear case, the presence of nonlinearity prevents a direct analysis. To address this, we first establish the concentration of the empirical full gradient, leveraging the fact that the empirical gradient approximates its expectation closely when the sample size is sufficiently large.

Subsequently, we utilize tools from Hermite decomposition to derive useful properties of the expected gradients. These properties are then transferred back to the empirical gradients through concentration results. Finally, since low-rank adapters under **(Spectral-init)** represent the best r -rank approximation of \mathbf{G}^\natural , we apply matrix analysis techniques to derive the desired results. Also, the concentration results in this part can serve as an important component for the later convergence analysis.

C.1.1 Computation of Full Population Gradients

First, we can simplify $\mathbf{\Gamma}_{1,t}$ and $\mathbf{\Gamma}_{2,t}$ which defined in Eq. (C.2) to be

$$\mathbf{\Gamma}_{1,t} = \frac{1}{N} \sum_{i=1}^N \tilde{\mathbf{x}}_i \left[\sigma(\tilde{\mathbf{x}}_i^\top \tilde{\mathbf{w}}_1^\natural) \sigma'(\tilde{\mathbf{x}}_i^\top \mathbf{w}_{t,1}) \quad \dots \quad \sigma(\tilde{\mathbf{x}}_i^\top \tilde{\mathbf{w}}_k^\natural) \sigma'(\tilde{\mathbf{x}}_i^\top \mathbf{w}_{t,k}) \right],$$

and

$$\mathbf{\Gamma}_{2,t} = \frac{1}{N} \sum_{i=1}^N \tilde{\mathbf{x}}_i \left[\sigma(\tilde{\mathbf{x}}_i^\top \mathbf{w}_{t,1}) \sigma'(\tilde{\mathbf{x}}_i^\top \mathbf{w}_{t,1}) \quad \dots \quad \sigma(\tilde{\mathbf{x}}_i^\top \mathbf{w}_{t,k}) \sigma'(\tilde{\mathbf{x}}_i^\top \mathbf{w}_{t,k}) \right],$$

where

$$\begin{aligned}
\boldsymbol{\Psi}_t(n) &= \frac{1}{4\pi} \frac{\text{Diag} \left(\langle \mathbf{w}_{t,1}, \mathbf{w}_{t,1} \rangle^n - \langle \tilde{\mathbf{w}}_1^\natural, \mathbf{w}_{t,1} \rangle^n, \dots, \langle \mathbf{w}_{t,k}, \mathbf{w}_{t,k} \rangle^n - \langle \tilde{\mathbf{w}}_k^\natural, \mathbf{w}_{t,k} \rangle^n \right)}{2^n n^2 n! n!} \widetilde{\mathbf{W}}^\natural \\
&+ \frac{1}{4\pi} \frac{\text{Diag} \left(\langle \mathbf{w}_{t,1}, \mathbf{w}_{t,1} \rangle^n, \dots, \langle \mathbf{w}_{t,k}, \mathbf{w}_{t,k} \rangle^n \right)}{2^n n^2 n! n!} (\mathbf{A}_t \mathbf{B}_t - \Delta) \\
&- \frac{1}{4\pi} \frac{\text{Diag} \left(\langle \mathbf{w}_{t,1}, \mathbf{w}_{t,1} \rangle^{n+1} - \langle \tilde{\mathbf{w}}_1^\natural, \mathbf{w}_{t,1} \rangle^{n+1}, \dots, \langle \mathbf{w}_{t,k}, \mathbf{w}_{t,k} \rangle^{n+1} - \langle \tilde{\mathbf{w}}_k^\natural, \mathbf{w}_{t,k} \rangle^{n+1} \right)}{2^{n+1} n(n+2)(n+1)!(n+3)!} \mathbf{W}_t.
\end{aligned}$$

Also, we have

$$\begin{aligned}
\|\boldsymbol{\Psi}_t(n)\|_{\text{F}} &\leq \left(\frac{\|\widetilde{\mathbf{W}}^\natural\|_{\text{op}} \max \left\{ \left(1 + \|\mathbf{A}_t \mathbf{B}_t - \Delta\|_{\text{op}} + \|\Delta\|_{\text{op}} \right), \|\widetilde{\mathbf{W}}^\natural\|_{\text{op}} \right\}}{4\pi 2^n n(n!)^2} \right)^{2n-1} \\
&+ \frac{\left(\|\widetilde{\mathbf{W}}^\natural\|_{\text{op}} + \|\mathbf{A}_t \mathbf{B}_t - \Delta\|_{\text{op}} \right) \max \left\{ \left(1 + \|\mathbf{A}_t \mathbf{B}_t - \Delta\|_{\text{op}} + \|\Delta\|_{\text{op}} \right), \|\widetilde{\mathbf{W}}^\natural\|_{\text{op}} \right\}}{4\pi 2^{n+1} n(n+2)n!(n+3)!} \right)^{2n+1} \\
&+ \left(\frac{\left(1 + \|\mathbf{A}_t \mathbf{B}_t - \Delta\|_{\text{op}} + \|\Delta\|_{\text{op}} \right)^{2n}}{4\pi 2^n n(n!)^2} \right) \|\mathbf{A}_t \mathbf{B}_t - \Delta\|_{\text{F}}.
\end{aligned}$$

Proof. We first give some notations here. Let $\mathbf{w}_{t,m}$ be the m -th column of $\mathbf{W}_t \in \mathbb{R}^{d \times k}$, \mathbf{w}_m^\natural be the m -th column of $\widetilde{\mathbf{W}}^\natural$, Δ_m as the m -th of the low-rank shift Δ , $[\mathbf{A}_t \mathbf{B}_t]_m$ as the m -th column of $\mathbf{A}_t \mathbf{B}_t$.

By Lemma C.1, we can derive m -th column of $\mathbb{E}_{\tilde{\mathbf{x}}} [\mathbf{J}_{\mathbf{W}_t}]$ for any $m = 1, 2, \dots, k$ as

$$\begin{aligned}
&\mathbb{E}_{\tilde{\mathbf{x}}} \left[\frac{1}{N} \sum_{i=1}^N \left(\sigma \left(\tilde{\mathbf{x}}_i^\top \mathbf{w}_{t,m} \right) - \sigma \left(\tilde{\mathbf{x}}_i^\top \tilde{\mathbf{w}}_m^\natural \right) \right) \sigma' \left(\tilde{\mathbf{x}}_i^\top \mathbf{w}_{t,m} \right) \tilde{\mathbf{x}}_i \right] \\
&= \sum_{j=0}^{\infty} \frac{c_{j+1}^2}{(j+1)!(j+1)!} \langle \mathbf{w}_{t,m}, \mathbf{w}_{t,m} \rangle^j \mathbf{w}_{t,m} + \sum_{j=0}^{\infty} \frac{c_{j+2} c_j}{j!(j+2)!} \langle \mathbf{w}_{t,m}, \mathbf{w}_{t,m} \rangle^j \mathbf{w}_{t,m} \\
&\quad - \sum_{j=0}^{\infty} \frac{c_{j+1}^2}{(j+1)!(j+1)!} \langle \tilde{\mathbf{w}}_m^\natural, \mathbf{w}_{t,m} \rangle^j \tilde{\mathbf{w}}_m^\natural - \sum_{j=0}^{\infty} \frac{c_{j+2} c_j}{j!(j+2)!} \langle \tilde{\mathbf{w}}_m^\natural, \mathbf{w}_{t,m} \rangle^j \mathbf{w}_{t,m} \\
&= (c_1^2 + c_0 c_2 / 2) \left(\mathbf{w}_{t,m} - \tilde{\mathbf{w}}_m^\natural \right) \\
&\quad + \sum_{j=1}^{\infty} \frac{c_{2j}^2}{(2j)!(2j)!} \langle \mathbf{w}_{t,m}, \mathbf{w}_{t,m} \rangle^{2j-1} \mathbf{w}_{t,m} + \sum_{j=1}^{\infty} \frac{c_{2j+2} c_{2j}}{(2j)!(2j+2)!} \langle \mathbf{w}_{t,m}, \mathbf{w}_{t,m} \rangle^{2j} \mathbf{w}_{t,m} \\
&\quad - \sum_{j=1}^{\infty} \frac{c_{2j}^2}{(2j)!(2j)!} \langle \tilde{\mathbf{w}}_m^\natural, \mathbf{w}_{t,m} \rangle^{2j-1} \tilde{\mathbf{w}}_m^\natural - \sum_{j=1}^{\infty} \frac{c_{2j+2} c_{2j}}{(2j)!(2j+2)!} \langle \tilde{\mathbf{w}}_m^\natural, \mathbf{w}_{t,m} \rangle^{2j} \mathbf{w}_{t,m}.
\end{aligned}$$

By re-arranging the index of infinite sum, we can obtain

$$\begin{aligned}
& \mathbb{E}_{\tilde{\mathbf{x}}} \left[\frac{1}{N} \sum_{i=1}^N \left(\sigma \left(\tilde{\mathbf{x}}_i^\top \mathbf{w}_{t,m} \right) - \sigma \left(\tilde{\mathbf{x}}_i^\top \tilde{\mathbf{w}}_m^\natural \right) \right) \sigma' \left(\tilde{\mathbf{x}}_i^\top \mathbf{w}_{t,m} \right) \tilde{\mathbf{x}}_i \right] \\
&= (c_1^2 + c_0 c_2 / 2) ([\mathbf{A}_t \mathbf{B}_t]_m - \Delta_m) \\
&+ \frac{1}{4\pi} \sum_{\substack{n \geq 1, \\ n \text{ odd}}} \frac{\left(\langle \mathbf{w}_{t,m}, \mathbf{w}_{t,m} \rangle^n - \langle \tilde{\mathbf{w}}_m^\natural, \mathbf{w}_{t,m} \rangle^n \right)}{2^n n^2 n! n!} \tilde{\mathbf{w}}_m^\natural \\
&+ \frac{1}{4\pi} \sum_{\substack{n \geq 1, \\ n \text{ odd}}} \frac{\langle \mathbf{w}_{t,m}, \mathbf{w}_{t,m} \rangle^n}{2^n n^2 n! n!} ([\mathbf{A}_t \mathbf{B}_t]_m - \Delta_m) \\
&- \frac{1}{4\pi} \sum_{\substack{n \geq 1, \\ n \text{ odd}}} \frac{\left(\langle \mathbf{w}_{t,m}, \mathbf{w}_{t,m} \rangle^{n+1} - \langle \tilde{\mathbf{w}}_m^\natural, \mathbf{w}_{t,m} \rangle^{n+1} \right)}{2^{n+1} n(n+2)(n+1)!(n+3)!} \mathbf{w}_{t,m}.
\end{aligned}$$

Then, for the last three terms, we define the m -th residual vector of order- n of them as

$$\begin{aligned}
\mathbf{r}_m(n) &:= \frac{1}{4\pi} \frac{\left(\langle \mathbf{w}_{t,m}, \mathbf{w}_{t,m} \rangle^n - \langle \tilde{\mathbf{w}}_m^\natural, \mathbf{w}_{t,m} \rangle^n \right)}{2^n n^2 n! n!} \tilde{\mathbf{w}}_m^\natural + \frac{1}{4\pi} \frac{\langle \mathbf{w}_{t,m}, \mathbf{w}_{t,m} \rangle^n}{2^n n^2 n! n!} ([\mathbf{A}_t \mathbf{B}_t]_m - \Delta_m) \\
&- \frac{1}{4\pi} \frac{\left(\langle \mathbf{w}_{t,m}, \mathbf{w}_{t,m} \rangle^{n+1} - \langle \tilde{\mathbf{w}}_m^\natural, \mathbf{w}_{t,m} \rangle^{n+1} \right)}{2^{n+1} n(n+2)(n+1)!(n+3)!} \mathbf{w}_{t,m}.
\end{aligned}$$

Combining the above equations, we can write in matrix form as

$$\mathbb{E}_{\tilde{\mathbf{x}}} [\mathbf{J} \mathbf{W}_t] = (c_1^2 + c_0 c_2 / 2) (\mathbf{A}_t \mathbf{B}_t - \Delta) + \sum_{\substack{n \geq 1, \\ n \text{ odd}}} \underbrace{[\mathbf{r}_1(n) \quad \dots \quad \mathbf{r}_k(n)]}_{:= \Psi_t(n)},$$

where $\Psi_t(n)$ can be formulated as

$$\mathbf{\Psi}_t(n) = \frac{1}{4\pi} \frac{\text{Diag} \left(\langle \mathbf{w}_{t,1}, \mathbf{w}_{t,1} \rangle^n - \langle \tilde{\mathbf{w}}_1^\natural, \mathbf{w}_{t,1} \rangle^n, \dots, \langle \mathbf{w}_{t,k}, \mathbf{w}_{t,k} \rangle^n - \langle \tilde{\mathbf{w}}_k^\natural, \mathbf{w}_{t,k} \rangle^n \right)}{2^n n^2 n! n!} \widetilde{\mathbf{W}}^\natural \quad (\text{C.7})$$

$$+ \frac{1}{4\pi} \frac{\text{Diag} \left(\langle \mathbf{w}_{t,1}, \mathbf{w}_{t,1} \rangle^n, \dots, \langle \mathbf{w}_{t,k}, \mathbf{w}_{t,k} \rangle^n \right)}{2^n n^2 n! n!} (\mathbf{A}_t \mathbf{B}_t - \Delta) \quad (\text{C.8})$$

$$- \frac{1}{4\pi} \frac{\text{Diag} \left(\langle \mathbf{w}_{t,1}, \mathbf{w}_{t,1} \rangle^{n+1} - \langle \tilde{\mathbf{w}}_1^\natural, \mathbf{w}_{t,1} \rangle^{n+1}, \dots, \langle \mathbf{w}_{t,k}, \mathbf{w}_{t,k} \rangle^{n+1} - \langle \tilde{\mathbf{w}}_k^\natural, \mathbf{w}_{t,k} \rangle^{n+1} \right)}{2^{n+1} n(n+2)(n+1)!(n+3)!} \mathbf{W}_t. \quad (\text{C.9})$$

Now we aim to upper bound the Frobenius norm of $\Psi_t(n)$ for $n \geq 1$. We handle these three terms

of $\Psi_t(n)$ respectively. Regarding the first term (C.7), we have

$$\begin{aligned}
& \left\| \frac{1}{4\pi} \frac{\text{Diag} \left(\langle \mathbf{w}_{t,1}, \mathbf{w}_{t,1} \rangle^n - \langle \tilde{\mathbf{w}}_1^\natural, \mathbf{w}_{t,1} \rangle^n, \dots, \langle \mathbf{w}_{t,k}, \mathbf{w}_{t,k} \rangle^n - \langle \tilde{\mathbf{w}}_k^\natural, \mathbf{w}_{t,k} \rangle^n \right)}{2^n n^2 n! n!} \tilde{\mathbf{W}}^\natural \right\|_{\text{F}}^2 \\
& \leq \frac{\|\tilde{\mathbf{W}}^\natural\|_{\text{op}}^2}{16\pi^2 2^{2n} n^4 (n!)^4} \sum_{m=1}^k \left(\langle \mathbf{w}_{t,m}, \mathbf{w}_{t,m} \rangle^n - \langle \tilde{\mathbf{w}}_m^\natural, \mathbf{w}_{t,m} \rangle^n \right)^2 \\
& \leq \frac{\|\tilde{\mathbf{W}}^\natural\|_{\text{op}}^2}{16\pi^2 2^{2n} n^4 (n!)^4} \sum_{m=1}^k \left(n \max \left\{ \|\mathbf{w}_{t,m}\|_2, \|\tilde{\mathbf{w}}_m^\natural\|_2 \right\}^{2n-1} \|\mathbf{A}_t \mathbf{B}_t\|_m - \Delta_m\|_2 \right)^2 \\
& \quad \left[\text{by } |\langle \mathbf{u}, \mathbf{u} \rangle^j - \langle \mathbf{u}, \mathbf{v} \rangle^j| \leq j \max \{ \|\mathbf{u}\|_2, \|\mathbf{v}\|_2 \}^{2j-1} \|\mathbf{u} - \mathbf{v}\|_2 \text{ in Lemma D.5} \right] \\
& \leq \frac{\|\tilde{\mathbf{W}}^\natural\|_{\text{op}}^2}{16\pi^2 2^{2n} n^2 (n!)^4} \sum_{m=1}^k \left(\max \left\{ (1 + \|\mathbf{A}_t \mathbf{B}_t\|_m - \Delta_m\|_2 + \|\Delta_m\|_2), \|\tilde{\mathbf{w}}_m^\natural\|_2 \right\}^{2n-1} \|\mathbf{A}_t \mathbf{B}_t\|_m - \Delta_m\|_2 \right)^2 \\
& \quad \left[\text{by Assumption 4.1 and triangle inequality } \|\mathbf{w}_{t,m}\|_2 \leq 1 + \|\mathbf{A}_t \mathbf{B}_t\|_m - \Delta_m\|_2 + \|\Delta_m\|_2 \right] \\
& \leq \frac{\|\tilde{\mathbf{W}}^\natural\|_{\text{op}}^2}{16\pi^2 2^{2n} n^2 (n!)^4} \max \left\{ \left(1 + \|\mathbf{A}_t \mathbf{B}_t - \Delta\|_{\text{op}} + \|\Delta\|_{\text{op}} \right), \|\tilde{\mathbf{W}}^\natural\|_{\text{op}} \right\}^{4n-2} \|\mathbf{A}_t \mathbf{B}_t - \Delta\|_{\text{F}}^2,
\end{aligned}$$

where the last inequality holds by $\max_j \|\mathbf{a}_j\|_2 \leq \|\mathbf{A}\|_{\text{op}}$ for any matrix $\mathbf{A} = [\mathbf{a}_1, \mathbf{a}_2, \dots, \mathbf{a}_k] \in \mathbb{R}^{d \times k}$.

Accordingly, we have

$$\begin{aligned}
& \left\| \frac{1}{4\pi} \frac{\text{Diag} \left(\langle \mathbf{w}_{t,1}, \mathbf{w}_{t,1} \rangle^n - \langle \tilde{\mathbf{w}}_1^\natural, \mathbf{w}_{t,1} \rangle^n, \dots, \langle \mathbf{w}_{t,k}, \mathbf{w}_{t,k} \rangle^n - \langle \tilde{\mathbf{w}}_k^\natural, \mathbf{w}_{t,k} \rangle^n \right)}{2^n n^2 n! n!} \tilde{\mathbf{W}}^\natural \right\|_{\text{F}} \\
& \leq \frac{\|\tilde{\mathbf{W}}^\natural\|_{\text{op}} \max \left\{ \left(1 + \|\mathbf{A}_t \mathbf{B}_t - \Delta\|_{\text{op}} + \|\Delta\|_{\text{op}} \right), \|\tilde{\mathbf{W}}^\natural\|_{\text{op}} \right\}^{2n-1}}{4\pi 2^n n (n!)^2} \|\mathbf{A}_t \mathbf{B}_t - \Delta\|_{\text{F}}.
\end{aligned}$$

Regarding the second term (C.8), we have

$$\begin{aligned}
& \left\| \frac{1}{4\pi} \frac{\text{Diag} \left(\langle \mathbf{w}_{t,1}, \mathbf{w}_{t,1} \rangle^n, \dots, \langle \mathbf{w}_{t,k}, \mathbf{w}_{t,k} \rangle^n \right)}{2^n n^2 n! n!} (\mathbf{A}_t \mathbf{B}_t - \Delta) \right\|_{\text{F}} \\
& \leq \frac{\left(1 + \|\mathbf{A}_t \mathbf{B}_t - \Delta\|_{\text{op}} + \|\Delta\|_{\text{op}} \right)^{2n}}{4\pi 2^n n (n!)^2} \|\mathbf{A}_t \mathbf{B}_t - \Delta\|_{\text{F}}.
\end{aligned}$$

Regarding the third term (C.9), we can also have

$$\begin{aligned}
& \left\| \frac{1}{4\pi} \text{Diag} \left(\langle \mathbf{w}_{t,1}, \mathbf{w}_{t,1} \rangle^{n+1} - \langle \tilde{\mathbf{w}}_1^\natural, \mathbf{w}_{t,1} \rangle^{n+1}, \dots, \langle \mathbf{w}_{t,k}, \mathbf{w}_{t,k} \rangle^{n+1} - \langle \tilde{\mathbf{w}}_k^\natural, \mathbf{w}_{t,k} \rangle^{n+1} \right) \mathbf{W}_t \right\|_{\text{F}}^2 \\
& \leq \left(\frac{\|\mathbf{W}_t\|_{\text{op}}}{4\pi 2^{n+1} n(n+2)(n+1)!(n+3)!} \right)^2 \sum_{m=1}^k \left(\langle \mathbf{w}_{t,m}, \mathbf{w}_{t,m} \rangle^{n+1} - \langle \tilde{\mathbf{w}}_m^\natural, \mathbf{w}_{t,m} \rangle^{n+1} \right)^2 \\
& \leq \left(\frac{\|\mathbf{W}_t\|_{\text{op}}}{4\pi 2^{n+1} n(n+2)(n+1)!(n+3)!} \right)^2 \sum_{m=1}^k \left((n+1) \max \left\{ \|\mathbf{w}_{t,m}\|_2, \|\tilde{\mathbf{w}}_m^\natural\|_2 \right\}^{2n+1} \|\mathbf{A}_t \mathbf{B}_t\|_m - \Delta_m \right)^2 \\
& \quad \left[\text{by } |\langle \mathbf{u}, \mathbf{u} \rangle^j - \langle \mathbf{u}, \mathbf{v} \rangle^j| \leq j \max \{ \|\mathbf{u}\|_2, \|\mathbf{v}\|_2 \}^{2j-1} \|\mathbf{u} - \mathbf{v}\|_2 \text{ in Lemma D.5} \right] \\
& \leq \left(\frac{\left(\|\tilde{\mathbf{W}}^\natural\|_{\text{op}} + \|\mathbf{A}_t \mathbf{B}_t - \Delta\|_{\text{op}} \right) \max \left\{ \left(1 + \|\mathbf{A}_t \mathbf{B}_t - \Delta\|_{\text{op}} + \|\Delta\|_{\text{op}} \right), \|\tilde{\mathbf{W}}^\natural\|_{\text{op}} \right\}^{2n+1}}{4\pi 2^{n+1} n(n+2)n!(n+3)!} \right)^2 \|\mathbf{A}_t \mathbf{B}_t - \Delta\|_{\text{F}}^2.
\end{aligned}$$

Finally, combining the above three terms, we obtain

$$\begin{aligned}
\|\Psi_t(n)\|_{\text{F}} & \leq \left(\frac{\|\tilde{\mathbf{W}}^\natural\|_{\text{op}} \max \left\{ \left(1 + \|\mathbf{A}_t \mathbf{B}_t - \Delta\|_{\text{op}} + \|\Delta\|_{\text{op}} \right), \|\tilde{\mathbf{W}}^\natural\|_{\text{op}} \right\}^{2n-1}}{4\pi 2^n n(n!)^2} \right. \\
& \quad + \frac{\left(\|\tilde{\mathbf{W}}^\natural\|_{\text{op}} + \|\mathbf{A}_t \mathbf{B}_t - \Delta\|_{\text{op}} \right) \max \left\{ \left(1 + \|\mathbf{A}_t \mathbf{B}_t - \Delta\|_{\text{op}} + \|\Delta\|_{\text{op}} \right), \|\tilde{\mathbf{W}}^\natural\|_{\text{op}} \right\}^{2n+1}}{4\pi 2^{n+1} n(n+2)n!(n+3)!} \\
& \quad \left. + \frac{\left(1 + \|\mathbf{A}_t \mathbf{B}_t - \Delta\|_{\text{op}} + \|\Delta\|_{\text{op}} \right)^{2n}}{4\pi 2^n n(n!)^2} \right) \|\mathbf{A}_t \mathbf{B}_t - \Delta\|_{\text{F}},
\end{aligned}$$

which completes the proof. \square

C.1.2 Concentration of Empirical Gradients

In this part, we aim to provide the concentration of empirical gradient $\mathbf{J}_{\mathbf{W}_t} := \mathbf{\Gamma}_{1,t} - \mathbf{\Gamma}_{2,t} \in \mathbb{R}^{d \times k}$ in Frobenius norm. Recall $\mathbf{W}_t := \mathbf{W}^\natural + \mathbf{A}_t \mathbf{B}_t$ and $\mathbf{w}_{t,m}$ is the corresponding m -th column of \mathbf{W}_t , denote $\tilde{x}_{i,j}$ as the j -th element of $\tilde{\mathbf{x}}_i$, for notational simplicity, we define each element of $\mathbf{J}_{\mathbf{W}_t} := \mathbf{\Gamma}_{1,t} - \mathbf{\Gamma}_{2,t}$ as

$$c_{t,m}^j(\tilde{\mathbf{x}}_i) := \left(\sigma \left(\tilde{\mathbf{x}}_i^\top \tilde{\mathbf{w}}_m^\natural \right) - \sigma \left(\tilde{\mathbf{x}}_i^\top \mathbf{w}_{t,m}^\natural \right) \right) \sigma' \left(\tilde{\mathbf{x}}_i^\top \mathbf{w}_{t,m}^\natural \right) \tilde{x}_{i,j} \in \mathbb{R}, \quad \text{for } 1 \leq m \leq k, 1 \leq i \leq N, 1 \leq j \leq d,$$

Then, we can write $\mathbf{J}_{\mathbf{W}_t}$ in an element-wise way

$$\mathbf{J}_{\mathbf{W}_t} = \frac{1}{N} \sum_{i=1}^N \begin{bmatrix} c_{t,1}^1(\tilde{\mathbf{x}}_i) & \dots & c_{t,k}^1(\tilde{\mathbf{x}}_i) \\ \vdots & \ddots & \vdots \\ c_{t,1}^d(\tilde{\mathbf{x}}_i) & \dots & c_{t,k}^d(\tilde{\mathbf{x}}_i) \end{bmatrix} \in \mathbb{R}^{d \times k},$$

and

$$\left\| \mathbf{J}\mathbf{w}_t - \mathbb{E}_{\tilde{\mathbf{x}}} [\mathbf{J}\mathbf{w}_t] \right\|_{\text{F}}^2 = \sum_{j=1}^d \sum_{m=1}^k \left(\frac{1}{N} \sum_{i=1}^N c_{t,m}^j(\tilde{\mathbf{x}}_i) - \mathbb{E}_{\tilde{\mathbf{x}}} [c_{t,m}^j(\tilde{\mathbf{x}})] \right)^2.$$

Next, we have the following lemma.

Lemma C.3. For $1 \leq m \leq k$, $1 \leq j \leq d$, under assumptions in Section 2.1 for the nonlinear setting, with probability at least $1 - 2C \exp(-N\epsilon^2)$ for a universal constant $C > 0$ and $\epsilon \in (0, 1)$, we have

$$\left| \frac{1}{N} \sum_{i=1}^N c_{t,m}^j(\tilde{\mathbf{x}}_i) - \mathbb{E}_{\tilde{\mathbf{x}}} [c_{t,m}^j(\tilde{\mathbf{x}})] \right| \leq C^* K^2 \epsilon \|\tilde{\mathbf{w}}_m^{\natural} - \mathbf{w}_{t,m}^{\natural}\|_2,$$

for some absolute constant $C^* > 0$ and $K = \sqrt{8/3}$.

Proof. Since $\tilde{x}_{i,j} \sim \mathcal{N}(0, 1)$ for $\forall 1 \leq m \leq k$ and $\forall 1 \leq j \leq d$, then we have that $K := \|\tilde{x}_{i,j}\|_{\psi_2} = \sqrt{8/3}$. By the Orlicz-based definition of subgaussian norm, the subgaussian norm of random variable is identical to its absolute value. Then, for any $\lambda \in \mathbb{R}$, we have the following moment generating function

$$\begin{aligned} & \mathbb{E} \left[\exp \left(\lambda \left| \left(\sigma \left(\tilde{\mathbf{x}}_i^{\top} \tilde{\mathbf{w}}_m^{\natural} \right) - \sigma \left(\tilde{\mathbf{x}}_i^{\top} \mathbf{w}_{t,m}^{\natural} \right) \right) \sigma' \left(\tilde{\mathbf{x}}_i^{\top} \mathbf{w}_{t,m}^{\natural} \right) \right| \right) \right] \\ & \leq \mathbb{E} \left[\exp \left(\lambda \left| \left\langle \tilde{\mathbf{x}}_i, \tilde{\mathbf{w}}_m^{\natural} - \mathbf{w}_{t,m}^{\natural} \right\rangle \right| \right) \right] \quad \text{[by Lipschitz continuity of } \sigma \text{ and } \sigma'] \\ & \leq \mathbb{E} \left[\exp \left((C^*)^2 \lambda^2 \left\| \left\langle \tilde{\mathbf{x}}_i, \tilde{\mathbf{w}}_m^{\natural} - \mathbf{w}_{t,m}^{\natural} \right\rangle \right\|_{\psi_2}^2 \right) \right], \quad \text{[by subgaussian property]} \end{aligned}$$

for some constant $C^* > 0$, which implies

$$\left\| \left(\sigma \left(\tilde{\mathbf{x}}_i^{\top} \tilde{\mathbf{w}}_m^{\natural} \right) - \sigma \left(\tilde{\mathbf{x}}_i^{\top} \mathbf{w}_{t,m}^{\natural} \right) \right) \sigma' \left(\tilde{\mathbf{x}}_i^{\top} \mathbf{w}_{t,m}^{\natural} \right) \right\|_{\psi_2}^2 \leq (C^*)^2 \left\| \left\langle \tilde{\mathbf{x}}_i, \tilde{\mathbf{w}}_m^{\natural} - \mathbf{w}_{t,m}^{\natural} \right\rangle \right\|_{\psi_2}^2 = (C^* K)^2 \|\tilde{\mathbf{w}}_m^{\natural} - \mathbf{w}_{t,m}^{\natural}\|_2^2,$$

where the last inequality follows from the fact that $\|X\|_{\psi_2} = Ks$ if $X \sim \mathcal{N}(0, s^2)$. Therefore, by Vershynin (2018, Lemma 2.7.7), this implies $c_{t,m}^j(\tilde{\mathbf{x}}_i)$ is sub-exponential with

$$B_{t,m} := \|c_{t,m}^j(\tilde{\mathbf{x}})\|_{\psi_1} \leq \|\tilde{x}_{i,j}\|_{\psi_2} \left\| \left(\sigma \left(\tilde{\mathbf{x}}_i^{\top} \tilde{\mathbf{w}}_m^{\natural} \right) - \sigma \left(\tilde{\mathbf{x}}_i^{\top} \mathbf{w}_{t,m}^{\natural} \right) \right) \sigma' \left(\tilde{\mathbf{x}}_i^{\top} \mathbf{w}_{t,m}^{\natural} \right) \right\|_{\psi_2} \leq C^* K^2 \|\tilde{\mathbf{w}}_m^{\natural} - \mathbf{w}_{t,m}^{\natural}\|_2. \quad (\text{C.10})$$

Then, let $\epsilon_{t,m} = C^* K^2 \epsilon \|\tilde{\mathbf{w}}_m^{\natural} - \mathbf{w}_{t,m}^{\natural}\|_2$ for $\epsilon \in (0, 1)$, we can apply Bernstein's inequality for sub-exponential variables Vershynin (2018, Corollary 2.8.3)

$$\begin{aligned} & \mathbb{P} \left(\left| \frac{1}{N} \sum_{i=1}^N c_{t,m}^j(\tilde{\mathbf{x}}_i) - \mathbb{E}_{\tilde{\mathbf{x}}} [c_{t,m}^j(\tilde{\mathbf{x}})] \right| \geq \epsilon_{t,m} \right) \\ & \leq 2C \exp \left(-N \min \left\{ \frac{\epsilon_{t,m}}{B_{t,m}}, \frac{\epsilon_{t,m}^2}{B_{t,m}^2} \right\} \right) \quad \text{[for some constant } C > 0] \\ & \leq 2C \exp(-N\epsilon^2) \quad \text{[by Eq. (C.10) and } \epsilon \in (0, 1)] \end{aligned}$$

□

Theorem C.4. Suppose $\epsilon \in (0, 1)$, under assumptions in Section 2.1 for the nonlinear setting, then with probability at least $1 - 2Cdk \exp(-N\epsilon^2)$ for a universal constant $C > 0$, we have

$$\left\| \mathbf{J}_{\mathbf{W}_t} - \mathbb{E}_{\tilde{\mathbf{x}}}[\mathbf{J}_{\mathbf{W}_t}] \right\|_{\mathbb{F}} \leq C^* K^2 \sqrt{d} \epsilon \|\mathbf{A}_t \mathbf{B}_t - \Delta\|_{\mathbb{F}},$$

for some absolute constant $C^* > 0$ and $K = \sqrt{8/3}$.

Proof. By a union bound argument and Lemma C.3, with probability at least $1 - 2Cdk \exp(-N\epsilon^2)$ for a universal constant $C > 0$, we have

$$\begin{aligned} \left\| \mathbf{J}_{\mathbf{W}_t} - \mathbb{E}_{\tilde{\mathbf{x}}}[\mathbf{J}_{\mathbf{W}_t}] \right\|_{\mathbb{F}}^2 &= \sum_{j=1}^d \sum_{m=1}^k \left(\frac{1}{N} \sum_{i=1}^N c_{t,m}^j(\tilde{\mathbf{x}}_i) - \mathbb{E}_{\tilde{\mathbf{x}}}[c_{t,m}^j(\tilde{\mathbf{x}})] \right)^2 \\ &\leq \sum_{j=1}^d \sum_{m=1}^k \epsilon_{t,m}^2 \\ &\leq \sum_{j=1}^d \sum_{m=1}^k (C^* K^2)^2 \epsilon^2 \|\tilde{\mathbf{w}}_m^\dagger - \mathbf{w}_{t,m}^\dagger\|_2^2 \\ &= d(C^* K^2)^2 \epsilon^2 \|\mathbf{A}_t \mathbf{B}_t - \Delta\|_{\mathbb{F}}^2, \end{aligned}$$

which implies

$$\left\| \mathbf{J}_{\mathbf{W}_t} - \mathbb{E}_{\tilde{\mathbf{x}}}[\mathbf{J}_{\mathbf{W}_t}] \right\|_{\mathbb{F}} \leq C^* K^2 \sqrt{d} \epsilon \|\mathbf{A}_t \mathbf{B}_t - \Delta\|_{\mathbb{F}},$$

which finishes the proof. \square

Lemma C.5. Recall $\mathbf{G}^\dagger := -\nabla L(\mathbf{W}^\dagger) = \mathbf{J}_{\mathbf{W}^\dagger}$, under assumptions in Section 2.1 for the nonlinear setting and Assumption 4.1, with (Spectral-init), suppose $\epsilon \leq \frac{\rho}{3C^* K^2 \gamma \sqrt{2dr^* \kappa}}$ for some $\rho > 0$ and we set

$$\gamma \in \left[\frac{1}{c_{\text{H}}} - \frac{\rho}{3c_{\text{H}} \kappa \sqrt{2r^*}}, \frac{1}{c_{\text{H}}} + \frac{\rho}{3c_{\text{H}} \kappa \sqrt{2r^*}} \right], \quad \text{with } c_{\text{H}} := \frac{1}{4} + \frac{1}{4\pi} \sum_{\substack{n \geq 1, \\ n \text{ odd}}} 2^{-n} n^{-2} (n!)^{-2}, \quad (\text{C.11})$$

then with probability at least $1 - 2Cdk \exp(-N\epsilon^2)$ for a universal constant $C > 0$, it holds that

$$\|\mathbf{A}_0 \mathbf{B}_0 - \Delta\|_{\mathbb{F}} \leq \rho \lambda_{r^*}^*.$$

Remark Notice that computing the exact value of c_{H} is difficult. However, because of the super-fast decay of Hermite coefficients of ReLU σ , we can approximate c_{H} very well by only three higher order terms, i.e. $n \in \{1, 3, 5\}$, which is $c_{\text{H}} \simeq 0.28982$. The residual terms which the corresponding order bigger than 5 are negligible. For example, when $n = 7$, $\frac{1}{4\pi 2^n n^2 (n!)^2} \simeq 4.99 \times 10^{-13}$.

Proof. Recall $\mathbf{\Gamma}_1^{\natural}$ and $\mathbf{\Gamma}_2^{\natural}$ defined in Eq. (C.4), by Lemma C.1, we can obtain

$$\begin{aligned}
\mathbb{E}_{\tilde{\mathbf{x}}} \left[\mathbf{\Gamma}_1^{\natural} \right] &= \sum_{j=0}^{\infty} \left\{ \frac{c_{j+1}^2}{(j+1)!(j+1)!} \text{Diag} \left(\left(\mathbf{W}^{\natural} + \Delta \right)^{\top} \mathbf{W}^{\natural} \right)^j \left(\mathbf{W}^{\natural} + \Delta \right) \right. \\
&\quad \left. + \frac{c_{j+2}c_j}{j!(j+2)!} \text{Diag} \left(\left(\mathbf{W}^{\natural} + \Delta \right)^{\top} \mathbf{W}^{\natural} \right)^j \mathbf{W}^{\natural} \right\} \\
&= \sum_{j=0}^{\infty} \left\{ \frac{c_{j+1}^2}{(j+1)!(j+1)!} \text{Diag} \left(\left(\mathbf{W}^{\natural} \right)^{\top} \mathbf{W}^{\natural} \right)^j \left(\mathbf{W}^{\natural} + \Delta \right) \right. \\
&\quad \left. + \frac{c_{j+2}c_j}{j!(j+2)!} \text{Diag} \left(\left(\mathbf{W}^{\natural} \right)^{\top} \mathbf{W}^{\natural} \right)^j \mathbf{W}^{\natural} \right\}, \tag{by Assumption 4.1}
\end{aligned}$$

and

$$\mathbb{E}_{\tilde{\mathbf{x}}} \left[\mathbf{\Gamma}_2^{\natural} \right] = \sum_{j=0}^{\infty} \left(\frac{c_{j+1}^2}{(j+1)!(j+1)!} \text{Diag} \left(\left(\mathbf{W}^{\natural} \right)^{\top} \mathbf{W}^{\natural} \right)^j + \frac{c_{j+2}c_j}{j!(j+2)!} \text{Diag} \left(\left(\mathbf{W}^{\natural} \right)^{\top} \mathbf{W}^{\natural} \right)^j \right) \mathbf{W}^{\natural}.$$

Therefore, taking the Hermite coefficients by Eq. (D.3), we have

$$\mathbb{E}_{\tilde{\mathbf{x}}} \left[\mathbf{G}^{\natural} \right] = \sum_{j=0}^{\infty} \left(\frac{c_{j+1}^2}{(j+1)!(j+1)!} \text{Diag} \left(\left(\mathbf{W}^{\natural} \right)^{\top} \mathbf{W}^{\natural} \right)^j \left(\mathbf{W}^{\natural} + \Delta \right) \right. \tag{C.12}$$

$$\left. - \frac{c_{j+1}^2}{(j+1)!(j+1)!} \text{Diag} \left(\left(\mathbf{W}^{\natural} \right)^{\top} \mathbf{W}^{\natural} \right)^j \mathbf{W}^{\natural} \right)$$

$$= \sum_{j=0}^{\infty} \frac{c_{j+1}^2}{(j+1)!(j+1)!} \text{Diag} \left(\left(\mathbf{W}^{\natural} \right)^{\top} \mathbf{W}^{\natural} \right)^j \Delta$$

$$= \sum_{j=0}^{\infty} \frac{c_{j+1}^2}{(j+1)!(j+1)!} \Delta \tag{by Assumption 4.1}$$

$$= \underbrace{\left(c_1^2 + \frac{1}{4\pi} \sum_{\substack{n \geq 1, \\ n \text{ odd}}} \frac{1}{2^n n^2 (n!)^2} \right)}_{:=c_{\text{H}}} \Delta. \tag{C.13}$$

Following Theorem C.4, we replace \mathbf{W}_t with \mathbf{W}^{\natural} and then obtain the following concentration with the probability at least $1 - 2Cdk \exp(-N\epsilon^2)$ for a universal constant $C > 0$

$$\left\| \mathbf{G}^{\natural} - \mathbb{E}_{\tilde{\mathbf{x}}} \left[\mathbf{G}^{\natural} \right] \right\|_{\text{F}} \leq \frac{\rho \|\Delta\|_{\text{F}}}{3\sqrt{2}r^*\gamma\kappa} \leq \frac{\rho\sqrt{r^*}\|\Delta\|_{\text{op}}}{3\sqrt{2}r^*\gamma\kappa} = \frac{\rho\lambda_{r^*}^*}{3\sqrt{2}r^*\gamma},$$

where $\epsilon \leq \frac{\rho}{2C^*K^2\gamma\sqrt{2dr^*\kappa}}$ for $\rho > 0$. Besides, we have

$$\begin{aligned}
\left| \gamma \lambda_{r^*+1} \left(\mathbf{G}^\natural \right) - \lambda_{r^*+1} \left(\gamma \mathbb{E}_{\tilde{\mathbf{x}}} \left[\mathbf{G}^\natural \right] \right) \right| &= \left| \gamma \lambda_{r^*+1} \left(\mathbf{G}^\natural \right) - \lambda_{r^*+1} \left(\Delta \right) \right| \\
&= \gamma \lambda_{r^*+1} \left(\mathbf{G}^\natural \right) && \text{[since Rank}(\Delta) = r^* \text{]} \\
&\leq \gamma \left\| \mathbf{G}^\natural - \mathbb{E}_{\tilde{\mathbf{x}}} \left[\mathbf{G}^\natural \right] \right\|_{op} && \text{[by Weyl's inequality]} \\
&\leq \gamma \left\| \mathbf{G}^\natural - \mathbb{E}_{\tilde{\mathbf{x}}} \left[\mathbf{G}^\natural \right] \right\|_F \\
&\leq \frac{\rho \lambda_{r^*}^*}{3\sqrt{2r^*}}, && \text{[by Eq. (C.11)]}
\end{aligned}$$

which implies

$$\lambda_{r^*+1} \left(\mathbf{G}^\natural \right) \leq \frac{\rho \lambda_{r^*}^*}{3\sqrt{2r^*} \gamma}, \quad (\text{C.14})$$

due to $\text{Rank} \left(\mathbb{E}_{\tilde{\mathbf{x}}} \left[\mathbf{G}^\natural \right] \right) = \text{Rank}(\Delta) = r^*$ by Eq. (C.13). Then, we have

$$\begin{aligned}
\| \mathbf{A}_0 \mathbf{B}_0 - \Delta \|_{op} &\leq \left\| \mathbf{A}_0 \mathbf{B}_0 - \gamma \mathbf{G}^\natural \right\|_{op} + \gamma \left\| \mathbf{G}^\natural - \mathbb{E}_{\tilde{\mathbf{x}}} \left[\mathbf{G}^\natural \right] \right\|_{op} + \left\| \gamma \mathbb{E}_{\tilde{\mathbf{x}}} \left[\mathbf{G}^\natural \right] - \Delta \right\|_{op} \\
&\leq \left\| \mathbf{A}_0 \mathbf{B}_0 - \gamma \mathbf{G}^\natural \right\|_{op} + \gamma \left\| \mathbf{G}^\natural - \mathbb{E}_{\tilde{\mathbf{x}}} \left[\mathbf{G}^\natural \right] \right\|_F + |\gamma c_H - 1| \|\Delta\|_{op} && \text{[by Eq. (C.13)]} \\
&\leq \left\| \mathbf{A}_0 \mathbf{B}_0 - \gamma \mathbf{G}^\natural \right\|_{op} + \frac{2\rho \lambda_{r^*}^*}{3\sqrt{2r^*}} \\
&\quad \left[\text{by Eq. (C.11) and } \gamma \in \left[\frac{1}{c_H} - \frac{\rho}{3c_H \kappa \sqrt{2r^*}}, \frac{1}{c_H} + \frac{\rho}{3c_H \kappa \sqrt{2r^*}} \right] \right] \\
&\leq \gamma \lambda_{r^*+1} \left(\mathbf{G}^\natural \right) + \frac{2\rho \lambda_{r^*}^*}{3\sqrt{2r^*}} \\
&\leq \frac{\rho \lambda_{r^*}^*}{\sqrt{2r^*}}. && \text{[by Eq. (C.14)]}
\end{aligned}$$

Since we work in the exact-rank case $\text{Rank}(\mathbf{A}_t \mathbf{B}_t) \leq r = r^*$ with $\text{Rank}(\Delta) = r^*$, then $\text{Rank}(\mathbf{A}_0 \mathbf{B}_0 - \Delta) \leq 2r^*$, which implies

$$\| \mathbf{A}_0 \mathbf{B}_0 - \Delta \|_F \leq \sqrt{2r^*} \| \mathbf{A}_0 \mathbf{B}_0 - \Delta \|_{op} \leq \rho \lambda_{r^*}^*.$$

□

C.2 LoRA Training under Spectral Initialization

C.2.1 Preconditioned Gradient Descent

Recall the loss of LoRA fine-tuning:

$$\tilde{L}(\mathbf{A}_t, \mathbf{B}_t) = \frac{1}{2N} \left\| \sigma \left(\tilde{\mathbf{X}} \left(\mathbf{W}^\natural + \mathbf{A}_t \mathbf{B}_t \right) \right) - \sigma \left(\tilde{\mathbf{X}} \tilde{\mathbf{W}}^\natural \right) \right\|_F^2.$$

Then, we employ the following preconditioned gradient updates for LoRA fine-tuning

$$\mathbf{A}_{t+1} = \mathbf{A}_t + \eta \mathbf{J}_{\mathbf{W}_t} \mathbf{B}_t^\top \left(\mathbf{B}_t \mathbf{B}_t^\top \right)^{-1}, \quad (\text{C.15})$$

and

$$\mathbf{B}_{t+1} = \mathbf{B}_t + \eta \left(\mathbf{A}_t^\top \mathbf{A}_t \right)^{-1} \mathbf{A}_t^\top \mathbf{J}_{\mathbf{W}_t}. \quad (\text{C.16})$$

Similar to the linear case, we define the following notations

- SVD of product matrix $\mathbf{A}_t \mathbf{B}_t := \mathcal{U}_t \mathcal{S}_t \mathcal{V}_t^\top$, where $\mathcal{U}_t \in \mathbb{R}^{d \times r}$, $\mathcal{S}_t \in \mathbb{R}^{r^* \times r}$, and $\mathcal{V}_t \in \mathbb{R}^{k \times r}$.
- The left singular matrix of \mathbf{A}_t as $\mathbf{U}_{\mathbf{A}_t} \in \mathbb{R}^{d \times r}$.
- The right singular matrix of \mathbf{B}_t as $\mathbf{V}_{\mathbf{B}_t} \in \mathbb{R}^{k \times r}$.

Lemma C.6. Under assumptions in Section 2.1 for the nonlinear setting, we update \mathbf{A}_t and \mathbf{B}_t via Eq. (C.15) and Eq. (C.16) under spectral initialization (**Spectral-init**), then we have the following recursion

$$\begin{aligned} \mathbf{A}_{t+1} \mathbf{B}_{t+1} - \Delta &= (1 - 2\eta c_H) \mathbf{U}_{\mathbf{A}_t} \mathbf{U}_{\mathbf{A}_t}^\top (\mathbf{A}_t \mathbf{B}_t - \Delta) \mathbf{V}_{\mathbf{B}_t} \mathbf{V}_{\mathbf{B}_t}^\top \\ &\quad + (1 - \eta c_H) \left(\mathbf{I}_d - \mathbf{U}_{\mathbf{A}_t} \mathbf{U}_{\mathbf{A}_t}^\top \right) (\mathbf{A}_t \mathbf{B}_t - \Delta) \mathbf{V}_{\mathbf{B}_t} \mathbf{V}_{\mathbf{B}_t}^\top \\ &\quad + (1 - \eta c_H) \mathbf{U}_{\mathbf{A}_t} \mathbf{U}_{\mathbf{A}_t}^\top (\mathbf{A}_t \mathbf{B}_t - \Delta) \left(\mathbf{I}_k - \mathbf{V}_{\mathbf{B}_t} \mathbf{V}_{\mathbf{B}_t}^\top \right) \\ &\quad + \left(\mathbf{I}_d - \mathbf{U}_{\mathbf{A}_t} \mathbf{U}_{\mathbf{A}_t}^\top \right) (\mathbf{A}_t \mathbf{B}_t - \Delta) \left(\mathbf{I}_k - \mathbf{V}_{\mathbf{B}_t} \mathbf{V}_{\mathbf{B}_t}^\top \right) \\ &\quad + \eta \boldsymbol{\Xi}_t \mathbf{V}_{\mathbf{B}_t} \mathbf{V}_{\mathbf{B}_t}^\top + \eta \mathbf{U}_{\mathbf{A}_t} \mathbf{U}_{\mathbf{A}_t}^\top \boldsymbol{\Xi}_t + \eta^2 \mathbf{J}_{\mathbf{W}_t} \mathcal{V}_t \mathcal{S}_t^{-1} \mathcal{U}_t^\top \mathbf{J}_{\mathbf{W}_t}, \end{aligned} \quad (\text{C.17})$$

where c_H is defined in Eq. (C.13) and

$$\boldsymbol{\Xi}_t := \mathbf{J}_{\mathbf{W}_t} - c_H (\mathbf{A}_t \mathbf{B}_t - \Delta).$$

Then, by choosing $\eta \in (0, \frac{1}{2c_H})$, we have the associated upper bound in Frobenius norm

$$\begin{aligned} &\| \mathbf{A}_{t+1} \mathbf{B}_{t+1} - \Delta \|_{\text{F}} \quad (\text{C.18}) \\ &\leq (1 - 2\eta c_H) \left\| \mathbf{U}_{\mathbf{A}_t} \mathbf{U}_{\mathbf{A}_t}^\top (\mathbf{A}_t \mathbf{B}_t - \Delta) \mathbf{V}_{\mathbf{B}_t} \mathbf{V}_{\mathbf{B}_t}^\top \right\|_{\text{F}} \\ &\quad + (1 - c_H \eta) \left\| \left(\mathbf{I}_d - \mathbf{U}_{\mathbf{A}_t} \mathbf{U}_{\mathbf{A}_t}^\top \right) (\mathbf{A}_t \mathbf{B}_t - \Delta) \mathbf{V}_{\mathbf{B}_t} \mathbf{V}_{\mathbf{B}_t}^\top + \mathbf{U}_{\mathbf{A}_t} \mathbf{U}_{\mathbf{A}_t}^\top (\mathbf{A}_t \mathbf{B}_t - \Delta) \left(\mathbf{I}_k - \mathbf{V}_{\mathbf{B}_t} \mathbf{V}_{\mathbf{B}_t}^\top \right) \right\|_{\text{F}} \\ &\quad + \left\| \left(\mathbf{I}_d - \mathbf{U}_{\mathbf{A}_t} \mathbf{U}_{\mathbf{A}_t}^\top \right) (\mathbf{A}_t \mathbf{B}_t - \Delta) \left(\mathbf{I}_k - \mathbf{V}_{\mathbf{B}_t} \mathbf{V}_{\mathbf{B}_t}^\top \right) \right\|_{\text{F}} \\ &\quad + 2\eta \| \boldsymbol{\Xi}_t \|_{\text{F}} + \eta^2 \left\| \mathbf{J}_{\mathbf{W}_t} \mathcal{V}_t \mathcal{S}_t^{-1} \mathcal{U}_t^\top \mathbf{J}_{\mathbf{W}_t} \right\|_{\text{F}}. \end{aligned} \quad (\text{C.19})$$

Proof. By the preconditioned update in Eq. (C.15) and Eq. (C.16), we can construct

$$\begin{aligned}
\mathbf{A}_{t+1}\mathbf{B}_{t+1} - \Delta &= \mathbf{A}_t\mathbf{B}_t - \Delta \\
&\quad - \eta\mathbf{J}_{\mathbf{W}_t}\mathbf{B}_t^\top \left(\mathbf{B}_t\mathbf{B}_t^\top\right)^{-1} \mathbf{B}_t - \eta\mathbf{A}_t \left(\mathbf{A}_t^\top\mathbf{A}_t\right)^{-1} \mathbf{A}_t^\top\mathbf{J}_{\mathbf{W}_t} \\
&\quad + \eta^2\mathbf{J}_{\mathbf{W}_t}\mathbf{B}_t^\top \left(\mathbf{B}_t\mathbf{B}_t^\top\right)^{-1} \left(\mathbf{A}_t^\top\mathbf{A}_t\right)^{-1} \mathbf{A}_t^\top\mathbf{J}_{\mathbf{W}_t} \\
&= \mathbf{A}_t\mathbf{B}_t - \Delta \\
&\quad - \eta c_{\text{H}}(\mathbf{A}_t\mathbf{B}_t - \Delta)\mathbf{B}_t^\top \left(\mathbf{B}_t\mathbf{B}_t^\top\right)^{-1} \mathbf{B}_t + \eta\boldsymbol{\Xi}_t\mathbf{B}_t^\top \left(\mathbf{B}_t\mathbf{B}_t^\top\right)^{-1} \mathbf{B}_t \\
&\quad - \eta c_{\text{H}}\mathbf{A}_t \left(\mathbf{A}_t^\top\mathbf{A}_t\right)^{-1} \mathbf{A}_t^\top(\mathbf{A}_t\mathbf{B}_t - \Delta) + \eta\mathbf{A}_t \left(\mathbf{A}_t^\top\mathbf{A}_t\right)^{-1} \mathbf{A}_t^\top\boldsymbol{\Xi}_t \\
&\quad + \eta^2\mathbf{J}_{\mathbf{W}_t}\mathbf{B}_t^\top \left(\mathbf{B}_t\mathbf{B}_t^\top\right)^{-1} \left(\mathbf{A}_t^\top\mathbf{A}_t\right)^{-1} \mathbf{A}_t^\top\mathbf{J}_{\mathbf{W}_t} \\
&= \mathbf{A}_t\mathbf{B}_t - \Delta \\
&\quad - \eta c_{\text{H}}(\mathbf{A}_t\mathbf{B}_t - \Delta)\mathbf{V}_{\mathbf{B}_t}\mathbf{V}_{\mathbf{B}_t}^\top + \eta\boldsymbol{\Xi}_t\mathbf{V}_{\mathbf{B}_t}\mathbf{V}_{\mathbf{B}_t}^\top \\
&\quad - \eta c_{\text{H}}\mathbf{U}_{\mathbf{A}_t}\mathbf{U}_{\mathbf{A}_t}^\top(\mathbf{A}_t\mathbf{B}_t - \Delta) + \eta\mathbf{U}_{\mathbf{A}_t}\mathbf{U}_{\mathbf{A}_t}^\top\boldsymbol{\Xi}_t \\
&\quad + \eta^2\mathbf{J}_{\mathbf{W}_t}\boldsymbol{\nu}_t\mathcal{S}_t^{-1}\mathcal{U}_t^\top\mathbf{J}_{\mathbf{W}_t}, \\
&\hspace{10em} [\text{by pseudo inverse theorem and Jia et al. (2024, Lemma 14)}]
\end{aligned}$$

from our definition on $c_{\text{H}} > 0$ in Eq. (C.13) and $\boldsymbol{\Xi}_t := \mathbf{J}_{\mathbf{W}_t} - c_{\text{H}}(\mathbf{A}_t\mathbf{B}_t - \Delta)$. We can continue to expand

$$\begin{aligned}
\mathbf{A}_{t+1}\mathbf{B}_{t+1} - \Delta &= \left(\mathbf{I}_d - \mathbf{U}_{\mathbf{A}_t}\mathbf{U}_{\mathbf{A}_t}^\top + \mathbf{U}_{\mathbf{A}_t}\mathbf{U}_{\mathbf{A}_t}^\top\right) (\mathbf{A}_t\mathbf{B}_t - \Delta) \left(\mathbf{I}_d - \mathbf{V}_{\mathbf{B}_t}\mathbf{V}_{\mathbf{B}_t}^\top + \mathbf{V}_{\mathbf{B}_t}\mathbf{V}_{\mathbf{B}_t}^\top\right) \\
&\quad - \eta c_{\text{H}} \left(\mathbf{I}_d - \mathbf{U}_{\mathbf{A}_t}\mathbf{U}_{\mathbf{A}_t}^\top + \mathbf{U}_{\mathbf{A}_t}\mathbf{U}_{\mathbf{A}_t}^\top\right) (\mathbf{A}_t\mathbf{B}_t - \Delta)\mathbf{V}_{\mathbf{B}_t}\mathbf{V}_{\mathbf{B}_t}^\top \\
&\quad - \eta c_{\text{H}}\mathbf{U}_{\mathbf{A}_t}\mathbf{U}_{\mathbf{A}_t}^\top(\mathbf{A}_t\mathbf{B}_t - \Delta) \left(\mathbf{I}_d - \mathbf{V}_{\mathbf{B}_t}\mathbf{V}_{\mathbf{B}_t}^\top + \mathbf{V}_{\mathbf{B}_t}\mathbf{V}_{\mathbf{B}_t}^\top\right) \\
&\quad + \eta\boldsymbol{\Xi}_t\mathbf{V}_{\mathbf{B}_t}\mathbf{V}_{\mathbf{B}_t}^\top + \eta\mathbf{U}_{\mathbf{A}_t}\mathbf{U}_{\mathbf{A}_t}^\top\boldsymbol{\Xi}_t + \eta^2\mathbf{J}_{\mathbf{W}_t}\boldsymbol{\nu}_t\mathcal{S}_t^{-1}\mathcal{U}_t^\top\mathbf{J}_{\mathbf{W}_t} \\
&= (1 - 2\eta c_{\text{H}})\mathbf{U}_{\mathbf{A}_t}\mathbf{U}_{\mathbf{A}_t}^\top(\mathbf{A}_t\mathbf{B}_t - \Delta)\mathbf{V}_{\mathbf{B}_t}\mathbf{V}_{\mathbf{B}_t}^\top \\
&\quad + (1 - \eta c_{\text{H}}) \left(\mathbf{I}_d - \mathbf{U}_{\mathbf{A}_t}\mathbf{U}_{\mathbf{A}_t}^\top\right) (\mathbf{A}_t\mathbf{B}_t - \Delta)\mathbf{V}_{\mathbf{B}_t}\mathbf{V}_{\mathbf{B}_t}^\top \\
&\quad + (1 - \eta c_{\text{H}})\mathbf{U}_{\mathbf{A}_t}\mathbf{U}_{\mathbf{A}_t}^\top(\mathbf{A}_t\mathbf{B}_t - \Delta) \left(\mathbf{I}_k - \mathbf{V}_{\mathbf{B}_t}\mathbf{V}_{\mathbf{B}_t}^\top\right) \\
&\quad + \left(\mathbf{I}_d - \mathbf{U}_{\mathbf{A}_t}\mathbf{U}_{\mathbf{A}_t}^\top\right) (\mathbf{A}_t\mathbf{B}_t - \Delta) \left(\mathbf{I}_k - \mathbf{V}_{\mathbf{B}_t}\mathbf{V}_{\mathbf{B}_t}^\top\right) \\
&\quad + \eta\boldsymbol{\Xi}_t\mathbf{V}_{\mathbf{B}_t}\mathbf{V}_{\mathbf{B}_t}^\top + \eta\mathbf{U}_{\mathbf{A}_t}\mathbf{U}_{\mathbf{A}_t}^\top\boldsymbol{\Xi}_t + \eta^2\mathbf{J}_{\mathbf{W}_t}\boldsymbol{\nu}_t\mathcal{S}_t^{-1}\mathcal{U}_t^\top\mathbf{J}_{\mathbf{W}_t}.
\end{aligned}$$

Based on the above formulation, suppose $\eta \in \left(0, \frac{1}{2c_{\text{H}}}\right)$, we can derive the following upper bound by

triangle inequality

$$\begin{aligned}
& \|\mathbf{A}_{t+1}\mathbf{B}_{t+1} - \Delta\|_{\text{F}} \tag{C.20} \\
& \leq \left\| (1 - 2\eta c_{\text{H}}) \mathbf{U}_{\mathbf{A}_t} \mathbf{U}_{\mathbf{A}_t}^{\top} (\mathbf{A}_t \mathbf{B}_t - \Delta) \mathbf{V}_{\mathbf{B}_t} \mathbf{V}_{\mathbf{B}_t}^{\top} \right\|_{\text{F}} \\
& \quad + \left\| (1 - \eta c_{\text{H}}) \left(\mathbf{I}_d - \mathbf{U}_{\mathbf{A}_t} \mathbf{U}_{\mathbf{A}_t}^{\top} \right) (\mathbf{A}_t \mathbf{B}_t - \Delta) \mathbf{V}_{\mathbf{B}_t} \mathbf{V}_{\mathbf{B}_t}^{\top} \right\|_{\text{F}} \\
& \quad + \left\| (1 - \eta c_{\text{H}}) \mathbf{U}_{\mathbf{A}_t} \mathbf{U}_{\mathbf{A}_t}^{\top} (\mathbf{A}_t \mathbf{B}_t - \Delta) \left(\mathbf{I}_k - \mathbf{V}_{\mathbf{B}_t} \mathbf{V}_{\mathbf{B}_t}^{\top} \right) \right\|_{\text{F}} \\
& \quad + \left\| \left(\mathbf{I}_d - \mathbf{U}_{\mathbf{A}_t} \mathbf{U}_{\mathbf{A}_t}^{\top} \right) (\mathbf{A}_t \mathbf{B}_t - \Delta) \left(\mathbf{I}_k - \mathbf{V}_{\mathbf{B}_t} \mathbf{V}_{\mathbf{B}_t}^{\top} \right) \right\|_{\text{F}} \\
& \quad + \eta \left\| \boldsymbol{\Xi}_t \mathbf{V}_{\mathbf{B}_t} \mathbf{V}_{\mathbf{B}_t}^{\top} \right\|_{\text{F}} + \eta \left\| \mathbf{U}_{\mathbf{A}_t} \mathbf{U}_{\mathbf{A}_t}^{\top} \boldsymbol{\Xi}_t \right\|_{\text{F}} + \eta^2 \left\| \mathbf{J}_{\mathbf{W}_t} \mathcal{V}_t \mathcal{S}_t^{-1} \mathcal{U}_t^{\top} \mathbf{J}_{\mathbf{W}_t} \right\|_{\text{F}} \quad \text{[by triangle inequality]} \\
& \leq (1 - 2\eta c_{\text{H}}) \left\| \mathbf{U}_{\mathbf{A}_t} \mathbf{U}_{\mathbf{A}_t}^{\top} (\mathbf{A}_t \mathbf{B}_t - \Delta) \mathbf{V}_{\mathbf{B}_t} \mathbf{V}_{\mathbf{B}_t}^{\top} \right\|_{\text{F}} \\
& \quad + (1 - c_{\text{H}} \eta) \left\| \left(\mathbf{I}_d - \mathbf{U}_{\mathbf{A}_t} \mathbf{U}_{\mathbf{A}_t}^{\top} \right) (\mathbf{A}_t \mathbf{B}_t - \Delta) \mathbf{V}_{\mathbf{B}_t} \mathbf{V}_{\mathbf{B}_t}^{\top} + \mathbf{U}_{\mathbf{A}_t} \mathbf{U}_{\mathbf{A}_t}^{\top} (\mathbf{A}_t \mathbf{B}_t - \Delta) \left(\mathbf{I}_k - \mathbf{V}_{\mathbf{B}_t} \mathbf{V}_{\mathbf{B}_t}^{\top} \right) \right\|_{\text{F}} \\
& \quad + \left\| \left(\mathbf{I}_d - \mathbf{U}_{\mathbf{A}_t} \mathbf{U}_{\mathbf{A}_t}^{\top} \right) (\mathbf{A}_t \mathbf{B}_t - \Delta) \left(\mathbf{I}_k - \mathbf{V}_{\mathbf{B}_t} \mathbf{V}_{\mathbf{B}_t}^{\top} \right) \right\|_{\text{F}} \\
& \quad + 2\eta \|\boldsymbol{\Xi}_t\|_{\text{F}} + \eta^2 \left\| \mathbf{J}_{\mathbf{W}_t} \mathcal{V}_t \mathcal{S}_t^{-1} \mathcal{U}_t^{\top} \mathbf{J}_{\mathbf{W}_t} \right\|_{\text{F}}, \quad \text{[since } \eta \in (0, \frac{1}{2c_{\text{H}}}) \text{]}
\end{aligned}$$

which proves the claim. \square

In order to derive the convergence rate of $\|\mathbf{A}_{t+1}\mathbf{B}_{t+1} - \Delta\|_{\text{F}}$ in the above terms, we need to provide the estimation of the following four terms

$$\begin{aligned}
& \|\boldsymbol{\Xi}_t\|_{\text{F}}, \quad \left\| \mathbf{J}_{\mathbf{W}_t} \mathcal{V}_t \mathcal{S}_t^{-1} \mathcal{U}_t^{\top} \mathbf{J}_{\mathbf{W}_t} \right\|_{\text{F}}, \\
& \left\| \left(\mathbf{I}_d - \mathbf{U}_{\mathbf{A}_t} \mathbf{U}_{\mathbf{A}_t}^{\top} \right) (\mathbf{A}_t \mathbf{B}_t - \Delta) \mathbf{V}_{\mathbf{B}_t} \mathbf{V}_{\mathbf{B}_t}^{\top} + \mathbf{U}_{\mathbf{A}_t} \mathbf{U}_{\mathbf{A}_t}^{\top} (\mathbf{A}_t \mathbf{B}_t - \Delta) \left(\mathbf{I}_k - \mathbf{V}_{\mathbf{B}_t} \mathbf{V}_{\mathbf{B}_t}^{\top} \right) \right\|_{\text{F}}, \\
& \left\| \left(\mathbf{I}_d - \mathbf{U}_{\mathbf{A}_t} \mathbf{U}_{\mathbf{A}_t}^{\top} \right) (\mathbf{A}_t \mathbf{B}_t - \Delta) \left(\mathbf{I}_k - \mathbf{V}_{\mathbf{B}_t} \mathbf{V}_{\mathbf{B}_t}^{\top} \right) \right\|_{\text{F}}.
\end{aligned}$$

which are important elements in Eq. (C.18). We firstly prove the upper bound for $\|\boldsymbol{\Xi}_t\|_{\text{F}}$ and $\left\| \mathbf{J}_{\mathbf{W}_t} \mathcal{V}_t \mathcal{S}_t^{-1} \mathcal{U}_t^{\top} \mathbf{J}_{\mathbf{W}_t} \right\|_{\text{F}}$ since they are relatively straightforward. After that, we will handle with the remaining three terms which are the most technical part. All of these three terms rely on the condition $\|\mathbf{A}_t \mathbf{B}_t - \Delta\|_{\text{F}} \leq \rho \lambda_{r^*}^*$ and we will prove it by induction finally in Theorem C.10.

Lemma C.7. For any $\rho \in (0, 1)$, suppose $\epsilon \leq \frac{\rho}{3C^* K^2 \gamma \sqrt{2d} r^* \kappa}$ with $\gamma \in \left[\frac{1}{c_{\text{H}}} - \frac{\rho}{3c_{\text{H}} \kappa \sqrt{2} r^*}, \frac{1}{c_{\text{H}}} + \frac{\rho}{3c_{\text{H}} \kappa \sqrt{2} r^*} \right]$, where c_{H} is defined in Eq. (C.13), assume $\|\mathbf{A}_t \mathbf{B}_t - \Delta\|_{\text{F}} \leq \rho \lambda_{r^*}^*$, under assumptions in Section 2.1 for the nonlinear setting, Assumption 4.1, and Assumption 4.2, then with probability at least $1 - 2Cdk \exp(-\epsilon^2 N)$ for a universal constant $C > 0$, we have

$$\|\boldsymbol{\Xi}_t\|_{\text{F}} \leq \left(h(\rho) + C^* K^2 \sqrt{d} \epsilon \right) \|\mathbf{A}_t \mathbf{B}_t - \Delta\|_{\text{F}},$$

where

$$h(\rho) := \left(\frac{\frac{\sqrt{2}+1}{2} \left(\frac{\sqrt{2}+1}{2} + \frac{\rho(\sqrt{2}-1)}{2} \right) + \left(\frac{\sqrt{2}+1}{2} + \frac{\rho(\sqrt{2}-1)}{2} \right)^2}{8\pi} + \frac{\left(\frac{\sqrt{2}+1}{2} + \frac{\rho(\sqrt{2}-1)}{2} \right)^4}{1152\pi} \right. \\ \left. + \frac{\frac{\sqrt{2}+1}{2} \left(\frac{\sqrt{2}+1}{2} + \frac{\rho(\sqrt{2}-1)}{2} \right)^5 + \left(\frac{\sqrt{2}+1}{2} + \frac{\rho(\sqrt{2}-1)}{2} \right)^6}{1728\pi} + \frac{\left(\frac{\sqrt{2}+1}{2} + \frac{\rho(\sqrt{2}-1)}{2} \right)^8}{2073600\pi} \right). \quad (\text{C.21})$$

Proof. Recall $\Xi_t := \mathbf{J}\mathbf{W}_t - c_H(\mathbf{A}_t\mathbf{B}_t - \Delta)$, then with probability at least $1 - 2Cdk \exp(-\epsilon^2 N)$ for a universal constant $C > 0$, we have

$$\begin{aligned} \|\Xi_t\|_{\text{F}} &= \|c_H(\mathbf{A}_t\mathbf{B}_t - \Delta) - \mathbb{E}_{\tilde{\mathbf{x}}}[\mathbf{J}\mathbf{W}_t] + \mathbb{E}_{\tilde{\mathbf{x}}}[\mathbf{J}\mathbf{W}_t] - \mathbf{J}\mathbf{W}_t\|_{\text{F}} \\ &\leq \|c_H(\mathbf{A}_t\mathbf{B}_t - \Delta) - \mathbb{E}_{\tilde{\mathbf{x}}}[\mathbf{J}\mathbf{W}_t]\|_{\text{F}} + \|\mathbb{E}_{\tilde{\mathbf{x}}}[\mathbf{J}\mathbf{W}_t] - \mathbf{J}\mathbf{W}_t\|_{\text{F}} \\ &= \left\| \sum_{\substack{n \geq 1, \\ n \text{ odd}}} \Psi_t(n) \right\|_{\text{F}} + \|\mathbb{E}_{\tilde{\mathbf{x}}}[\mathbf{J}\mathbf{W}_t] - \mathbf{J}\mathbf{W}_t\|_{\text{F}} && \text{[by Lemma C.2]} \\ &\leq \sum_{\substack{n \geq 1, \\ n \text{ odd}}} \|\Psi_t(n)\|_{\text{F}} + \|\mathbb{E}_{\tilde{\mathbf{x}}}[\mathbf{J}\mathbf{W}_t] - \mathbf{J}\mathbf{W}_t\|_{\text{F}} \\ &\leq \left(\frac{\|\widetilde{\mathbf{W}}^\natural\|_{\text{op}} \max \left\{ \left(1 + \|\mathbf{A}_t\mathbf{B}_t - \Delta\|_{\text{op}} + \|\Delta\|_{\text{op}} \right), \|\widetilde{\mathbf{W}}^\natural\|_{\text{op}} \right\}^{2n-1}}{4\pi 2^n n(n!)^2} \right. \\ &\quad \left. + \frac{\left(\|\widetilde{\mathbf{W}}^\natural\|_{\text{op}} + \|\mathbf{A}_t\mathbf{B}_t - \Delta\|_{\text{op}} \right) \max \left\{ \left(1 + \|\mathbf{A}_t\mathbf{B}_t - \Delta\|_{\text{op}} + \|\Delta\|_{\text{op}} \right), \|\widetilde{\mathbf{W}}^\natural\|_{\text{op}} \right\}^{2n+1}}{4\pi 2^{n+1} n(n+2)n!(n+3)!} \right. \\ &\quad \left. + \frac{\left(1 + \|\mathbf{A}_t\mathbf{B}_t - \Delta\|_{\text{op}} + \|\Delta\|_{\text{op}} \right)^{2n}}{4\pi 2^n n(n!)^2} \right) \|\mathbf{A}_t\mathbf{B}_t - \Delta\|_{\text{F}} && \text{[by Lemma C.2]} \\ &\quad + C^* K^2 \sqrt{d\epsilon} \|\mathbf{A}_t\mathbf{B}_t - \Delta\|_{\text{F}}. && \text{[by Theorem C.4]} \end{aligned}$$

Note that for any odd $n \geq 1$, we have

$$\frac{n(n!)^2}{(n+2)((n+2)!)^2} = \frac{n}{(n+2)^3(n+1)^2} < \frac{1}{2}, \quad \frac{n(n+2)n!(n+3)!}{(n+2)(n+4)(n+2)!(n+5)!} < \frac{1}{2}.$$

According to our assumption $\|\mathbf{A}_t\mathbf{B}_t - \Delta\|_{\text{F}} \leq \rho\lambda_{r^*}$ for $\rho \in (0, 1)$, then by Assumption 4.1 and Assumption 4.2, we have

$$1 + \|\mathbf{A}_t\mathbf{B}_t - \Delta\|_{\text{op}} + \|\Delta\|_{\text{op}} \leq 1 + (1 + \rho) \|\Delta\|_{\text{op}} \leq \frac{\sqrt{2}+1}{2} + \frac{\rho(\sqrt{2}-1)}{2},$$

and

$$\|\widetilde{\mathbf{W}}^\natural\|_{\text{op}} \leq 1 + \|\Delta\|_{\text{op}} \leq \frac{\sqrt{2}+1}{2},$$

which implies

$$\begin{aligned}
& \frac{\|\widetilde{\mathbf{W}}^\natural\|_{op} \max \left\{ \left(1 + \|\mathbf{A}_t \mathbf{B}_t - \Delta\|_{op} + \|\Delta\|_{op}\right), \|\widetilde{\mathbf{W}}^\natural\|_{op} \right\}^{2n-1}}{2^n} \leq \frac{\frac{\sqrt{2}+1}{2} \left(\frac{\sqrt{2}+1}{2} + \frac{\rho(\sqrt{2}-1)}{2} \right)^{2n-1}}{2^n} \leq 1, \\
& \frac{\left(1 + \|\mathbf{A}_t \mathbf{B}_t - \Delta\|_{op} + \|\Delta\|_{op}\right)^{2n}}{4\pi 2^n n(n!)^2} \leq \frac{\left(\frac{\sqrt{2}+1}{2} + \frac{\rho(\sqrt{2}-1)}{2} \right)^{2n}}{2^n} \leq 1, \\
& \frac{\left(\|\widetilde{\mathbf{W}}^\natural\|_{op} + \|\mathbf{A}_t \mathbf{B}_t - \Delta\|_{op} \right) \max \left\{ \left(1 + \|\mathbf{A}_t \mathbf{B}_t - \Delta\|_{op} + \|\Delta\|_{op}\right), \|\widetilde{\mathbf{W}}^\natural\|_{op} \right\}^{2n+1}}{2^{n+1}} \\
& \leq \frac{\left(\frac{\sqrt{2}+1}{2} + \frac{\rho(\sqrt{2}-1)}{2} \right)^{2(n+1)}}{2^{n+1}} \leq 1.
\end{aligned}$$

Through above characterization of the decay, to obtain a tight upper bound, here we propose to use

$$\begin{aligned}
& \sum_{\substack{n \geq 1, \\ n \text{ odd}}} \|\Psi_t(n)\|_{\mathbb{F}} \leq \|\Psi_t(1)\|_{\mathbb{F}} + 2\|\Psi_t(3)\|_{\mathbb{F}} \\
& \leq \left(\frac{\frac{\sqrt{2}+1}{2} \left(\frac{\sqrt{2}+1}{2} + \frac{\rho(\sqrt{2}-1)}{2} \right) + \left(\frac{\sqrt{2}+1}{2} + \frac{\rho(\sqrt{2}-1)}{2} \right)^2}{8\pi} + \frac{\left(\frac{\sqrt{2}+1}{2} + \frac{\rho(\sqrt{2}-1)}{2} \right)^4}{1152\pi} \right. \\
& \quad \left. + \frac{\frac{\sqrt{2}+1}{2} \left(\frac{\sqrt{2}+1}{2} + \frac{\rho(\sqrt{2}-1)}{2} \right)^5 + \left(\frac{\sqrt{2}+1}{2} + \frac{\rho(\sqrt{2}-1)}{2} \right)^6}{1728\pi} + \frac{\left(\frac{\sqrt{2}+1}{2} + \frac{\rho(\sqrt{2}-1)}{2} \right)^8}{2073600\pi} \right) \|\mathbf{A}_t \mathbf{B}_t - \Delta\|_{\mathbb{F}},
\end{aligned}$$

which completes the proof. \square

Lemma C.8. Under assumptions in Section 2.1 for the nonlinear setting, suppose $\|\mathbf{A}_t \mathbf{B}_t - \Delta\|_{\mathbb{F}} \leq \rho \lambda_{r^*}$ for $\rho > 0$, with probability at least $1 - 2C \exp(-\epsilon^2 N)$ for some constants $C > 0$, it holds that

$$\left\| \mathbf{J}_{\mathbf{W}_t} \mathcal{V}_t \mathcal{S}_t^{-1} \mathcal{U}_t^\top \mathbf{J}_{\mathbf{W}_t} \right\|_{\mathbb{F}} \leq (1 + \epsilon)^2 \frac{\rho}{1 - \rho} \|\mathbf{A}_t \mathbf{B}_t - \Delta\|_{\mathbb{F}}.$$

Proof. First, with probability at least $1 - 2C \exp(-\epsilon^2 N)$ for some constants $C > 0$, we can derive

$$\begin{aligned}
& \left\| \mathbf{J}_{\mathbf{W}_t} \mathcal{V}_t \mathcal{S}_t^{-1} \mathcal{U}_t^\top \mathbf{J}_{\mathbf{W}_t} \right\|_{\mathbb{F}} \leq \left\| \mathbf{J}_{\mathbf{W}_t} \right\|_{\mathbb{F}}^2 \left\| \mathcal{V}_t \mathcal{S}_t^{-1} \mathcal{U}_t^\top \right\|_{op} \\
& = \frac{\left\| \frac{1}{N} \widetilde{\mathbf{X}}^\top \left(\sigma \left(\widetilde{\mathbf{X}} (\mathbf{W}^\natural + \mathbf{A}_t \mathbf{B}_t) \right) - \sigma \left(\widetilde{\mathbf{X}} \widetilde{\mathbf{W}}^\natural \right) \right) \odot \sigma' \left(\widetilde{\mathbf{X}} (\mathbf{W}^\natural + \mathbf{A}_t \mathbf{B}_t) \right) \right\|_{\mathbb{F}}^2}{\lambda_r(\mathbf{A}_t \mathbf{B}_t)} \\
& \leq \frac{\left\| \frac{1}{N} \widetilde{\mathbf{X}}^\top \widetilde{\mathbf{X}} (\mathbf{A}_t \mathbf{B}_t - \Delta) \right\|_{\mathbb{F}}^2}{\lambda_r(\mathbf{A}_t \mathbf{B}_t)} \quad \text{[by Lipschitz continuity of } \sigma, \sigma'] \\
& \leq \left(\frac{1}{N} \lambda_1^2(\widetilde{\mathbf{X}}) \right)^2 \frac{\|\mathbf{A}_t \mathbf{B}_t - \Delta\|_{\mathbb{F}}^2}{\lambda_r(\mathbf{A}_t \mathbf{B}_t)} \\
& \leq (1 + \epsilon)^2 \frac{\rho}{1 - \rho} \|\mathbf{A}_t \mathbf{B}_t - \Delta\|_{\mathbb{F}}, \quad \text{[by concentration of operator norm]}
\end{aligned}$$

where the last equality follows from $r = r^*$ and

$$\lambda_r(\mathbf{A}_t \mathbf{B}_t) \geq \lambda_{r^*}(\Delta) - \|\mathbf{A}_t \mathbf{B}_t - \Delta\|_{\text{F}} \geq (1 - \rho) \lambda_{r^*}(\Delta).$$

□

With Lemma C.7 and Lemma C.8, now we can prove for the other three terms.

Lemma C.9. Suppose $\|\mathbf{A}_t \mathbf{B}_t - \Delta\|_{\text{F}} \leq \rho \lambda_{r^*}^*$ with $\rho \in [0, 1/4]$, then it holds that

$$\left\| \left(\mathbf{I}_d - \mathbf{U}_{\mathbf{A}_t} \mathbf{U}_{\mathbf{A}_t}^\top \right) \Delta \left(\mathbf{I}_k - \mathbf{V}_{\mathbf{B}_t} \mathbf{V}_{\mathbf{B}_t}^\top \right) \right\|_{\text{F}} \leq \frac{\rho}{\sqrt{1 - 8\rho^2}} \|\mathbf{A}_t \mathbf{B}_t - \Delta\|_{\text{F}},$$

and

$$\left\| \left(\mathbf{I}_d - \mathbf{U}_{\mathbf{A}_t} \mathbf{U}_{\mathbf{A}_t}^\top \right) \Delta \mathbf{V}_{\mathbf{B}_t} \mathbf{V}_{\mathbf{B}_t}^\top + \mathbf{U}_{\mathbf{A}_t} \mathbf{U}_{\mathbf{A}_t}^\top \Delta \left(\mathbf{I}_k - \mathbf{V}_{\mathbf{B}_t} \mathbf{V}_{\mathbf{B}_t}^\top \right) \right\|_{\text{F}} \leq \|\mathbf{A}_t \mathbf{B}_t - \Delta\|_{\text{F}}.$$

Proof. First, we recall

$$\mathbf{Z}_t = \begin{bmatrix} \mathbf{A}_t \\ \mathbf{B}_t^\top \end{bmatrix}, \quad \underline{\mathbf{Z}}_t = \begin{bmatrix} \mathbf{A}_t \\ -\mathbf{B}_t^\top \end{bmatrix},$$

and define a preconditioned operator \mathcal{P} and symmetrized downstream feature shift matrix $\widehat{\Delta}$ as

$$\mathcal{P}(\mathbf{Z}_t) := \begin{bmatrix} \mathbf{A}_t (\mathbf{A}_t^\top \mathbf{A}_t)^{-1} \\ \mathbf{B}_t^\top (\mathbf{B}_t \mathbf{B}_t^\top)^{-1} \end{bmatrix}, \quad \mathcal{P}(\underline{\mathbf{Z}}_t) := \begin{bmatrix} \mathbf{A}_t (\mathbf{A}_t^\top \mathbf{A}_t)^{-1} \\ -\mathbf{B}_t^\top (\mathbf{B}_t \mathbf{B}_t^\top)^{-1} \end{bmatrix}, \quad \widehat{\Delta} := \begin{bmatrix} \mathbf{0}_{d \times d} & \Delta \\ \Delta^\top & \mathbf{0}_{k \times k} \end{bmatrix}.$$

Next, we observe that

$$\frac{1}{2} \left(\mathbf{Z}_t \mathbf{Z}_t^\top - \underline{\mathbf{Z}}_t \underline{\mathbf{Z}}_t^\top \right) - \widehat{\Delta} = \begin{bmatrix} \mathbf{0}_{d \times d} & \mathbf{A}_t \mathbf{B}_t - \Delta \\ (\mathbf{A}_t \mathbf{B}_t - \Delta)^\top & \mathbf{0}_{k \times k} \end{bmatrix},$$

leading to

$$\left\| \frac{1}{2} \left(\mathbf{Z}_t \mathbf{Z}_t^\top - \underline{\mathbf{Z}}_t \underline{\mathbf{Z}}_t^\top \right) - \widehat{\Delta} \right\|_{op} = \|\mathbf{A}_t \mathbf{B}_t - \Delta\|_{op}, \quad \left\| \frac{1}{2} \left(\mathbf{Z}_t \mathbf{Z}_t^\top - \underline{\mathbf{Z}}_t \underline{\mathbf{Z}}_t^\top \right) - \widehat{\Delta} \right\|_{\text{F}} = \sqrt{2} \|\mathbf{A}_t \mathbf{B}_t - \Delta\|_{\text{F}}.$$

Based on the compact SVD of Δ in Eq. (2.1), we can write out the eigendecomposition of $\widehat{\Delta}$ as

$$\widehat{\Delta} = \begin{bmatrix} \Phi & \underline{\Phi} \end{bmatrix} \begin{bmatrix} \mathbf{S}^* & \mathbf{0}_{r^* \times r^*} \\ \mathbf{0}_{r^* \times r^*} & -\mathbf{S}^* \end{bmatrix} \begin{bmatrix} \Phi & \underline{\Phi} \end{bmatrix}^\top = \Phi \mathbf{S}^* \Phi^\top - \underline{\Phi} \mathbf{S}^* \underline{\Phi}^\top, \quad \text{where } \Phi = \frac{1}{\sqrt{2}} \begin{bmatrix} \mathbf{U} \\ \mathbf{V} \end{bmatrix}, \underline{\Phi} = \frac{1}{\sqrt{2}} \begin{bmatrix} \mathbf{U} \\ -\mathbf{V} \end{bmatrix}. \quad (\text{C.22})$$

Notice that we can also obtain the SVD of $\widehat{\Delta}$ as

$$\widehat{\Delta} = \widehat{\mathbf{U}} \widehat{\mathbf{S}} \widehat{\mathbf{V}}^\top = \underbrace{\begin{bmatrix} \Phi & \underline{\Phi} \end{bmatrix}}_{:=\widehat{\mathbf{U}}} \underbrace{\begin{bmatrix} \mathbf{S}^* & \mathbf{0}_{r^* \times r^*} \\ \mathbf{0}_{r^* \times r^*} & \mathbf{S}^* \end{bmatrix}}_{:=\widehat{\mathbf{S}}} \underbrace{\begin{bmatrix} \Phi & -\underline{\Phi} \end{bmatrix}^\top}_{:=\widehat{\mathbf{V}}^\top}. \quad (\text{C.23})$$

Notice that $\widehat{\Delta}$ is a low-rank matrix with rank- $2r^*$ because of $\text{Rank}(\Delta) = r^*$. If $\frac{1}{2} (\mathbf{Z}_t \mathbf{Z}_t^\top - \underline{\mathbf{Z}}_t \underline{\mathbf{Z}}_t^\top)$

recovers $\widehat{\Delta}$, this indicates that the top- $2r^*$ subspace of $\frac{1}{2}(\mathbf{Z}_t\mathbf{Z}_t^\top - \underline{\mathbf{Z}}_t\underline{\mathbf{Z}}_t^\top)$ will align to $\widehat{\Delta}$ perfectly. Next, we can derive the projection matrix for the top- $2r^*$ subspace of $\frac{1}{2}(\mathbf{Z}_t\mathbf{Z}_t^\top - \underline{\mathbf{Z}}_t\underline{\mathbf{Z}}_t^\top)$. First, we have

$$\mathbf{Z}_t\mathcal{P}^\top(\mathbf{Z}_t) = \begin{bmatrix} \mathbf{A}_t(\mathbf{A}_t^\top\mathbf{A}_t)^{-1}\mathbf{A}_t^\top & \mathbf{A}_t(\mathbf{B}_t\mathbf{B}_t^\top)^{-1}\mathbf{B}_t \\ \mathbf{B}_t^\top(\mathbf{A}_t^\top\mathbf{A}_t)^{-1}\mathbf{A}_t^\top & \mathbf{B}_t^\top(\mathbf{B}_t\mathbf{B}_t^\top)^{-1}\mathbf{B}_t \end{bmatrix},$$

which can imply

$$\begin{aligned} \frac{1}{2}\mathbf{Z}_t\mathcal{P}^\top(\mathbf{Z}_t)\mathbf{Z}_t\mathbf{Z}_t^\top &= \frac{1}{2} \begin{bmatrix} \mathbf{A}_t(\mathbf{A}_t^\top\mathbf{A}_t)^{-1}\mathbf{A}_t^\top & \mathbf{A}_t(\mathbf{B}_t\mathbf{B}_t^\top)^{-1}\mathbf{B}_t \\ \mathbf{B}_t^\top(\mathbf{A}_t^\top\mathbf{A}_t)^{-1}\mathbf{A}_t^\top & \mathbf{B}_t^\top(\mathbf{B}_t\mathbf{B}_t^\top)^{-1}\mathbf{B}_t \end{bmatrix} \begin{bmatrix} \mathbf{A}_t\mathbf{A}_t^\top & \mathbf{A}_t\mathbf{B}_t \\ \mathbf{B}_t^\top\mathbf{A}_t^\top & \mathbf{B}_t^\top\mathbf{B}_t \end{bmatrix} \\ &= \frac{1}{2} \begin{bmatrix} \mathbf{A}_t\mathbf{A}_t^\top & \mathbf{A}_t\mathbf{B}_t \\ \mathbf{B}_t^\top\mathbf{A}_t^\top & \mathbf{B}_t^\top\mathbf{B}_t \end{bmatrix} = \frac{1}{2}\mathbf{Z}_t\mathbf{Z}_t^\top. \end{aligned}$$

Similarly, we can derive

$$\frac{1}{2}\underline{\mathbf{Z}}_t\mathcal{P}^\top(\underline{\mathbf{Z}}_t)\underline{\mathbf{Z}}_t\underline{\mathbf{Z}}_t^\top = \frac{1}{2} \begin{bmatrix} \mathbf{A}_t\mathbf{A}_t^\top & -\mathbf{A}_t\mathbf{B}_t \\ -\mathbf{B}_t^\top\mathbf{A}_t^\top & \mathbf{B}_t^\top\mathbf{B}_t \end{bmatrix} = \frac{1}{2}\underline{\mathbf{Z}}_t\underline{\mathbf{Z}}_t^\top.$$

Additionally, we have

$$\frac{1}{2}\underline{\mathbf{Z}}_t\mathcal{P}^\top(\underline{\mathbf{Z}}_t)\mathbf{Z}_t\mathbf{Z}_t^\top = \mathbf{0}_{(d+k)\times(d+k)}, \quad \frac{1}{2}\mathbf{Z}_t\mathcal{P}^\top(\mathbf{Z}_t)\underline{\mathbf{Z}}_t\underline{\mathbf{Z}}_t^\top = \mathbf{0}_{(d+k)\times(d+k)}.$$

Base on the above identity, we can obtain that the subspace of $\mathbf{Z}_t\mathbf{Z}_t^\top$ is orthogonal to the subspace of $\underline{\mathbf{Z}}_t\underline{\mathbf{Z}}_t^\top$. Since $\text{Rank}(\mathbf{Z}_t\mathbf{Z}_t^\top) \leq r$ and $\text{Rank}(\underline{\mathbf{Z}}_t\underline{\mathbf{Z}}_t^\top) \leq r$, then we have that $\text{Rank}(\mathbf{Z}_t\mathbf{Z}_t^\top - \underline{\mathbf{Z}}_t\underline{\mathbf{Z}}_t^\top) \leq 2r^*$ since $r = r^*$. Therefore, we can construct a valid projection matrix

$$\mathbf{P}_t := \mathbf{Z}_t\mathcal{P}^\top(\mathbf{Z}_t) + \underline{\mathbf{Z}}_t\mathcal{P}^\top(\underline{\mathbf{Z}}_t), \quad (\text{C.24})$$

which satisfies

$$\frac{1}{2}\mathbf{P}_t \left(\mathbf{Z}_t\mathbf{Z}_t^\top - \underline{\mathbf{Z}}_t\underline{\mathbf{Z}}_t^\top \right) = \frac{1}{2} \left(\mathbf{Z}_t\mathbf{Z}_t^\top - \underline{\mathbf{Z}}_t\underline{\mathbf{Z}}_t^\top \right),$$

and

$$\frac{1}{2}(\mathbf{I}_{d+k} - \mathbf{P}_t) \left(\mathbf{Z}_t\mathbf{Z}_t^\top - \underline{\mathbf{Z}}_t\underline{\mathbf{Z}}_t^\top \right) = \mathbf{0}_{(d+k)\times(d+k)}. \quad (\text{C.25})$$

Also, we can verify that \mathbf{P}_t is symmetric and $\mathbf{P}_t\mathbf{P}_t = \mathbf{P}_t$. Therefore we can conclude that \mathbf{P}_t is the projection matrix which maps matrices or vectors to the top- $2r$ subspace of $\frac{1}{2}(\mathbf{Z}_t\mathbf{Z}_t^\top - \underline{\mathbf{Z}}_t\underline{\mathbf{Z}}_t^\top)$. For notational simplicity, here we fix the timestamp t and denote

$$\mathbf{F} := \frac{1}{2\sqrt{2}} \left(\mathbf{Z}_t\mathbf{Z}_t^\top - \underline{\mathbf{Z}}_t\underline{\mathbf{Z}}_t^\top \right),$$

which means

$$\left\| \mathbf{F} - \frac{\widehat{\Delta}}{\sqrt{2}} \right\|_{\text{F}} = \|\mathbf{A}_t\mathbf{B}_t - \Delta\|_{\text{F}} \leq \rho\lambda_{r^*}^*. \quad (\text{C.26})$$

Next, we define $\mathbf{P}_t := \mathbf{L}\mathbf{L}^\top \in \mathbb{R}^{(d+k) \times (d+k)}$ with

$$\mathbf{L} = \begin{bmatrix} \mathbf{U}_{\mathbf{A}_t} & \mathbf{0}_{d \times r} \\ \mathbf{0}_{k \times r} & \mathbf{V}_{\mathbf{B}_t} \end{bmatrix} \in \mathbb{R}^{(d+k) \times 2r},$$

and $(\mathbf{I}_{d+k} - \mathbf{P}_t) = \mathbf{L}_\perp \mathbf{L}_\perp^\top$ where

$$\mathbf{L}_\perp = \begin{bmatrix} \mathbf{U}_{\mathbf{A}_t, \perp} & \mathbf{0}_{d \times (k-r)} \\ \mathbf{0}_{k \times (d-r)} & \mathbf{V}_{\mathbf{B}_t, \perp} \end{bmatrix} \in \mathbb{R}^{(d+k) \times (d+k-2r)},$$

then we have

$$\begin{aligned} \left\| \mathbf{F} - \frac{\widehat{\Delta}}{\sqrt{2}} \right\|_{\mathbb{F}}^2 &= \left\| \begin{bmatrix} \mathbf{L}^\top \\ \mathbf{L}_\perp^\top \end{bmatrix} \left(\mathbf{F} - \frac{\widehat{\Delta}}{\sqrt{2}} \right) \begin{bmatrix} \mathbf{L} & \mathbf{L}_\perp \end{bmatrix} \right\|_{\mathbb{F}} \\ &= \left\| \begin{bmatrix} \mathbf{L}^\top \mathbf{F} \mathbf{L} - \mathbf{L}^\top \frac{\widehat{\Delta}}{\sqrt{2}} \mathbf{L} & -\mathbf{L}^\top \frac{\widehat{\Delta}}{\sqrt{2}} \mathbf{L}_\perp \\ -\mathbf{L}_\perp^\top \frac{\widehat{\Delta}}{\sqrt{2}} \mathbf{L} & \mathbf{L}_\perp^\top \frac{\widehat{\Delta}}{\sqrt{2}} \mathbf{L}_\perp \end{bmatrix} \right\|_{\mathbb{F}}^2 && \text{[by Eq. (C.25)]} \\ &= \left\| \mathbf{L}^\top \mathbf{F} \mathbf{L} - \frac{1}{\sqrt{2}} \mathbf{L}^\top \widehat{\Delta} \mathbf{L} \right\|_{\mathbb{F}}^2 + \frac{1}{2} \left\| \mathbf{L}_\perp^\top \widehat{\Delta} \mathbf{L} \right\|_{\mathbb{F}}^2 + \frac{1}{2} \left\| \mathbf{L}^\top \widehat{\Delta} \mathbf{L}_\perp \right\|_{\mathbb{F}}^2 + \frac{1}{2} \left\| \mathbf{L}_\perp^\top \widehat{\Delta} \mathbf{L}_\perp \right\|_{\mathbb{F}}^2. \end{aligned} \quad (\text{C.27})$$

Since $\mathbf{I}_{d+k} - \mathbf{P}_t = \mathbf{L}_\perp \mathbf{L}_\perp^\top$, then we have

$$\left\| \left(\mathbf{I}_d - \mathbf{U}_{\mathbf{A}_t} \mathbf{U}_{\mathbf{A}_t}^\top \right) \Delta \left(\mathbf{I}_k - \mathbf{V}_{\mathbf{B}_t} \mathbf{V}_{\mathbf{B}_t}^\top \right) \right\|_{\mathbb{F}} = \frac{1}{\sqrt{2}} \left\| \mathbf{L}_\perp^\top \widehat{\Delta} \mathbf{L}_\perp \right\|_{\mathbb{F}}. \quad (\text{C.28})$$

Next, by Eq. (C.27), we have $\left\| \mathbf{F} - \frac{\widehat{\Delta}}{\sqrt{2}} \right\|_{\mathbb{F}}^2 \geq \frac{1}{2} \left\| \mathbf{L}_\perp^\top \widehat{\Delta} \mathbf{L} \right\|_{\mathbb{F}}^2 + \frac{1}{2} \left\| \mathbf{L}^\top \widehat{\Delta} \mathbf{L}_\perp \right\|_{\mathbb{F}}^2$, leading to

$$\frac{\frac{1}{2} \left\| \mathbf{L}_\perp^\top \widehat{\Delta} \mathbf{L}_\perp \right\|_{\mathbb{F}}^2}{\left\| \mathbf{F} - \frac{\widehat{\Delta}}{\sqrt{2}} \right\|_{\mathbb{F}}^2} \leq \frac{\frac{1}{2} \left\| \mathbf{L}_\perp^\top \widehat{\Delta} \mathbf{L}_\perp \right\|_{\mathbb{F}}^2}{\frac{1}{2} \left\| \mathbf{L}_\perp^\top \widehat{\Delta} \mathbf{L} \right\|_{\mathbb{F}}^2 + \frac{1}{2} \left\| \mathbf{L}^\top \widehat{\Delta} \mathbf{L}_\perp \right\|_{\mathbb{F}}^2}. \quad (\text{C.29})$$

The technical part is to lower bound $\left\| \mathbf{L}_\perp^\top \widehat{\Delta} \mathbf{L} \right\|_{\mathbb{F}}^2$ and $\left\| \mathbf{L}^\top \widehat{\Delta} \mathbf{L}_\perp \right\|_{\mathbb{F}}^2$, we will rely on the following decomposition which based on Eq. (C.23), i.e.

$$\begin{aligned} \left\| \mathbf{L}_\perp^\top \widehat{\Delta} \mathbf{L} \right\|_{\mathbb{F}}^2 &= \left\| \mathbf{L}_\perp^\top \widehat{\mathbf{U}} \widehat{\mathbf{S}} \widehat{\mathbf{V}}^\top \mathbf{L} \right\|_{\mathbb{F}}^2 \\ &= \left\| \left(\mathbf{L}_\perp^\top \widehat{\mathbf{U}} \widehat{\mathbf{S}}^{1/2} \right) \left(\mathbf{L}^\top \widehat{\mathbf{V}} \widehat{\mathbf{S}}^{1/2} \right)^\top \right\|_{\mathbb{F}}^2 \\ &= \text{tr} \left(\left(\mathbf{L}^\top \widehat{\mathbf{V}} \widehat{\mathbf{S}}^{1/2} \right) \left(\mathbf{L}_\perp^\top \widehat{\mathbf{U}} \widehat{\mathbf{S}}^{1/2} \right)^\top \left(\mathbf{L}_\perp^\top \widehat{\mathbf{U}} \widehat{\mathbf{S}}^{1/2} \right) \left(\mathbf{L}^\top \widehat{\mathbf{V}} \widehat{\mathbf{S}}^{1/2} \right)^\top \right) \\ &= \text{tr} \left(\left(\mathbf{L}^\top \widehat{\mathbf{V}} \widehat{\mathbf{S}}^{1/2} \right)^\top \left(\mathbf{L}^\top \widehat{\mathbf{V}} \widehat{\mathbf{S}}^{1/2} \right) \left(\mathbf{L}_\perp^\top \widehat{\mathbf{U}} \widehat{\mathbf{S}}^{1/2} \right)^\top \left(\mathbf{L}_\perp^\top \widehat{\mathbf{U}} \widehat{\mathbf{S}}^{1/2} \right) \right) \\ &= \text{tr} \left(\left(\widehat{\mathbf{S}}^{1/2} \widehat{\mathbf{V}}^\top \mathbf{L} \mathbf{L}^\top \widehat{\mathbf{V}} \widehat{\mathbf{S}}^{1/2} \right) \left(\widehat{\mathbf{S}}^{1/2} \widehat{\mathbf{U}}^\top \mathbf{L}_\perp \mathbf{L}_\perp^\top \widehat{\mathbf{U}} \widehat{\mathbf{S}}^{1/2} \right) \right). \end{aligned}$$

Notice that $\widehat{\mathbf{S}}^{1/2}\widehat{\mathbf{V}}^\top\mathbf{L}\mathbf{L}^\top\widehat{\mathbf{V}}\widehat{\mathbf{S}}^{1/2}$ and $\widehat{\mathbf{S}}^{1/2}\widehat{\mathbf{U}}^\top\mathbf{L}_\perp\mathbf{L}_\perp^\top\widehat{\mathbf{U}}\widehat{\mathbf{S}}^{1/2}$ are two positive semi-definite matrices, then by lower bound of trace of product of positive semi-definite matrices, using Weyl inequality, we have

$$\begin{aligned}\left\|\mathbf{L}_\perp^\top\widehat{\Delta}\mathbf{L}\right\|_{\text{F}}^2 &\geq \lambda_{2r^*}\left(\widehat{\mathbf{S}}^{1/2}\widehat{\mathbf{V}}^\top\mathbf{L}\mathbf{L}^\top\widehat{\mathbf{V}}\widehat{\mathbf{S}}^{1/2}\right)\left\|\widehat{\mathbf{S}}^{1/2}\widehat{\mathbf{U}}^\top\mathbf{L}_\perp\mathbf{L}_\perp^\top\widehat{\mathbf{U}}\widehat{\mathbf{S}}^{1/2}\right\|_{\text{F}} \\ &\geq \lambda_{r^*}^*\times\lambda_{2r^*}\left(\widehat{\mathbf{V}}^\top\mathbf{L}\mathbf{L}^\top\widehat{\mathbf{V}}\right)\left\|\widehat{\mathbf{S}}^{1/2}\widehat{\mathbf{U}}^\top\mathbf{L}_\perp\mathbf{L}_\perp^\top\widehat{\mathbf{U}}\widehat{\mathbf{S}}^{1/2}\right\|_{\text{F}} \\ &= \lambda_{r^*}^*\times\lambda_{2r^*}\left(\widehat{\mathbf{V}}^\top\mathbf{L}\mathbf{L}^\top\widehat{\mathbf{V}}\right)\left\|\mathbf{L}_\perp\mathbf{L}_\perp^\top\widehat{\mathbf{U}}\widehat{\mathbf{S}}\widehat{\mathbf{U}}^\top\mathbf{L}_\perp\mathbf{L}_\perp^\top\right\|_{\text{F}},\end{aligned}$$

where the last equality follows from

$$\begin{aligned}\left\|\widehat{\mathbf{S}}^{1/2}\widehat{\mathbf{U}}^\top\mathbf{L}_\perp\mathbf{L}_\perp^\top\widehat{\mathbf{U}}\widehat{\mathbf{S}}^{1/2}\right\|_{\text{F}}^2 &= \text{tr}\left(\widehat{\mathbf{S}}^{1/2}\widehat{\mathbf{U}}^\top\mathbf{L}_\perp\mathbf{L}_\perp^\top\widehat{\mathbf{U}}\widehat{\mathbf{S}}\widehat{\mathbf{U}}^\top\mathbf{L}_\perp\mathbf{L}_\perp^\top\widehat{\mathbf{U}}\widehat{\mathbf{S}}^{1/2}\right) \\ &= \text{tr}\left(\widehat{\mathbf{S}}^{1/2}\widehat{\mathbf{U}}^\top\mathbf{L}_\perp\mathbf{L}_\perp^\top\left(\mathbf{L}_\perp\mathbf{L}_\perp^\top\widehat{\mathbf{U}}\widehat{\mathbf{S}}\widehat{\mathbf{U}}^\top\mathbf{L}_\perp\mathbf{L}_\perp^\top\right)\mathbf{L}_\perp\mathbf{L}_\perp^\top\widehat{\mathbf{U}}\widehat{\mathbf{S}}^{1/2}\right) \\ &= \text{tr}\left(\left(\mathbf{L}_\perp\mathbf{L}_\perp^\top\widehat{\mathbf{U}}\widehat{\mathbf{S}}\widehat{\mathbf{U}}^\top\mathbf{L}_\perp\mathbf{L}_\perp^\top\right)\left(\mathbf{L}_\perp\mathbf{L}_\perp^\top\widehat{\mathbf{U}}\widehat{\mathbf{S}}\widehat{\mathbf{U}}^\top\mathbf{L}_\perp\mathbf{L}_\perp^\top\right)\right) \\ &= \left\|\mathbf{L}_\perp\mathbf{L}_\perp^\top\widehat{\mathbf{U}}\widehat{\mathbf{S}}\widehat{\mathbf{U}}^\top\mathbf{L}_\perp\mathbf{L}_\perp^\top\right\|_{\text{F}}^2.\end{aligned}$$

Similarly, we have

$$\left\|\mathbf{L}^\top\widehat{\Delta}\mathbf{L}_\perp\right\|_{\text{F}}^2 \geq \lambda_{r^*}^*\times\lambda_{2r^*}\left(\widehat{\mathbf{U}}^\top\mathbf{L}\mathbf{L}^\top\widehat{\mathbf{U}}\right)\left\|\mathbf{L}_\perp\mathbf{L}_\perp^\top\widehat{\mathbf{V}}\widehat{\mathbf{S}}\widehat{\mathbf{V}}^\top\mathbf{L}_\perp\mathbf{L}_\perp^\top\right\|_{\text{F}}.$$

Next, we can derive

$$\begin{aligned}\left\|\mathbf{L}_\perp\mathbf{L}_\perp^\top\widehat{\mathbf{U}}\widehat{\mathbf{S}}\widehat{\mathbf{U}}^\top\mathbf{L}_\perp\mathbf{L}_\perp^\top\right\|_{\text{F}}^2 &= \left\|\mathbf{L}_\perp\mathbf{L}_\perp^\top\left(\underline{\Phi}\mathbf{S}^*\underline{\Phi}^\top+\underline{\Phi}\mathbf{S}^*\underline{\Phi}^\top\right)\mathbf{L}_\perp\mathbf{L}_\perp^\top\right\|_{\text{F}}^2 \quad [\text{by Eq. (C.22)}] \\ &= \left\|\mathbf{L}_\perp\mathbf{L}_\perp^\top\underline{\Phi}\mathbf{S}^*\underline{\Phi}^\top\mathbf{L}_\perp\mathbf{L}_\perp^\top\right\|_{\text{F}}^2+\left\|\mathbf{L}_\perp\mathbf{L}_\perp^\top\Phi\mathbf{S}^*\Phi^\top\mathbf{L}_\perp\mathbf{L}_\perp^\top\right\|_{\text{F}}^2 \\ &\quad +2\left\langle\mathbf{L}_\perp\mathbf{L}_\perp^\top\underline{\Phi}\mathbf{S}^*\underline{\Phi}^\top\mathbf{L}_\perp\mathbf{L}_\perp^\top,\mathbf{L}_\perp\mathbf{L}_\perp^\top\Phi\mathbf{S}^*\Phi^\top\mathbf{L}_\perp\mathbf{L}_\perp^\top\right\rangle,\end{aligned}$$

and

$$\begin{aligned}\left\|\mathbf{L}_\perp\mathbf{L}_\perp^\top\widehat{\mathbf{V}}\widehat{\mathbf{S}}\widehat{\mathbf{V}}^\top\mathbf{L}_\perp\mathbf{L}_\perp^\top\right\|_{\text{F}}^2 &= \left\|\mathbf{L}_\perp\mathbf{L}_\perp^\top\left(\underline{\Phi}\mathbf{S}^*\underline{\Phi}^\top+\underline{\Phi}\mathbf{S}^*\underline{\Phi}^\top\right)\mathbf{L}_\perp\mathbf{L}_\perp^\top\right\|_{\text{F}}^2 \quad [\text{by Eq. (C.22)}] \\ &= \left\|\mathbf{L}_\perp\mathbf{L}_\perp^\top\underline{\Phi}\mathbf{S}^*\underline{\Phi}^\top\mathbf{L}_\perp\mathbf{L}_\perp^\top\right\|_{\text{F}}^2+\left\|\mathbf{L}_\perp\mathbf{L}_\perp^\top\Phi\mathbf{S}^*\Phi^\top\mathbf{L}_\perp\mathbf{L}_\perp^\top\right\|_{\text{F}}^2 \\ &\quad +2\left\langle\mathbf{L}_\perp\mathbf{L}_\perp^\top\underline{\Phi}\mathbf{S}^*\underline{\Phi}^\top\mathbf{L}_\perp\mathbf{L}_\perp^\top,\mathbf{L}_\perp\mathbf{L}_\perp^\top\Phi\mathbf{S}^*\Phi^\top\mathbf{L}_\perp\mathbf{L}_\perp^\top\right\rangle.\end{aligned}$$

Also, we can obtain

$$\begin{aligned}\left\|\mathbf{L}_\perp^\top\widehat{\Delta}\mathbf{L}_\perp\right\|_{\text{F}}^2 &= \left\|\mathbf{L}_\perp\mathbf{L}_\perp^\top\widehat{\mathbf{U}}\widehat{\mathbf{S}}\widehat{\mathbf{V}}^\top\mathbf{L}_\perp\mathbf{L}_\perp^\top\right\|_{\text{F}}^2 \\ &= \left\|\mathbf{L}_\perp\mathbf{L}_\perp^\top\left(\underline{\Phi}\mathbf{S}^*\underline{\Phi}^\top-\underline{\Phi}\mathbf{S}^*\underline{\Phi}^\top\right)\mathbf{L}_\perp\mathbf{L}_\perp^\top\right\|_{\text{F}}^2 \quad [\text{by Eq. (C.22)}] \\ &= \left\|\mathbf{L}_\perp\mathbf{L}_\perp^\top\underline{\Phi}\mathbf{S}^*\underline{\Phi}^\top\mathbf{L}_\perp\mathbf{L}_\perp^\top\right\|_{\text{F}}^2+\left\|\mathbf{L}_\perp\mathbf{L}_\perp^\top\Phi\mathbf{S}^*\Phi^\top\mathbf{L}_\perp\mathbf{L}_\perp^\top\right\|_{\text{F}}^2-2\left\langle\mathbf{L}_\perp\mathbf{L}_\perp^\top\underline{\Phi}\mathbf{S}^*\underline{\Phi}^\top\mathbf{L}_\perp\mathbf{L}_\perp^\top,\mathbf{L}_\perp\mathbf{L}_\perp^\top\Phi\mathbf{S}^*\Phi^\top\mathbf{L}_\perp\mathbf{L}_\perp^\top\right\rangle.\end{aligned}$$

Notice that the matrix inner product term is the inner product of two positive semi-definite matrices, then by trace inequality for positive semi-definite matrices, we can obtain

$$\left\langle \mathbf{L}_\perp \mathbf{L}_\perp^\top \underline{\Phi} \mathbf{S}^* \underline{\Phi}^\top \mathbf{L}_\perp \mathbf{L}_\perp^\top, \mathbf{L}_\perp \mathbf{L}_\perp^\top \Phi \mathbf{S}^* \Phi^\top \mathbf{L}_\perp \mathbf{L}_\perp^\top \right\rangle = \text{tr} \left(\left(\mathbf{L}_\perp \mathbf{L}_\perp^\top \underline{\Phi} \mathbf{S}^* \underline{\Phi}^\top \mathbf{L}_\perp \mathbf{L}_\perp^\top \right) \left(\mathbf{L}_\perp \mathbf{L}_\perp^\top \Phi \mathbf{S}^* \Phi^\top \mathbf{L}_\perp \mathbf{L}_\perp^\top \right) \right) \geq 0.$$

Then, we can claim

$$\left\| \mathbf{L}_\perp \mathbf{L}_\perp^\top \widehat{\mathbf{U}} \widehat{\mathbf{S}} \widehat{\mathbf{U}}^\top \mathbf{L}_\perp \mathbf{L}_\perp^\top \right\|_{\mathbb{F}}^2, \left\| \mathbf{L}_\perp \mathbf{L}_\perp^\top \widehat{\mathbf{V}} \widehat{\mathbf{S}} \widehat{\mathbf{V}}^\top \mathbf{L}_\perp \mathbf{L}_\perp^\top \right\|_{\mathbb{F}}^2 \geq \left\| \mathbf{L}_\perp^\top \widehat{\Delta} \mathbf{L}_\perp \right\|_{\mathbb{F}}^2. \quad (\text{C.30})$$

Next, we can obtain

$$\begin{aligned} \left\| \mathbf{L}_\perp^\top \widehat{\Delta} \mathbf{L}_\perp \right\|_{\mathbb{F}}^2 + \left\| \mathbf{L}_\perp^\top \widehat{\Delta} \mathbf{L}_\perp \right\|_{\mathbb{F}}^2 &\geq \lambda_{r^*}^* \times \lambda_{2r^*} \left(\widehat{\mathbf{U}}^\top \mathbf{L} \mathbf{L}^\top \widehat{\mathbf{U}} \right) \left\| \mathbf{L}_\perp \mathbf{L}_\perp^\top \widehat{\mathbf{V}} \widehat{\mathbf{S}} \widehat{\mathbf{V}}^\top \mathbf{L}_\perp \mathbf{L}_\perp^\top \right\|_{\mathbb{F}} \\ &\quad + \lambda_{r^*}^* \times \lambda_{2r^*} \left(\widehat{\mathbf{V}}^\top \mathbf{L} \mathbf{L}^\top \widehat{\mathbf{V}} \right) \left\| \mathbf{L}_\perp \mathbf{L}_\perp^\top \widehat{\mathbf{U}} \widehat{\mathbf{S}} \widehat{\mathbf{U}}^\top \mathbf{L}_\perp \mathbf{L}_\perp^\top \right\|_{\mathbb{F}} \\ &\geq \lambda_{r^*}^* \min \left\{ \lambda_{2r^*} \left(\widehat{\mathbf{U}}^\top \mathbf{L} \mathbf{L}^\top \widehat{\mathbf{U}} \right), \lambda_{2r^*} \left(\widehat{\mathbf{V}}^\top \mathbf{L} \mathbf{L}^\top \widehat{\mathbf{V}} \right) \right\} \\ &\quad \times \left(\left\| \mathbf{L}_\perp \mathbf{L}_\perp^\top \widehat{\mathbf{V}} \widehat{\mathbf{S}} \widehat{\mathbf{V}}^\top \mathbf{L}_\perp \mathbf{L}_\perp^\top \right\|_{\mathbb{F}} + \left\| \mathbf{L}_\perp \mathbf{L}_\perp^\top \widehat{\mathbf{U}} \widehat{\mathbf{S}} \widehat{\mathbf{U}}^\top \mathbf{L}_\perp \mathbf{L}_\perp^\top \right\|_{\mathbb{F}} \right) \\ &\geq 2\lambda_{r^*}^* \min \left\{ \lambda_{2r^*} \left(\widehat{\mathbf{U}}^\top \mathbf{L} \mathbf{L}^\top \widehat{\mathbf{U}} \right), \lambda_{2r^*} \left(\widehat{\mathbf{V}}^\top \mathbf{L} \mathbf{L}^\top \widehat{\mathbf{V}} \right) \right\} \left\| \mathbf{L}_\perp^\top \widehat{\Delta} \mathbf{L}_\perp \right\|_{\mathbb{F}}. \end{aligned}$$

[by Eq. (C.30)]

Then, combining the above inequality and Eq. (C.29), we have

$$\begin{aligned} \frac{\frac{1}{2} \left\| \mathbf{L}_\perp^\top \widehat{\Delta} \mathbf{L}_\perp \right\|_{\mathbb{F}}^2}{\left\| \mathbf{F} - \frac{\widehat{\Delta}}{\sqrt{2}} \right\|_{\mathbb{F}}^2} &\leq \frac{\left\| \mathbf{L}_\perp^\top \widehat{\Delta} \mathbf{L}_\perp \right\|_{\mathbb{F}}^2}{2\lambda_{r^*}^* \min \left\{ \lambda_{2r^*} \left(\widehat{\mathbf{U}}^\top \mathbf{L} \mathbf{L}^\top \widehat{\mathbf{U}} \right), \lambda_{2r^*} \left(\widehat{\mathbf{V}}^\top \mathbf{L} \mathbf{L}^\top \widehat{\mathbf{V}} \right) \right\} \left\| \mathbf{L}_\perp^\top \widehat{\Delta} \mathbf{L}_\perp \right\|_{\mathbb{F}}} \\ &= \frac{\left\| \mathbf{L}_\perp^\top \widehat{\Delta} \mathbf{L}_\perp \right\|_{\mathbb{F}}}{2\lambda_{r^*}^* \min \left\{ \lambda_{2r^*} \left(\widehat{\mathbf{U}}^\top \mathbf{L} \mathbf{L}^\top \widehat{\mathbf{U}} \right), \lambda_{2r^*} \left(\widehat{\mathbf{V}}^\top \mathbf{L} \mathbf{L}^\top \widehat{\mathbf{V}} \right) \right\}}. \end{aligned}$$

Next, we will focus on the lower bound of $\lambda_{2r^*} \left(\widehat{\mathbf{U}}^\top \mathbf{L} \mathbf{L}^\top \widehat{\mathbf{U}} \right)$ and $\lambda_{2r^*} \left(\widehat{\mathbf{V}}^\top \mathbf{L} \mathbf{L}^\top \widehat{\mathbf{V}} \right)$. Due to symmetry, the technique is identical to each other, so here we only prove for $\lambda_{2r^*} \left(\widehat{\mathbf{U}}^\top \mathbf{L} \mathbf{L}^\top \widehat{\mathbf{U}} \right)$. First, $\lambda_{2r^*} \left(\widehat{\mathbf{U}}^\top \mathbf{L} \mathbf{L}^\top \widehat{\mathbf{U}} \right) = \lambda_{2r^*}^2 \left(\mathbf{L}^\top \widehat{\mathbf{U}} \right)$ since $\widehat{\mathbf{U}}^\top \mathbf{L} \mathbf{L}^\top \widehat{\mathbf{U}}$ is symmetric. Next, we have

$$\lambda_{2r^*}^2 \left(\mathbf{L}^\top \widehat{\mathbf{U}} \right) = 1 - \left\| \mathbf{L}_\perp^\top \widehat{\mathbf{U}} \right\|_{op}^2,$$

where $\left\| \mathbf{L}_\perp^\top \widehat{\mathbf{U}} \right\|_{op}$ can be upper bounded by Wedin's $\sin(\Theta)$ theorem, here we use a variant from in Chen et al. (2021b, Theorem 2.9) to obtain

$$\left\| \mathbf{L}_\perp^\top \widehat{\mathbf{U}} \right\|_{op} \leq \frac{2 \left\| \mathbf{F} - \frac{\widehat{\Delta}}{\sqrt{2}} \right\|_{op}}{\lambda_{2r^*}^* \left(\frac{\widehat{\Delta}}{\sqrt{2}} \right)} \leq \frac{2\sqrt{2} \left\| \mathbf{F} - \frac{\widehat{\Delta}}{\sqrt{2}} \right\|_{\mathbb{F}}}{\lambda_{r^*}^*} \leq 2\sqrt{2}\rho, \quad \left[\text{by } \left\| \mathbf{F} - \frac{\widehat{\Delta}}{\sqrt{2}} \right\|_{\mathbb{F}} \leq \rho\lambda_{r^*}^* \right]$$

which implies

$$\lambda_{2r^*}^2 \left(\mathbf{L}^\top \widehat{\mathbf{U}} \right) \geq 1 - 8\rho^2. \quad (\text{C.31})$$

Therefore, we have

$$\begin{aligned} \rho^2(\lambda_{r^*}^*)^2 &= \rho^2 \lambda_{2r^*}^2(\widehat{\Delta}) \geq \left\| \mathbf{F} - \frac{\widehat{\Delta}}{\sqrt{2}} \right\|_{\text{F}}^2 \\ &\geq \frac{1}{2} \left\| \mathbf{L}_\perp^\top \widehat{\Delta} \mathbf{L} \right\|_{\text{F}}^2 + \frac{1}{2} \left\| \mathbf{L}^\top \widehat{\Delta} \mathbf{L}_\perp \right\|_{\text{F}}^2 && \text{[by Eq. (C.27)]} \\ &\geq \lambda_{r^*}^* \min \left\{ \lambda_{2r^*} \left(\widehat{\mathbf{U}}^\top \mathbf{L} \mathbf{L}^\top \widehat{\mathbf{U}} \right), \lambda_{2r^*} \left(\widehat{\mathbf{V}}^\top \mathbf{L} \mathbf{L}^\top \widehat{\mathbf{V}} \right) \right\} \left\| \mathbf{L}_\perp^\top \widehat{\Delta} \mathbf{L}_\perp \right\|_{\text{F}} \\ &\geq \frac{1}{2} \lambda_{r^*}^* \left\| \mathbf{L}_\perp^\top \widehat{\Delta} \mathbf{L}_\perp \right\|_{\text{F}}, && \text{[by Eq. (C.31) and } \rho \leq 1/4 \text{]} \end{aligned}$$

which implies

$$\frac{\left\| \mathbf{L}_\perp^\top \widehat{\Delta} \mathbf{L}_\perp \right\|_{\text{F}}}{\lambda_{r^*}^*} \leq 2\rho^2.$$

Finally, combining Eq. (C.28), we can obtain

$$\left\| \left(\mathbf{I}_d - \mathbf{U}_{\mathbf{A}_t} \mathbf{U}_{\mathbf{A}_t}^\top \right) \Delta \left(\mathbf{I}_k - \mathbf{V}_{\mathbf{B}_t} \mathbf{V}_{\mathbf{B}_t}^\top \right) \right\|_{\text{F}}^2 = \frac{1}{2} \left\| \mathbf{L}_\perp^\top \widehat{\Delta} \mathbf{L}_\perp \right\|_{\text{F}}^2 \leq \frac{\rho^2}{1 - 8\rho^2} \left\| \mathbf{A}_t \mathbf{B}_t - \Delta \right\|_{\text{F}}^2.$$

Notice that

$$\begin{aligned} \frac{1}{2} \left\| \mathbf{L}_\perp^\top \widehat{\Delta} \mathbf{L} \right\|_{\text{F}}^2 + \frac{1}{2} \left\| \mathbf{L}^\top \widehat{\Delta} \mathbf{L}_\perp \right\|_{\text{F}}^2 &= \frac{1}{2} \left\| \mathbf{P}_t \widehat{\Delta} (\mathbf{I}_{d+k} - \mathbf{P}_t) \right\|_{\text{F}}^2 + \frac{1}{2} \left\| (\mathbf{I}_{d+k} - \mathbf{P}_t) \widehat{\Delta} \mathbf{P}_t \right\|_{\text{F}}^2 \\ &= \left\| \left(\mathbf{I}_d - \mathbf{U}_{\mathbf{A}_t} \mathbf{U}_{\mathbf{A}_t}^\top \right) \Delta \mathbf{V}_{\mathbf{B}_t} \mathbf{V}_{\mathbf{B}_t}^\top \right\|_{\text{F}}^2 + \left\| \mathbf{U}_{\mathbf{A}_t} \mathbf{U}_{\mathbf{A}_t}^\top \Delta \left(\mathbf{I}_k - \mathbf{V}_{\mathbf{B}_t} \mathbf{V}_{\mathbf{B}_t}^\top \right) \right\|_{\text{F}}^2 \\ &= \left\| \left(\mathbf{I}_d - \mathbf{U}_{\mathbf{A}_t} \mathbf{U}_{\mathbf{A}_t}^\top \right) \Delta \mathbf{V}_{\mathbf{B}_t} \mathbf{V}_{\mathbf{B}_t}^\top + \mathbf{U}_{\mathbf{A}_t} \mathbf{U}_{\mathbf{A}_t}^\top \Delta \left(\mathbf{I}_k - \mathbf{V}_{\mathbf{B}_t} \mathbf{V}_{\mathbf{B}_t}^\top \right) \right\|_{\text{F}}^2, \end{aligned}$$

then by the decomposition in Eq. (C.27), we can obtain

$$\left\| \left(\mathbf{I}_d - \mathbf{U}_{\mathbf{A}_t} \mathbf{U}_{\mathbf{A}_t}^\top \right) \Delta \mathbf{V}_{\mathbf{B}_t} \mathbf{V}_{\mathbf{B}_t}^\top + \mathbf{U}_{\mathbf{A}_t} \mathbf{U}_{\mathbf{A}_t}^\top \Delta \left(\mathbf{I}_k - \mathbf{V}_{\mathbf{B}_t} \mathbf{V}_{\mathbf{B}_t}^\top \right) \right\|_{\text{F}}^2 \leq \left\| \mathbf{F} - \frac{\widehat{\Delta}}{\sqrt{2}} \right\|_{\text{F}}^2 = \left\| \mathbf{A}_t \mathbf{B}_t - \Delta \right\|_{\text{F}}^2,$$

which completes the proof. \square

Based on the above estimation, we are ready to deliver the linear convergence rate of $\left\| \mathbf{A}_t \mathbf{B}_t - \Delta \right\|_{\text{F}}$.

Theorem C.10. Suppose $\epsilon \leq \frac{\rho}{3C^*K^2\gamma\sqrt{2dr^*\kappa}}$ for $\rho \leq 0.01$ and we take $\gamma \in \left[\frac{1}{c_{\text{H}}} - \frac{\rho}{3c_{\text{H}}\kappa\sqrt{2r^*}}, \frac{1}{c_{\text{H}}} + \frac{\rho}{3c_{\text{H}}\kappa\sqrt{2r^*}} \right]$ for (Spectral-init), where c_{H} is defined in Eq. (C.13), set $\eta \in \left(c_\eta, \frac{1}{2c_{\text{H}}} \right)$ where $c_\eta > 0$ is a small constant, under assumptions in Section 2.1 for the nonlinear setting, Assumption 4.1, and Assumption 4.2, then with probability at least $1 - 2Cdk \exp(-\epsilon^2 N)$ for a universal constant $C > 0$, we

have

$$\|\mathbf{A}_t \mathbf{B}_t - \Delta\|_{\text{F}} \leq \left(1 - \frac{c_{\text{H}}}{10} \eta\right)^t \rho \lambda_{r^*}^*.$$

Proof. We prove it by induction. The following hypothesis holds at $t = 0$ by Lemma C.5

$$\|\mathbf{A}_t \mathbf{B}_t - \Delta\|_{\text{F}} \leq \rho \lambda_{r^*}^*.$$

We suppose it also holds for at time t , showing that

$$\lambda_{r^*}(\mathbf{A}_t \mathbf{B}_t) \geq (1 - \rho) \lambda_{r^*}^*. \quad [\text{by Weyl's inequality}]$$

Next, by Eq. (C.18) from Lemma C.6, under initial conditions from Lemma C.5, for time $t + 1$, we can derive

$$\begin{aligned} & \|\mathbf{A}_{t+1} \mathbf{B}_{t+1} - \Delta\|_{\text{F}} \\ & \leq (1 - 2\eta c_{\text{H}}) \left\| \mathbf{U}_{\mathbf{A}_t} \mathbf{U}_{\mathbf{A}_t}^{\top} (\mathbf{A}_t \mathbf{B}_t - \Delta) \mathbf{V}_{\mathbf{B}_t} \mathbf{V}_{\mathbf{B}_t}^{\top} \right\|_{\text{F}} \\ & \quad + (1 - c_{\text{H}} \eta) \left\| \left(\mathbf{I}_d - \mathbf{U}_{\mathbf{A}_t} \mathbf{U}_{\mathbf{A}_t}^{\top} \right) (\mathbf{A}_t \mathbf{B}_t - \Delta) \mathbf{V}_{\mathbf{B}_t} \mathbf{V}_{\mathbf{B}_t}^{\top} + \mathbf{U}_{\mathbf{A}_t} \mathbf{U}_{\mathbf{A}_t}^{\top} (\mathbf{A}_t \mathbf{B}_t - \Delta) \left(\mathbf{I}_k - \mathbf{V}_{\mathbf{B}_t} \mathbf{V}_{\mathbf{B}_t}^{\top} \right) \right\|_{\text{F}} \\ & \quad + \left\| \left(\mathbf{I}_d - \mathbf{U}_{\mathbf{A}_t} \mathbf{U}_{\mathbf{A}_t}^{\top} \right) (\mathbf{A}_t \mathbf{B}_t - \Delta) \left(\mathbf{I}_k - \mathbf{V}_{\mathbf{B}_t} \mathbf{V}_{\mathbf{B}_t}^{\top} \right) \right\|_{\text{F}} \\ & \quad + 2\eta \|\boldsymbol{\Xi}_t\|_{\text{F}} + \eta^2 \left\| \mathbf{J}_{\mathbf{W}_t} \mathcal{V}_t \mathcal{S}_t^{-1} \mathcal{U}_t^{\top} \mathbf{J}_{\mathbf{W}_t} \right\|_{\text{F}} \\ & \leq (1 - 2\eta c_{\text{H}}) \|\mathbf{A}_t \mathbf{B}_t - \Delta\|_{\text{F}} \\ & \quad + \left(1 - \eta c_{\text{H}} + \frac{\rho}{\sqrt{1 - 8\rho^2}} \right) \|\mathbf{A}_t \mathbf{B}_t - \Delta\|_{\text{F}} \quad [\text{by Lemma C.9}] \\ & \quad + 2\eta \left(h(\rho) + C^* K^2 \sqrt{d\epsilon} \right) \|\mathbf{A}_t \mathbf{B}_t - \Delta\|_{\text{F}} \quad [\text{by Lemma C.7}] \\ & \quad + \eta^2 (1 + \epsilon)^2 \frac{\rho}{1 - \rho} \|\mathbf{A}_t \mathbf{B}_t - \Delta\|_{\text{F}} \quad [\text{by Lemma C.8}] \\ & \leq \left(2 - 3\eta c_{\text{H}} + \frac{\rho}{\sqrt{1 - 8\rho^2}} \right) \|\mathbf{A}_t \mathbf{B}_t - \Delta\|_{\text{F}} \\ & \quad + 2\eta \left(h(\rho) + \frac{\rho}{3\gamma \sqrt{2r^* \kappa}} \right) \|\mathbf{A}_t \mathbf{B}_t - \Delta\|_{\text{F}} \\ & \quad + \eta^2 \left(1 + \frac{\rho}{3C^* K^2 \gamma \sqrt{2dr^* \kappa}} \right)^2 \frac{\rho}{1 - \rho} \|\mathbf{A}_t \mathbf{B}_t - \Delta\|_{\text{F}}, \quad \left[\text{since } \epsilon \leq \frac{\rho}{3C^* K^2 \gamma \sqrt{2dr^* \kappa}} \right] \end{aligned}$$

with probability at least $1 - 2Cdk \exp(-\epsilon^2 N)$ for a universal constant $C > 0$. Since we take $\rho \leq 0.01$, $h(\rho)$ defined in Eq. (C.21) and $\frac{\rho}{\sqrt{1 - 8\rho^2}}$ is monotonically increasing, then we can continue

the above upper bound as

$$\begin{aligned} \|\mathbf{A}_{t+1}\mathbf{B}_{t+1} - \Delta\|_{\text{F}} &\leq \left(1 - \frac{c_{\text{H}}}{10}\eta\right) \|\mathbf{A}_t\mathbf{B}_t - \Delta\|_{\text{F}} \\ &\quad + \left\{ \left(1 + \frac{1}{300C^*K^2\gamma\sqrt{2dr^*\kappa}}\right)^2 \frac{1}{99}\eta^2 \right. \\ &\quad \left. + \eta \left(1 - \frac{29c_{\text{H}}}{10} + 2h(0.01) + \frac{1}{150\gamma\sqrt{2r^*\kappa}}\right) + \frac{\sqrt{2498}}{4996} \right\} \|\mathbf{A}_t\mathbf{B}_t - \Delta\|_{\text{F}}. \end{aligned}$$

Then, there exists a constant $c_\eta > 0$ such that for $\forall \eta \in \left(c_\eta, \frac{1}{2c_{\text{H}}}\right)$, we have

$$-\left(1 - \frac{c_{\text{H}}}{10}\eta\right) \leq \left(1 + \frac{1}{300C^*K^2\gamma\sqrt{2dr^*\kappa}}\right)^2 \frac{1}{99}\eta^2 + \eta \left(1 - \frac{29c_{\text{H}}}{10} + 2h(0.01) + \frac{1}{150\gamma\sqrt{2r^*\kappa}}\right) + \frac{\sqrt{2498}}{4996} \leq 0,$$

which implies

$$\|\mathbf{A}_{t+1}\mathbf{B}_{t+1} - \Delta\|_{\text{F}} \leq \left(1 - \frac{c_{\text{H}}}{10}\eta\right) \|\mathbf{A}_t\mathbf{B}_t - \Delta\|_{\text{F}}.$$

Then, we can obtain the inductive hypothesis at $t + 1$ and prove the claim. \square

C.2.2 Preconditioned Smoothed-Gradient Descent

We can remove Assumption 4.1 and Assumption 4.2 in analysis if we drop the mask matrix (derivative of σ : σ') in the gradient, which improves the smoothness of gradient. By defining

$$-\mathbf{J}_{\mathbf{W}_t}^{\text{GLM}} := \frac{1}{N} \widetilde{\mathbf{X}}^\top \left(\sigma \left(\widetilde{\mathbf{X}} \mathbf{W}_t \right) - \sigma \left(\widetilde{\mathbf{X}} \widetilde{\mathbf{W}}^\natural \right) \right),$$

we present the preconditioned smoothed-gradient updates for LoRA fine-tuning as

$$\mathbf{A}_{t+1} = \mathbf{A}_t + \eta \mathbf{J}_{\mathbf{W}_t}^{\text{GLM}} \mathbf{B}_t^\top \left(\mathbf{B}_t \mathbf{B}_t^\top \right)^{-1}, \quad (\text{C.32})$$

and

$$\mathbf{B}_{t+1} = \mathbf{B}_t + \eta \left(\mathbf{A}_t^\top \mathbf{A}_t \right)^{-1} \mathbf{A}_t^\top \mathbf{J}_{\mathbf{W}_t}^{\text{GLM}}. \quad (\text{C.33})$$

Similarly, we propose to use $\mathbf{G}^\natural := \mathbf{J}_{\mathbf{W}^\natural}^{\text{GLM}}$ for (Spectral-init) to initialize \mathbf{A}_0 and \mathbf{B}_0 .

First, we compute the expectation of $\mathbf{J}_{\mathbf{W}_t}^{\text{GLM}}$.

Lemma C.11. Under assumptions in Section 2.1 for the nonlinear setting, we have

$$\mathbb{E}_{\tilde{\mathbf{x}}} \left[-\mathbf{J}_{\mathbf{W}_t}^{\text{GLM}} \right] = \frac{1}{2} (\mathbf{A}_t \mathbf{B}_t - \Delta).$$

Proof. For $\forall 1 \leq m \leq k$, we can show

$$\mathbb{E}_{\tilde{\mathbf{x}}} \left[\tilde{\mathbf{x}} \sigma \left(\tilde{\mathbf{x}}^\top \mathbf{w}_{t,m} \right) \right] = \mathbb{E}_{\tilde{\mathbf{x}}} \left[\nabla_{\tilde{\mathbf{x}}} \sigma \left(\tilde{\mathbf{x}}^\top \mathbf{w}_{t,m} \right) \right] = c_1 \mathbf{w}_{t,m}. \quad [\text{by Stein's Lemma and Lemma D.4}]$$

Similarly, we have

$$\mathbb{E}_{\tilde{\mathbf{x}}} \left[\tilde{\mathbf{x}} \sigma \left(\tilde{\mathbf{x}}^\top \tilde{\mathbf{w}}_m^\natural \right) \right] = c_1 \tilde{\mathbf{w}}_m^\natural.$$

Then, we can obtain

$$\mathbb{E}_{\tilde{\mathbf{x}}} \left[-\mathbf{J}_{\mathbf{W}_t}^{\text{GLM}} \right] = \frac{1}{N} \sum_{i=1}^N \left[\left[\sigma \left(\tilde{\mathbf{x}}_i^\top \mathbf{w}_{t,1} \right) - \sigma \left(\tilde{\mathbf{x}}_i^\top \tilde{\mathbf{w}}_1^\natural \right) \right] \tilde{\mathbf{x}}_i \cdots \left[\sigma \left(\tilde{\mathbf{x}}_i^\top \mathbf{w}_{t,1} \right) - \sigma \left(\tilde{\mathbf{x}}_i^\top \tilde{\mathbf{w}}_1^\natural \right) \right] \tilde{\mathbf{x}}_i \right] = \frac{1}{2} (\mathbf{A}_t \mathbf{B}_t - \Delta),$$

[by Eq. (D.3)]

which completes the proof. \square

By the same proof strategies with Theorem C.4, we can obtain the concentration of smoothed $\mathbf{J}_{\mathbf{W}_t}^{\text{GLM}}$ via the following theorem.

Theorem C.12. Suppose $\epsilon \in (0, 1)$, under assumptions in Section 2.1 for the nonlinear setting, then with probability at least $1 - 2dkC \exp(-N\epsilon^2)$ for a universal constant $C > 0$, we have

$$\left\| \mathbf{J}_{\mathbf{W}_t}^{\text{GLM}} - \mathbb{E}_{\tilde{\mathbf{x}}} \left[\mathbf{J}_{\mathbf{W}_t}^{\text{GLM}} \right] \right\|_{\text{F}} \leq C^* K^2 \sqrt{d} \epsilon \|\mathbf{A}_t \mathbf{B}_t - \Delta\|_{\text{F}},$$

for some absolute constant $C^* > 0$ and $K = \sqrt{8/3}$.

Proof. Identical to Theorem C.4 so we omit details here. \square

Next, we can obtain the initial condition under (Spectral-init) using $\mathbf{G}^\natural = \mathbf{J}_{\mathbf{W}_1}^{\text{GLM}}$.

Lemma C.13. Let $\mathbf{G}^\natural := \mathbf{J}_{\mathbf{W}_1}^{\text{GLM}}$, under assumptions in Section 2.1 for the nonlinear setting, with (Spectral-init), suppose $\epsilon \leq \frac{\rho}{3C^* K^2 \gamma \sqrt{2dr^* \kappa}}$ for some $\rho > 0$ and we set

$$\gamma \in \left[2 - \frac{2\rho}{3\kappa\sqrt{2r^*}}, 2 + \frac{2\rho}{3\kappa\sqrt{2r^*}} \right],$$

then with probability at least $1 - 2Cdk \exp(-N\epsilon^2)$ for a universal constant $C > 0$, it holds that

$$\|\mathbf{A}_0 \mathbf{B}_0 - \Delta\|_{\text{F}} \leq \rho \lambda_{r^*}^*.$$

Proof. By Lemma C.11, we can obtain

$$\mathbb{E}_{\tilde{\mathbf{x}}} \left[\mathbf{G}^\natural \right] = \mathbb{E}_{\tilde{\mathbf{x}}} \left[\mathbf{J}_{\mathbf{W}_1}^{\text{GLM}} \right] = \frac{1}{2} \Delta. \quad (\text{C.34})$$

By Theorem C.12, with the probability at least $1 - 2Cdk \exp(-N\epsilon^2)$ for a universal constant $C > 0$, we have

$$\left\| \mathbf{G}^\natural - \mathbb{E}_{\tilde{\mathbf{x}}} \left[\mathbf{G}^\natural \right] \right\|_{\text{F}} \leq \frac{\rho \|\Delta\|_{\text{F}}}{3\sqrt{2r^* \gamma \kappa}} \leq \frac{\rho \sqrt{r^*} \|\Delta\|_{\text{op}}}{3\sqrt{2r^* \gamma \kappa}} = \frac{\rho \lambda_{r^*}^*}{3\sqrt{2r^* \gamma}}, \quad (\text{C.35})$$

where $\epsilon \leq \frac{\rho}{2C^*K^2\gamma\sqrt{2dr^*\kappa}}$ for $\rho > 0$. Similar to Lemma C.5, we can derive

$$\lambda_{r^*+1} \left(\mathbf{G}^\natural \right) \leq \frac{\rho\lambda_{r^*}^*}{3\sqrt{2r^*\gamma}}, \quad (\text{C.36})$$

due to $\text{Rank}(\mathbb{E}_{\tilde{\mathbf{x}}}[\mathbf{G}^\natural]) = \text{Rank}(\Delta) = r^*$ by Eq. (C.34). Then, we have

$$\begin{aligned} \|\mathbf{A}_0\mathbf{B}_0 - \Delta\|_{op} &\leq \left\| \mathbf{A}_0\mathbf{B}_0 - \gamma\mathbf{G}^\natural \right\|_{op} + \gamma \left\| \mathbf{G}^\natural - \mathbb{E}_{\tilde{\mathbf{x}}}[\mathbf{G}^\natural] \right\|_{op} + \left\| \gamma\mathbb{E}_{\tilde{\mathbf{x}}}[\mathbf{G}^\natural] - \Delta \right\|_{op} \\ &\leq \left\| \mathbf{A}_0\mathbf{B}_0 - \gamma\mathbf{G}^\natural \right\|_{op} + \gamma \left\| \mathbf{G}^\natural - \mathbb{E}_{\tilde{\mathbf{x}}}[\mathbf{G}^\natural] \right\|_{\text{F}} + |\gamma c_{\text{H}} - 1| \|\Delta\|_{op} \quad [\text{by Eq. (C.34)}] \\ &\leq \left\| \mathbf{A}_0\mathbf{B}_0 - \gamma\mathbf{G}^\natural \right\|_{op} + \frac{2\rho\lambda_{r^*}^*}{3\sqrt{2r^*}} \\ &\quad \left[\text{by Eq. (C.35) and } \gamma \in \left[2 - \frac{2\rho}{3\kappa\sqrt{2r^*}}, 2 + \frac{2\rho}{3\kappa\sqrt{2r^*}} \right] \right] \\ &\leq \gamma\lambda_{r^*+1} \left(\mathbf{G}^\natural \right) + \frac{2\rho\lambda_{r^*}^*}{3\sqrt{2r^*}} \\ &\leq \frac{\rho\lambda_{r^*}^*}{\sqrt{2r^*}}. \quad [\text{by Eq. (C.36)}] \end{aligned}$$

Since $\text{Rank}(\mathbf{A}_t\mathbf{B}_t) \leq r = r^*$ and $\text{Rank}(\Delta) = r^*$, then $\text{Rank}(\mathbf{A}_0\mathbf{B}_0 - \Delta) \leq 2r^*$, which implies

$$\|\mathbf{A}_0\mathbf{B}_0 - \Delta\|_{\text{F}} \leq \sqrt{2r^*} \|\mathbf{A}_0\mathbf{B}_0 - \Delta\|_{op} \leq \rho\lambda_{r^*}^*.$$

□

With simple modifications to Lemma C.6, we can obtain the following lemma.

Lemma C.14. Under assumptions in Section 2.1 for the nonlinear setting, suppose $\eta \in (0, 1)$, we update \mathbf{A}_t and \mathbf{B}_t via Eq. (C.32) and Eq. (C.33), then we have the following recursion

$$\begin{aligned} \mathbf{A}_{t+1}\mathbf{B}_{t+1} - \Delta &= (1 - \eta)\mathbf{U}_{\mathbf{A}_t}\mathbf{U}_{\mathbf{A}_t}^\top (\mathbf{A}_t\mathbf{B}_t - \Delta)\mathbf{V}_{\mathbf{B}_t}\mathbf{V}_{\mathbf{B}_t}^\top \\ &\quad + (1 - \eta/2) \left(\mathbf{I}_d - \mathbf{U}_{\mathbf{A}_t}\mathbf{U}_{\mathbf{A}_t}^\top \right) (\mathbf{A}_t\mathbf{B}_t - \Delta)\mathbf{V}_{\mathbf{B}_t}\mathbf{V}_{\mathbf{B}_t}^\top \\ &\quad + (1 - \eta/2)\mathbf{U}_{\mathbf{A}_t}\mathbf{U}_{\mathbf{A}_t}^\top (\mathbf{A}_t\mathbf{B}_t - \Delta) \left(\mathbf{I}_k - \mathbf{V}_{\mathbf{B}_t}\mathbf{V}_{\mathbf{B}_t}^\top \right) \\ &\quad + \left(\mathbf{I}_d - \mathbf{U}_{\mathbf{A}_t}\mathbf{U}_{\mathbf{A}_t}^\top \right) (\mathbf{A}_t\mathbf{B}_t - \Delta) \left(\mathbf{I}_k - \mathbf{V}_{\mathbf{B}_t}\mathbf{V}_{\mathbf{B}_t}^\top \right) \\ &\quad + \eta\Xi_t^{\text{GLM}}\mathbf{V}_{\mathbf{B}_t}\mathbf{V}_{\mathbf{B}_t}^\top + \eta\mathbf{U}_{\mathbf{A}_t}\mathbf{U}_{\mathbf{A}_t}^\top\Xi_t^{\text{GLM}} + \eta^2\mathbf{J}_{\mathbf{W}_t}^{\text{GLM}}\mathcal{V}_t\mathcal{S}_t^{-1}\mathcal{U}_t^\top\mathbf{J}_{\mathbf{W}_t}^{\text{GLM}}, \quad (\text{C.37}) \end{aligned}$$

where $\Xi_t^{\text{GLM}} := \mathbf{J}_{\mathbf{W}_t}^{\text{GLM}} - \frac{1}{2}(\mathbf{A}_t\mathbf{B}_t - \Delta)$. Then, the associated upper bound in Frobenius norm is

$$\begin{aligned} &\|\mathbf{A}_{t+1}\mathbf{B}_{t+1} - \Delta\|_{\text{F}} \quad (\text{C.38}) \\ &\leq (1 - \eta) \left\| \mathbf{U}_{\mathbf{A}_t}\mathbf{U}_{\mathbf{A}_t}^\top (\mathbf{A}_t\mathbf{B}_t - \Delta)\mathbf{V}_{\mathbf{B}_t}\mathbf{V}_{\mathbf{B}_t}^\top \right\|_{\text{F}} \\ &\quad + (1 - \eta/2) \left\| \left(\mathbf{I}_d - \mathbf{U}_{\mathbf{A}_t}\mathbf{U}_{\mathbf{A}_t}^\top \right) (\mathbf{A}_t\mathbf{B}_t - \Delta)\mathbf{V}_{\mathbf{B}_t}\mathbf{V}_{\mathbf{B}_t}^\top + \mathbf{U}_{\mathbf{A}_t}\mathbf{U}_{\mathbf{A}_t}^\top (\mathbf{A}_t\mathbf{B}_t - \Delta) \left(\mathbf{I}_k - \mathbf{V}_{\mathbf{B}_t}\mathbf{V}_{\mathbf{B}_t}^\top \right) \right\|_{\text{F}} \\ &\quad + \left\| \left(\mathbf{I}_d - \mathbf{U}_{\mathbf{A}_t}\mathbf{U}_{\mathbf{A}_t}^\top \right) (\mathbf{A}_t\mathbf{B}_t - \Delta) \left(\mathbf{I}_k - \mathbf{V}_{\mathbf{B}_t}\mathbf{V}_{\mathbf{B}_t}^\top \right) \right\|_{\text{F}} + 2\eta \|\Xi_t^{\text{GLM}}\|_{\text{F}} + \eta^2 \left\| \mathbf{J}_{\mathbf{W}_t}^{\text{GLM}}\mathcal{V}_t\mathcal{S}_t^{-1}\mathcal{U}_t^\top\mathbf{J}_{\mathbf{W}_t}^{\text{GLM}} \right\|_{\text{F}}. \quad (\text{C.39}) \end{aligned}$$

Notice that Lemma C.8 and Lemma C.9 are still applied in this case. Thanks to Lemma C.11, we do not have the residual terms $\Psi_t(n)$ in Lemma C.7, then Theorem C.12 suffices to bound $\|\Xi_t^{\text{GLM}}\|_{\text{F}}$. Now, we can prove the following theorem.

Theorem C.15. Suppose $\epsilon \leq \frac{\rho}{3C^*K^2\gamma\sqrt{2dr^*\kappa}}$ for $\rho \leq \frac{1}{20}$ and we take $\gamma \in \left[2 - \frac{2\rho}{3\kappa\sqrt{2r^*}}, 2 + \frac{2\rho}{3\kappa\sqrt{2r^*}}\right]$ for (Spectral-init), set $\eta \in (c_\eta^{\text{GLM}}, 1)$ where $c_\eta^{\text{GLM}} > 0$ is a small constant, under assumptions in Section 2.1 for the nonlinear setting, then with probability at least $1 - 2Cdk \exp(-\epsilon^2N)$ for a universal constant $C > 0$, we have

$$\|\mathbf{A}_t\mathbf{B}_t - \Delta\|_{\text{F}} \leq \left(1 - \frac{\eta}{4}\right)^t \rho\lambda_{r^*}^*.$$

Proof. Similar to Theorem C.10, the following statement holds for $t = 0$ by C.13 and is assumed to be true at time t

$$\|\mathbf{A}_t\mathbf{B}_t - \Delta\|_{\text{F}} \leq \rho\lambda_{r^*}^*, \quad \Rightarrow \quad \lambda_{r^*}(\mathbf{A}_t\mathbf{B}_t) \geq (1 - \rho)\lambda_{r^*}^*. \quad [\text{by Weyl's inequality}]$$

Next, by Eq. (C.38) from Lemma C.14, under initial conditions from Lemma C.13, for time $t + 1$, we can derive

$$\begin{aligned} & \|\mathbf{A}_{t+1}\mathbf{B}_{t+1} - \Delta\|_{\text{F}} \\ & \leq (1 - \eta) \left\| \mathbf{U}_{\mathbf{A}_t}\mathbf{U}_{\mathbf{A}_t}^\top (\mathbf{A}_t\mathbf{B}_t - \Delta) \mathbf{V}_{\mathbf{B}_t}\mathbf{V}_{\mathbf{B}_t}^\top \right\|_{\text{F}} \\ & \quad + (1 - \eta/2) \left\| \left(\mathbf{I}_d - \mathbf{U}_{\mathbf{A}_t}\mathbf{U}_{\mathbf{A}_t}^\top \right) (\mathbf{A}_t\mathbf{B}_t - \Delta) \mathbf{V}_{\mathbf{B}_t}\mathbf{V}_{\mathbf{B}_t}^\top + \mathbf{U}_{\mathbf{A}_t}\mathbf{U}_{\mathbf{A}_t}^\top (\mathbf{A}_t\mathbf{B}_t - \Delta) \left(\mathbf{I}_k - \mathbf{V}_{\mathbf{B}_t}\mathbf{V}_{\mathbf{B}_t}^\top \right) \right\|_{\text{F}} \\ & \quad + \left\| \left(\mathbf{I}_d - \mathbf{U}_{\mathbf{A}_t}\mathbf{U}_{\mathbf{A}_t}^\top \right) (\mathbf{A}_t\mathbf{B}_t - \Delta) \left(\mathbf{I}_k - \mathbf{V}_{\mathbf{B}_t}\mathbf{V}_{\mathbf{B}_t}^\top \right) \right\|_{\text{F}} \\ & \quad + 2\eta \|\Xi_t^{\text{GLM}}\|_{\text{F}} + \eta^2 \left\| \mathbf{J}_{\mathbf{W}_t}^{\text{GLM}} \mathcal{V}_t \mathcal{S}_t^{-1} \mathcal{U}_t^\top \mathbf{J}_{\mathbf{W}_t}^{\text{GLM}} \right\|_{\text{F}} \\ & \leq (1 - \eta) \|\mathbf{A}_t\mathbf{B}_t - \Delta\|_{\text{F}} \\ & \quad + \left(1 - \eta/2 + \frac{\rho}{\sqrt{1 - 8\rho^2}} \right) \|\mathbf{A}_t\mathbf{B}_t - \Delta\|_{\text{F}} \quad [\text{by Lemma C.9}] \\ & \quad + 2\eta C^* K^2 \sqrt{d}\epsilon \|\mathbf{A}_t\mathbf{B}_t - \Delta\|_{\text{F}} \quad [\text{by Theorem C.12}] \\ & \quad + \eta^2 (1 + \epsilon)^2 \frac{\rho}{1 - \rho} \|\mathbf{A}_t\mathbf{B}_t - \Delta\|_{\text{F}} \quad [\text{by Lemma C.8}] \\ & \leq \left(2 - 3\eta/2 + \frac{\rho}{\sqrt{1 - 8\rho^2}} \right) \|\mathbf{A}_t\mathbf{B}_t - \Delta\|_{\text{F}} \\ & \quad + \eta \frac{2\rho}{3\gamma\sqrt{2r^*\kappa}} \|\mathbf{A}_t\mathbf{B}_t - \Delta\|_{\text{F}} \\ & \quad + \eta^2 \left(1 + \frac{\rho}{3C^*K^2\gamma\sqrt{2dr^*\kappa}} \right)^2 \frac{\rho}{1 - \rho} \|\mathbf{A}_t\mathbf{B}_t - \Delta\|_{\text{F}}. \quad \left[\text{since } \epsilon \leq \frac{\rho}{3C^*K^2\gamma\sqrt{2dr^*\kappa}} \right] \end{aligned}$$

with probability at least $1 - 2Cdk \exp(-\epsilon^2N)$ for a universal constant $C > 0$. Since $\rho \leq \frac{1}{20}$, then

we can sort the above upper bound as

$$\begin{aligned} \|\mathbf{A}_{t+1}\mathbf{B}_{t+1} - \Delta\|_{\text{F}} &\leq \left(1 - \frac{\eta}{4}\right) \|\mathbf{A}_t\mathbf{B}_t - \Delta\|_{\text{F}} \\ &\quad + \left\{ \left(1 + \frac{1}{60C^*K^2\gamma\sqrt{2dr^*\kappa}}\right)^2 \frac{1}{19}\eta^2 \right. \\ &\quad \left. + \eta \left(1 - 5\eta/4 + \frac{1}{30\gamma\sqrt{2r^*\kappa}}\right) + \frac{\sqrt{2}}{28} \right\} \|\mathbf{A}_t\mathbf{B}_t - \Delta\|_{\text{F}} . \end{aligned}$$

Then, there exists a constant $c_\eta^{\text{GLM}} > 0$ such that for $\forall \eta \in (c_\eta^{\text{GLM}}, 1)$, we have

$$-\left(1 - \frac{\eta}{4}\right) \leq \left(1 + \frac{1}{60C^*K^2\gamma\sqrt{2dr^*\kappa}}\right)^2 \frac{1}{19}\eta^2 + \eta \left(1 - 5\eta/4 + \frac{1}{30\gamma\sqrt{2r^*\kappa}}\right) + \frac{\sqrt{2}}{28} \leq 0,$$

which implies

$$\|\mathbf{A}_{t+1}\mathbf{B}_{t+1} - \Delta\|_{\text{F}} \leq \left(1 - \frac{\eta}{4}\right) \|\mathbf{A}_t\mathbf{B}_t - \Delta\|_{\text{F}} .$$

Then, we can obtain the inductive hypothesis at $t + 1$ and prove the claim. \square

D Auxiliary Results for Proofs

In this subsection, we present some auxiliary results that are needed for our proof. First, we present the estimation of the spectral norm of random matrices. It can be easily derived from [Vershynin \(2018\)](#) and we put it here for the completeness.

Lemma D.1. ([Vershynin, 2018](#), Adapted from Theorem 4.6.1) For a random sub-Gaussian matrix $\widetilde{\mathbf{X}} \in \mathbb{R}^{N \times d}$ whose rows are i.i.d. isotropic sub-gaussian random vector with sub-Gaussian norm K , then we have the following statement

$$\mathbb{P} \left(\left\| \frac{1}{N} \widetilde{\mathbf{X}}^\top \widetilde{\mathbf{X}} - \mathbf{I}_d \right\|_{\text{op}} > \delta \right) \leq 2 \exp(-CN \min(\delta^2, \delta)) .$$

for a universal constant C depending only on K .

Lemma D.2. ([Vershynin, 2010](#), Adapted from Corollary 5.35) For a random standard Gaussian matrix $\mathbf{S} \in \mathbb{R}^{d \times r}$ with $[\mathbf{S}]_{ij} \sim \mathcal{N}(0, 1)$, if $d > 2r$, we have

$$\frac{\sqrt{d}}{2} \leq \|\mathbf{S}\|_{\text{op}} \leq (2\sqrt{d} + \sqrt{r}), \tag{D.1}$$

with probability at least $1 - C \exp(-d)$ for some positive constants C .

The following results are modified from the proof of [Stöger and Soltanolkotabi \(2021, Lemma 8.7\)](#).

Lemma D.3. Suppose $\mathbf{S} \in \mathbb{R}^{d \times r}$ is a random standard Gaussian matrix with $[\mathbf{S}]_{ij} \sim \mathcal{N}(0, 1)$ and $\mathbf{U} \in \mathbb{R}^{d \times r^*}$ has orthonormal columns. If $r \geq 2r^*$, with probability at least $1 - C \exp(-r)$ for some

positive constants C , we have

$$\lambda_{\min}(\mathbf{U}^\top \mathbf{S}) \gtrsim 1.$$

If $r^* \leq r < 2r^*$, by choosing $\xi > 0$ appropriately, with probability at least $1 - (C\xi)^{r-r^*+1} - C' \exp(-r)$ for some positive constants C, C' , we have

$$\lambda_{\min}(\mathbf{U}^\top \mathbf{S}) \gtrsim \frac{\xi}{r}.$$

Next, we give a short description of the Hermite expansion of ReLU function via Hermite polynomials. Details can be found in [Damian et al. \(2022, A.1.1\)](#) and [Arous et al. \(2021\)](#). To be specific, the Hermite expansion of ReLU function $\sigma(x)$ is

$$\sigma(x) = \sum_{j=1}^{\infty} \frac{c_j}{j!} \text{He}_j(x) = \frac{1}{\sqrt{2\pi}} + \frac{1}{2}x + \frac{1}{\sqrt{2\pi}} \sum_{j \geq 1} \frac{(-1)^{j-1}}{j!2^j(2j-1)} \text{He}_{2j}(x), \quad (\text{D.2})$$

which implies that we can express the Hermite coefficients as

$$\begin{cases} c_0 = \frac{1}{\sqrt{2\pi}}, \\ c_1 = \frac{1}{2}, \\ c_{2j} = \frac{(-1)^{j-1}}{\sqrt{2\pi}2^j(2j-1)} \quad \text{for } j \geq 1. \end{cases} \quad (\text{D.3})$$

Furthermore, the derivative of $\sigma(x)$ admits

$$\sigma'(x) = \frac{1}{2} + \frac{1}{\sqrt{2\pi}} \sum_{j \geq 0} \frac{(-1)^j}{j!2^j(2j+1)} \text{He}_{2j+1}(x). \quad (\text{D.4})$$

Lemma D.4. ([Oko et al., 2024, Corollary 9](#)) $\mathbb{E}_{\tilde{\mathbf{x}}}[\nabla^k \sigma(\langle \mathbf{w}, \tilde{\mathbf{x}} \rangle)] = c_k \mathbf{w}^{\otimes k}$ for any k such that $c_k \neq 0$.

Lemma D.5. For any vectors \mathbf{u} and \mathbf{v} , we have

$$|\langle \mathbf{u}, \mathbf{u} \rangle^j - \langle \mathbf{u}, \mathbf{v} \rangle^j| \leq j \max\{\|\mathbf{u}\|_2, \|\mathbf{v}\|_2\}^{2j-1} \|\mathbf{u} - \mathbf{v}\|_2.$$

Proof. First, we analyze the following two scalar variables case

$$|x^j - y^j|.$$

By algebraic identity $\sum_{j=1}^{t-1} x^{t-j-1} y^j = \frac{x^t - y^t}{x-y}$ which is valid for $\forall j \in \mathbb{N}^+$, we have

$$|x^j - y^j| = \left| (x-y) \sum_{i=0}^{j-1} x^{j-i-1} y^i \right| \leq |x-y| \sum_{i=0}^{j-1} \max\{|x|, |y|\}^{j-1} = j|x-y| \max\{|x|, |y|\}^{j-1}.$$

Now we define $x := \langle \mathbf{u}, \mathbf{u} \rangle$ and $y := \langle \mathbf{u}, \mathbf{v} \rangle$, then we can obtain

$$\begin{aligned}
|\langle \mathbf{u}, \mathbf{u} \rangle^j - \langle \mathbf{u}, \mathbf{v} \rangle^j| &\leq j \max \{ |\langle \mathbf{u}, \mathbf{u} \rangle|, |\langle \mathbf{u}, \mathbf{v} \rangle| \}^{j-1} |\langle \mathbf{u}, \mathbf{u} \rangle - \langle \mathbf{u}, \mathbf{v} \rangle| \\
&\leq j \max \left\{ \|\mathbf{u}\|_2^2, \|\mathbf{u}\|_2 \|\mathbf{v}\|_2 \right\}^{j-1} \|\mathbf{u}\|_2 \|\mathbf{u} - \mathbf{v}\|_2 \\
&\hspace{15em} \text{[by Cauchy-Schwartz inequality]} \\
&= j \max \{ \|\mathbf{u}\|_2, \|\mathbf{v}\|_2 \}^{2j-1} \|\mathbf{u} - \mathbf{v}\|_2 .
\end{aligned}$$

□

E Discussion on Prior Work Based on Gradient Alignment

Our initialization strategy in Algorithm 1 (line 4-6) shares some similarity with prior work on gradient alignment, e.g., LoRA-GA (Wang et al., 2024a), and LoRA-pro (Wang et al., 2024b). However, the motivation behind these gradient alignment work differs significantly from ours. The above gradient alignment based algorithms are driven by how to approximate the full fine-tuning gradient by low-rank updates. Instead, our our work is motivated by which subspace ($\mathbf{A}_t, \mathbf{B}_t$) will align with and then how to achieve this alignment efficiently so as to finally recover Δ .

Here we take LoRA-GA as an example to explain the potential issue that the spirit of LoRA-GA might not help recover Δ , both theoretically and empirically. To be specific, LoRA-GA (Wang et al., 2024a) also computes the SVD of $\nabla_{\mathbf{W}} L(\mathbf{W}^\natural)$. To ensure the pre-trained model remains unchanged at $t = 0$, LoRA-GA the following strategy

$$\begin{aligned}
\mathbf{A}_0 &= -\sqrt{\gamma} \left[\tilde{\mathbf{U}}_{\mathbf{G}^\natural} \right]_{[:,1:r]}, \mathbf{B}_0 = \sqrt{\gamma} \left[\tilde{\mathbf{V}}_{\mathbf{G}^\natural} \right]_{[:,r+1:2r]}^\top, \\
\mathbf{W}_{\text{off}}^\natural &:= \mathbf{W}^\natural - \frac{\alpha}{\sqrt{r}} \mathbf{A}_0 \mathbf{B}_0.
\end{aligned} \tag{LoRA-GA}$$

Theoretically, LoRA-GA observes $\text{rank}(\nabla_{\mathbf{A}} \tilde{L}(\mathbf{A}_t, \mathbf{B}_t) + \nabla_{\mathbf{B}} \tilde{L}(\mathbf{A}_t, \mathbf{B}_t)) \leq 2r$ and then proposes to find the best $2r$ -rank approximation of one-step full gradient to the first step of LoRA. Accordingly, LoRA-GA chooses the first r singular values for \mathbf{A}_0 and $(r + 1)$ th to $2r$ th singular values for \mathbf{B}_0 . However, as pointed by our theory, \mathbf{B}_t will also align to the right-side rank- r^* singular subspace of \mathbf{G}^\natural under random initialization. That means, due to the way LoRA-GA chooses the $(r + 1)$ th to $2r$ th singular values for \mathbf{B}_0 , the iterate \mathbf{B}_t does not lie in the desired subspace and may not escape an undesirable subspace.

Empirically, the mismatch of singular subspace induced by corresponding singular values in LoRA-GA might bring unfavorable performance even in a toy model. We consider the exact-ranked case ($r = r^*$) for fine-tuning task in the linear setting. We compare the generalization risk of three initialization strategies: (Spectral-init), Algorithm 1 without preconditioners, and LoRA-GA trained via vanilla GD. The results are shown in Fig. 2. We can empirically observe that LoRA-GA fails to generalize and remain at a high-risk level throughout training. In contrast, (Spectral-init) and Algorithm 1 both can generalize well. This empirically demonstrates the optimality of choosing top- r singular subspace of \mathbf{G}^\natural .

Before the submission deadline we became aware of the concurrent work Pongshe et al. (2024), which uses the same initialization for \mathbf{B}_0 as in line 6 of our Algorithm 1. However, the motivation, problem setting, and theoretical analysis are totally different between our work and theirs. Moreover,

our Algorithm 1 also introduces the preconditioners and is able to efficiently handle ill-conditioned cases, and this is not available in Punkshe et al. (2024).

F Experimental Settings and Additional Results

In Appendix F.1, we firstly provide the experimental details of small-scale experiments in our main text, e.g., Fig. 2 and Fig. 3. Experimental settings of NLP tasks in the main text are given by Appendix F.2. We also include the fine-tuning experiments on LLMs in Appendix F.3. More ablation study is given by Appendix F.4. Finally, we visualize the singular values of both the pre-trained weights and the difference weights after fine-tuning in Appendix F.5. All small-scale experiments were performed on AMD EPYC 7B12 CPU. All experiments for T5 base model and Llama 2-7B were performed on Nvidia A100 GPU (40GB).

F.1 Small-Scale Experiments

Here we give the experimental details of Fig. 2 and Fig. 3. Besides, we plot the GD trajectories under (Spectral-init) and (LoRA-init) for comparison.

Details for Fig. 2: For the exact-ranked setting, we take $d = k = 100$, $N = 1600$, and $r = r^* = 4$. We sample each element of \mathbf{W}^\natural independently from $\mathcal{N}(0, 1)$. We construct $\Delta := \mathbf{U}\mathbf{V}^\top$ where $\mathbf{U} \in \mathbb{R}^{100 \times 4}$ and $\mathbf{V} \in \mathbb{R}^{100 \times 4}$ are obtained from the SVD of a matrix whose elements are independently sampled from $\mathcal{N}(0, 1)$. For LoRA-One (-) and LoRA-GA (-), we use learning rate $\eta = \frac{1}{35}$ and stable parameter $s = 2$. For (Spectral-init) (-), we use learning rate $\eta = \frac{1}{10}$ and $\gamma = 1$.

For the ill-conditioned setting, we take $d = k = 100$, $N = 1600$, $r^* = 4$, and $r = 8$. We construct $\Delta := \mathbf{U}\mathbf{S}^*\mathbf{V}^\top$ where $\mathbf{U} \in \mathbb{R}^{100 \times 4}$ and $\mathbf{V} \in \mathbb{R}^{100 \times 4}$ are obtained from the SVD of a matrix whose elements are independently sampled from $\mathcal{N}(0, 1)$, and $\mathbf{S}^* = \text{Diag}(1, 0.75, 0.5, 0.25)$. For algorithms without preconditioners, we set the learning rate to be $\eta = \frac{1}{20}$. For algorithms with preconditioners, we set the learning rate to be $\eta = \frac{1}{2}$. For LoRA-One, LoRA-One (-), LoRA-GA (-), and LoRA-GA (+), we set the stable parameter $s = 2$. For (Spectral-init) (-) and (Spectral-init) (+), we take $\gamma = 1$. All damping parameters λ for preconditioners are set to be 0.001.

Details for Fig. 3: We examine for dimension $d = k = 100$ and $d = k = 1000$. We set $N = 16d$, $r^* = 4$, and $r = 8$. We construct $\Delta := \mathbf{U}\mathbf{V}^\top$ where $\mathbf{U} \in \mathbb{R}^{100 \times 4}$ and $\mathbf{V} \in \mathbb{R}^{100 \times 4}$ are obtained from the SVD of a matrix whose elements are independently sampled from $\mathcal{N}(0, 1)$. We initialize \mathbf{A}_0 and \mathbf{B}_0 via (LoRA-init) over variance $\alpha^2 \in \{1, 0.1, 0.01, 0.001, 0.0001\}$. We set learning rate $\eta = \frac{1}{64}$. We run 1500 GD steps for each case.

Comparison on GD trajectories of Fig. 1: Here we conduct a toy experiment to intuitively compare the GD trajectories under (Spectral-init) and (LoRA-init). We fine-tune a simple pre-trained model $y = \mathbf{x}^\top \mathbf{w}^\natural$ on downstream data generated by $\tilde{y} = \tilde{\mathbf{x}}^\top (\mathbf{w}^\natural + \mathbf{w})$, where $\mathbf{x}^\top, \tilde{\mathbf{x}}, \mathbf{w}^\natural, \mathbf{w} \in \mathbb{R}^2$ and $y, \tilde{y} \in \mathbb{R}$. We propose to use LoRA to fine-tune this model by $\hat{y} = \tilde{\mathbf{x}}^\top (\mathbf{w}^\natural + b\mathbf{a})$ where $\mathbf{a} = [a_1 \ a_2]^\top \in \mathbb{R}^2$ and $b \in \mathbb{R}$. Without loss of generality, we set $\mathbf{w}^\natural = \mathbf{0}$ and $\mathbf{w} = [2 \ 1]^\top$. The set of global minimizers to this problem is $\{a_1^* = 2/t, a_2^* = 1/t, b^* = t \mid t \in \mathbb{R}\}$. We generate 4 data points $(\tilde{\mathbf{x}}_1, \tilde{\mathbf{x}}_2, \tilde{\mathbf{x}}_3, \tilde{\mathbf{x}}_4)$ whose elements are independently sampled from $\mathcal{N}(0, 1)$ and calculate for $(\tilde{y}_1, \tilde{y}_2, \tilde{y}_3, \tilde{y}_4)$. We use the squared loss $\frac{1}{8} \sum_{i=1}^4 (\tilde{y}_i - b\tilde{\mathbf{x}}_i^\top \mathbf{a})^2$. For (LoRA-init), we initialize each element of \mathbf{a}_0 from $\mathcal{N}(0, 1)$ and $b_0 = 0$. Notice that the variance 1 follows from the Kaiming

initialization (He et al., 2015). For (Spectral-init), we first calculate the one-step full gradient, i.e. $\mathbf{g}^h := \frac{1}{4} \sum_{i=1}^4 \tilde{y}_i^2 \tilde{\mathbf{x}}_i$. Accordingly, we initialize $\mathbf{a}_0 = \frac{\mathbf{g}^h}{\sqrt{\|\mathbf{g}^h\|_2}}$ and $b_0 = \sqrt{\|\mathbf{g}^h\|_2}$. Next, we run GD to train \mathbf{a} and b for 1000 steps with learning rate $\eta = 0.1$. For each initialization strategy and data generation, we run for 3 different seeds. The starting points and stopping points with corresponding loss values are presented in Table 8 for (Spectral-init) and Table 9 for (LoRA-init). Our experiments in Fig. 1 show that spectral initialization enables faster convergence to the global minimizer compared to LoRA initialization.

Table 8: The details of starting points with initial loss and stopping points with final loss under (Spectral-init) over 3 runs.

	Starting Point	Initial Loss	Stopping Point	Final Loss
Run 1	$\mathbf{a} = [0.26, 0.55]^\top, b = 0.61$	0.39	$\mathbf{a} = [1.34, 0.67]^\top, b = 1.49$	5×10^{-13}
Run 2	$\mathbf{a} = [1.10, -0.27]^\top, b = 1.10$	0.38	$\mathbf{a} = [1.35, 0.68]^\top, b = 1.48$	1×10^{-13}
Run 3	$\mathbf{a} = [0.96, 0.35]^\top, b = 1.02$	0.34	$\mathbf{a} = [1.34, 0.67]^\top, b = 1.49$	4×10^{-13}

Table 9: The details of starting points with initial loss and stopping points with final loss under (LoRA-init) over 3 runs.

	Starting Point	Initial Loss	Stopping Point	Final Loss
Run 1	$\mathbf{a} = [-0.35, 2.63]^\top, b = -0.03$	0.43	$\mathbf{a} = [-2.49, -1.24]^\top, b = -0.80$	1×10^{-10}
Run 2	$\mathbf{a} = [0.14, -1.68]^\top, b = 0.10$	0.82	$\mathbf{a} = [1.81, 0.91]^\top, b = 1.10$	1×10^{-13}
Run 3	$\mathbf{a} = [-1.44, 0.98]^\top, b = 0.03$	0.97	$\mathbf{a} = [1.84, 0.92]^\top, b = 1.08$	6×10^{-13}

F.2 Natural Language Understanding

In the main text of Section 5, we have presented the experimental comparisons between Algorithm 1 and typical LoRA based algorithms. For experimental details, we follow the configuration of prompt tuning as Wang et al. (2024a). The general hyperparameter settings are provided in Table 10. Also, we employ the scaling parameter $\sqrt{\frac{d_{\text{out}}}{s}}$ for LoRA-One (Algorithm 1) derived in Wang et al. (2024a) which is proven to be numerically stable. To ensure a fair comparison, we tune the learning rate via grid search over $\{1 \times 10^{-3}, 5 \times 10^{-4}, 2 \times 10^{-4}, 1 \times 10^{-4}, 5 \times 10^{-5}, 2 \times 10^{-5}, 1 \times 10^{-5}\}$.

Furthermore, we fine-tune the model using one step update from full-batch gradient descent under full fine-tuning. To optimize GPU memory usage, we adopt the averaged gradient computation method from Lv et al. (2023); Wang et al. (2024a) to compute the full gradient, which is then manually added to the pre-trained weights, scaled by the learning rate.

Besides, we notice that the test accuracy on the MNLI dataset remains 0.0% for the first dozen steps in both full fine-tuning and LoRA fine-tuning. So we omit results on this dataset. We conjecture that this is due to the significant discrepancy between pre-trained tasks and downstream tasks. For SST-2, CoLA, QNLI, and MRPC, the learning rates are set to be $\{5 \times 10^{-4}, 1 \times 10^{-2}, 2 \times 10^{-2}, 0.5\}$.

Table 10: Hyperparameters for LoRA fine-tuning on T5-base model.

Epoch	Optimizer	(β_1, β_2)	ϵ	Batch Size
1	AdamW	(0.9, 0.999)	1×10^{-8}	32
Warm-up Ratio	LoRA Alpha	s (if needed)	λ (if needed)	#Runs
0.03	16	16	1×10^{-6}	3
Weight Decay	LR Scheduler	Sequence Length	Precision	
0	cosine	128	FP32	

F.3 Experiments on LLM

We use a stronger baseline for full fine-tuning, as provided in Wang et al. (2024b), compared to those in Wang et al. (2024a). For vanilla LoRA, due to the limitation of computational resources, we use the results of LoRA with rank 8 from Wang et al. (2024a). For LoRA-GA, we pick the best results from (Wang et al., 2024a). We align our generation configuration and stable parameter s with LoRA-GA Wang et al. (2024a) to ensure a fair comparison. The hyperparameter settings are provided in Table 11. For the learning rates of LoRA-One, we conduct a grid search over $\{5 \times 10^{-5}, 2 \times 10^{-5}, 1 \times 10^{-5}\}$, following the configuration used in Wang et al. (2024a).

Table 11: Hyperparameters for LoRA fine-tuning on Llama 2-7B model.

Epoch	Optimizer	(β_1, β_2)	ϵ	Batch Size
1	AdamW	(0.9, 0.999)	1×10^{-8}	32
Warm-up Ratio	LoRA Alpha	s (if needed)	λ (if needed)	#Runs
0.03	16	64	1×10^{-6}	3
Weight Decay	LR Scheduler	Sequence Length	Precision	
0	cosine	1024	FP32	

F.4 Ablation Study

In this subsection, we compare 5 algorithms to provide insights for practical algorithm design. The details of 5 algorithms are summarized in Table 12. The details of means and standard deviations over 3 runs are shown in Table 13 for CoLA and Table 14 for MRPC. The hyperparameter settings for LoRA-One, LoRA-One (-), LoRA-GA (-), and LoRA-GA (+) are same as the settings used in Appendix F.2. We tune the learning rates via grid search over $\{1 \times 10^{-3}, 5 \times 10^{-4}, 2 \times 10^{-4}, 1 \times 10^{-4}, 5 \times 10^{-5}, 2 \times 10^{-5}, 1 \times 10^{-5}\}$ to ensure a fair comparison. The implement details of Spectral (-) are provided in Algorithm 2, which is a scaled version of (Spectral-init) without preconditioning. We notice that Spectral (-) is highly sensitive to hyperparameters which makes it hard to tune. The general hyperparameters of Spectral (-) is same as the settings used in Appendix F.2. Here we provide the LoRA alpha and learning rates for Spectral (-) in Table 15.

Table 12: Initialization strategies and corresponding optimizers for ablation study.

	Initialization	Optimizer
LoRA-One	Algorithm 1 (1-8)	Prec-AdamW
LoRA-One (-)	Algorithm 1 (1-8)	AdamW
Spectral (-)	Algorithm 2 (1-5)	AdamW
LoRA-GA (-)	(LoRA-GA)	AdamW
LoRA-GA (+)	(LoRA-GA)	Prec-AdamW

Table 13: Accuracy comparison across different methods on CoLA under three ranks, i.e. $r = 8, 32, 128$. LoRA-One (-) stands for training with AdamW without preconditioning under initialization by line 1-8 in Algorithm 1.

Rank	LoRA-One	LoRA-One (-)	Spectral (-)	LoRA-GA (-)	LoRA-GA (+)
8	81.08 \pm 0.36	80.83 \pm 0.54	81.40 \pm 0.31	80.57 \pm 0.20	80.57 \pm 0.12
32	81.34 \pm 0.51	81.30 \pm 0.16	81.18 \pm 0.30	80.86 \pm 0.23	80.92 \pm 0.34
128	81.53 \pm 0.36	81.34 \pm 0.12	81.62 \pm 0.48	80.95 \pm 0.35	80.02 \pm 0.64

Table 14: Accuracy comparison across different methods on MRPC under three ranks, i.e. $r = 8, 32, 128$. LoRA-One (-) stands for training with AdamW without preconditioning under initialization by line 1-8 in Algorithm 1.

Rank	LoRA-One	LoRA-One (-)	Spectral (-)	LoRA-GA (-)	LoRA-GA (+)
8	86.77 \pm 0.53	87.50 \pm 0.60	86.19 \pm 0.42	85.29 \pm 0.24	85.87 \pm 0.31
32	87.34 \pm 0.31	87.34 \pm 0.42	86.02 \pm 0.20	86.36 \pm 0.42	85.78 \pm 0.20
128	88.40 \pm 0.70	87.26 \pm 0.20	86.03 \pm 0.20	85.46 \pm 0.23	87.01 \pm 0.35

Algorithm 2 (Spectral-init) training for a specific layer

Input: Pre-trained weight \mathbf{W}^\natural , batched data $\{\mathcal{D}_t\}_{t=1}^T$, LoRA rank r , LoRA alpha α , loss function L , scaling parameter γ

Initialize:

- 1: Compute $\mathbf{G}^\natural \leftarrow -\nabla_{\mathbf{W}} L(\mathbf{W}^\natural)$
- 2: $\mathbf{U}, \mathbf{S}, \mathbf{V} \leftarrow \text{SVD}(\mathbf{G}^\natural)$
- 3: $\mathbf{A}_0 \leftarrow \sqrt{\gamma} \cdot \mathbf{U}_{[:,1:r]} \mathbf{S}_{[1:r]}^{1/2}$
- 4: $\mathbf{B}_0 \leftarrow \sqrt{\gamma} \cdot \mathbf{S}_{[1:r]}^{1/2} \mathbf{V}_{[:,1:r]}^\top$
- 5: Clear \mathbf{G}^\natural

Train:

- 6: **for** $t = 1, \dots, T$ **do**
- 7: Update parameters \mathbf{A}_t and \mathbf{B}_t by AdamW given \mathcal{D}_t
- 8: **end for**

Return: $\mathbf{W}^\natural + \frac{\alpha}{\sqrt{r}} \mathbf{A}_T \mathbf{B}_T$

Table 15: Specific hyperparameter settings for Spectral (-) (see details in Algorithm 2) used in Appendix F.4.

Rank	CoLA			MRPC		
	LR	LoRA Alpha	γ	LR	LoRA Alpha	γ
8	2×10^{-3}	$\sqrt{8}$	0.01	6×10^{-4}	1	0.01
32	2×10^{-3}	$\sqrt{32}$	0.01	2×10^{-3}	16	0.01
128	2×10^{-3}	1	0.01	9×10^{-4}	1	0.01

F.5 Comparison of Singular Values

First, we collect top-32 singular values for each pre-trained layer \mathbf{W}^d of pre-trained T5-base model (Raffel et al., 2020). Next, we perform full fine-tuning to the pre-trained model on SST-2 dataset from GLUE. To ensure better convergence, we take the hyperparameter settings which are presented in Table 16. After training, we collect top-32 singular values for each difference weights, i.e. $\Delta \mathbf{W} = \mathbf{W}_{\text{fine-tuned}} - \mathbf{W}^d$. The results are shown in Fig. 4. The hyperparameter settings for full fine-tuning are provided in Table 16.

We observe that, across all layers, the singular values of the pre-trained weights are significantly larger than those of the difference weights.

Table 16: Hyperparameters for full fine-tuning on T5-base model used for Appendix F.5.

Epoch	Optimizer	(β_1, β_2)	ϵ	Batchsize
10	AdamW	(0.9, 0.999)	1×10^{-8}	32
Weight Decay	LR	LR Scheduler	Warm-up Ratio	
0.1	1×10^{-4}	cosine	0.03	